



## City Research Online

### City, University of London Institutional Repository

---

**Citation:** Chappell, D. C. (1991). Fluorescent labelling of proteins - Volume 1.  
(Unpublished Doctoral thesis, City, University of London)

This is the accepted version of the paper.

This version of the publication may differ from the final published version.

---

**Permanent repository link:** <https://openaccess.city.ac.uk/id/eprint/28491/>

**Link to published version:**

**Copyright:** City Research Online aims to make research outputs of City, University of London available to a wider audience. Copyright and Moral Rights remain with the author(s) and/or copyright holders. URLs from City Research Online may be freely distributed and linked to.

**Reuse:** Copies of full items can be used for personal research or study, educational, or not-for-profit purposes without prior permission or charge. Provided that the authors, title and full bibliographic details are credited, a hyperlink and/or URL is given for the original metadata page and the content is not changed in any way.

FLUORESCENT  
LABELLING  
OF PROTEINS

VOLUME 1.

by

DAVID CLIVE CHAPPELL

A thesis submitted for the Degree of  
DOCTOR OF PHILOSOPHY  
in the Chemistry Department of  
The City University, London.

April, 1991.

CHAPTER 1 - GENERAL INTRODUCTION	1
1.1 Fundamentals of Photochemistry	1
1.1.1 Electronically Excited States	2
1.1.2 Excited Singlet and Triplet States	4
1.1.3 Fluorescence	6
1.1.4 Lifetime and Quantum Yield of Fluorescence	8
1.1.5 Phosphorescence	8
1.1.6 Non-radiative Decay	9
1.1.7 The Jablonski Diagram	10
1.2 Fluorescent Probes	12
1.2.1 Fluorescent Calcium Probes and Their Use	13
1.3 Some Known Functions of cGMP	24
1.4 The Objectives of the Project and the Approach Adopted	27
1.5 References	
CHAPTER 2 - FLUORESCENT PROBES AND THEIR USES	29
2.1 Introduction	29
2.2 The Major Factors to be Considered in the Fluorescent Labelling of Biomolecules	29
2.2.1 The Reactive Sites on Proteins	30
2.2.2 The Reactive Moieties on Fluorescent Probes	33
2.2.3 Characteristics of an Ideal Fluorescent Probe	35
2.3 Covalent Labelling of Biomolecules	36
2.3.1 Solubilisation of the Fluorophore	36
2.3.2 The Mechanism of Covalent Modification	38
2.3.3 Purification of the Biomolecule-Probe Conjugate	39
2.4 Procedures and Fluorophores Utilised for Selective Modification Reactions	40
2.4.1 Thiol Modification	40
2.4.2 Amine Modification	48
2.4.3 Histidine Modification	56
2.4.4 Methionine Modification	56
2.4.5 Tyrosine Modification	57
2.4.6 Carboxylic Acid Modification	57
2.4.7 Modification of Other Residues in Proteins	58

	<u>PAGE</u>
2.5 Probes that are Sensitive to the pH of Their Environment	60
2.6 Fluorescent Probes which Undergo Energy Transfer	62
2.7 Fluorescent Probes that are Sensitive to the Polarity of Their Environment	63
2.8 Fluorescent Redox Potential Probes	64
2.9 Fluorescent Probes for Measuring Enzyme Activities	65
2.10 Photo-activatable Fluorophores	68
2.11 Non-covalently Associating Fluorescent Probes	69
2.11.1 pH Probes that Partition Between Compartments with Different pH	69
2.11.2 Probes for the Visualisation of Membrane and Lipid Compartments	70
2.11.3 DNA and RNA Probes	71
2.11.4 Membrane Potential Probes	72
2.12 Summary	74
2.13 References	
 CHAPTER 3 - cAMP RECEPTOR PROTEIN	 75
3.1 Discovery of cAMP Receptor Protein	75
3.2 Location, Isolation and Purification of CRP	75
3.3 Physical and Chemical Properties of CRP	77
3.4 The Primary Structure of CRP	77
3.5 The Secondary Structure of CRP	79
3.5.1 The $\beta$ -Roll Structure	81
3.5.2 The Hinge Region Structure	82
3.5.3 Interdomain Interactions	83
3.5.4 The Carboxyl-Terminal Domain Structure	85
3.5.5 Intersubunit Interactions	86
3.6 Binding of the cAMP Molecule to CRP: Mechanism of Action	87
3.7 Homology Between CRP and the Regulatory Subunit of cAMP-Dependent Protein Kinase	90

	<u>PAGE</u>
3.8 Evidence for a Conformational Change Elicited in CRP by cAMP	94
3.9 Binding of the CRP-cAMP Complex to DNA: Mechanism of Action	100
3.10 Summary	107
3.11 References	
 CHAPTER 4 - EXPERIMENTAL PROCEDURES FOR THE SYNTHESIS OF FLUORESCENT PROBES	 108
4.1 Synthesis of Bis (1,10-phenanthroline) (Bathophen- anthroline disulphonyl chloride) ruthenium (II) hexafluorophosphate dihydrate	108
4.1.1 Preparation of Bis (1,10-phenanthroline) dichloride ruthenium (II) dihydrate	108
4.1.2 Preparation of Bis (1,10-phenanthroline) (Bathophenanthroline disulphonic acid, disodium salt) ruthenium (II) dihydrate	110
4.1.3 Preparation of Bis (1,10-phenanthroline) (Bathophenanthroline disulphonyl chloride) ruthenium (II) hexafluorophosphate dihydrate	112
4.2 Synthesis of N-(1-Pyrene) Maleimide	114
4.2.1 Preparation of N-(1-Pyrene) Maleamic Acid	114
4.2.2 Preparation of N-(1-Pyrene) Maleimide	116
4.3 Synthesis of N-(Iodoacetylaminoethyl)-1-naphthylamine -8-Sulphonic Acid	118
4.3.1 Preparation of 1-Naphthol-8-Sulphonic Acid	118
4.3.2 Preparation of 1-Naphthol-8-Sulphonic Acid, Sodium Salt	120
4.3.3 Preparation of p-Nitrophenyl Iodoacetate	121
4.3.4 Preparation of N-(Aminoethyl)-1-naphthylamine -8-Sulphonic Acid	124
4.3.5 Preparation of N-(Iodoacetylaminoethyl)-1- naphthylamine-8-Sulphonic Acid	127
4.4 Synthesis of N-(1-anilinonaphthyl-4) Maleimide	129
4.4.1 Preparation of 4-p-sulphobenzeneazo-1- anilinonaphthalene	129
4.4.2 Preparation of 1-anilino-4-aminonaphthalene	132
4.4.3 Preparation of N-(1-anilinonaphthyl-4) Maleamic Acid	134

	<u>PAGE</u>
4.4.4 Preparation of N-(1-anilinonaphthyl-4) Maleimide	136
4.5 Synthesis of the Maleimidyl Benzoate Ester of Benz(c,d)indol-2(1H)-one	138
4.5.1 Preparation of Benz(c,d)indol-2(1H)-one	138
4.5.2 Preparation of 1-hydroxy-methylbenz(c,d)indol-2(1H)-one	140
4.5.3 Preparation of 1-chloro-methylbenz(c,d)indol-2(1H)-one	142
4.5.4 Preparation of N-(p-benzoic acid) Maleamic Acid	144
4.5.5 Preparation of N-(p-benzoic acid) Maleimide	146
4.5.6 Preparation of the Maleimidyl Benzoate Ester of Benz(c,d)indol-2(1H)-one	148
4.6 Synthesis of Succinimidyl Trans-Parinaric Acid	150
4.7 Synthesis of 9-Bromomethylacridine	152
4.7.1 Preparation of 9-Methylacridine	152
4.7.2. Preparation of 9-Bromomethylacridine	154
4.8 References	
CHAPTER 5 - EXPERIMENTAL PROCEDURES FOR THE FLUORESCENT MODIFICATION OF cAMP RECEPTOR PROTEIN	156
5.1 Introduction	156
5.2 CRP Assay	156
5.2.1 Experimental Procedure	156
5.2.2 Results	157
5.3 Experimental Procedures for the Modification of the $\epsilon$ -amino Group of Lysine Residues in CRP	159
5.3.1 Fluorescent Modification of CRP Using Bis (1,10-phenanthroline) (Bathophenanthroline disulphonyl chloride) ruthenium (II) hexafluorophosphate dihydrate	159
5.3.2 Fluorescent Modification of CRP Using Succinimidyl Trans-Parinaric Acid	161
5.3.3 Fluorescent Modification of CRP Using Sulphorhodamine Acid Chloride	162
5.3.4 Fluorescent Modification of CRP Using Succinimidyl 7-amino-4-methylcoumarin-3-acetic acid	164

5.3.5	Fluorescent Modification of CRP Using 5-dimethylaminonaphthalene-1-Sulphonyl Chloride	165
5.4	Experimental Procedures for the Modification of the Thiol Group of Cysteine Residues in CRP	167
5.4.1	Fluorescent Modification of CRP Using Bis (2,2'-bipyridine) (4-vinyl-4'-methyl-2,2'-bipyridine) ruthenium (II) hexafluorophosphate	167
5.4.2	Fluorescent Modification of CRP Using 9-Bromomethylacridine	168
5.4.3	Fluorescent Modification of CRP Using N-(9-acridinyl) Maleimide	170
5.4.4	Fluorescent Modification of CRP Using Tetramethylrhodamine-5-Iodoacetamide	171
5.4.5	Fluorescent Modification of CRP Using 5-Iodoacetamidofluorescein	173
5.4.6	Fluorescent Modification of CRP Using 4-chloro-7-nitrobenz-2-oxa-1,3-diazole	174
5.4.7	Fluorescent Modification of CRP Using Protoporphyrin IX	175
5.4.8	Fluorescent Modification of CRP Using Bilirubin	177
5.4.9	Fluorescent Modification of CRP Using N-(1-Pyrene) Maleimide	178
5.4.10	Fluorescent Modification of CRP Using Lucifer Yellow	180
5.4.11	Fluorescent Modification of CRP Using N-(7-dimethylamino-4-methylcoumarinyl) Maleimide	181
5.4.12	Fluorescent Modification of CRP Using Maleimidyl Benzoate Ester of Benz(c,d)indol-2(1H)-one	183
5.4.13	Fluorescent Modification of CRP Using N-(1-anilinonaphthyl-4) Maleimide	184
5.4.14	Fluorescent Modification of CRP Using 2-(4'-iodoacetamidoanilino)naphthalene-6-sulphonic acid, sodium salt	186
5.4.15	Fluorescent Modification of CRP Using N-(Iodoacetylaminoethyl)-1-naphthylamine-8-Sulphonic Acid	187
5.4.16	Fluorescent Modification of CRP Using 6-acryloyl-2-dimethylaminonaphthalene	188
5.5	References	

	<u>PAGE</u>
CHAPTER 6 - RESULTS AND DISCUSSION	190
6.1 Investigation of the Interaction of cAMP with the Unlabelled and Labelled cAMP Receptor Protein	190
6.1.1 CRP Assay	190
6.1.1.1 Experimental Procedure	190
6.1.1.2 Results	192
6.1.2 cAMP Binding Assay of Unlabelled CRP	193
6.1.2.1 Experimental Procedure	193
6.1.2.2 Results	195
6.1.3 cAMP Binding Assay of 6-acryloyl-2-dimethylaminonaphthalene Labelled CRP	196
6.1.3.1 Experimental Procedure	196
6.1.3.2 Results	198
6.1.4 cAMP binding Assay of Bis (1,10-phenanthroline) (Bathophenanthroline disulphonyl chloride) ruthenium (II) hexafluorophosphate Labelled CRP	198
6.1.4.1 Experimental Procedure	199
6.1.4.2 Results	200
6.1.4.3 Conclusion	201
6.1.5 cAMP Binding Assay of Unlabelled CRP Using the Aspirator Separation Method	202
6.1.5.1 Experimental Procedure	202
6.1.5.2 Results	203
6.1.5.3 Conclusion	205
6.2 Investigation of the Conformational Change Induced in CRP, by cAMP Binding, as Reported by a Range of Fluorophores	205
6.2.1 Fluorescence Data Derived from CRP Labelled Via $\epsilon$ -amino Groups	205
6.2.1.1 Bis (1,10-phenanthroline) (Bathophenanthroline disulphonyl chloride) ruthenium (II) hexafluorophosphate Labelled CRP and Derivatized n-butylamine	205
6.2.1.2 Succinimidyl Trans-Parinaric Acid Labelled CRP and Derivatized n-butylamine	206
6.2.1.3 Sulphorhodamine Acid Chloride Labelled CRP and Derivatized n-butylamine	208
6.2.1.4 Succinimidyl 7-amino-4-methylcoumarin-3-acetic acid Labelled CRP and Derivatized n-butylamine	209

	<u>PAGE</u>
6.2.1.5 5-dimethylaminonaphthalene-1-sulphonyl chloride Labelled CRP and Derivatised n-butylamine	210
6.2.2 Fluorescence Data Derived from CRP Labelled Via Thiol Groups	211
6.2.2.1 Bis (2,2'-bipyridine) (4-vinyl-4'-methyl-2,2'-bipyridine) ruthenium (II) hexafluorophosphate Labelled CRP and Derivatised Cysteine	211
6.2.2.2 9-bromomethylacridine Labelled CRP, Derivatised Cysteine and the Free Probe	213
6.2.2.3 N-(9-acridinyl) Maleimide Labelled CRP, Derivatised Cysteine and the Free Probe	214
6.2.2.4 Tetramethylrhodamine-5-Iodoacetamide Labelled CRP, Derivatised Cysteine and the Free Probe	215
6.2.2.5 5-iodoacetamidofluorescein Labelled CRP, Derivatised Cysteine and the Free Probe	217
6.2.2.6 4-chloro-7-nitrobenz-2-oxa-1,3-diazole Labelled CRP, Derivatised Cysteine and the Free Probe	218
6.2.2.7 Protoporphyrin IX Labelled CRP and Derivatised Cysteine	219
6.2.2.8 Bilirubin Labelled CRP and Derivatised Cysteine	220
6.2.2.9 N-(1-Pyrene) Maleimide Labelled CRP, Derivatised Cysteine and the Free Probe	222
6.2.2.10 Dilithium-4-amino-N-(3-(vinylsulphonyl) phenyl naphthalimide-3,6-disulphonate Labelled CRP and Derivatised Cysteine	223
6.2.2.11 N-(7-dimethylamino-4-methylcoumarinyl) Maleimide Labelled CRP, Derivatised Cysteine and the Free Probe	224
6.2.2.12 Maleimidyl Benzoate Ester of Benz(c,d)indol-2(1H)-one Labelled CRP, Derivatised Cysteine and the Free Probe	225
6.2.2.13 N-(1-Anilidonaphthyl-4) Maleimide Labelled CRP, Derivatised Cysteine and the Free Probe	227
6.2.2.14 2-(4'-iodoacetamidoanilino)naphthalene-6-sulphonate Labelled CRP, Derivatised Cysteine and the Free Probe	229
6.2.2.15 N-(Iodoacetyl aminoethyl)-1-naphthylamine-8-sulphonic acid Labelled CRP, Derivatised Cysteine and the Free Probe	230
6.2.2.16 6-acryloyl-2-dimethylaminonaphthalene Labelled CRP and Derivatised Cysteine	232

	<u>PAGE</u>
6.2.3 Discussion of the Performance of the Various Fluorophores Utilised	234
6.3 Correlation of the Polarity of the Hydrophobic Pocket of CRP, with a Range of Organic Solvents Possessing Different Polarities	247
6.3.1 Experimental Procedure	247
6.3.2 Results	248
6.3.3 Conclusion	248
6.4 Determination of the Effect of cAMP on the Ability of CRP to Undergo Thiol Modification	249
6.4.1 Experimental Procedure	249
6.4.2 Results	251
6.4.3 Conclusion	251
6.5 Investigation of the Nature of the CRP-Probe Conjugate	251
6.5.1 Determination of the Stoichiometry of the Labelling of CRP Via Thiol Modification	252
6.5.1.1 Experimental Procedure	252
6.5.1.2 Results	252
6.5.2 Determination of the Specificity of the Labelling of CRP Via Thiol Groups	253
6.5.2.1 Experimental Procedure	254
6.5.2.2 Results	255
6.5.3 Conclusion	255
6.5.4 Discussion	256
6.6 Investigation of the Interaction of cAMP with the cAMP Binding Site of CRP and R <sub>II</sub>	259
6.6.1 cABS and R <sub>II</sub> Assay	260
6.6.1.1 Experimental Procedure	260
6.6.1.2 Results	260
6.6.2 cAMP Binding Assay of Unlabelled cABS and R <sub>II</sub>	261
6.6.2.1 Experimental Procedure	261
6.6.2.2 Results	262
6.6.3 Conclusion	263
6.7 Investigation of the Nature of the Protein-Probe Conjugates	264
6.7.1 Determination of the Stoichiometry of Labelling	264
6.7.1.1 Calculation of the Molar Extinction Coefficient of cABS	264

	<u>PAGE</u>
6.7.1.2 Calculation of the Stoichiometry of the Labelling of cABS Via Thiol Modification	265
6.7.2 Determination of the Specificity of Labelling	266
6.7.2.1 Experimental Procedure	266
6.7.2.2 Results	266
6.7.3 Conclusion	267
6.8 Determination of the Effect of Thiol Modification of cABS and $R_{II}$ on the Capacity for cAMP Binding	267
6.8.1 Experimental Procedure	267
6.8.2 Results	267
6.8.3 Conclusion	268
6.9 Determination of the Ability of cAMP Bound cABS and $R_{II}$ to Undergo Thiol Modification	268
6.9.1 Experimental Procedure	268
6.9.2 Results	269
6.9.3 Discussion	269
6.10 Ideas for Further Work	270
6.11 Summary	274
6.12 References	

## ACKNOWLEDGEMENTS

I would like to express my appreciation to the following:-

Prof. R. Stephen Davidson for his guidance, encouragement and for proof-reading the individual chapters.

Past and present organic photochemists at the City University for their friendship, and especially: Jeff Abrahams, Nergis Arsu, Richard Bowser, Grant Bradley, Eleanor Cockburn, Stephen Collins, Paul Crick, Phil Duncanson, Niaz Khan, Paul Kidd, Sandy Lewis, Dr. Trish Moran, Audrey O'Donnell, Adrian Taylor, Shaun Tranter, Yulin Xue, Dr. Graham Yearwood, for creating such a pleasant environment.

Anthony 'Spud' Murphy for elemental analyses, and for weighing minuscule quantities of fluorescent compounds.

Dr. Martin Hilchenbach for collaboration, and for the fluorescence lifetime measurements.

Dr. Ken Murray of SmithKline Beecham Pharmaceuticals, for his guidance, and for proof-reading Chapter 3.

Dr. Geoff Barnard for reading the manuscript, and for his helpful comments and suggestions.

The SERC for a maintenance grant.

SmithKline Beecham Pharmaceuticals for co-sponsorship, allowing me to conduct certain experiments at their laboratories, and for funds to attend the XIIIth IUPAC Symposium on Photochemistry at The University of Warwick, July, 1990.

DECLARATION

I grant powers of discretion to the University Librarian to allow this thesis to be copied, in whole or in part, without further reference to me. This permission covers only single copies made for study purposes, subject to normal conditions of acknowledgement.

D. Chappell

## ABSTRACT

A range of fluorescent probes were utilised for the fluorescent modification, via both amine and thiol groups, of a protein that binds cAMP. The protein concerned, called cAMP Receptor Protein, undergoes a conformational change on cAMP binding, and as a consequence, the microenvironment of the probe is altered with regard to polarity. The probes were then screened in order to ascertain the degree of sensitivity to the polarity of their environment. This property was monitored via alterations in the fluorescence characteristics of the probe, particularly fluorescence enhancement and/or shifts in peak emission. The most suitable probes may then be applied to a protein that binds cGMP, and the alteration in the fluorescence characteristics induced in the probe via cGMP binding, may then be utilised in order to determine the intracellular cGMP concentration within the intact cell.

DEDICATED TO

MUM AND DAD

WITH LOVE

CHAPTER 1.

GENERAL INTRODUCTION.

1.1. FUNDAMENTALS OF PHOTOCHEMISTRY.

When single atomic orbitals on each of two adjacent atoms are combined, two molecular orbitals are produced; one of lower energy (called the highest occupied molecular orbital (HOMO) or the bonding orbital), and one of higher energy (called the lowest unoccupied molecular orbital (LUMO) or the antibonding orbital).

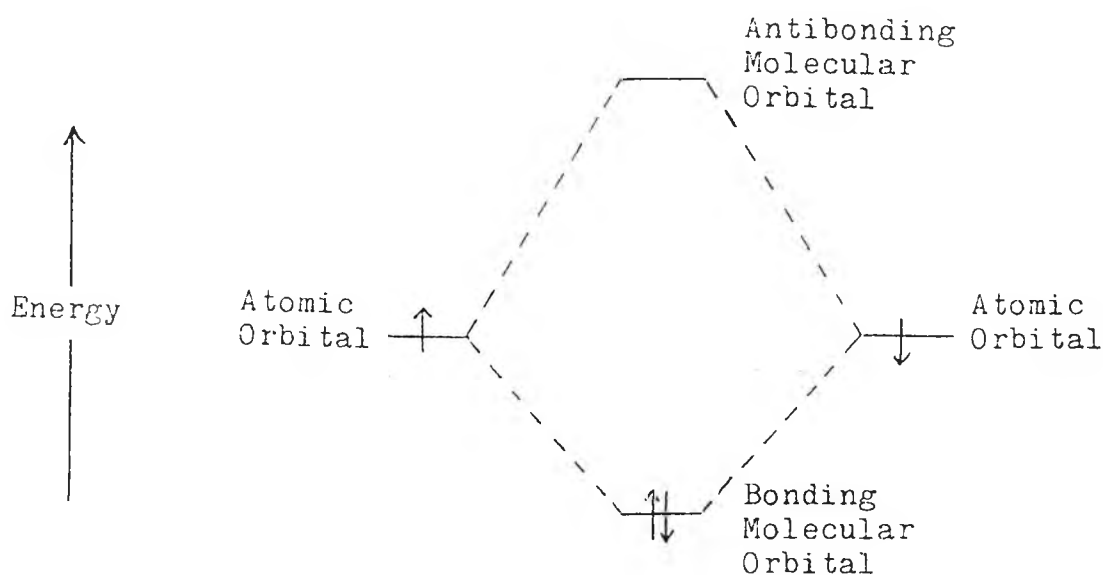


Fig. 1.1. A molecular orbital diagram for a two-electron bond between the atoms.

In a typical two-electron bond between the atoms, both electrons will normally occupy the bonding orbital.

In addition to its wave-like properties, light may be considered to be composed of discrete units called quanta or photons. Each photon possesses a quantity of energy (E) given by the relationship:

$$E = h\nu$$

where  $h$  = Planck's constant =  $6.63 \times 10^{-34}$  Joule second, and  $\nu$  = frequency of the light. On electronic excitation, for example by a photon, an electron from the bonding orbital may be promoted to the antibonding orbital. This process produces an electronically excited state.

Completely symmetrical orbitals about the inter-nuclear axis, are called sigma ( $\sigma$ ) or sigma-star ( $\sigma^*$ ) orbitals, according to whether they are bonding or antibonding respectively. Orbitals that are anti-symmetrical about the inter-nuclear axis are called pi ( $\pi$ ) or pi-star ( $\pi^*$ ) orbitals. A third type of orbital is denoted as an n-orbital. These orbitals are non-bonding, and a 'lone pair' of electrons on a particular atom, may be envisaged as occupying this orbital.

#### 1.1.1. Electronically Excited States.

Absorption of a photon by an organic molecule, occurs in an extremely short period of time (approximately  $10^{-15}$  sec.), and it is assumed, therefore, that the positions of the nuclei within the molecule do not change during this period. This is known as the Franck-Condon Principle, and therefore the major change is in the electronic structure; to produce an electronically excited state. This state is a distinct molecular species, whose electrons are arranged in a way that is not the lowest energy configuration. Electrons present in the bonding  $\pi$  or n-orbitals, may be promoted to the antibonding  $\pi^*$  or  $\sigma^*$  orbitals, depending upon the wavelength of the exciting radiation. The electronically

excited state has a finite lifetime, and possesses physical and chemical properties that differ from those of the natural or ground state.

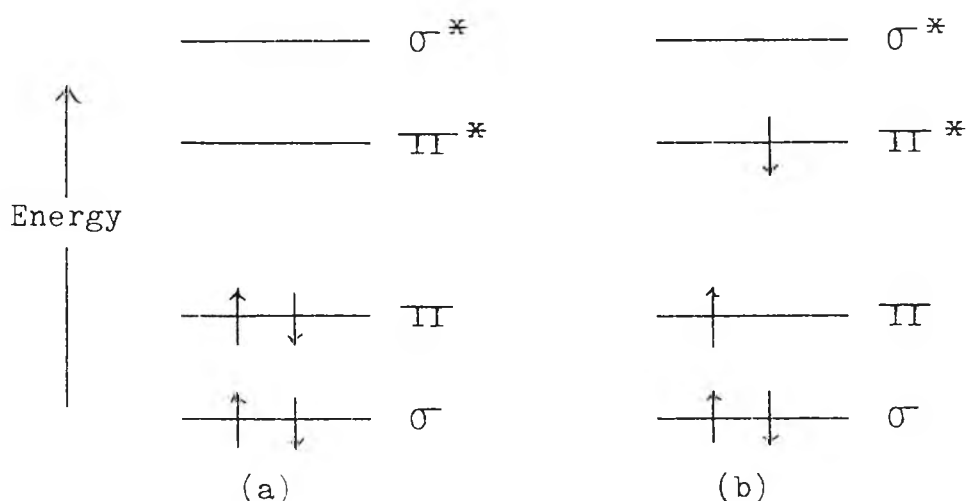


Fig. 1.2. The electronic configuration of an alkene, showing the occupancy of the carbon-carbon bond orbitals: (a) in the ground state; and (b) in the ( $\pi, \pi^*$ ) excited singlet state, after absorption of a photon of wavelength approximately 180 nm.

For excitation wavelengths in excess of 200 nm, three general classes of electronically excited states may be considered. These are ( $n, \pi^*$ ), ( $\pi, \pi^*$ ) and ( $n, \sigma^*$ ) arising from  $n \rightarrow \pi^*$ ,  $\pi \rightarrow \pi^*$  and  $n \rightarrow \sigma^*$  transitions respectively.

At a particular wavelength, the bulk absorption properties of the molecule may be represented by the Beer-Lambert law. This states that the absorbance (D), which equals the base-10 logarithm of the ratio of incident light intensity ( $I_0$ ) to transmitted light intensity (I), is directly proportional to the concentration (c) of the

compound, and the pathlength (l) of the radiation through the sample. The proportionality constant ( $\epsilon$ ) is called the absorption coefficient, or more specifically, the molar extinction coefficient with units of litre mol<sup>-1</sup> cm<sup>-1</sup>, if concentration is in mol litre<sup>-1</sup>, and the pathlength is in cm.

$$\log_{10} (I_0/I) = D = \epsilon c l.$$

Generally,  $\pi \rightarrow \pi^*$  transitions, which may occur on excitation of alkenes, exhibit molar extinction coefficients of  $5 \times 10^3$  to  $1 \times 10^5$  litre mol<sup>-1</sup> cm<sup>-1</sup>.  $n \rightarrow \sigma^*$  transitions, which generally occur in saturated molecules, show  $\epsilon$  values of  $1 \times 10^2$  to  $1 \times 10^3$  litre mol<sup>-1</sup> cm<sup>-1</sup>; whilst  $n \rightarrow \pi^*$  transitions, which may occur on excitation of ketones, exhibit the lowest values of  $\epsilon$  ranging from 1 to  $4 \times 10^2$  litre mol<sup>-1</sup> cm<sup>-1</sup>.

Electronically excited states can also be produced by electrical discharge, ionising radiation (for example,  $\alpha$  and  $\beta$  particles as well as  $\gamma$  radiation), extreme temperatures, electron transfer reactions, the decomposition of peroxide compounds, and by chemical activation (for example, via chemiluminescence (1,2)).

### 1.1.2. Excited Singlet and Triplet States.

Each orbital within a molecule possesses a definite energy and angular momentum, due to the movement of the electrons around the nuclei. Additionally, electrons rotate about their axes and, therefore, they themselves have a spin

angular momentum, which is assigned the value of  $\frac{1}{2}$  unit per electron. In the ground state, The Pauli Exclusion Principle limits the number of electrons in a non-degenerative molecular orbital to two, such that the net spin is zero (one electron =  $+\frac{1}{2}$  and the other =  $-\frac{1}{2}$ ). The multiplicity is given by  $2S + 1$ , where  $S$  is the total spin angular momentum. Since, in this case,  $S = 0$  then the multiplicity equates to 1. This is therefore referred to as a 'singlet' state, and it is likely that the singlet status will be retained upon production of the electronically excited state, by direct absorption of a photon.

However, upon excitation, the promotion of one electron into an antibonding molecular orbital, means that The Pauli Exclusion Principle no longer applies. It is now possible for an electron to undergo spin inversion. The total spin angular momentum becomes 1, giving a multiplicity of 3. The excited molecule is therefore referred to as a 'triplet' state.

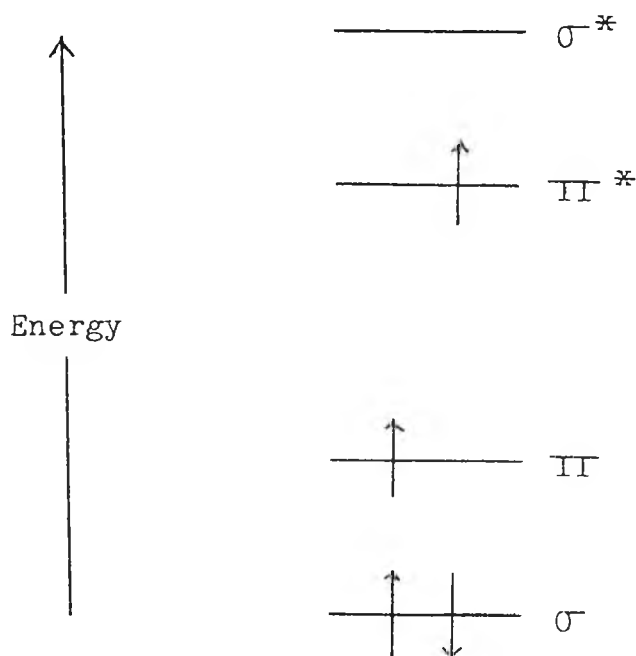


Fig. 1.3. The electronic configuration of the ( $\pi, \pi^*$ ) triplet state of an alkene.

The triplet state, which is not readily produced by direct absorption of a photon, is of a lower energy with regard to the singlet state, because of the repulsive nature of interactions between electrons of the same spin.

The difference in energy between singlet and triplet excited states, is considerably smaller for (  $n, \overline{\text{II}}^*$  ) states than for (  $\overline{\text{II}}, \overline{\text{II}}^*$  ) states. The elucidation of the energy of an excited state is useful in order to deduce the feasibility of a particular transformation.

An excited state has a characteristic lifetime under given conditions of solvent, concentration of substrate, temperature and of other species in the solution. These lifetimes are short, varying from less than  $10^{-12}$  sec. for some of the shortest-lived singlet states, to more than 10 sec. at liquid nitrogen temperature ( $-80^\circ\text{C}$ ) for some of the longest-lived triplet states. The lifetime is defined as the reciprocal of the sum of all the first-order (or pseudo-first-order) rate constants for processes that the excited state undergoes, and the enormous range of lifetimes (more than thirteen orders of magnitude), encompasses the wide variety of photochemical and photophysical processes that can occur for an excited state.

### 1.1.3. Fluorescence.

In the absence of interaction with another chemical species, an electronically excited state may undergo one of two transformations; it may either change into a different compound, or it may change into a different electronic state

of the same compound. The first of these events is a photochemical reaction, and the second (which is more pertinent to the present discussion) is a photophysical process.

Intramolecular photophysical processes may be subdivided into two groups; i) radiative (or luminescent) processes, in which a photon of ultra-violet or visible radiation is emitted, and ii) non-radiative processes, in which no such emission occurs. Luminescence is a commonly observed property of electronically excited states, and the energy of the emitted radiation is less than that of the exciting radiation. This is because energy is lost by conversion into rotational and vibrational motion, thus it is possible for visible light to be emitted as a consequence of ultra-violet excitation. The difference (in nm.) between the wavelength of fluorescent emission, and the excitation wavelength of a particular species is called the Stokes Shift (3). The emission of a photon by an excited singlet state, returns the latter to the ground state, which is also a singlet state. Such a process is 'spin-allowed' since there is no overall change of spin; and the luminescence produced is called fluorescence. The emission observed is most commonly that produced by decay of the singlet state, produced on excitation. This observation is due to the greater rate of non-radiative decay, from a higher excited singlet state to the lowest excited singlet state, than that of radiative decay to the ground state. As a consequence, the fluorescence spectrum is not affected by the excitation wavelength.

#### 1.1.4. Lifetime and Quantum Yield of Fluorescence.

Two useful fluorescence parameters are the lifetime and the quantum yield. The lifetime of fluorescence is measured directly by following the decay of fluorescence intensity with time, after interruption of the exciting radiation. Lifetime values are of use since they provide, in reciprocal form, the overall sum of rate constants for singlet state decay, which may be used to determine the individual rate constants for excited-state processes. Since the fluorescence lifetime is sensitive to environmental conditions (for example, solvent polarity), it may be employed to probe heterogeneous environments.

The quantum yield of fluorescence is a measure of the efficiency with which absorbed radiation, causes the molecule to undergo a specified change. It may be defined, thus:

$$\text{Quantum Yield for Fluorescence } (\phi_f) = \frac{\text{Number of Photons Emitted.}}{\text{Number of Photons Absorbed.}}$$

Quantum yield values normally fall in the range from 0 to 1.0, and it follows that the higher the value of the quantum yield, the greater the intensity of the fluorescence output.

#### 1.1.5. Phosphorescence.

Luminescence that originates from an excited triplet state, is called phosphorescence. Almost all phosphorescence is produced by decay of the lowest excited triplet state to the ground state. Since a change in spin multiplicity occurs,

phosphorescence is regarded as a 'spin forbidden' process, and consequently has a longer lifetime than does fluorescence. While fluorescence may be studied in a fluid medium at room temperature, phosphorescence must be investigated in a rigid, glass matrix at very low temperature, usually 77°K. These conditions are necessary since triplet states in solution at room temperature, are generally deactivated very rapidly in bimolecular processes with other molecular species.

#### 1.1.6. Non-Radiative Decay.

Non-radiative decay processes involve conversion of one electronic state into another, without emission of light. Like radiative processes, they may be divided into two categories according to whether or not there is an overall change in spin multiplicity, during the process. If there is no spin change, the non-radiative process is called internal conversion. By this process, higher excited singlet states decay to the lowest excited singlet state prior to any other photophysical process. Higher triplet states may also decay to the lowest triplet state, via internal conversion. Internal conversion may also occur from the lowest excited singlet state to the ground state, in direct competition with fluorescence. The rate of internal conversion, is related inversely to the energy difference between the initial and final states. Thus, the smaller the energy gap, the greater is the rate of internal conversion. The difference in energy between the ground state and the lowest excited singlet state, is always greater than that between the lowest excited singlet

state and the higher excited singlet states. As a consequence, fluorescence usually prevails over the much slower non-radiative decay to the ground state, via internal conversion.

When non-radiative decay involves a change in spin multiplicity, it is called intersystem crossing. There are two important intersystem crossing processes, which may be considered when dealing with organic molecules. The first of these, is the non-radiative decay which is in competition with the phosphorescent decay of the lowest triplet state, to the ground state. The second, is the process whereby the lowest excited singlet state may be converted into the lowest excited triplet state. Therefore, this process is in competition with both the internal conversion from the lowest excited singlet state, and with fluorescence, and it allows the production of many triplet states via the absorption of a photon to produce the excited singlet state, followed by intersystem crossing to the triplet state.

#### 1.1.7. The Jablonski Diagram.

These diverse processes may be represented schematically by the use of a Jablonski Diagram (4). In the left-hand portion of the diagram are the singlet states of the molecule, namely the ground state ( $S_0$ ) and the excited singlet states ( $S_1$ ,  $S_2$  etc.), on a vertical scale of increasing energy. In the right-hand portion, are the triplet states ( $T_1$ ,  $T_2$  etc.) in order of increasing energy. Each bold horizontal line represents a different electronic state of the molecule.

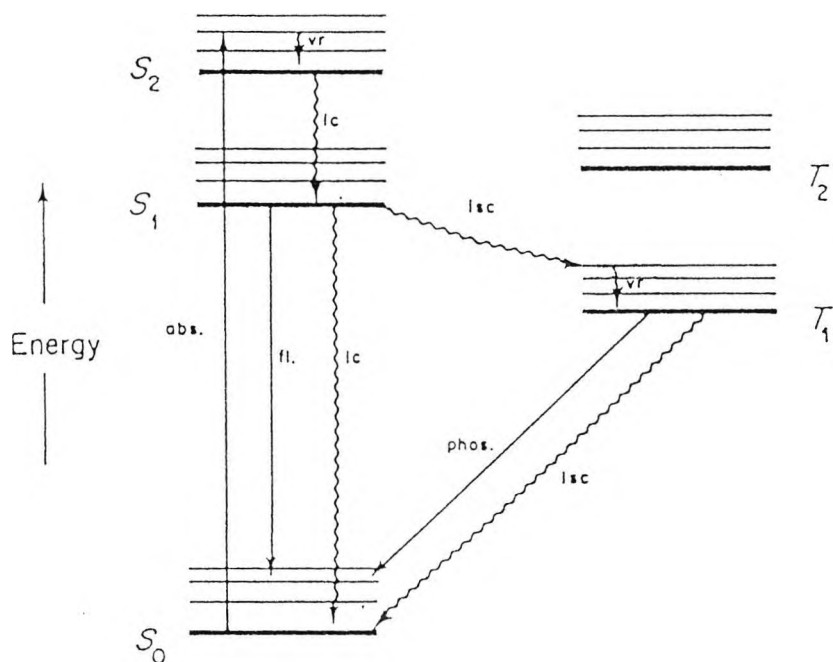


Fig. 1.4. The Jablonski Diagram.

The electronic states may have varying amounts of vibrational energy, and this is indicated by the series of lighter horizontal lines ('vibrational levels') for each state. Photophysical processes are represented by lines connecting the states. Straight lines are used for radiative processes: vertically upwards for absorption (abs), vertically downwards for fluorescence (fl), and downwards at an angle for phosphorescence (phos), to indicate that it involves a change of multiplicity. Wavy lines represent radiationless transitions: vertically downwards for internal conversion (ic), or for vibrational relaxation (vr) within a particular state, and at an angle for intersystem crossing (isc).

## 1.2. FLUORESCENT PROBES.

A chemical species which, when suitably excited, displays fluorescent emission is called a fluorescent probe or fluorophore. Almost all fluorophores of practical use for biochemical investigations, are derivatives of aromatic compounds, usually possessing one to five conjugated rings. Possible exceptions with regard to aromaticity, include some rare-earth chelates and certain polyenes, such as parinaric acid and retinol. The usual range of useful spectral absorption and emission for extrinsic fluorescent probes, is from 300 nm to approximately 650 nm.

The ultimate intensity detected by the fluorescence spectrophotometer, is an important consideration for many applications of fluorescence studies. Two factors affect this intensity; these are the molar extinction coefficient at the excitation wavelength and the quantum yield of fluorescence. Both properties are innate to the conjugated fluorophores at a particular light intensity, and it is essentially the product of these two factors that determines the ultimate sensitivity obtainable.

Generally, chromophores with extended conjugation and resonance, have more allowed transitions and higher extinction coefficients for their longest wavelength absorptions. Compounds with one or two aromatic rings have low absorptivity (under  $10^4$  litre mol<sup>-1</sup> cm<sup>-1</sup>), while fluorophores with several rings and especially those with two equivalent resonance forms, such as rhodamines and symmetrical carbocyanines, can have extinction coefficients up to  $2 \times 10^5$

litre mol<sup>-1</sup> cm<sup>-1</sup>, although values of  $1 \times 10^4$  to  $5 \times 10^4$  litre mol<sup>-1</sup> cm<sup>-1</sup> are more common. The vast majority of organic compounds has a quantum yield of less than 0.01, and are therefore useless as extrinsic fluorescent probes.

### 1.2.1. Fluorescent Calcium Probes and Their Use.

Absolutely critical to the fuller understanding of the role of any intracellular molecule, such as a second messenger, is the ability to monitor its free concentration in the cytosol of living cells. Rapid advances in our understanding of the role of calcium, followed the introduction of cell penetrant fluorescent indicators that report the intracellular free-calcium concentration.

Such an indicator is 1,2-bis(o-aminophenoxy)ethane-N,N,N',N'-tetra-acetic acid, (BAPTA) (5).

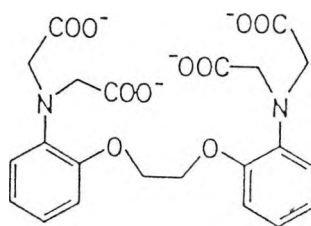


Fig. 1.5. The Molecular Structure of 1,2-bis(o-aminophenoxy)ethane-N,N,N',N'-tetra-acetic acid, (BAPTA).

In the absence of Ca<sup>2+</sup>, the absorption spectrum shows a maximum at 254 nm ( $\epsilon = 1.6 \times 10^4$  litre mol<sup>-1</sup> cm<sup>-1</sup>), with a

shoulder at 287 nm ( $\epsilon = 5.6 \times 10^3$  litre mol<sup>-1</sup> cm<sup>-1</sup>). Ca<sup>2+</sup> binding causes a major hypsochromic (blue) shift, toward a limiting spectrum having a small maximum at 274 nm ( $\epsilon = 4.2 \times 10^3$  litre mol<sup>-1</sup> cm<sup>-1</sup>), and the main peak at 203 nm ( $\epsilon = 4.1 \times 10^4$  litre mol<sup>-1</sup> cm<sup>-1</sup>). The stoichiometry of Ca<sup>2+</sup> binding was found to be 1 : 1.

The fluorescence emission spectrum of BAPTA, shows a peak at 363 nm with no fine structure. Binding of Ca<sup>2+</sup> reduces the emission intensity by a factor of 2.8, without significantly altering the shape of the band or the wavelength of its peak.

The cation affinity of BAPTA can be tuned up or down by appropriate electron-donating or withdrawing substituents. Thus, substitution of methyl groups at the 4-carbon positions, strengthens calcium binding. Substitution of bromine atoms at the same positions, weakens calcium binding, and consequently reduces the quantum yield of fluorescence.

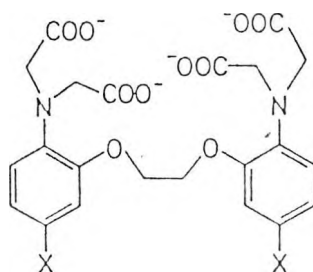


Fig. 1.6. The Molecular Structure of BAPTA indicating the 4-carbon positions (marked by 'X'). Substitution of methyl (electron-donating) groups, strengthens calcium binding. Substitution of bromine (electron-withdrawing) atoms, weakens calcium binding (5).

The binding affinity for  $\text{Ca}^{2+}$ , may be further modified by replacing one of the ether oxygens by an  $\text{sp}^2$  hybridised heterocyclic nitrogen atom, to produce a substituted quinoline.

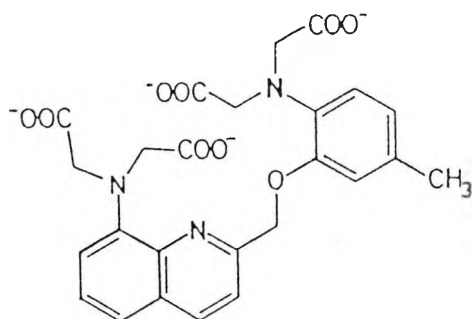


Fig. 1.7. The molecular Structure of a Substituted Quinoline.

Since such nitrogen atoms are considerably more basic than the ether oxygen atoms, it follows that this modification increases the affinity of the indicator for  $\text{Ca}^{2+}$ . The quantum yield of fluorescence of the indicator is increased approximately five-fold (from approximately 0.012 to 0.057), on binding  $\text{Ca}^{2+}$ . The increased size and conjugation of the chromophore, shifts the wavelengths of absorption and fluorescence to 350 nm and 520 nm respectively. This molecule also chelates  $\text{Mg}^{2+}$  to an appreciable extent, but the quantum efficiency is only minimally increased.

If a methoxy group is introduced meta to the 8-amino group, the resulting molecule possesses an emission maximum at 510 nm and a quantum yield of approximately 0.029; some  $2\frac{1}{2}$  times higher than the quinoline devoid of the methoxy group.

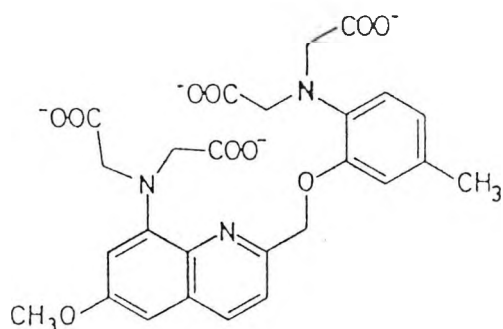


Fig. 1.8. The Molecular Structure of a Substituted Quinoline exhibiting a methoxy group, meta to the 8-amino group.

Again,  $\text{Ca}^{2+}$  binding causes a very slight shift of emission to approximately 525 nm, and a five-fold enhancement of quantum yield to 0.14.

BAPTA and its derivatives are of use for the elucidation of calcium levels in vitro. However, they are not suitable for determining the intracellular calcium concentration, due to their high intrinsic polarity, which would prevent passage across the cell membrane. Micro-injection of these indicators directly into the cell is not practicable, due to the perturbation of the cell membrane which invariably ensues.

A means of allowing transport of the indicator across the cell membrane, is by the use of esterified indicators. BAPTA, possessing a methyl group at one of the 4-carbon positions is known as Quin-2 (6), and this indicator may be esterified to produce the acetoxymethyl tetra-ester of Quin-2.

Cells (for example, thymocytes), usually in suspension, are incubated with the ester for periods ranging from a few

minutes to two hours. The acetoxymethyl tetra-ester of Quin-2 traverses the cell membrane and is cleaved by endogenous esterases to the Quin-2 indicator; which is now trapped.

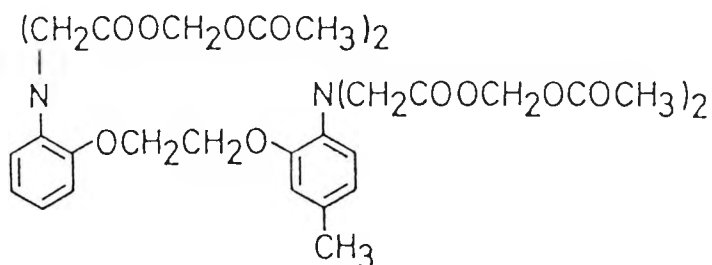


Fig. 1.9. The Molecular Structure of the Acetoxymethyl tetra-ester of Quin-2 (6).

The simplest esters (methyl or ethyl) of this chelator are not hydrolysed in mouse thymocytes. Trimethylsilyl esters are too rapidly hydrolysed extracellularly, while *t*-butyldimethylsilyl esters are potentially cytolytic. Anhydrides, imidazolides or activated aryl esters were not considered, because the end products would probably include chelator molecules irreversibly bound to intracellular nucleophiles. Use of this probe, has shown that the intracellular concentration of  $\text{Ca}^{2+}$ , in the resting mouse thymocyte, is  $123 \pm 6$  nM. The available evidence shows that the dye is distributed throughout the cytosol and nucleus, but does not enter mitochondria, lysosomes, endoplasmic reticulum or secretory granules. The cells are then washed and loaded into a cuvette in a conventional fluorescence spectrophotometer, and their fluorescence is monitored during the experimental manipulations under investigation.

Cells, such as lymphocytes (7), erythrocytes (8) and macrophages (9), in which intracellular calcium levels have been reduced below the normal resting level by loading with large quantities of chelator, in the absence of external  $\text{Ca}^{2+}$ , seen to have an abnormally high  $\text{Ca}^{2+}$  permeability dependent upon their lowered intracellular calcium concentration ( $[\text{Ca}^{2+}]_i$ ). This conclusion was reached after it was observed that when the external  $\text{Ca}^{2+}$  concentration ( $[\text{Ca}^{2+}]_o$ ) is restored to normal,  $[\text{Ca}^{2+}]_i$  rises to a near-normal level remarkably quickly. A  $\text{Ca}^{2+}$ -leak induced by low  $[\text{Ca}^{2+}]_i$  could be a valuable negative-feedback mechanism for regulating resting  $[\text{Ca}^{2+}]_i$ , and also helps explain why increasing the chelator loading, does not lower the measured resting  $[\text{Ca}^{2+}]_i$  provided the loading is performed with normal  $[\text{Ca}^{2+}]_o$  present (10,11,12,13).

In the human erythrocyte, it has been shown (8) that the  $\text{Ca}^{2+}$  pump rate is proportional to the square of  $[\text{Ca}^{2+}]_i$ , at least up to normal resting  $[\text{Ca}^{2+}]_i$ . In thymocytes (14) and neutrophils (15,16), it has been found that the tumour promoter 12-0-tetradecanoyl-phorbol-13-acetate (TPA), could lower  $[\text{Ca}^{2+}]_i$ . The BAPTA family of  $\text{Ca}^{2+}$  indicators have provided confirmation of  $[\text{Ca}^{2+}]_i$  rises, associated with lymphocyte mitogen stimulation (14,17), neutrophil (18,19) and platelet (12,20) activation, glycolytic activation of pancreatic insulinoma cells (21),  $\alpha$ -adrenergic stimulation of hepatocytes (22) and depolarisation of pheochromocytoma cells (13), synaptosomes (13) and adrenal medullary cells (11).

It is possible to assess the relative contributions of

extracellular calcium versus intracellular stores in generating a rise in  $[Ca^{2+}]_i$ . This may be done by comparing the  $[Ca^{2+}]_i$  rise in normal medium with that observed when external  $Ca^{2+}$  is absent, or chelated with ethylene-glycol-bis-( $\beta$ -aminoethylether)-N,N,N',N'-tetra-acetic acid (EGTA). The EGTA should not be added until just before the stimulus, so that internal stores have no time to be depleted. In some systems, such as  $K^+$  depolarised neurosecretory cells (11, 13,23) and lectin stimulated thymocytes (14), the  $[Ca^{2+}]_i$  rise is completely dependent upon  $[Ca^{2+}]_o$ . However, in B-lymphocytes (10), neutrophils (18,19) and platelets (12), stimulated with anti-immunoglobulin, f-Met-Leu-Phe and thrombin respectively, removal of  $[Ca^{2+}]_o$  reduces, but does not eliminate,  $[Ca^{2+}]_i$  rises, showing a significant contribution from internal stores. An example of  $[Ca^{2+}]_i$  increases dependent only on internal stores not on  $[Ca^{2+}]_o$ , seems to be in hepatocytes stimulated with glycogenolytic hormones (22).

In zero  $[Ca^{2+}]_o$ , addition of calcium ionophores should release nearly all calcium that was actively accumulated inside membrane enclosed organelles (7,10). It has been found that after ionophore pre-treatment, other stimuli cannot release any further internal  $Ca^{2+}$  stores (10,12,18). This implies that the releasable  $Ca^{2+}$  was actively sequestered in membrane-enclosed organelles, and provides evidence that the releasable pool includes calcium complexed with components of the cytosol, or bound to the cytosolic surface of cell membranes.

A comparison has been made between the  $[Ca^{2+}]_i$  within blood platelets reported by Quin-2, and the photoprotein aequorin (24). Aequorin is a  $Ca^{2+}$ -sensitive photoprotein of 20000 daltons, obtained from the photocytes of the jelly-fish *Aequorea aequorea*. A procedure has been developed, whereby aequorin may be incorporated within vascular smooth muscle cells, without the use of microinjection (25). This technique was adapted to effect the loading of aequorin into blood platelets.

No platelet abnormalities were detected after aequorin incorporation, and the resting  $[Ca^{2+}]_i$  was found to be 2-4  $\mu M$ , in media containing 1 mM  $Ca^{2+}$ . Quin-2 reported a resting  $[Ca^{2+}]_i$  of less than 1  $\mu M$ . This discrepancy may be explained by the difference in the response to  $[Ca^{2+}]_i$  detected by the indicators.

Quin-2 elicits an essentially linear response to  $\log [Ca^{2+}]_i$  increments, and therefore requires large, diffuse changes in  $[Ca^{2+}]_i$  to provide signals. Aequorin furnishes a log luminescent response to  $\log [Ca^{2+}]_i$  increments, increasing as the 2.5 power of  $[Ca^{2+}]_i$ .

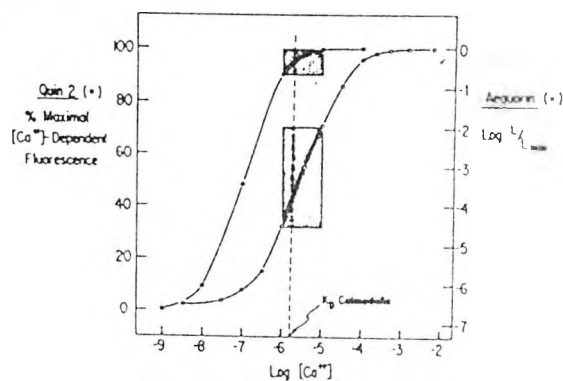


Fig. 1.10. Aequorin luminescence ( $\log L/L_{max}$ ) and Quin-2 fluorescence (% maximal  $Ca^{2+}$ -dependent fluorescence) at various  $[Ca^{2+}]_i$ . Shaded regions encompass the 1-10  $\mu M$   $Ca^{2+}$  range. In this region, aequorin is highly sensitive relative to Quin-2 (24).

This property allows the aequorin to produce intense signals, from even small zones of the cytosol exposed to local fluctuating  $[Ca^{2+}]_i$ . This indicates that calcium may be distributed heterogeneously throughout the blood platelet.

Quin-2 suffers from a number of disadvantages. Firstly, its preferred excitation wavelength of 339 nm, excites some auto-fluorescence from endogenous compounds, such as reduced pyridine nucleotides, and this could interfere with the fluorescence of Quin-2. Secondly, no investigations have been reported using the chelator trapping method on plants, fungi or bacteria. Some tissues, such as sea urchin eggs and frog muscle, which may only be manipulated at low temperatures, appear to load the indicator too slowly (26). Thirdly, the high affinity of Quin-2 for  $Ca^{2+}$  means that the dye is saturated at  $[Ca^{2+}]_i$ , in excess of 2  $\mu M$ . Finally, the main response of Quin-2 to  $Ca^{2+}$  is a change in fluorescence intensity, rather than a shift in fluorescence emission.

As a consequence, a new group of  $Ca^{2+}$  indicators was developed (27), offering improved fluorescence characteristics. The six compounds developed, (the so-called stil-, indo- and fura-series), combine an 8-coordinate tetracarboxylate-chelating site with stilbene chromophores, and offer up to 30-fold brighter fluorescence, slightly lower affinities for  $Ca^{2+}$ , slightly longer wavelengths of excitation, considerably improved selectivity for  $Ca^{2+}$  over other divalent cations, and major changes in wavelength, not just intensity, on  $Ca^{2+}$  binding.

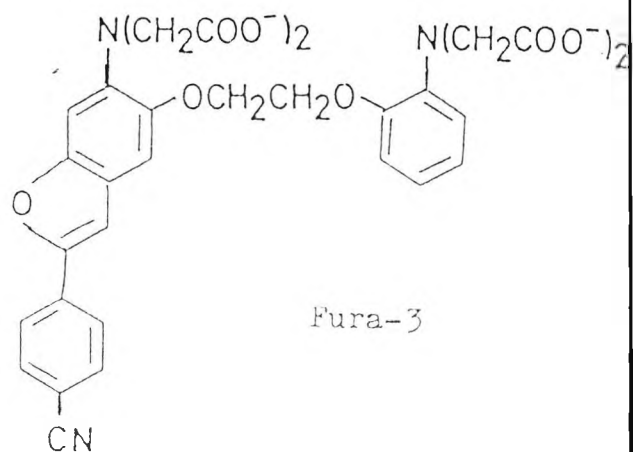
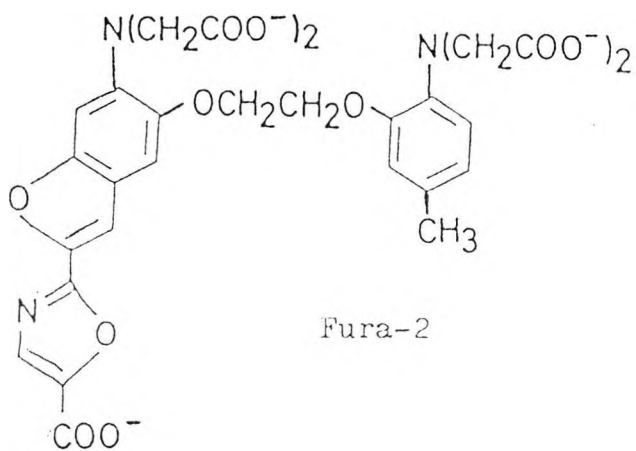
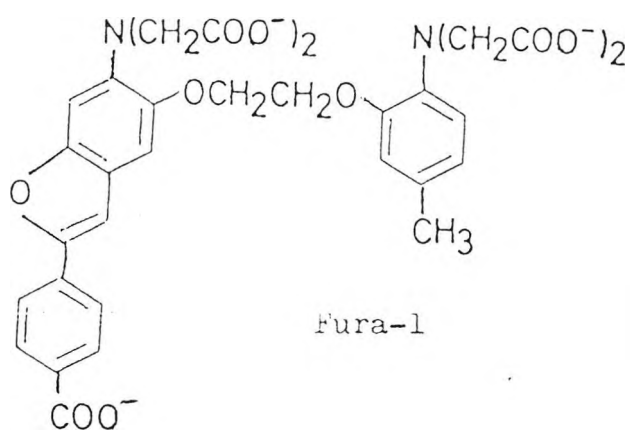
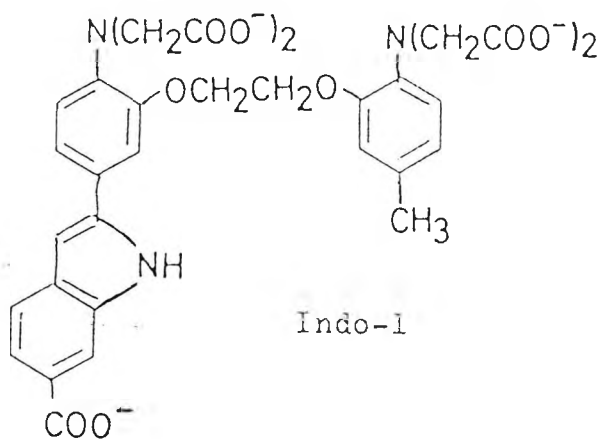
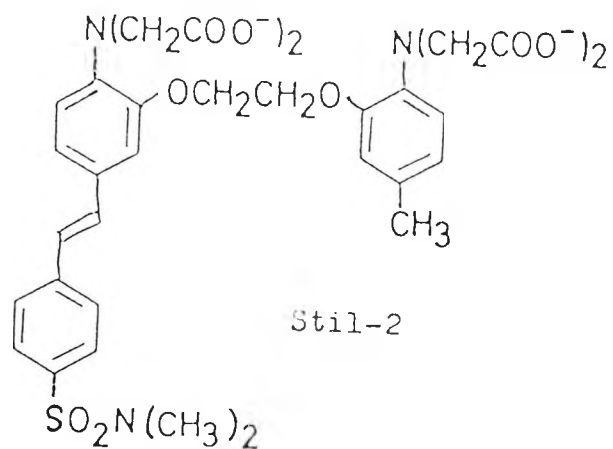
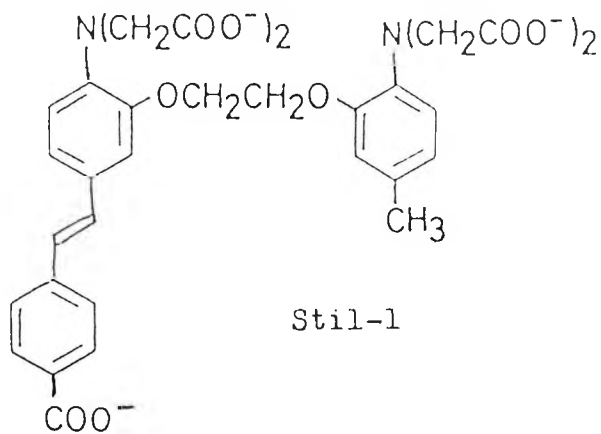


Fig. 1.11. The Molecular Structures of a range of fluorescent indicators of  $\text{Ca}^{2+}$ .

Dye	Absorption maxima		Emission maxima		Fluorescence quantum efficiency	
	Free anion	Ca complex	Free anion	Ca complex	Free anion	Ca complex
stil-1	362 (27)	329 (34)	537 (585)	529 (ND <sup>a</sup> )	0.14	ND
stil-2	352 (12)	326 (12)	564 (590)	560 (587)	0.11	0.15
indo-1	349 (34)	331 (34)	485 (482)	410 (398)	0.38	0.56
fura-1	350 (21)	334 (27)	534 (585)	522 (548)	0.14	0.20
fura-2	362 (27)	335 (33)	512 (518)	505 (510)	0.23	0.49
fura-3	370 (14)	343 (25)	564 (588)	551 (599)	0.13	0.21

Table 1.1. The properties of new fluorescent indicators of Ca<sup>2+</sup>. Absorption maxima refer to the dominant peaks at longest wavelength, measured at 22 ± 2<sup>o</sup>C in 100 mM KCl. The first number is the wavelength in nanometres, followed, in parentheses, by the corresponding extinction coefficient (x 10<sup>-3</sup> litre mol<sup>-1</sup> cm<sup>-1</sup>). ND = Not Determined (27).

Absorbance maxima are in the near ultra-violet, with extinction coefficients in the range 2 x 10<sup>4</sup> to 3 x 10<sup>4</sup> litre mol<sup>-1</sup> cm<sup>-1</sup>. The binding of Ca<sup>2+</sup> shifts all of the absorbance spectra to shorter wavelengths.

The stilbene derived dyes exhibit excitation and emission wavelengths only slightly longer than those of Quin-2. Nevertheless, whereas the response of Quin-2 to Ca<sup>2+</sup> falls off sharply between 339 nm and 350 nm, fura-2 shows considerable sensitivity to Ca<sup>2+</sup> at 350 nm and 380-385 nm. Since conventional fluorescence microscopes with glass optics, usually cut off at wavelengths between 340 nm and 350 nm, fura-2 is much easier to use. The hypsochromic shift in absorption and excitation spectra, upon binding Ca<sup>2+</sup>, is well documented (5). The twisting of the bond between the ring and the nitrogen atom, is brought about by the Ca<sup>2+</sup> present in the vicinity of the lone-pair of electrons, on the amino nitrogen atom. As a consequence, the conjugation between the

lone pair and the remainder of the chromophore is thereby disrupted.

Of the range of  $\text{Ca}^{2+}$  indicators, fura-2 appears to be the preferred dye, due to its high quantum yield of fluorescence, and its desirable absorption and emission wavelengths.

### 1.3. SOME KNOWN FUNCTIONS OF cGMP.

Following the success of the investigation into the role of calcium within the cell, attention was turned to another second messenger, namely guanosine 3',5'-cyclic monophosphate (cGMP).

It has been shown (28) that when smooth muscle (for example, rat thoracic aorta), is challenged with nor-epinephrine in the presence of either acetylcholine, histamine or the calcium ionophore A23187, endothelium derived relaxing factor is produced which stimulates the muscle guanylate cyclase. As a consequence, concentrations of cGMP were elevated forty-fold, (from 0.8 to 32 pmol per mg protein).



It was therefore concluded that cGMP mediates the relaxation of smooth muscle, when antagonised with nor-epinephrine.

cGMP has been found also to have a role in vertebrate vision (29). It acts as a phototransducer within the light sensitive region of the rod cell; the rod outer segment (ROS),



In darkness, the total concentration of cGMP in the outer segment is about 70  $\mu\text{M}$ , but the majority of this is bound, and effectively the free concentration is approximately 10  $\mu\text{M}$ . At this concentration, cGMP maintains the plasma membranes open, allowing the  $\text{Na}^+$  and  $\text{Ca}^{2+}$  ions to flood in, and depolarise the cell. The hydrolysis of cGMP in the light causes fewer channels to remain open, thus reducing the circulating current and thereby hyperpolarising the cell. A consequence of light induced closure of channels, is that the cytoplasmic calcium concentration declines as the  $\text{Ca}^{2+}$  extrusion mechanisms continue to operate.

These investigations have served to regenerate interest in the roles of cGMP as a second messenger. However, our knowledge of the cellular function of cGMP is considerably less than that of adenosine 3',5'-cyclic monophosphate (cAMP) for several reasons. Firstly, whereas cAMP elicits its effects via activation of cAMP-dependent protein kinase, cGMP, which in addition to activating its own protein kinase, may also bind to other intracellular proteins. These include two independent cyclic nucleotide phosphodiesterases (30). Secondly, although cGMP-dependent protein kinase is the major protein involved in cGMP action, very little is known about its substrates. Thirdly, whereas cAMP is used as a second messenger in a large number of tissues, cGMP is much less ubiquitous, being found in a few selected tissues, (for example, smooth muscle, brain and heart).

#### 1.4. THE OBJECTIVES OF THE PROJECT AND THE APPROACH ADOPTED.

Total intracellular levels of cGMP, have hitherto been determined via assay following tissue homogenisation. This is an unreliable means of quantification, and it is therefore desirable to produce a fluorescent indicator for cGMP. It is not presently known how to construct a small molecule which would have the required affinity and selectivity of binding to cGMP. It is therefore proposed to subvert the biological solution to this problem, by fluorescently modifying a protein which will bind cGMP.

The probe should ideally satisfy the following criteria:

- i) the label should exhibit a substantial Stokes Shift. This is important for any fluorochrome to be used in fluorescence microscopy, since we are using dichroic mirrors to separate the excitation light from the fluorescence;
- ii) the fluorescence quantum yield should be as near unity as possible, as we are likely to be visualising femtomoles of material with the naked eye. Thus green/yellow emission is ideal, since this is the region of the visible spectrum which is most sensitive to the eye;
- iii) the extinction coefficient of the fluorochrome at the excitation wavelength, should be high; this is because the optical pathlength for excitation is very short;
- iv) the fluorochromated protein should undergo a spectral shift on binding to cGMP.

From the experience gained using probes directed against  $\text{Ca}^{2+}$  ions, it is desirable to produce an indicator with a substantial spectral shift on either or both of excitation

and emission, and this criterion is the primary goal. Also, since the fluorophores will be visualised using standard fluorescence microscopy, we would like excitation and emission wavelengths in the visible part of the spectrum.

Thus, the approach adopted was to examine different ways of covalently labelling the protein with fluorescent derivatives, to produce a fluorescent peptide, which will exhibit substantial spectral changes when cGMP binds, thereby providing a fluorescent indicator of free cGMP concentration. After fluorescence derivatisation is complete, it is essential that protein-bound indicator is removed from the free indicator, since the emission characteristics of the latter may interfere with those of the former.

Owing to the ease of availability of cAMP Receptor Protein (CRP) isolated from *Escherichia coli*, this protein was utilised in the protein modification procedures. The most suitable fluorophores obtained may then be applied to a protein which interacts favourably with cGMP.

1.5. REFERENCES.

1. McCapra, F.  
(1966) Quart. Rev. Chem. Soc. 20 485
2. Schuster, G.B.  
(1979) Acc. Chem. Res. 12 366
3. Stokes, G.G.  
(1852) Phil. Trans. Roy. Soc. London 142 463
4. Jablonski, A.  
(1935) Z. Phys. 94 38
5. Tsien, R.Y.  
(1980) Biochemistry 19 2396
6. Tsien, R.Y.  
(1981) Nature 290 527
7. Tsien, R.Y., Pozzan, T. & Rink, T.J.  
(1982) J. Cell Biol. 94 325
8. Lew, V.L., Tsien, R.Y., Miner, C. & Bookchin, R.M.  
(1982) Nature 298 478
9. Kesteven, N.T.  
(1982) J. Physiol. (London) 332 119P
10. Pozzan, T., Arslan, P., Tsien, R.Y. & Rink, T.J.  
(1982) J. Cell Biol. 94 335
11. Knight, D.E. & Kesteven, N.T.  
(1983) Proc. Roy. Soc. London B218 177
12. Rink, T.J., Smith, S.W. & Tsien, R.Y.  
(1982) FEBS Letters 148 21
13. Meldolesi, J., Huttner, W.B., Tsien, R.Y. & Pozzan, T.  
(1984) Proc. Natl. Acad. Sci. USA 81 620
14. Tsien, R.Y., Pozzan, T. & Rink, T.J.  
(1982) Nature 295 68
15. Sha'afi, R.I., White, J.R., Molski, T.F.P., Shefcyk, J., Volpi, M., Naccache, P.H. & Feinstein, M.B.  
(1983) Biochem. Biophys. Res. Commun. 114 638

16. Lagast, H., Pozzan, T., Lew, P.D. & Waldvogel, F.A.  
(1983) Clin. Res. 31 410A
17. Hesketh, T.R., Smith, G.A., Moore, J.P., Taylor, M.V.  
& Metcalfe, J.C.  
(1983) J. Biol. Chem. 258 4876
18. Pozzan, T., Lew, D.P., Wollheim, C.B. & Tsien, R.Y.  
(1983) Science 221 1413
19. White, J.R., Naccache, P.H., Molski, T.F.P., Borgeat, P.  
& Sha'afi, R.I.  
(1983) Biochem. Biophys. Res. Commun. 113 44
20. Feinstein, M.B., Egan, J.J., Sha'afi, R.I. & White, J.  
(1983) Biochem. Biophys. Res. Commun. 113 598
21. Wollheim, C.B. & Pozzan, T.  
(1984) J. Biol. Chem. 259 2262
22. Charest, R., Blackmore, P.F., Berthon, B. & Exton, J.H.  
(1983) J. Biol. Chem. 258 8769
23. Gershengorn, M.C. & Thaw, C.  
(1983) Endocrinology 113 1522
24. Johnson, P.C., Ware, J.A., Cliveden, P.B., Smith, M.,  
Dvorak, A.M. & Salzman, E.W.  
(1985) J. Biol. Chem. 260 2069
25. Morgan, J.P. & Morgan, K.G.  
(1982) Pflugers Arch. 395 75
26. Tsien, R.Y.  
(1983) Ann. Rev. Biophys. Bioeng. 12 91
27. Gryniewicz, G., Poenie, M. & Tsien, R.Y.  
(1985) J. Biol. Chem. 260 3440
28. Furchgott, R.F.  
(1983) Circ. Res. 53 557
29. Lamb, T.D.  
(1986) Trends in Neurosciences 9 224
30. Hurwitz, R.L., Hansen, R.S., Harrison, S.A., Martins, T.J.,  
Mumby, M.C. & Beavo, J.A.  
(1984) Adv. Cyc. Nucl. Res. 16 89

CHAPTER 2.

FLUORESCENT PROBES AND THEIR USES.

## 2.1. INTRODUCTION.

In addition to the use of fluorophores for the deduction of the intracellular concentration of calcium, a plethora of probes have been utilised for the investigation of a wide range of scientific observations, and for the solution to specific problems.

It is frequently necessary to introduce fluorophores with experimentally advantageous fluorescence properties, when applying fluorescence techniques to biomolecules (for example, protein, nucleic acid, polysaccharide, cell membrane or related material). Those fluorescent probes for use in the modification of biomolecules, can be of two types:

i) the covalent fluorescent probes which form strong chemical bonds with specific atoms on the biomolecule, and usually are irreversibly bound; and ii) the non-covalent probes which form a reversible association with the biomolecule, by a combination of ionic, dipole-dipole and hydrophobic interactions. The two types of probe are complementary and each has advantages, limitations and specific applications to fluorescence studies.

## 2.2. THE MAJOR FACTORS TO BE CONSIDERED IN THE FLUORESCENT LABELLING OF BIOMOLECULES.

In the covalent modification of a biomolecule (for example, protein), it is important to select a fluorescent chromophore with spectral characteristics appropriate to the phenomenon under investigation, and the fluorescence technique employed. Two other major factors must be considered:

firstly, an investigation into the potentially reactive groups on the protein; and secondly, the use of a chemically reactive moiety, which is usually an integral part of the fluorescent probe.

### 2.2.1. The Reactive Sites on Proteins.

The reactive residues on proteins are predominantly nucleophiles, and consequently, their reactions with probes are mainly examples of nucleophilic substitution, or addition reactions. When low levels of probe are utilised, different nucleophilic moieties present on the protein, will compete for modification. 'Nucleophilicity' is a major factor when considering reaction rates. Since high nucleophilicity is partially determined by base strength, aliphatic amines, such as the epsilon-amino group of lysine in peptides, (pKa approximately 10), is rapidly modified by several reagents. However, other factors affect nucleophilicity, and the weaker base mercaptide (or thiolate) of cysteine, (pKa approximately 8), usually undergoes nucleophilic substitution faster than lysine.

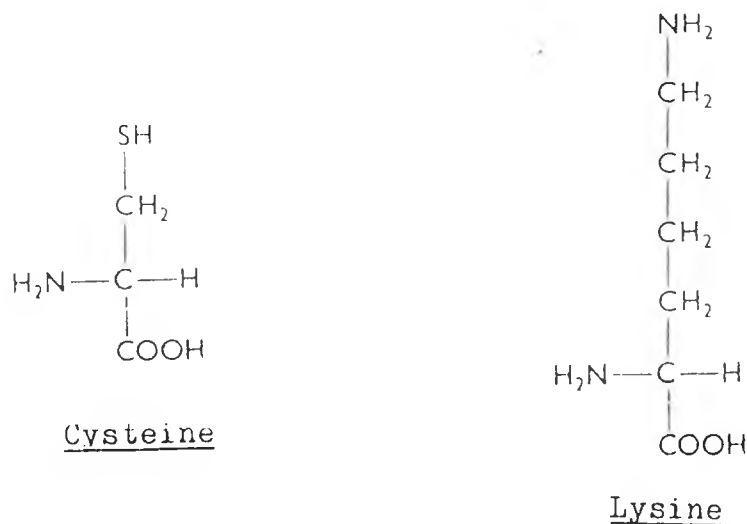


Fig. 2.1. The Molecular Structures of Cysteine and Lysine.

The pH of the reaction medium plays an important role, in dictating the reactivity of certain moieties on the protein. At pH 7, less than 1% of the lysine residues present in the protein, are in the form of unprotonated nucleophiles ( $R-NH_2$ ). Since the protonated lysines ( $R-NH_3^+$ ) are totally unreactive, the overall rate of modification is very slow at low pH. Due to the fact that the alpha-amino terminus of peptides is a much weaker base (pKa approximately 7), a significant proportion remains unprotonated, and the alpha-amino group can be selectively modified at physiological pH. As a result of the high intrinsic nucleophilicity of the mercaptide anion ( $RS^-$ ), cysteine is rapidly modified by many reagents. It remains fairly reactive in the acidic ( $R-SH$ ) state.

Reactions in which phenolic residues, such as tyrosine, are the nucleophiles, are also highly pH dependent and are most rapid above the phenol ionisation constant. One common amino acid whose rate of side-chain modification is not highly pH sensitive, is methionine.

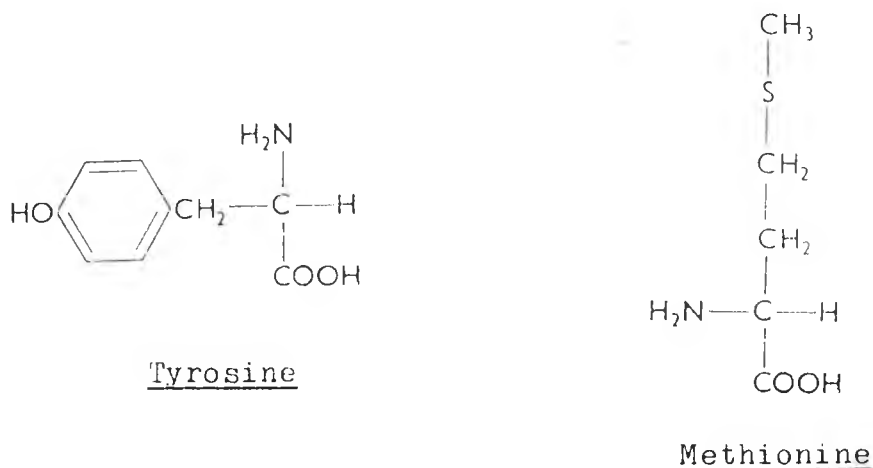


Fig. 2.2. The Molecular Structures of Tyrosine and Methionine.

Methionine alkylation has been achieved in proteins devoid of cysteine, using a relatively low pH to suppress reaction with other nucleophiles, to give specific modification of methionine.

The heterocyclic ring of histidine undergoes some reactions, usually as a relatively poor nucleophile below its pKa value of approximately 7. The guanidinium group of arginine remains protonated, and hence generally unreactive, up to pH 12 or 13; however it may undergo modification at more acidic pH, by the utilisation of specific reagents.

Due to the fact that most biochemical modification reactions are performed in aqueous solution, specific reaction of the weakly nucleophilic hydroxyl groups, present in serine or threonine, is impractical, owing to competitive reactions with water.

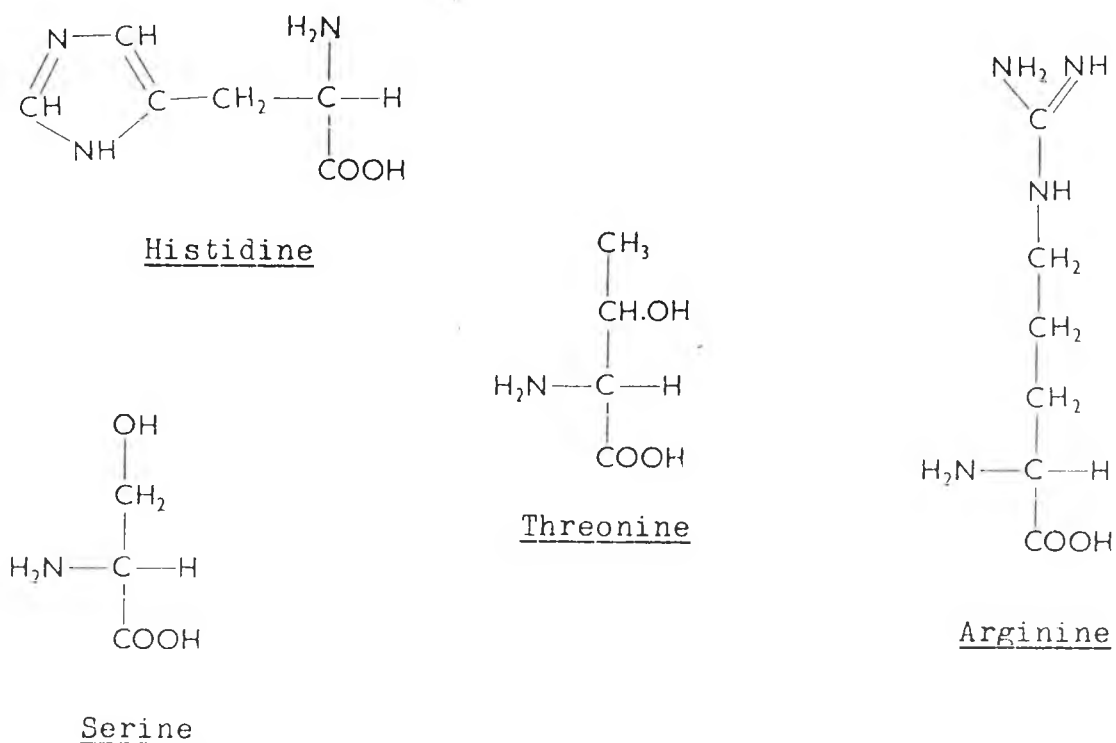
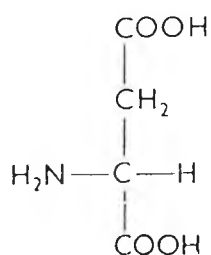
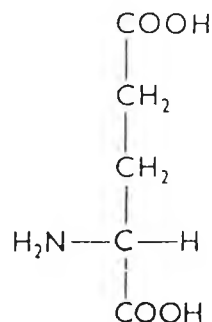


Fig. 2.3. The Molecular Structures of Histidine, Arginine, Serine and Threonine.

Modification of carboxyl groups present in aspartic acid and glutamic acid, usually requires reactions in which it functions as other than a nucleophile.



Aspartic Acid



Glutamic Acid

Fig. 2.4. The Molecular Structures of Aspartic Acid and Glutamic Acid.

### 2.2.2. The Reactive Moieties on Fluorescent Probes.

In the majority of cases, the chemically reactive group is an integral part of the fluorophore. These reactive moieties are predominantly electron-deficient groups, that interact with the electron-rich nucleophiles on the biomolecule. Since we need to achieve an appreciable reaction rate, usually below 40°C, it is usual to utilise a relatively unstable reactive group on the probe. The use of unstable reactive groups introduces problems such as storage. With most useful probes, a balance between high reactivity and storage stability must be achieved; however, all covalent probes should be regarded as unstable.

The factors that will determine which nucleophiles on the biomolecule are modified (for example, thiols versus amines), are related to the reactive moieties on the probes. Fluorescent probes, and the reactions they undergo with

biomolecules, can be classified as one of the following types: i) alkylating; ii) acylating; iii) aldehyde and ketone reactive; iv) photo-activatable; or v) miscellaneous.

The alkylating reagents include the functional groups: haloacetyl, (for example, iodoacetamides), maleimides, epoxides, aziridines and alkyl and aryl halides. All preferentially react with the thiol group of cysteine residues within proteins, if they are present, but may also react with lysine, histidine, methionine, tyrosine and possibly carboxylic acids.

Acylating probes are reactive derivatives of carboxylic, sulphonic, phosphoric or boric acids, and include acid halides, anhydrides, imidoesters, 'active' esters and isothiocyanates. Stable products are formed with lysine or tyrosine at elevated pH, while several are selective or specific for serine proteases, for example, chymotrypsin. Their reaction products with cysteine, histidine or carboxylic acids in proteins, are frequently hydrolytically and thermodynamically unstable, and they do not react with methionine.

Aldehyde and ketone reagents are almost all derivatives of hydrazine, or potentially, hydroxylamine. Photo-activatable fluorophores are chemically non-reactive, until photolysed to a reactive intermediate, which may then form a covalent linkage with the appropriate amino acid residue. Miscellaneous reagents include disulphides, mercurials and those used in non-nucleophilic, or enzyme-assisted, modification of biomolecules.

### 2.2.3. Characteristics of an Ideal Fluorescent Probe.

Generally, the ideal fluorescent probe should satisfy six criteria:

- i) Large Extinction Coefficient ( $\epsilon$ ) at the Excitation Wavelength: The extinction coefficient should be at least as high as that for fluorescein (approximately  $7 \times 10^4$  litre  $\text{mol}^{-1} \text{cm}^{-1}$ ), and preferably as high as the multichromophore phycobiliproteins, which attain values of  $2 \times 10^6$  litre  $\text{mol}^{-1} \text{cm}^{-1}$  (1);
- ii) High Quantum Yield of Fluorescence: The quantum yield of the probe-biomolecule conjugate, should be greater than 0.3 when in its solvent environment, where fluorescence measurement is made. Fluorescein labelled proteins have quantum yields of 0.2 to 0.7 at pH 8, but decreases rapidly with decreasing pH. Rhodamine is much less sensitive to pH, and is still fluorescent at high acid concentrations;
- iii) Photostability: Fluorescein can survive between  $10^4$  and  $10^5$  excitations, before decomposing. This property is important for detecting a small number of probes in solution. Removal of oxygen is the most effective step that can be taken, but this is not always possible, for example, in studies involving living cells;
- iv) Optimal Excitation Wavelength: This is a primary consideration when studying cells. Cells excited at wavelengths below 500 nm, produce considerable auto-fluorescence from flavins, flavoproteins, NADH etc. (2);
- v) Minimal Perturbation by Probe: The fluorophore should not perturb the function of the cell, organelle, or target

molecule by reacting with key groups in active sites, or by causing steric perturbation because of its size. If the probe disrupts its binding partner to a large degree, non-specific binding of a labelled protein could occur.

Also, the probe should not be photo-toxic;

vi) Large Stokes Shift: The probe should exhibit as large a Stokes Shift as possible. (This is the difference between the excitation wavelength and the wavelength of peak fluorescence emission). A large Stokes Shift is desirable so that excitation light does not interfere with the detection of fluorescence emission.

Very few fluorescent probes satisfy all of these requirements, so we need to select the probe which is best suited to the task undertaken.

### 2.3. COVALENT LABELLING OF BIOMOLECULES.

Each fluorescent probe has different characteristics with regard to stability, solubility and reactivity. As a result, there is no major protocol for fluorescent labelling of biomolecules. However, some generalisations can be made.

#### 2.3.1. Solubilisation of the Fluorophore.

Before chemical reactions can occur, it is necessary to dissolve the probe in a solvent or buffer. Although biomolecules can be labelled in biphasic mixtures such as crystals, suspensions, amorphous solids or even in vivo, better reproducibility in labelling usually occurs when they are dissolved in true solutions, where standard kinetics

controls the rate of modification. Unfortunately, many spectrally useful probes are almost totally water insoluble. In order to overcome this problem, we may add the probe from a concentrated stock solution in an organic solvent to the aqueous biomolecule. Probably the best single organic solvent to use is N,N-dimethylformamide (DMF). This highly polar, aprotic solvent dissolves almost all fluorescent probes. It is non-nucleophilic and is compatible with many biomolecules. Dimethyl sulphoxide (DMSO) has been used similarly, but some probes such as dimethylaminonaphthalene sulphonyl ('dansyl') chloride, react exothermically with DMSO to yield decomposition products (3). DMSO usually contains traces of dimethyl sulphide and this may react with iodoacetamides. Other solvents used include the lower alcohols, acetone, tetrahydrofuran (THF), 1,4-dioxane and acetonitrile, all of which are completely water miscible. Alcohols, being weak nucleophiles, should not be used with most acylating reagents. Acetone may potentially form Schiff bases when reacted with epsilon-amino groups in proteins, especially at higher pH, and obviously cannot be used when modifying aldehyde or ketone moieties on biomolecules. THF and 1,4-dioxane commonly contain high levels of organic peroxides, which may oxidise thiols and other groups. Acetonitrile is excellent provided it dissolves the probe. Owing to the highly reactive nature of most probe molecules, fresh stock solutions should be prepared frequently for maximum reproducibility of labelling. It is advantageous to dilute the dissolved probe into the concentrated biomolecule solution, by rapid mixing, in order to avoid high local concentrations

of organic solvent, which may denature the biomolecule.

The crystals of some probes are very slow to dissolve in water or aqueous buffer. Dissolution is much faster if the probe is dissolved in a volatile solvent such as ether, and mixed with the buffer, followed by partial evaporation. Sonication may also be used to disperse a water-insoluble probe by increasing the surface area of the probe in contact with the aqueous biomolecule.

A greater surface area may be achieved by the use of diatomaceous earth (Celite). The water-insoluble probe is adsorbed onto Celite by evaporating the probe from an organic solution onto Celite, that had been previously dried at 200°C, so that the probe-to-Celite ratio is approximately 1 to 10. The use of Celite generally increases the rate of modification, however, the location of labelling may be different from that performed in homogeneous solution. For example,  $\alpha$ -chymotrypsin labelled with 'dansyl' chloride on Celite predominantly modifies surface lysine, while in solution, the buried active-site serine residue is modified, resulting in loss of biological activity.

Another alternative for increasing aqueous probe solubility is encapsulation of the probe within  $\beta$ -cyclodextrin (cyclohepta-amylose) (4,5). This partially water-soluble clathrate forms a moderately polar cavity around the probe, and has been used to solubilise fluorescamine and 'dansyl' chloride, and may be used with most two-ring fluorophores.

### 2.3.2. The Mechanism of Covalent Modification.

The biomolecule and probe concentrations should be kept

as high as possible, for the greatest rate of labelling. The high biomolecule concentration also helps to solubilise the probe. At low biomolecule concentrations, rates of decomposition or hydrolysis of the probe may exceed the rate of labelling, resulting in a low degree of labelling, particularly when the probe concentration is also low.

In general, it is prudent to use the highest practical concentration of biomolecule with about 0.01 to 0.1 mM probe, at the appropriate pH for either two hours at room temperature or overnight at 4°C.

When labelling with any reactive probe, it is advisable to remove reducing agents such as mercaptoethanol and dithiothreitol, unless these have been shown to be non-reactive with the probe. It is inadvisable to use tris-hydroxymethyl-aminomethane (Tris) and related buffers, since these introduce a high concentration of reactive nucleophiles. Phosphate, borate and carbonate buffers are generally used.

Some modification procedures need to be performed in the dark, since a few reactive moieties on the fluorophores (for example, azides and iodoacetamides) are light sensitive. Generally, most common fluorophores and their reactive moieties are oxygen stable.

### 2.3.3. Purification of the Biomolecule-Probe Conjugate.

After labelling, it is necessary to remove the non-conjugated probe from the modified biomolecule. Various methods are available in order to achieve this. With water-soluble biomolecules, the most rapid method is chromatography on a

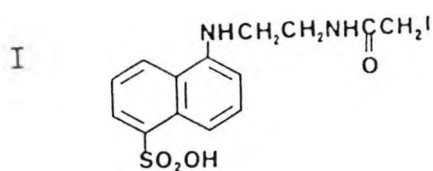
molecular-weight exclusion column, such as Sephadex G-25, with the low-molecular-weight probe being tightly bound, and the biomolecule passing through with the void volume. Dialysis, or membrane filtration, can also be used with water-soluble probes. Another general method useful for water-soluble biomolecules, is to adsorb the non-conjugated probe onto activated charcoal, followed by filtration or centrifugation. This procedure may be used in order to remove the last traces of probe from fluorescein isothiocyanate conjugates, and also to remove free rhodamine from its conjugates, since both are characteristically strongly adsorbed non-covalently.

#### 2.4. PROCEDURES AND FLUOROPHORES UTILISED FOR SELECTIVE MODIFICATION REACTIONS.

##### 2.4.1. Thiol Modification.

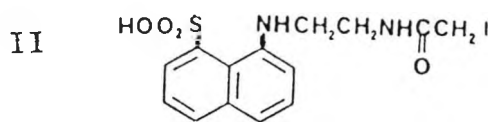
Free thiol (sulphydryl) groups occur primarily as cysteine in proteins. In order to selectively label cysteine, a pH of 7 to 8 is optimum. Above this pH, the reaction rate with tyrosine and lysine becomes more significant. Below this pH, the thiol is primarily in the protonated form and histidine modification may proceed at a comparable rate.

Three major classes of reactive alkylating groups have been used for selective thiol modification: haloacetyls, aziridines and maleimides. A selection of thiol reactive probes and their absorption and emission characteristics, are as shown.



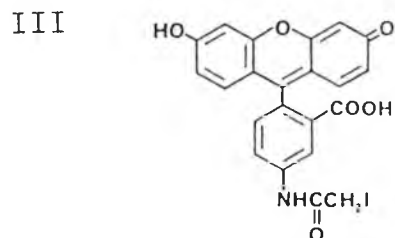
5-(2-((iodoacetyl)amino)ethyl) aminonaphthalene-1-sulphonic acid  
(1,5-IAEDANS)

Excitation  $\lambda = 337$  nm  
Emission  $\lambda = 520$  nm



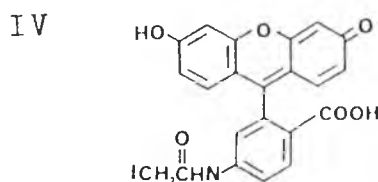
1,8-IAEDANS

Excitation  $\lambda = 340$  nm  
Emission  $\lambda = 515$  nm



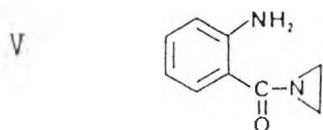
5-iodoacetamido-fluorescein  
(5-IAF)

Excitation  $\lambda = 490$  nm  
Emission  $\lambda = 520$  nm



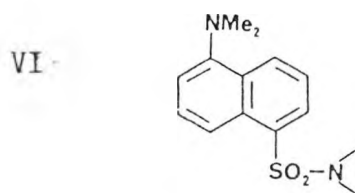
6-IAF

Excitation  $\lambda = 490$  nm  
Emission  $\lambda = 520$  nm



Anthraniloyl aziridine

Excitation  $\lambda = 330$  nm  
Emission  $\lambda = 420$  nm

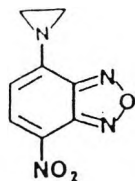


5-dimethylamino naphthalene-1-sulphonyl aziridine  
('Dansyl' aziridine)

Excitation  $\lambda = 345$  nm  
Emission  $\lambda = 485$  nm

Fig. 2.5. The structures and spectral characteristics of a range of thiol-reactive fluorophores.

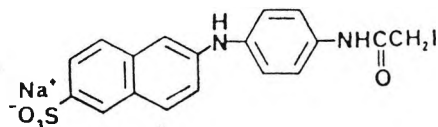
VII



4-aziridine-7-nitrobenz-  
2-oxa-1,3-diazole  
(NBD-Aziridine)

Excitation  $\lambda = 465$  nm  
Emission  $\lambda = 520$  nm

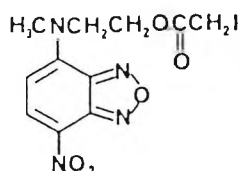
VIII



2-(4'-iodoacetamidoanilino)  
naphthalene-6-sulphonic acid  
(IAANS)

Excitation  $\lambda = 330$  nm  
Emission  $\lambda = 440$  nm

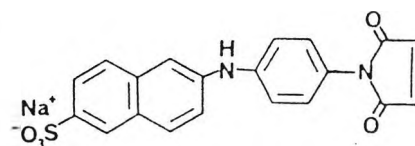
IX



NBD-Iodoacetate

Excitation  $\lambda = 495$  nm  
Emission  $\lambda = 550$  nm

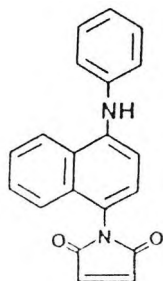
X



2-(4'-maleimidylanilino)  
naphthalene-6-sulphonic acid  
(MIANS)

Excitation  $\lambda = 322$  nm  
Emission  $\lambda = 417$  nm

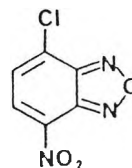
XI



N-(1-anilinonaphthyl-4)  
maleimide

Excitation  $\lambda = 350$  nm  
Emission  $\lambda = 430$  nm

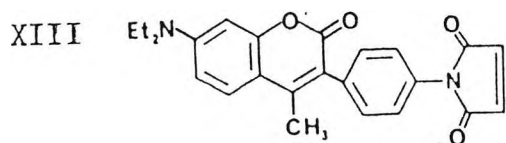
XII



4-chloro-7-nitrobenz-  
2-oxa-1,3-diazole  
(NBD-Chloride)

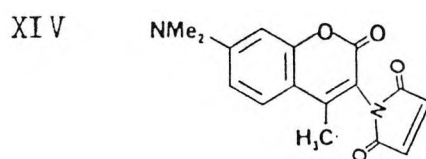
Excitation  $\lambda = 425$  nm  
Emission  $\lambda = 550$  nm

Fig. 2.6. The structures and spectral characteristics of a range of thiol-reactive fluorophores.



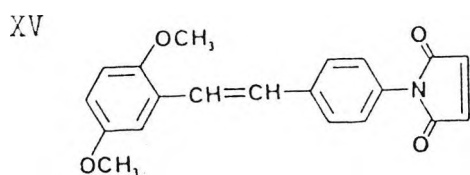
7-diethylamino-3-(4'-maleimidylphenyl)-4-methylcoumarin (CPM)

Excitation  $\lambda = 387$  nm  
Emission  $\lambda = 465$  nm



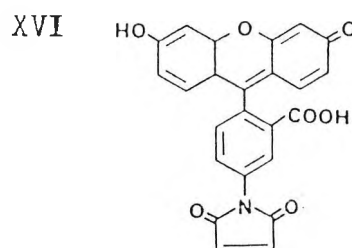
N-(7-dimethylamino-4-methylcoumarinyl) maleimide (DACM)

Excitation  $\lambda = 385$  nm  
Emission  $\lambda =$  Non-fluorescent  
Emission  $\lambda = 476$  nm (thiol adduct)



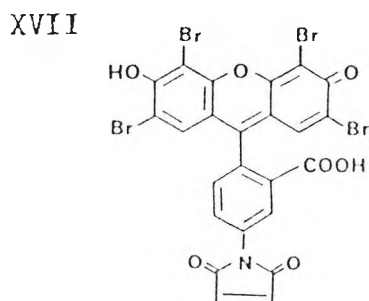
2,5-dimethoxystilbene-4'-maleimide

Excitation  $\lambda = 364$  nm  
Emission  $\lambda = 430$  nm



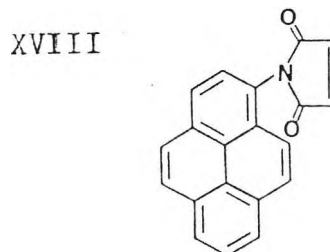
Fluorescein-5-maleimide

Excitation  $\lambda = 490$  nm  
Emission  $\lambda = 520$  nm



Eosin-5-maleimide

Excitation  $\lambda = 520$  nm  
Emission  $\lambda = 550$  nm

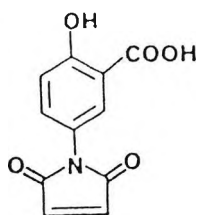


N-(1-pyrene)maleimide

Excitation  $\lambda = 343$  nm  
Emission  $\lambda = 376$  nm, 396 nm and 415 nm.

Fig. 2.7. The structures and spectral characteristics of a range of thiol-reactive fluorophores.

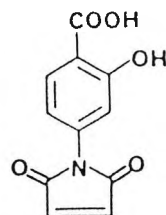
XIX



4-maleimidyl-  
salicylic acid

Excitation  $\lambda = 313$  nm  
Emission  $\lambda = 408$  nm

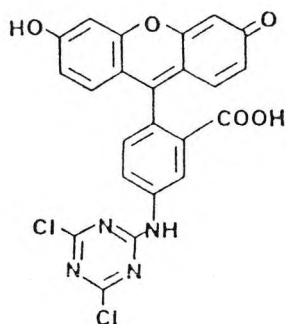
XX



5-maleimidyl-  
salicylic acid

Excitation  $\lambda = 343$  nm  
Emission  $\lambda = 435$  nm

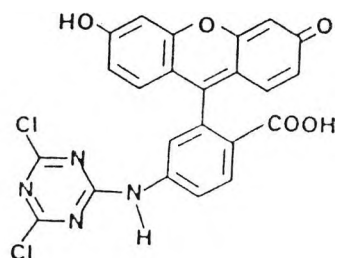
XXI



5-(4,6-dichlorotriazinyl)  
aminofluorescein (5-DTAF)

Excitation  $\lambda = 492$  nm  
Emission  $\lambda = 513$  nm

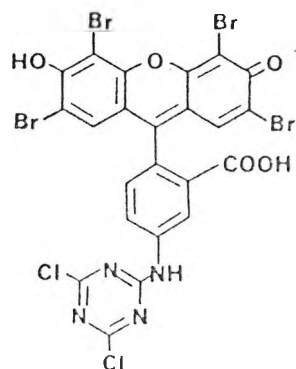
XXII



6-DTAF

Excitation  $\lambda = 492$  nm  
Emission  $\lambda = 513$  nm

XXIII



Eosin-5-dichlorotriazine

Fig. 2.8. The structures and spectral characteristics of a range of thiol-reactive fluorophores.

Haloacetyl probes, of which the fluorescent iodoacetamides are the most common, have been widely used. 1,5-IAEDANS (I) and 5-iodoacetamido-fluorescein (III), are appreciably water-soluble above pH 7 but, like all iodoacetamides, are rapidly photo-lysed by ultra-violet radiation. The 1,5-IAEDANS has a relatively long lifetime (approximately 20 nsec.), making it valuable for rotational correlation and segmental flexibility studies of proteins of molecular weight up to  $5 \times 10^5$  daltons (6,7). The spectral overlap of the fluorescence of 1,5-IAEDANS and absorbance of 5-iodoacetamido-fluorescein, permits efficient fluorescence energy transfer between sites labelled with this pair, whereby an approximate distance of 5 nm produces quenching of 50% (8,9,10,11). The fluorescein derivative absorbs more strongly ( $\epsilon = 77000 \text{ litre mol}^{-1} \text{ cm}^{-1}$ ) than does 1,5-IAEDANS ( $\epsilon = 6100 \text{ litre mol}^{-1} \text{ cm}^{-1}$ ), and has emission of high quantum yield that is somewhat pH sensitive. Actin labelled with 5-iodoacetamido-fluorescein retains full biological activity when injected into living cells, and becomes regionally concentrated during different stages of cell division (12,13,14).

Aziridines can be divided chemically into 'activated' and 'inactivated' classes. The activated aziridines are amides of carboxylic acids, such as anthranilic acid (V), and of sulphonic acids, such as 'dansyl' (VI). The inactivated aziridines are N-alkyl- or N-arylethylenimine derivatives such as NBD-Aziridine (VII). Activated aziridines undergo ring-opening nucleophilic reactions with thiols or amines in basic solution, while the inactivated aziridines are very

stable in base and undergo ring-opening reactions only with acid catalysis. The most widely used fluorescent aziridine has been 'dansyl' aziridine, particularly with the muscle proteins; actin, myosin and troponin C. On actin, one cysteine is modified with high selectivity (15), while on the cysteine-free troponin C, the site of reaction is a methionine residue (16,17).

The iodoacetyl derivatives of anilinonaphthalene sulphonic acid (ANS) and of nitrobenzoxadiazole (NBD), IAANS (VIII) and IANBD (IX) respectively, and the maleimide derivatives of ANS (MIANS (X)) and anilinonaphthalene (ANM (XI)), are predominantly thiol reactive and are very environment sensitive. NBD-Chloride (XII) and all other NBD derivatives share this same degree of environmentally sensitive fluorescence. This property allows the fluorescence characteristics of these probes to respond to conformational changes induced by substrate, allosteric mediator or inorganic ion binding. The fluorescence intensity of proteins labelled with covalent hydrophobic probes is sensitive to the folding of the protein, and is eventually reduced on exposure to water during denaturation.

Most of the maleimide derivatives of fluorophores have the property of being non-fluorescent until after conjugation of a reactive nucleophile, across the maleimide double bond. In addition to ANM and the maleimide derivatives of ANS, other useful maleimides include maleimides of stilbene and coumarin (XIII, XIV, XV) with both high absorbance and quantum yield, fluorescein and eosin maleimides (XVI and XVII) with the longest-wavelength fluorescence and high intensity, pyrene

maleimide (XVIII) with a fluorescence lifetime up to 100 nsec., and derivatives of salicylic acid (XIX and XX) which are highly water-soluble and reported to be membrane impermeant (18). The coumarin maleimides; CPM (XIII) and DACM (XIV), appear to be the reagents of choice for histochemical demonstration of thiols.

The chemical instability of the maleimide ring-attaching group, introduces some limitations in its use. Ring-opening hydrolysis of the anhydride-like maleimide ring occurs at an appreciable rate above pH 8 (19). Since selective modification of thiols is usually conducted below this pH and the maleimide reagent is usually used in excess, this is often not critical. A more significant problem exists when the protein-thiol adduct of the maleimide ring opens after conjugation to the biomolecule, since the fluorescence properties of the closed-ring thiol adduct and the open-ring adduct, are sometimes significantly different. An application of this ring instability is the potential cross-linking of the maleimide adduct with a spatially adjacent lysine residue, to form a diamide derivative. This has been reported to occur for the pyrene maleimide derivative of serum albumin (20). Pyrene maleimide also exhibits the phenomenon of excimer fluorescence when two probes are on spatially adjacent thiols, as occurs in tropomyosin (21).

Two types of fluorophore possess cysteine reactive moieties that are most appropriately termed 'aryllating reagents' rather than 'alkylating reagents.' These are NBD-Chloride (XII) and several dichlorotriazine probes (XXI, XXII, XXIII). Both

of these groups of fluorophores rapidly form moderately stable adducts with thiols, and may also react with amines. Absorption of the NBD-thiol adduct is about 425 nm while that of the amine adduct is near 475 nm, so that the type of residue modified can be readily determined. The fluorescence of the NBD-thiol adduct is very weak, especially in an aqueous environment. When reacted with 2-mercaptoethylamine (cysteamine), the initial site of reaction is the thiol. This is followed by an intramolecular transfer of the nitrobenzoxadiazole to the amine. An identical sulphur to nitrogen transfer appears to occur in actin where initial reaction of a thiol is transferred to a spatially adjacent lysine.

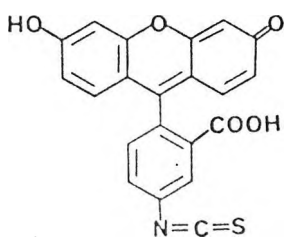
The dichlorotriazinylamine derivatives of fluorescein (XXI and XXII) have been proposed as alternatives to fluorescein isothiocyanate for immunofluorescence tracing, since they are equally fluorescent and the conjugation proceeds with greater ease and reproducibility at a lower pH (22,23).

#### 2.4.2. Amine Modification.

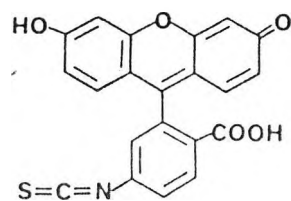
Selective modification of the epsilon-amino group of lysine in proteins occurs quite readily provided the pH can be raised above pH 9, where the concentration of unprotonated amine begins to become significant. The protonated aliphatic amine is non-reactive and modification by any reagent, will be very slow below this pH. In contrast, the pKa of the alpha-amino group of peptides is approximately 7,

so that selective modification of the amino-terminus can be accomplished, provided it is free. The most widely used covalent fluorescent probes for lysine modification are fluorescein isothiocyanate, 'dansyl' chloride, fluorescamine and o-phthalaldehyde.

Fluorescein isothiocyanate (FITC) is almost an ideal covalent fluorescent probe. It suffers from a small Stokes Shift of approximately 25 nm, which necessitates the use of sharp cut-off filters or monochromators, and it has a tendency toward photo-bleaching. Its advantages are high extinction coefficient, high quantum yield and water solubility. The spectra are far removed from the auto-fluorescence of biomolecules. In the synthesis of FITC, two isomers are formed, originally called isomer I and isomer II, which correspond to fluorescein-5-isothiocyanate and fluorescein-6-isothiocyanate respectively. These isomers differ in the point of attachment of the isothiocyanate group to the single benzene ring.



Fluorescein-5-  
Isothiocyanate  
(Isomer I)

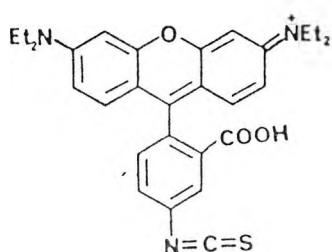


Fluorescein-6-  
Isothiocyanate  
(Isomer II)

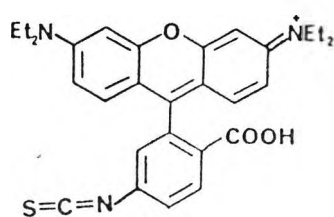
Fig. 2.9. The molecular structures of FITC Isomers I & II.

The 5-isomer (Isomer I) has been most widely used although the spectral properties of the two isomers are quite similar, and some commercial preparations are a mixture of the two isomers. In contrast to the original isocyanates (24), the isothiocyanates undergo solvolysis only slowly in aqueous or alcoholic solutions. At extremes of pH, the thiourea adduct formed by reaction of an isothiocyanate with an amine is somewhat unstable to hydrolysis, producing a urea and hydrogen sulphide. Fluorescein conjugates are susceptible to concentration quenching, whenever two fluorescein chromophores are spatially adjacent. This can even occur at longer distances, by singlet-singlet energy transfer.

Rhodamine isothiocyanates have the advantage over FITC of greater photo-lytic stability; however, they have a lower quantum yield, are usually a mixture of the 5- and 6-isomers, and are difficult to dissolve in the conjugation medium.



Rhodamine-5-  
Isothiocyanate



Rhodamine-6-  
Isothiocyanate

Fig. 2.10. The molecular structures of Rhodamine-5-isothiocyanate and Rhodamine-6-isothiocyanate.

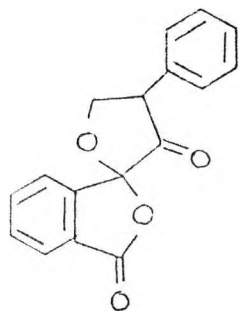
'Dansyl' chloride forms highly stable sulphonamide derivatives with amines.



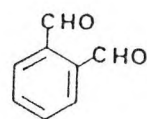
Fig. 2.11. The molecular structure of 'dansyl' chloride.

The extinction coefficient of the conjugate is very low (approximately 4500 litre mol<sup>-1</sup> cm<sup>-1</sup>) as compared with fluorescein (approximately 75000 litre mol<sup>-1</sup> cm<sup>-1</sup>). The quantum yield is also quite environment sensitive but is low, (less than 0.1), for sites exposed to water. The Stokes Shift of emission is extremely high, with emission up to 200 nm red-shifted from absorption. The reactivity of the reagent is quite high, therefore conjugation proceeds rapidly, but hydrolysis can occur at an appreciable rate. As a result, storage can cause problems. Under certain conditions, it also reacts with amino acids to yield aldehydes (25).

Fluorescamine and o-phthaldehyde are both reagents that have predominantly been used, in order to quantitate primary aliphatic amines.



Fluorescamine



o-phthaldehyde

Fig. 2.12. The structures of Fluorescamine and o-phthaldehyde.

Fluorescamine is an unusual probe in that neither it, nor its hydrolysis product, is fluorescent but its amine conjugates are. Conjugation is usually achieved by vortexing a solution of the biomolecule, with fluorescamine dissolved in acetone.

O-phthaldehyde usually undergoes reaction with amines in the presence of mercaptan, to yield a fluorescent isoindole derivative (26,27). It has been reported (26) that o-phthaldehyde detection of amines is five to ten times as sensitive as that of fluorescamine.

Several other lysine-reactive reagents have been developed for specific applications, and as alternatives to those previously mentioned, and a selection is as shown.

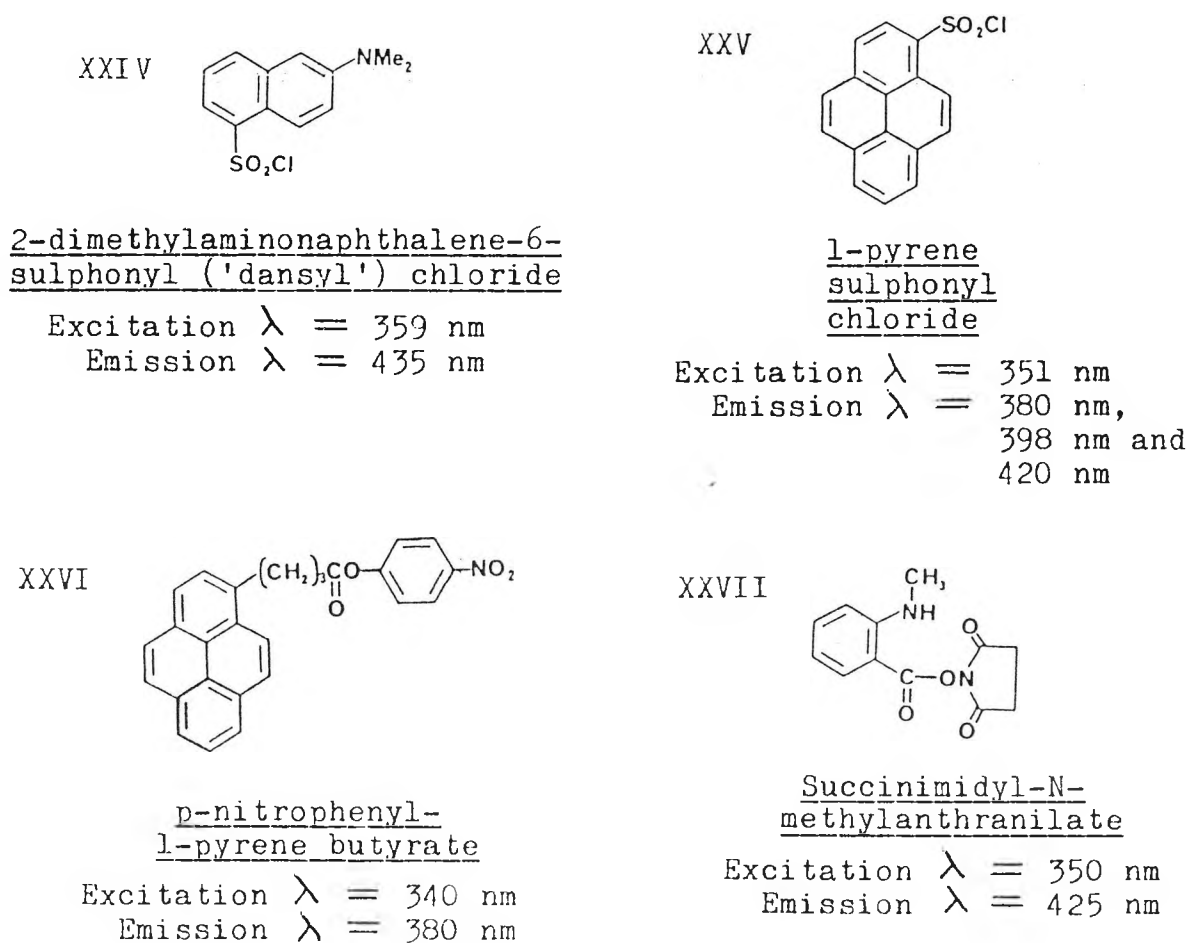
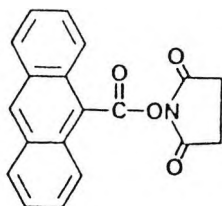


Fig. 2.13. The structures and spectral characteristics of a range of amine-reactive fluorophores.

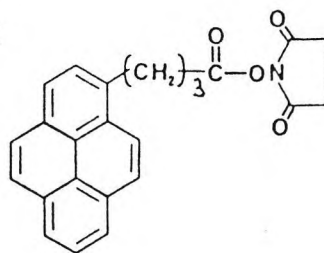
XXVIII



Succinimidyl-9-  
anthracene  
carboxylate

Excitation  $\lambda = 378$  nm  
Emission  $\lambda = 415$  nm

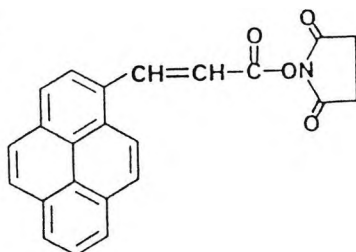
XXIX



Succinimidyl-  
1-pyrene butyrate

Excitation  $\lambda = 340$  nm  
Emission  $\lambda = 380$  nm and  
400 nm

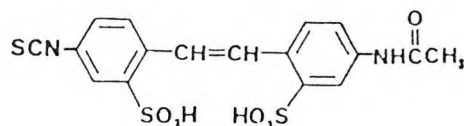
XXX



Succinimidyl-1-  
pyrene acrylate

Excitation  $\lambda = 373$  nm  
Emission  $\lambda = 463$  nm

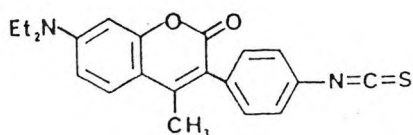
XXXI



4-acetamido-4'-isothio-  
cyanatostilbene-2,2'-  
disulphonic acid (SITS)

Excitation  $\lambda = 350$  nm  
Emission  $\lambda = 420$  nm

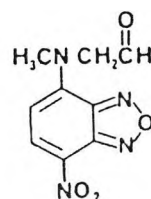
XXXII



7-diethylamino-3-(4'-isothio-  
cyanatophenyl)-4-methylcoumarin  
(CPI)

Excitation  $\lambda = 357$  nm  
Emission  $\lambda = 460$  nm

XXXIII



2-(7-nitrobenz-2-oxa-1,3-  
diazol-4-yl)methylamino  
acetaldehyde

Excitation  $\lambda = 470$  nm  
Emission  $\lambda = 530$  nm

Fig. 2.14. The structures and spectral characteristics of a  
range of amine-reactive fluorophores.

The 2,5- and 2,6-isomers of 'dansyl' chloride (XXIV), show a much greater Stokes Shift than does the 1,5-isomer, with the 2,5-isomer showing an exceptionally long fluorescent lifetime (approximately 30 nsec.). Pyrene sulphonyl chloride (XXV) has a quantum yield similar to 'dansyl' chloride, but significantly stronger absorbance, making its detectability greater. It also has a longer fluorescence lifetime.

Several methods exist for formation of simple amide derivatives between fluorescent carboxylic acids, and biomolecule amines. In order to achieve this, the carboxy-probe needs to be 'activated', to provide the necessary reaction mechanism. Carboxylic acid chlorides are usually not used due to their high reactivity, while simple esters are generally not sufficiently reactive. Esters of p-nitrophenol and N-hydroxysuccinimide may be used.

Nitrophenyl esters of aliphatic acids such as pyrene butyric acid (XXVI), readily acylate aliphatic (but not aromatic) amines. The reactivity of p-nitrophenyl esters of aromatic acids, depends, in part, on other substituents on the aromatic ring. Electron-withdrawing groups increase reactivity while donating substituents decrease reactivity. Succinimidyl esters of carboxylic acids (XXVII, XXVIII, XXIX and XXX), show high specificity for amine modification, while the much more reactive acyl imidazoles also acylate tyrosine and hydroxyl groups.

Fluorescent carboxylic acids can also be rendered protein reactive by conversion to anhydrides. Usually, the symmetrical

anhydride is not employed, since only half of an anhydride is incorporated when it reacts with nucleophiles. As a consequence, 'mixed anhydrides' are usually employed. Examples are mixed anhydrides with sulphur trioxide, ethyl chloroformate or trifluoroacetic anhydride. Carbodiimides, and particularly the water-soluble carbodiimides (such as 1-ethyl-3-(3-dimethylaminopropyl)-carbodiimide, EDC), have also been used to activate carboxylic acids, through formation of a mixed anhydride with the carbodiimides being converted to a urea (28).

A very water-soluble isothiocyanate derivative of stilbene, SITS (XXXI), has been used most frequently for its specific anion-transport inhibition (29), although it is also of use as the short wavelength 'third probe' for multiply labelled fluorescence-activated cell sorting, due to its fluorescence being spectrally well separated from the other probes used. Coumarin phenyl isothiocyanate (XXXII), is both an intensely absorbing and strongly emitting isothiocyanate.

The reversible reaction of aldehydes and ketones with amines to form Schiff bases, can be used for highly specific labelling of amines if the Schiff base is reduced with sodium borohydride or, in preference, sodium cyanoborohydride. This reductive alkylation reaction retains the basic character of the amine, and produces a highly stable derivative. A fluorescent reagent to take advantage of this reaction for covalent modification of amines, is an NBD-acetaldehyde derivative (XXXIII).

#### 2.4.3. Histidine Modification.

It has been found that the imidazole ring of histidine, has been alkylated by iodoacetamides. Use of reactive substrate analogues, may enable labelling of catalytically important histidine residues in proteins that do not contain cysteine residues. The histidine of lysozyme, has been selectively labelled at pH 6.2 by a dichlorotriazinyl spin label, which indicates that this reactive moiety on fluorescent probes 'XXI', 'XXII' and 'XXIII', may also be useful for histidine modification (30).

#### 2.4.4. Methionine Modification.

Dialkyl sulphides, such as methionine, are generally non-reactive; however, when they are protected from aqueous solvation in a protein, they are susceptible to alkylation to form a sulphonium salt. Aziridines and iodoacetamides may undergo the reaction, but the ternary salts formed, however, may not be completely stable since trialkyl sulphonium salts are themselves alkylating reagents for other nucleophiles (31). Moreover, iodoacetamide has been suggested as a reagent for the specific cleavage of peptides, at methionine residues (32). Methionine modification in the presence of cysteine is unlikely to be successful, unless cysteine residues are protected as disulphide linkages, such as by prior treatment with dithiobis-2-nitrobenzoic acid (DTNB). In the presence of other potential nucleophiles, such as lysine, histidine and tyrosine, advantage can be taken of the pH insensitivity of methionine modification to suppress the

reaction of other nucleophiles, by performing the reaction at the lowest practical pH.

#### 2.4.5. Tyrosine Modification.

Tyrosine in proteins can be modified by many fluorescent reagents, but usually with low selectivity in the presence of other common amino acids, such as cysteine and lysine. 'Dansyl' chloride gives stable sulphate derivatives and iodoacetamides, react readily at elevated pH. Specific modification may be achieved (33) by the nitration of tyrosine with tetranitromethane to form nitrotyrosine, followed by dithionite reduction to aminotyrosine. Being weakly basic, the aromatic amine could be modified at low pH with 'dansyl' chloride. Diazonium salts readily couple with tyrosine at neutral pH, to form azo-dyes. While azo-dyes are not generally fluorescent, the azo-dye derived by coupling diazotised o-aminophenol to tyrosine, forms a strongly fluorescent chelate with such cations as magnesium and aluminium (34).

#### 2.4.6. Carboxylic Acid Modification.

Due to the low nucleophilicity of the carboxylate anion, direct modification of carboxylic acids in biomolecules is usually difficult. An approach could be the reversal of the carbodiimide-mediated coupling of an amine with a carboxylic acid, to form an amide by utilising a fluorescent amine derivative to attack a carbodiimide-activated protein carboxyl group. Since a large number of carboxyl groups are usually

present, selectivity of modification depends on the ability of the carbodiimide to reach the carboxyl group, to form the mixed anhydride derivative. For surface carboxyl residues, a polar, water-soluble carbodiimide (for example, EDC), is probably most suitable, but for the buried carboxyl groups, a non-polar carbodiimide such as 1,3-dicyclohexylcarbodiimide (DCC) is most appropriate. Choice of the amine is also very important. In order to avoid protein cross-linking, a fluorescent amine with a low pKa (weak base) is necessary, since a significant concentration of free base can be maintained at pH 5-7, where essentially all of the lysine residues are in the unreactive protonated form. Glycine amides and esters, hydrazides and hydroxylamines all meet these requirements, by having a pKa of approximately 7 (35).

Some fluorescent reagents react with carboxylic acids and these may be extended for usage in protein modification. A candidate is 9-diazomethyl anthracene (36). Like diazomethane, this reagent esterifies carboxylic acids at room temperature. Halomethylcarbonyl compounds (for example, phenacyl bromide), are common carboxylic acid derivatisation reagents, and the 'dansyl' chloromethyl ketones have this structure. Aziridines, such as NBD-aziridine also react with carboxylic acids at low pH.

#### 2.4.7. Modification of Other Residues in Proteins.

Although guanidines, such as arginine, form fluorescent adducts with ninhydrin and o-phenanthrene quinone (37), the extremely basic conditions required, preclude their use at physiological pH. It has been reported (38,39) that

chromophoric glyoxal derivatives react reversibly with arginine, in the stoichiometry of two glyoxals per arginine. This may be extended for use with fluorescent glyoxal derivatives.

The non-reactivity of serine and threonine side-chain hydroxyl groups, to either alkylating or acylating reagents is not unexpected due to their low nucleophilicity. However, reactive serine residues at the active site of certain enzymes, may undergo fluorescent modification. 'Dansyl' fluoride, unlike its analogue 'dansyl' chloride, does not react with amines, and is very stable to hydrolysis.

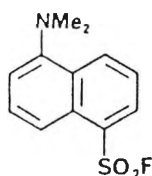


Fig. 2.15. The molecular structure of 'dansyl' fluoride

This reagent reacts with active-site serine in a number of enzymes such as chymotrypsin (40), thrombin (41) and cholinesterase (42). The fluorescent pyrene-phosphonofluoridate also specifically modifies serine of acetylcholinesterase (43,44).

Another method for specific modification of biomolecules, is enzyme-mediated fluorescence labelling. The hitherto most widely used system, has been guinea-pig liver transglutaminase-catalysed incorporation of 'dansyl' cadaverine into proteins (45,46,47). Protein glutamine residues are specifically converted to fluorescent glutamic acid amides. This has been reported for rhodopsin, actin, nitrate reductase, casein,

spectrin in erythrocyte ghosts and sarcoplasmic reticulum membrane proteins.

2.5. PROBES THAT ARE SENSITIVE TO THE pH  
OF THEIR ENVIRONMENT.

When certain dyes bind either hydrogen ions or metal ions, the electronic structure of the former is altered. If the hydrogen ion or metal ion is near the dissociation constant of the ground state, or the excited state of the dye then, respectively, the absorption properties or the fluorescence characteristics, or both, can be affected (48).

6-carboxyfluorescein is an example of a probe with an absorption spectrum, sensitive to pH within the physiological range.

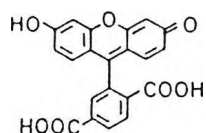


Fig. 2.16. The molecular  
structure of 6-carboxyfluorescein.

This probe has a ground state pKa near to 6.5. The peak absorption is present in the 440-450 nm region, at lower pH. As the pH is raised, the peak absorption shifts to near 490 nm (49). Thus, pH measurements are performed by exciting the molecule at both 496 nm and at 452 nm. The ratio of the emissions produced by these two excitations is then calculated.

1,4-dihydroxyphthalonitrile is another example of a probe which alters its emission characteristics, in response

to changes in the pH of its environment within the physiological range (50). The diacetoxy ester of this compound is a permeant molecule, which enters cells rapidly and is subsequently cleaved by endogenous esterases. The product, 1,4-dihydroxyphthalonitrile is relatively impermeable, and fluoresces, both in its acid form, which when excited at 366 nm shows fluorescence emission at 453 nm, and its base form, which when excited at 386 nm, exhibits fluorescence emission at 483 nm.

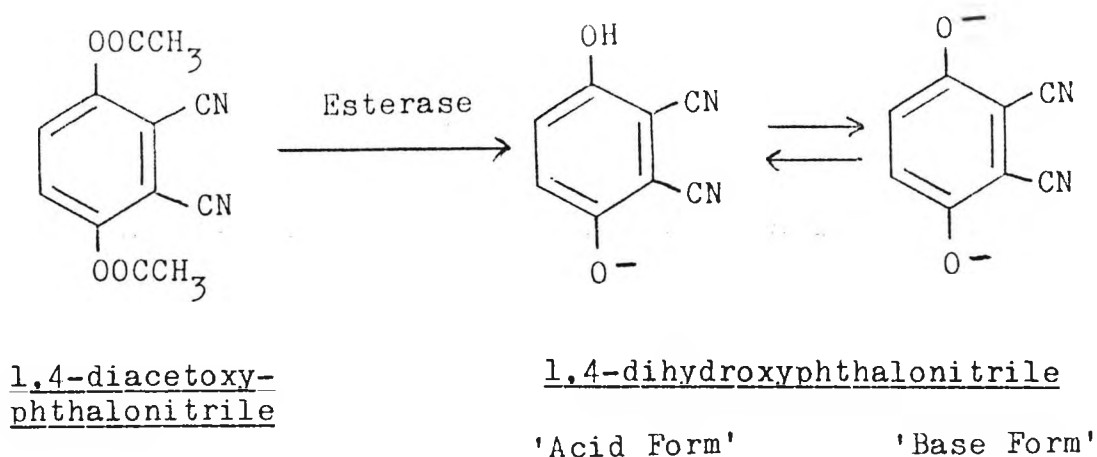


Fig. 2.17. The enzymatic hydrolysis of 1,4-diacetoxyphthalonitrile

8-hydroxy-1,3,6-pyrenetrisulphonate is a third example of a pH sensitive probe (51). The fluorescence intensity of this compound is strongly dependent upon the degree of ionisation of the 8-hydroxy group (pKa, 7.2). Thus, as the pH of the medium is increased from 5 to 10, the fluorescence emission at 520 nm of the molecule increases 90-fold when excited at 460 nm.

## 2.6. FLUORESCENT PROBES WHICH UNDERGO ENERGY TRANSFER.

Resonance energy transfer can occur between a fluorescent chromophore in the excited state which acts as a donor, and a nearby chromophore which may act as an acceptor. Provided the donor fluorescence spectrum significantly overlaps with the absorption spectrum of the acceptor, energy transfer may occur between two chromophores, separated by distances of tens of angstroms. The donor does not emit a photon which is absorbed by the acceptor, rather, if the acceptor is fluorescent, it may emit a photon as a consequence of excitation of the donor. Energy transfer is therefore a non-radiative process.

It has been found (52) that fluorescence energy transfer can be used as a spectroscopic ruler. Oligomers of poly-L-proline ( $n = 1-12$ ), were used to separate a naphthalene energy donor from a 'dansyl' energy acceptor by distances ranging from 12-46 Å. The observed energy transfer efficiencies, which ranged from 100% to 16%, varied with the inverse  $5.9 \pm 0.3$  power of the distance between the donor and acceptor. Thus, if the energy transfer efficiency between donor and acceptor is known, the distance between these two entities may be calculated.

More recently, energy transfer investigations (53) have centred on the determination of the cell surface using fluorescein (donor) and rhodamine (acceptor) (54). Energy transfer phenomena have also been utilised to investigate the self-assembly or binding events within living cells (55). Actin was fluorescently labelled at cysteine-373 with either

an energy donor (5-iodoacetamido-fluorescein), or an energy acceptor (tetramethylrhodamine iodoacetamide). Donor-labelled actin and acceptor-labelled actin were co-assembled.

Following determination of the energy transfer efficiency, it was calculated that the distance between the cysteine residue of one filament, and that of the other filament, was approximately  $35 \overset{0}{\text{A}}$ . This indicated that cysteine-373 is located near the outer surface of the filament.

In addition to energy transfer, it is possible for certain ions and molecules to directly quench fluorescence, by deactivation of the excited state. Direct quenching of probe fluorescence may occur in the presence of heavy atoms, oxygen and molecules that form charge transfer complexes.

## 2.7. FLUORESCENT PROBES THAT ARE SENSITIVE TO THE POLARITY OF THEIR ENVIRONMENT.

Almost all fluorescent molecules are sensitive, by varying degrees, to the polarity of their solvent environment. This is because the energy of the excited state is uptaken by the solvent, when polar solvent molecules re-orientate about the more dipolar structure of the excited molecule, shortly after excitation. Reduction of the distance between the excited and ground state, causes the emitted photons to possess lower energy. As a consequence, the fluorescence spectrum undergoes a bathochromic (red) shift.

Certain dyes are utilised for their sensitivity to their environment. Many dyes sensitive to membrane potential, are more fluorescent in lipophilic environments, such as membranes,

as a result, show fluorescence changes when driven by changes in membrane potential, to compartments of different polarity.

Solvent polarity sensitivity of certain probes, can be a disadvantage. Calcium probes, pH probes and energy transfer probes, may change their fluorescence characteristics in response to the polarity of their surroundings, as opposed to their primary function.

## 2.8. FLUORESCENT REDOX POTENTIAL PROBES.

Certain intracellular cofactors are themselves able to exhibit fluorescence, and may be used to determine the redox state of the cell. When excited at 488 nm, flavin adenine dinucleotide ( $\text{FAD}^+$ ) exhibits green fluorescence at 530 nm. As this cofactor is reduced, its fluorescence intensity falls. This allows the use of  $\text{FAD}^+$  to report the extent of reduction, within the cell (56).

Dichlorofluorescein has been used to monitor the release of hydrogen peroxide by phagocytic cells (57). The probe may be transported across the cell membrane by the use of the reduced di-acetate ester. Cleavage by endogenous esterases yields the non-fluorescent reduced dichlorofluorescein, which on oxidation by hydrogen peroxide, produces the highly fluorescent, oxidised dichlorofluorescein. When excited at 500 nm, dichlorofluorescein shows green emission at 530 nm.

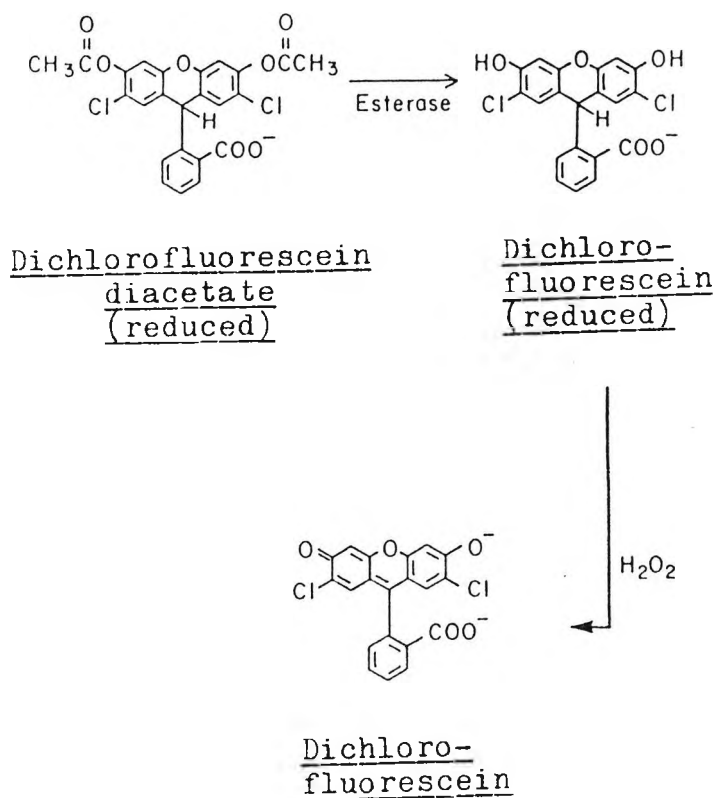


Fig. 2.18. Membrane-permeant diacetyl-dichloro-fluorescein is converted by cellular esterases to dichlorofluorescein. Peroxides released upon neutrophil stimulation oxidise the non-fluorescent dichlorofluorescein to the fluorescent dichloro-fluorescein (57).

## 2.9. FLUORESCENT PROBES FOR MEASURING ENZYME ACTIVITIES.

Fluorogenic substrates are used to investigate enzyme activities. The chromophores are converted by specific enzymes, into products that have either increased fluorescence or shifted spectra. It is desirable to be able to monitor lysosomal enzymes, such as proteases, esterases, phosphatases,

glycosidases and phosphodiesterases, since when control over these is lost, certain disease states are produced, for example, rheumatoid arthritis and tumour invasion, amongst others (58).

The majority of fluorogenic substrates are derived from chromophores possessing either an hydroxyl, or amino group, which may participate in the electronic conjugation. When a suitable amino acid sequence is attached to an amino-chromophore via an amide bond, the chromophoric molecule is usually rendered much less fluorescent. Cleavage of the amide bond of the substrate by an appropriate peptidase, releases the more fluorescent primary amine chromophore. Amino-coumarins, amino-quinolines and naphthylamine, have been used as chromophore bases for fluorogenic peptidase substrates.

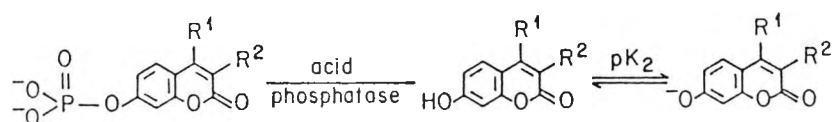


Fig. 2.19. Substituted coumarins may be utilised in order to measure enzyme activities. The R-groups are peptides specific for the enzyme of interest (59).

The R-groups may be varied so as to increase conjugation and thereby shift the fluorescence of these derivatives toward the visible region of the spectrum (59). A disadvantage of using these chromophores, is that ultra-violet irradiation is usually necessary for excitation. This invokes problems

associated with auto-fluorescence of the proteins. An advance has been made with the use of a rhodamine chromophore, which may be excited at 490 nm (60,61).

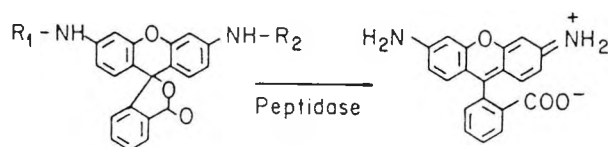


Fig. 2.20. The use of a substituted rhodamine for the determination of enzyme activities which allows the use of visible light for excitation (60).

A range of coupling reagents have been developed which convert products into insoluble coloured substances, which may be analysed by absorbance techniques. However, only one coupling reaction is available whose insoluble fluorescent product, stays within the cell. This is the coupling reaction between nitrosalicylaldehyde and the product from the proteolytic degradation of the methoxy-naphthylamine conjugate (62).

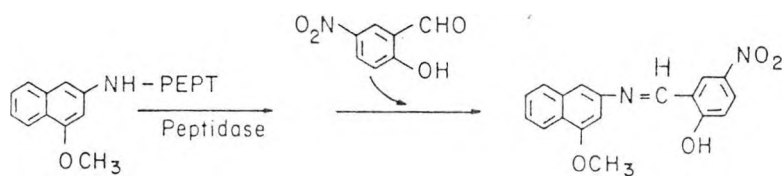


Fig. 2.21. The free amino group, which is made available when the peptide bond of peptidyl-methoxynaphthylamine is hydrolysed by a peptidase, couples with 5-nitrosalicylaldehyde, which is present during the reaction, to form the insoluble red-orange-fluorescing product (62).

A photo-activatable fluorophore (PAF) is a non-fluorescent molecule, that can be converted to a stable fluorescent molecule when irradiated by light. The desirable characteristics of a PAF, are as follows:

- i) Non-fluorescent;
- ii) Capable of covalent attachment to target molecules;
- iii) Activated by light which is not strongly absorbed by the ultimate fluorophore;
- iv) Chemically and thermally stable.

The photo-activation process should be:

- i) Selective, (that is, no other processes are to be induced);
- ii) Efficient, (the absorbing moiety should possess a high extinction coefficient);
- iii) Induced by relatively low energy light;
- iv) Clean, (that is, no damaging by-products should be generated),

The ultimate fluorophore should be:

- i) Highly fluorescent;
- ii) Excited by non-activating wavelength;
- iii) Chemically, thermally and photo-chemically stable.

Three general types of PAF may be considered: A type I PAF consists of a photo-removable quenching moiety, attached to a fluorescent molecule; a type II PAF is composed of two parts which react with each other or rearrange when irradiated, to form the ultimate fluorophore; a type III PAF might be considered a hybrid of the first two, whereby

the two parts are prevented from reacting together, by a photo-removable protecting group.

Photo-activatable fluorophores allow the long-term monitoring of the labelled species.

## 2.11. NON-COVALENTLY ASSOCIATING FLUORESCENT PROBES.

### 2.11.1. pH Probes that Partition Between Compartments with Different pH.

An ideal fluorescent probe for this purpose would have the following properties:

- i) The probe would be capable of rapid equilibration across membranes, in response to pH gradients;
- ii) The probe would be a mono-amine or mono-functional weak acid;
- iii) Fluorescent quenching, by whatever mechanism, would be complete when the molecule entered a membrane enclosed volume;
- iv) Intrinsic fluorescence of the probe would be independent of the composition of the external medium.

The quenching of 9-aminoacridine fluorescence has been quantitatively related to the magnitude of pH gradients across liposome membranes (63). Acridine orange has been shown to preferentially localise within the azurophilic granules, of the peripheral blood neutrophils (64). These granules contain the enzymes elastase and myeloperoxidase. Since loss of elastase from the granules results in a loss of red fluorescence, it is concluded that acridine orange associates with elastase.

2.11.2. Probes for the Visualisation of Membrane and Lipid Compartments.

Cell membranes are composed of a lipid bilayer into which proteins are inserted or applied. The lipids do not form a homogeneous medium, but tend to segregate into separate phases; fluid and gel (65,66).

It has been shown (67) that the 3,3'-diacylindocarbocyanine iodides accumulate in different locations, according to the length of the hydrocarbon chain.

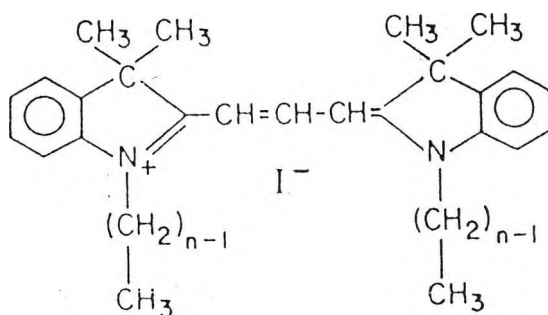


Fig. 2.22. The Molecular Structure of 3,3'-diacylindocarbocyanine iodide (67).

When the hydrocarbon chain is shorter than that of the lipid bilayer, the dye aggregates within the fluid. When the dye-hydrocarbon chain and the lipid-hydrocarbon chain are of comparable length, no preference is observed. If the dye chain is longer than the lipid chain, the former concentrates within the gel, while those much longer prefer the fluid.

Nile red (9-diethylamino-5H-benzo( $\alpha$ )phenoxazine-5-one),

has been shown to aggregate specifically within lipid droplets (68).

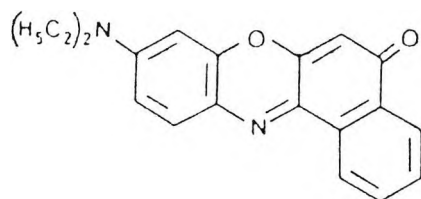


Fig. 2.23. The molecular Structure of Nile Red.

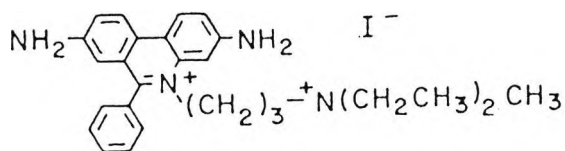
Abnormal accumulation of cytoplasmic lipid droplets occurs in a variety of pathological conditions. When excited at between 450 nm and 500 nm, the dye exhibits a yellow-gold fluorescence (at 528 nm). If it is excited at between 515 nm and 560 nm, it shows red fluorescence (at 590 nm). Low levels of lipid may be visualised by the use of yellow-gold fluorescence, due to the greater sensitivity of the human eye, to light of this wavelength. The red fluorescence exhibited by the dye, is extremely intense.

### 2.11.3. DNA and RNA Probes.

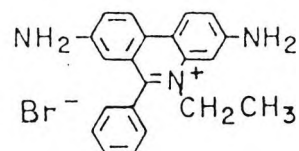
A series of DNA and RNA probes have been investigated with regard to their binding mechanism (69).

4',6-diamidino-2-phenylindole (DAPI), is thought to intercalate between the adenine and thymine bases of DNA. Ethidium bromide, propidium iodide, acridine orange and quinacrine, all intercalate, but show no preferential

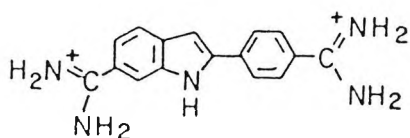
association site. Mithramycin, which needs magnesium ions for association, binds externally in the vicinity of guanine and cytosine bases.



Propidium Iodide



Ethidium Bromide



4',6-diamidino-2-phenylindole (DAPI)

Fig. 2.24. The Molecular Structure of Three DNA and RNA Probes.

Propidium iodide suffers from the disadvantage of not readily crossing the cell membrane. Acridine orange binds differently to single-stranded RNA and to DNA. The red fluorescence of acridine orange molecules associated with single-stranded RNA, can be readily measured separately from the green fluorescence of acridine orange, intercalating in DNA. Thus, RNA and DNA may be quantified simultaneously (70).

#### 2.11.4. Membrane Potential Probes.

Cyanine dyes have been used extensively as membrane potential probes. Cyanine dyes are positively charged molecules, and will therefore tend to migrate to areas of

negative potential. One particular cyanine dye, namely, 3,3'-dipropylthio-dicarbocyanine iodide (71),

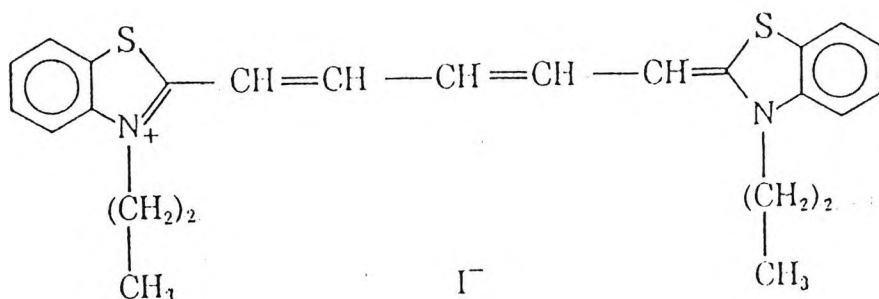


Fig. 2.25. The Molecular Structure of 3,3'-dipropylthio-dicarbocyanine iodide.

was introduced into a suspension of intact red blood cells. The cells were then hyperpolarised (that is, the interior of the cell possesses an overall negative charge), by valinomycin. Consequently, the cells uptake the dye, and an 80% change in fluorescence (at 670 nm) was observed. The dye was also found to minimally affect ion fluxes and transport across the membrane. With maximal hyperpolarisation, a ten-fold decrease of dye concentration was observed. Cell-associated dye is significantly less fluorescent than that present in the medium. Before hyperpolarisation, cell-associated dye, was one-fifth as fluorescent as the dye in the medium. After maximal hyperpolarisation, the amount of dye associated with the cells, was nearly doubled and the fluorescence of the cell-associated dye was found to be only one-twelfth of its relative intensity in the medium.

Similar experiments have been done using rhodamine 123

on mitochondrial suspensions, and the dye has also been found to accumulate within tumour cell lines (72).

## 2.12. SUMMARY.

Thus, a wide range of fluorescent probes is available to cater to the specific area of investigation. Proteins may be readily modified specifically via cysteine, lysine, histidine, methionine, tyrosine, aspartic acid and glutamic acid residues, by manipulating the conjugation conditions with regard to the reactive function of the probe, and the protein concentration, pH etc.

In order to function as a fluorophore, a fluorescent molecule must be chemically modified so as to interact with reactive moieties present on biomolecules, and must satisfy certain criteria, in order to be accorded the status of a fluorophore. The probe should: i) possess a high extinction coefficient; ii) have a high quantum yield; iii) be photo-stable; iv) exhibit an optimal excitation wavelength; v) produce little perturbation of the biomolecule; vi) have a large Stokes Shift.

Not all fluorophores associate covalently with the target molecule. Certain fluorophores exist which tend to associate in areas that are attractive, by virtue of the intrinsic nature of the fluorophore. Thus, positively charged fluorophores will associate in areas of negative potential. Similarly, hydrophobic probes will tend to aggregate in areas of low polarity, and planar fluorophores may associate with nucleic acids. These probes can provide much information regarding the nature of the areas they inhabit.

2.13. REFERENCES.

1. Glazer, A.N. & Stryer, L.  
(1984) Trends in Biochem. Sciences (Oct) 423
2. Benson, R.C., Meyer, R.A., Zaruba, M.E. & McKhann, G.M.  
(1979) J. Histochem. Cytochem. 27 44
3. Boyle, R.E.  
(1966) J. Org. Chem. 31 3880
4. Kinoshita, T., Iinuma, F. & Tsuji, A.  
(1974) Anal. Biochem. 61 632
5. Nakaya, K., Yabuta, M., Iinuma, F., Kinoshita, T.  
& Nakamura, Y.  
(1975) Biochem. Biophys. Res. Commun. 67 760
6. Mendelson, R.A., Morales, M.F. & Botts, J.  
(1973) Biochemistry 12 2250
7. Ikkai, T., Wahl, P. & Auchet, J.-C.  
(1979) Eur. J. Biochem. 93 397
8. Takashi, R.  
(1979) Biochemistry 18 5164
9. Eshaghpour, H., Dietrich, A.E., Cantor, C.R. & Crothers, D.M.  
(1980) Biochemistry 19 1797
10. Marsh, D.J. & Lowey, S.  
(1980) Biochemistry 19 774
11. Vanderkooi, J.M., Ierokomas, A., Nakamura, H. & Martonosi, A.  
(1977) Biochemistry 16 1262
12. Taylor, D.L. & Wang, Y.-L.  
(1980) Nature (London) 284 405
13. Wehland, J. & Weber, K.  
(1980) Exp. Cell. Res. 127 397
14. Wang, Y.-L. & Taylor, D.L.  
(1979) J. Cell Biol. 81 672

15. Lin, T.-I.  
(1978) Arch. Biochem. Biophys. 185 285
16. Johnson, J.D.  
(1978) J. Biol. Chem. 253 6451
17. Johnson, J.D., Charlton, S.C. & Potter, J.D.  
(1979) J. Biol. Chem. 254 3497
18. Mercado, E., Carvajal, G., Reyes, A. & Rosado, A.  
(1976) Biology of Reproduction 14 632
19. Machida, M., Machida, M.I. & Kanaoka, Y.  
(1977) Chem. Pharm. Bull. 25 2739
20. Wu, C.-W., Yarbrough, L.R. & Wu, F.-Y.H.  
(1976) Biochemistry 15 2863
21. Graceffa, P. & Lehrer, S.S.  
(1980) J. Biol. Chem. 255 11296
22. Blakeslee, D. & Baines, M.G.  
(1976) J. Immunol. Methods 13 305
23. Axelrod, D.  
(1980) Proc. Natl. Acad. Sci. USA 77 4823
24. Coons, A.H. & Kaplan, M.H.  
(1950) J. Exp. Med. 91 1
25. Neadle, D.J. & Pollitt, R.J.  
(1965) Biochem. J. 97 607
26. Benson, J.R. & Hare, P.E.  
(1975) Proc. Natl. Acad. Sci. USA 72 619
27. Chen, R.F., Scott, C. & Trepman, E.  
(1979) Biochim. Biophys. Acta 576 440
28. Bauminger, S. & Wilchek, M.  
(1980) Meth. Enzymol. 70 151
29. Knauf, P.A. & Rothstein, A.  
(1971) J. Gen. Physiol. 58 190
30. Likhtenshtein, G.I., Grebenshchikov, Y.B., Bobodzhanov, P.K.  
& Kokhanov, Y.V.  
(1970) Mol. Biol. 4 550

31. Horton, H.R. & Tucker, W.P.  
(1970) J. Biol. Chem. 245 3397
32. Lawson, W.B., Gross, E., Foltz, C.M. & Witkop, B.  
(1962) J. Amer. Chem. Soc. 84 1715
33. Kenner, R.A. & Neurath, H.  
(1971) Biochemistry 10 551
34. Guilbault, G.G.  
In Practical Fluorescence: Theory, Methods & Techniques.  
(Ed. Marcel Dekker, New York) pp 230-235 (1973)
35. Carraway, K.L. & Koshland, Jr., D.E.  
(1972) Meth. Enzymol. 25B 616
36. Barker, S.A., Monti, J.A., Christian, S.T., Benington, F.  
& Morin, R.D.  
(1980) Anal. Biochem. 107 116
37. Yasuda, K. & Chilton, W.S.  
(1976) Anal. Biochem. 74 609
38. Takahashi, K.  
(1968) J. Biol. Chem. 243 6171
39. Borders, Jr., C.L., Pearson, L.J., McLaughlin, A.E.,  
Gustafson, M.E., Vasiloff, J., An, F.Y. & Morgan, D.J.  
(1979) Biochim. Biophys. Acta 568 491
40. Vaz, W.L.C. & Schoellmann, G.  
(1976) Biochim. Biophys. Acta 439 194
41. Berliner, L.J. & Shen, Y.Y.L.  
(1977) Thrombosis Res. 12 15
42. Himel, C.M., Abond-Saad, W.G. & Uk, S.  
(1971) J. Agric. Food Chem. 19 1178
43. Berman, H.A. & Taylor, P.  
(1978) Biochemistry 17 1704
44. Berman, H.A., Yguerabide, J. & Taylor, P.  
(1980) Biochemistry 19 2226
45. Dutton, A. & Singer, S.J.  
(1975) Proc. Natl. Acad. Sci. USA 72 2568

46. Pober, J.S., Iwanij, V., Reich, E. & Stryer, L.  
(1978) *Biochemistry* 17 2163
47. Gard, D.L. & Lazarides, E.  
(1979) *J. Cell Biol.* 81 336
48. Schulman, S.G.  
*In Modern Fluorescence Spectroscopy*, Vol. 2.  
(Ed. E.L. Wehry, New York, Plenum Press) pp 239-275 (1976)
49. Thomas, J.A., Buchsbaum, R.N., Zimniak, A. & Racker, E.  
(1979) *Biochemistry* 18 2210
50. Kurtz, I. & Balaban, R.S.  
(1985) *Biophys. J.* 48 499
51. Clement, N.R. & Gould, J.M.  
(1981) *Biochemistry* 20 1534
52. Stryer, L. & Haugland, R.P.  
(1967) *Proc. Natl. Acad. Sci. USA* 58 719
53. Szollosi, J., Tron, L., Damjanovich, S., Helliwell, S.H.,  
Arndt-Jovin, D. & Jovin, T.M.  
(1984) *Cytometry* 5 210
54. Fernandez, S.M. & Berlin, R.D.  
(1976) *Nature* 264 411
55. Taylor, D.L., Reidler, J., Spudich, J.A. & Stryer, L.  
(1981) *J. Cell Biol.* 89 362
56. Theorell, B.  
(1983) *Cytometry* 4 61
57. Bass, D.A., Parce, J.W., Dechatelet, L.R., Szejda, P.,  
Seeds, M.C. & Thomas, M.  
(1983) *J. Immunol.* 130 1910
58. Struli, P., Barrett, A.J., Bauci, A.  
*In Proteinases and Tumour Invasion.*  
(New York, Raven Press) (1980)
59. Koller, E. & Wolfbeis, O.S.  
(1985) *Monatshefte Chemie* 116 65
60. Leytus, S.P., Patterson, W.L. & Mangel, W.F.  
(1983) *Biochemical J.* 215 253

61. Leytus, S.P., Melhado, L.L. & Mangel, W.F.  
(1983) *Biochemical J.* 209 299
62. Dolbeare, F.A. & Smith, R.E.  
(1977) *Clin. Chem.* 23 1485
63. Deamer, D.W., Prince, R.C. & Crofts, A.R.  
(1972) *Biochim. Biophys. Acta* 274 323
64. Abrams, W.R., Diamond, L.W. & Kane, A.B.  
(1983) *J. Histochem. Cytochem* 31 737
65. Verkleij, A.J., Ververgaert, P.H.J., Van Deenen, L.L.M.  
& Elbers, P.F.  
(1972) *Biochim. Biophys. Acta* 288 326
66. Stewart, T.P., Hui, S.W., Portis, Jr., A.R.  
& Papahadjopoulos, D.  
(1979) *Biochim. Biophys. Acta* 556 1
67. Klausner, R.D. & Wolf, D.E.  
(1980) *Biochemistry* 19 6199
68. Greenspan, P., Mayer, E.P. & Fowler, S.D.  
(1985) *J. Cell Biol.* 100 965
69. Darzynkiewicz, Z., Tragonos, F., Kapuscinski, J.,  
Staiano-Coico, L. & Melamed, M.R.  
(1984) *Cytometry* 5 355
70. Kapuscinski, J., Darzynkiewicz, Z. & Melamed, M.R.  
(1982) *Cytometry* 2 201
71. Sims, P.J., Waggoner, A.S., Wang, C.-H. & Hoffman, J.F.  
(1974) *Biochemistry* 13 3315
72. Johnson, L.V., Walsh, M.L., Bockus, B.J. & Chen, L.B.  
(1981) *J. Cell Biol.* 88 526

CHAPTER 3.

cAMP RECEPTOR PROTEIN.

### 3.1. DISCOVERY OF cAMP RECEPTOR PROTEIN.

In 1900, it was found (1) that the bacterial enzyme 'galactozymase' disappeared from cells grown in the presence of glucose. This phenomenon was later referred to as 'catabolite repression.'

A turning point in the understanding of catabolite repression was provided by the finding (2), that adenosine 3',5'-cyclic monophosphate (cAMP) was implicated in catabolite repression. It was found that cAMP attained levels of  $10^{-4}$  M within bacterial cells. In the presence of glucose, the intracellular concentration fell rapidly to  $10^{-7}$  M.

In 1968, two groups of researchers working independently (3,4), found that the repressing effect of glucose on the synthesis of enzymes concerned with the degradation of alternative carbon sources by certain bacteria, particularly *Escherichia coli* (*E. coli*), could be reversed by cAMP. This implied that cAMP is somehow affecting the DNA within the cell. Further investigation (5,6) provided evidence that a protein was implicated in the mechanism of cAMP action. This protein has been referred to as Catabolite Gene-Activator Protein (CAP), but is more widely known as cAMP Receptor Protein (CRP).

### 3.2. LOCATION, ISOLATION & PURIFICATION OF CRP.

It has been shown (7) that CRP is a cytoplasmic protein. This has been achieved using a particular strain of *E. coli* (strain P678-54) which buds to produce DNA-free (that is,

anucleate) minicells. After assay, CRP levels present within the minicells were found to be approximately equal to those found in parent cells. It follows therefore, that CRP is indeed cytoplasmic in origin.

There are from 300 to 1000 copies of CRP per bacterial cell. The high concentration of CRP is a reflection of the large number of genes it affects. Various purification procedures have been utilised (8,9,10) yielding varying degrees of purity and quantity. The most efficient method (11) of purification yielding high levels of pure protein, is outlined as follows:

Frozen *E. coli* cells (50 gm) were suspended in phosphate buffer, pH 7.5. The suspension was homogenised and immediately centrifuged with retention of the supernatant.

The supernatant was applied to a phosphocellulose column which had been previously equilibrated with the phosphate buffer. A linear gradient utilising increasing concentrations of KCl was applied, and eighty 5 ml fractions were collected. The CRP containing fractions were identified and pooled.

The pooled fractions were diluted and applied to an hydroxyapatite column. A linear gradient utilising increasing concentrations of orthophosphoric acid, was applied. Fifty 2 ml fractions were collected and the CRP containing fractions were again identified and pooled.

Subsequent to dialysis against Tris-HCl buffer, pH 8.15, the pooled fractions were then applied to a DNA cellulose-DEAE cellulose column, and the latter was eluted with this buffer. The CRP was seen to be present in the flow-through volume.

Prior to these manipulations, the total quantity of

protein within the crude extract equalled 10365 mg. Subsequent to these purification procedures, the total amount of protein recovered equalled 25.6 mg. Correspondingly, the specific activity of the refined material was 320 times that of the crude material, as deduced using a tritiated cAMP binding assay.

### 3.3. PHYSICAL & CHEMICAL PROPERTIES OF CRP.

CRP migrates on a G-100 Sephadex column as a molecule with a molecular weight of approximately 45000 daltons. After heating in 0.1% w/v sodium dodecyl sulphate (SDS), its electrophoretic migration rate on SDS-polyacrylamide gels indicates a homogeneous species, with a molecular weight of 22000 daltons. Since the heating in SDS step should dissociate a protein into its subunits, it was suggested that CRP is normally a dimer with subunits of approximately 22000 daltons molecular weight each (8).

CRP is a basic protein with an isoelectric point (pI) of 9.2. This high isoelectric point is due to the high glutamine and asparagine content of the protein (12).

### 3.4. THE PRIMARY STRUCTURE OF CRP.

Utilising various genetic techniques, it was found (13,14) that the region of *E. coli* (strain K 12 SG20062) DNA which codes for the CRP molecule, was located in the 930 base-pair region between two particular restriction endonucleases (Hind III and EcoRI). The DNA sequence of this region revealed

that the structural gene of CRP starts 25 nucleotides downstream from the Hind III cleavage site.

Having located the CRP structural gene, it was possible to deduce the amino acid sequence of the protein.

```

-200                                -150
      CCTGACGACCAGGCGGATTGCGCCAGAAAAGTTAACCCCTTCGACCCACTTCACTCGCGCTTGCATTTT
      GGACTGCTGGTCTCCGCCTAAAGCGGGTCTTTTCAATTCCGAAGCTGGGTCAAGTCAGCCGGAACCTAAAAA

      -100                                -50
      GCTACTCCACTGCGTCAATTTTCTGACAGAGTACCGGTACTAACC AAAATCGCGCAACGGAAGGCGACCTGCGTCA
      CGATGAGGTGACCGCAGTAAAAGGACTGTCTCATCGCCATGATTGGTTTAGCGCGTTGCTTCCGCTGGACCCAGTAC
      CACTTCCGCTCTG

      -1+1                                50
      ACCAGGAGACACAAAGCGAAAGCTATGCTTAAACAGTCAGGATGCTACAGTAATACATTGATGTACTGCAATG
      TATGCCAAAGGACGCTCACATGGTCTCTGTGTTCCGCTTTCCTACCGATTTGTCAGTCTACGATGTCATTATG
      TAACTACATGACGTACATACGTTTCCCTCCAGTGT

      100
      TTACCGTGCAGTACAGTTCATAGCCCTTCCCGAGGTAGCGGGAAGCATAATTTGGGCAATCCAGAGACAGCGCG
      GTTATCTGGCTCTCGAG AATGGCAGCTCATGCTCAACTATCGGGGAAGCGTCCATCGCCCTTCGATAAAGCGG
      TTAGGTCCTGTGCGCCGCAATAGACCCGACCTC

      150                                200
      AAAGCTTATAACAGACATAACCCGCCATGGTCTGGCAAACCGCAAACAGACCCGACTCTCGAATGGTCTTCTG
      CATTGCCACATTTCGCAATATTCCTATTGGCGCGTACCACGAAACCGTTTCCGCTTGTCTGGGCTGAGAGCTT
      ACCAAGAACAGAGTAACCGGTCAA

      1      10      20
      ValLeuGlyLysProGlnThrAspProThrLeuGluTroPheLeuSerHisCysHisIle

      250                                300
      CATAAGTACCCATCCAAGAGCACCCCTTATTCACCAGGGTGAAAAGCGGAAACCGCTGTACTACATCGTTAAAG
      GCTCTGTGGCAGTGTGTGTATTCATGCGTAGGTTCTCGTCCCAATAAAGTGTCCACTTTTTCCCTTTCCGACAT
      GATGTAGCAATTTCCGACACCCGTCACGAC

      30      40      50
      HisLysTyrProSerLysSerThrLeuIleHisGlnGlyGluLysAlaGluThrLeuTyrTyrIleValLysGlySer
      ValAlaValLeu

      350                                400
      ATCAAAGACGAAGAGCGGTAAGAAAATGATCCTCTCCTATCTGAATCAGGGTGATTTTATGGCGAACTGGGCT
      GTTTGAAAGAGGGCCAGTAGTTCCTGCTTCTCCCATTTCTTTACTAGGAGAGATAGACTTAGTCCCACATAAAAT
      AACCCCTTCACCCGGACAAAACCTCTCCCGGTC

      50      60      70      80
      IleLysAspGluGluGlyLysGluMetIleLeuSerTyrLeuAsnGlnGlyAspPheIleGlyGluLeuGlyLeuPhe
      GluGluGlyGln

      450                                500
      GAACGTAGCCCATGCGTACGTCGCAAAACCCCTCTGAAGTGGCTCAAATTTCCGTACAAAAAATTTCCGCAAT
      TGATTCAGGTAACCCCTCTTCGCATCGCGTACCCATGCAACGCTTTTGGCGGACACTTCACCGACTTTAAAGCAT
      GTTTTTTAAAGCGGTTAACTAAGTCCATTTCCGGC

      90      100      110
      GluArgSerAlaTrpValArgAlaLysThrAlaCysGluValAlaGluIleSerTyrLysLysPheArgGlnLeuIle
      GlnValAsnPro

      550
      GACATTCGATGCGTTTGTCTGCACAGATGGCGGCTCGTCTGCAAGTCACTTCAGAGAAAGTGGGCAACCTGCG
      GTTCCGACGTTGACGCTGCTAAGACTACGCCAAACAGACGCTGCTACCCGGCAGCAGAGCTTCAGTGAAGTCTCT
      TTCACCCGTTGGACCCGCAAGGAGCTGCACTGC

      120      130      140
      AspIleLeuMetArgLeuSerAlaGlnMetAlaArgArgLeuGlnValThrSerGluLysValGlyAsnLeuAlaPhe
      LeuAspValThr

      600                                650
      GCGCGCATTGCACAGACTCTGCTGAATCTGCCAAAACAACCAGACGCTATGACTCACCCGGACCGGTATGCCAAT
      CAAAATTACCCGTCAGCCGCTAACCTGCTGAGACGACTTAGACCGTTTGTTCGGTCTGGGATACTGAGTGGGCTG
      CCATACGTTTAGTTTTAATGGGCAGTCC

      150      160      170
      GlyArgIleAlaGlnThrLeuLeuAsnLeuAlaLysGlnProAspAlaMetThrHisProAspGlyMetGlnIleLys
      IleThrArgGln

      700                                750
      GAAATTCGTCAGATTCGCGGCTGTTCTCGTGAAAACCGTGGGACCGATTCTGAAGATGCTGGAAGATCAGAACC
      TGATCTCCGCACACCGTCTTTAACCCAGTCTAACAGCCGACAAGACACTTTGGCACCCCTCCGTAAGACTTCTAC
      GACCTTCTAGTCTTTGGACTAGACCGGCTGTGCCA

      180      190      200
      GluIleGlyGlnIleValGlyCysSerArgGluThrValGlyArgIleLeuLysMetLeuGluAspGlnAsnLeuIle
      SerAlaHisGly

      800                                850
      AAAACCATCTGCTTTTACCGCACTCGTTATCCCGTCCGAGTGGCGGTTACCTGGTAGCGCGCCATTTTGTIT
      TCCCGCGATGTGGCGCATTTTGGTAGCAGCAAATCCGTGACCAATTAGGGCAGCCTCACCCCGCAATCGACCAT
      CGCCCGGTAACAACAAGGGGGCTACACCCCGT

      209
      LysThrIleValValTyrGlyThrArgEND

      900
      GACTGATTTATCACCCCGATATCAACTATGCACCTTCGACAAAACCC
      CTGACTAAAATAGTCCGGCTATAGTTGATACCTGAAGCTGTTTCCG
  
```

Fig. 3.1. The Primary Structure of CRP (13).

The CRP structural gene spans a region of 627 nucleotides which corresponds to a polypeptide chain containing 209 amino acids. The molecular weight was found to be 23619 daltons. It may be seen from the primary structure that the CRP molecule is rich in both lysine and cysteine amino acid residues. This characteristic renders the molecule readily amenable to fluorescent modification.

The translation of CRP is terminated with an arginine codon at base pair 627, which is followed by an ochre codon TAA. About 30 base pairs downstream from the termination codon, there is a guanine-cytosine (G-C) rich inverted repeat sequence followed by a run of thymine (T) nucleotides. The transcription is thought to terminate somewhere in the thymine cluster.

### 3.5. THE SECONDARY STRUCTURE OF CRP.

The three-dimensional structure of CRP has been obtained by X-ray diffraction studies of crystals (15,16). The crystals, which are orthorhombic, were obtained in the presence of 0.5 mM cAMP.

It was found that the CRP monomer has two distinct structural domains. The amino-terminal domain, which has the overall dimensions of 25 x 30 x 35 Å, comprises approximately two-thirds of the monomer, binds cAMP, and forms the subunit-subunit contacts in the CRP dimer. As intimated earlier, the CRP molecule binds to DNA and the smaller carboxyl-terminal domain has been implicated in this action (17). The CRP dimer is asymmetric, and the asymmetry is a result of different relative orientations of the large and small domains in the

two subunits. One subunit is in an 'open' conformation, while the other is 'closed.'

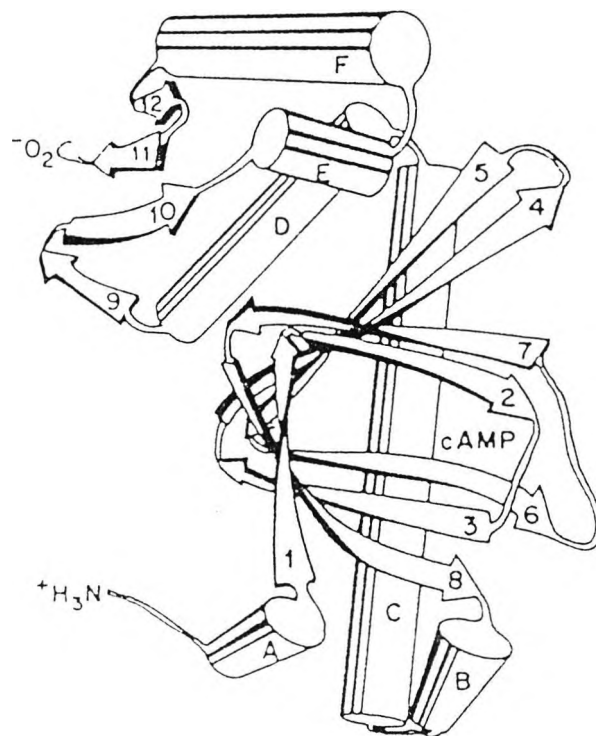


Fig. 3.2. Schematic diagram of the CRP monomer showing the regions that are in  $\alpha$ -helix and  $\beta$ -sheet conformation (15).

The  $\alpha$ -helices are lettered A-F and the  $\beta$ -strands are numbered 1-12. Overall, approximately 35-40% of the molecule is well defined  $\alpha$ -helix, and an equal fraction, 35-40%, is in antiparallel  $\beta$ -sheet conformation. The regions between the D and E helices and following the F helix, appear to be two pairs of short antiparallel  $\beta$ -strands. The pair between the D and E helices is labelled  $\beta_9$  and  $\beta_{10}$  and the two carboxyl-terminal strands are designated  $\beta_{11}$  and  $\beta_{12}$ .

A. <i><math>\alpha</math>-Helices</i>			
A	9-18	D	140-151
B	99-110	E	168-176
C	112-133	F	180-191
B. Strands forming $\beta$ -roll		C. $\beta$ -Sheet in small domain	
Strand	Residues	Strand	Residues
1	19-23	9	157-160
2	(26) 27-32 (33)	10	161-165
3	34-42 (43)	11	195-199
4	(46) 48-52	12	201-205
5	58-64 (66)		
6	68-70		
7	(79) 77-88 (89)		
8	90-98 (99)		

Table 3.1. The amino acid sequences spanning each area of secondary structure (18).

### 3.5.1. The $\beta$ -Roll Structure.

The amino-terminal (large) domain spans residues 1 to 129. Since a major feature of the domain is the antiparallel  $\beta$ -roll, the large domain is, therefore, most appropriately classified as an antiparallel  $\beta$ -structure. The  $\beta$ -roll in CRP contains a pocket which forms a major part of the cAMP binding site. The antiparallel  $\beta$ -roll of CRP, which includes residues 19-99, is a relatively compact structure, as there are only two short loops (residues 52-60 and 72-80) which diverge from the  $\beta$ -fold. The loop spanning residues 72-80 appears to be involved in subunit-subunit interactions.

The antiparallel ribbon would first form when a kink around amino acid residue 55, which allows residues 19 to 54 to align with residues 56 to 99. The ribbon would then curl up to form the eight-stranded supercoiled structure with hydrogen-bonds formed across four adjacent strands.

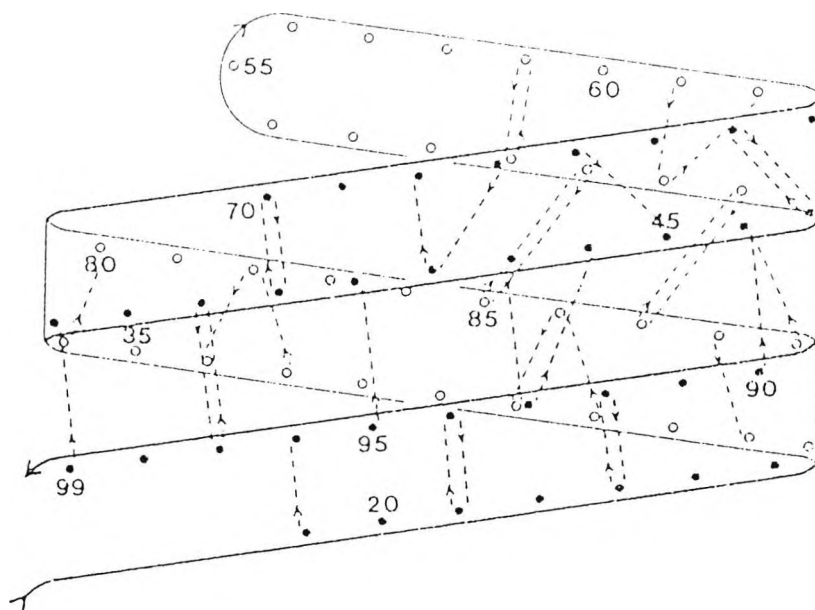


Fig. 3.3. An idealised view of the  $\beta$ -roll (18).

In general,  $\beta$ -strands tend to be mainly composed of polar amino acid residues near the ends, while the centre is rich in non-polar residues. In the case of CRP, the  $\beta$ -strands do not have an alternating polar/non-polar sequence; as there are several polar side-chains directed towards the interior of the structure, and several non-polar side-chains on the exterior surface.

### 3.5.2. The Hinge Region Structure.

The large and small domains are connected by a single covalent stretch of polypeptide that constitutes residues 130 to 138. The conformation of this polypeptide is different in each subunit, and provides a hinge region between each domain. Although a distinct cleft is present between the two domains of the CRP subunit, non-covalent interactions occur between them. These interactions are thought to stabilise the

relative orientations of the domains in each subunit.

The 'closed' subunit contains a non-helical region, composed of amino acids 133 to 138, between  $\alpha$ -helices C and D; while the non-helical region in the 'open' subunit consists of residues 130 to 138.

Several hydrogen-bonding interactions occur within the hinge region, as well as the hydrogen-bonds formed at the carboxyl-terminus of the C helix, and between the hinge and the amino-terminus of the D helix. The hinge region of the 'closed' subunit also provides further interactions with the small domain; amino acids Lys-130 to Ala-135 are close to Arg-142 and Gln-145 of the D helix, and Ile-175 to Val-176 of the E helix. There are hydrogen-bonds between the carbonyl group derived from Leu-134 and the amino group of Arg-142, and between the amino group of Asn-133 and the oxygen atom present in the amide side-chain of Gln-145 (18).

### 3.5.3. Interdomain Interactions.

The major contact region between the two domains within the CRP monomer, is between the strand  $\beta_5$  of the large domain and the E helix of the small domain.

The 'closed' subunit has hydrogen-bond interactions between residues 58 to 63 and 171 to 175, while in the 'open' subunit, the peptide backbone between residues 58 to 60 in the large domain appears to be within contact distance of the peptide backbone, at residue 174 in the small domain.

In the 'closed' subunit, there appears to be a network of polar side-chains that includes Lys-57, Glu-58, Lys-89,

Lys-130, Gln-170, Glu-171, Gln-174 and Arg-180. Three hydrogen-bonds are thought to be formed: between the side-chains of Glu-58 and Gln-174, the backbone interaction between the N-H group of Ile-60 and the carbonyl group of Gln-174, and between the side-chains of Tyr-63 and Glu-171. This last interaction occurs only in the 'closed' subunit. In the 'open' subunit, Tyr-63 and Glu-171 are too far apart ( $4.04 \text{ \AA}$ ).

As previously mentioned, the CRP dimer is asymmetric. In one subunit, the two domains form an 'open' cleft. The small domain of this 'open' subunit is packed tightly against a neighbouring molecule in the crystal. The other subunit is in a 'closed' conformation with the two domains more closely packed, and has no extensive contact between its small domain and a neighbouring molecule.

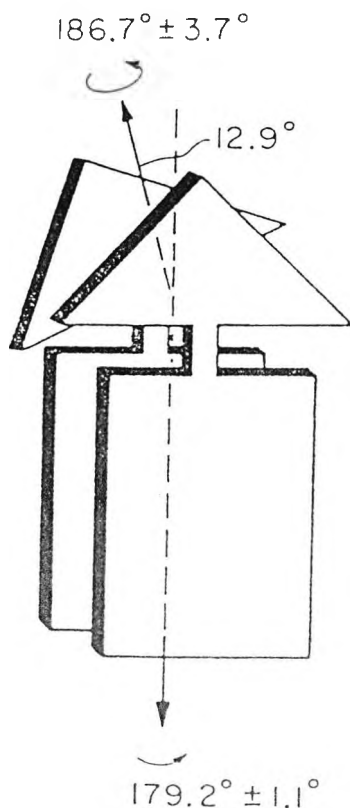


Fig. 3.4. Schematic diagram of the molecular symmetry of the CRP dimer. The rectangles represent the large amino-terminal domain, the triangles show the small carboxyl-terminal domain (16).

In addition to the contact between strand  $\beta_5$  and the E helix, the subunit in the 'closed' conformation has a second region of contact between the large and small domains. The second possible contact occurs between Asn-65 of strand  $\beta_5$  and Gln-153 between the D helix and strand  $\beta_9$ .

Although the relative proportion of polar and non-polar residues is approximately equal for the large and small domains, certain amino acids are distributed asymmetrically within the structure. Most of the aromatic residues are in the large domain: only two of the six histidine residues and one of the six tyrosine residues are found in the small domain, while one phenylalanine residue is found in the hinge region. Only two of the ten aromatic side chains in the antiparallel  $\beta$ -roll are on the interior of the roll, while the others lie on the exterior surface.

The specific function of some of the arginine residues is clear. Arg-103 may form a salt bridge to Glu-78 in the loop between strands  $\beta_6$  and  $\beta_7$ . Arg-123 forms an internal salt bridge to Asp-68 and Glu-72 in the interior of the  $\beta$ -roll. Arg-115 and Arg-122 are relatively accessible to solvent in the molecule.

#### 3.5.4. The Carboxyl-Terminal Domain Structure.

The carboxyl-terminal (small) domain, which has dimensions of 20 x 20 x 30  $\overset{\circ}{\text{A}}$ , includes residues 136 to 209, and is composed predominantly of three  $\alpha$ -helices (labelled D, E and F) and a short  $\beta$ -sheet; hence it may be classed as an antiparallel  $\alpha$ -domain. The small domain is a relatively open structure, with an apparent pocket between the 24  $\overset{\circ}{\text{A}}$  long D helix and the

E and F helices. The F helix is 22 Å long.

Several surface residues in the carboxyl-terminal domain form interactions with symmetry-related molecules in the crystal. In the 'closed' subunit, these residues are Asp-138, Arg-169, Thr-182, Lys-183, Gln-193 and Lys-201. In the carboxyl-terminal domain of the 'open' subunit, only the carbonyl group derived from Pro-160, Arg-185 and Asn-194, form such polar crystal packing interactions.

### 3.5.5. Intersubunit Interactions.

All of the subunit-subunit interactions in the CRP dimer are between the two large domains. A major source of subunit-subunit contact in the CRP dimer is provided by the two 17-residue long C helices which span residues 112 to 129, and extend the full length of the large domains. The helices terminate in the hinge region between the two domains, and are packed with an interhelical angle of approximately  $20^{\circ}$  and have a slight superhelical twist, allowing contact between them along their entire length.

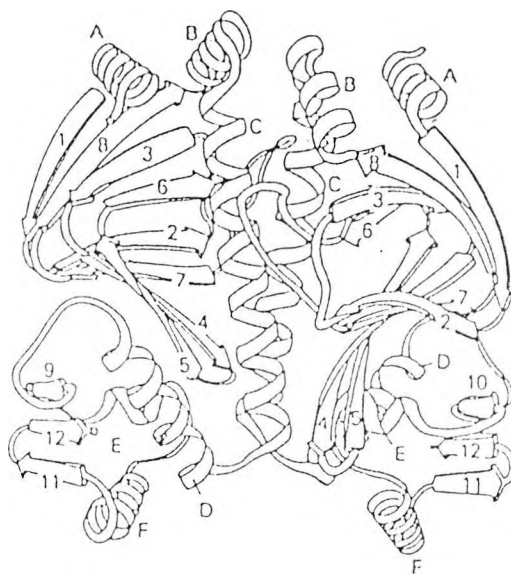


Fig. 3.5. The CRP Dimer (19).

Further subunit-subunit contacts are provided by a part of the  $\beta$ -roll of one subunit interacting with the 40 Å long C helix of the opposite subunit. Specifically, strands  $\beta_4$ ,  $\beta_5$ , the loop between  $\beta_6$  and  $\beta_7$  and strand  $\beta_7$  appear to form intersubunit contacts.

Most of the interactions between the subunits are hydrophobic, only two hydrogen-bonds are formed symmetrically between both subunits of the dimer. These are between the two Ser-117 side chains, and between Ser-128 and the cAMP molecule when the latter is bound.

### 3.6. BINDING OF THE cAMP MOLECULE TO CRP: MECHANISM OF ACTION.

In solution, cAMP exists in two conformational states. It may either exist in the 'anti' or 'syn' conformations. The 'anti' state accounts for approximately 70%, while the remainder is present in the 'syn' conformation (20).

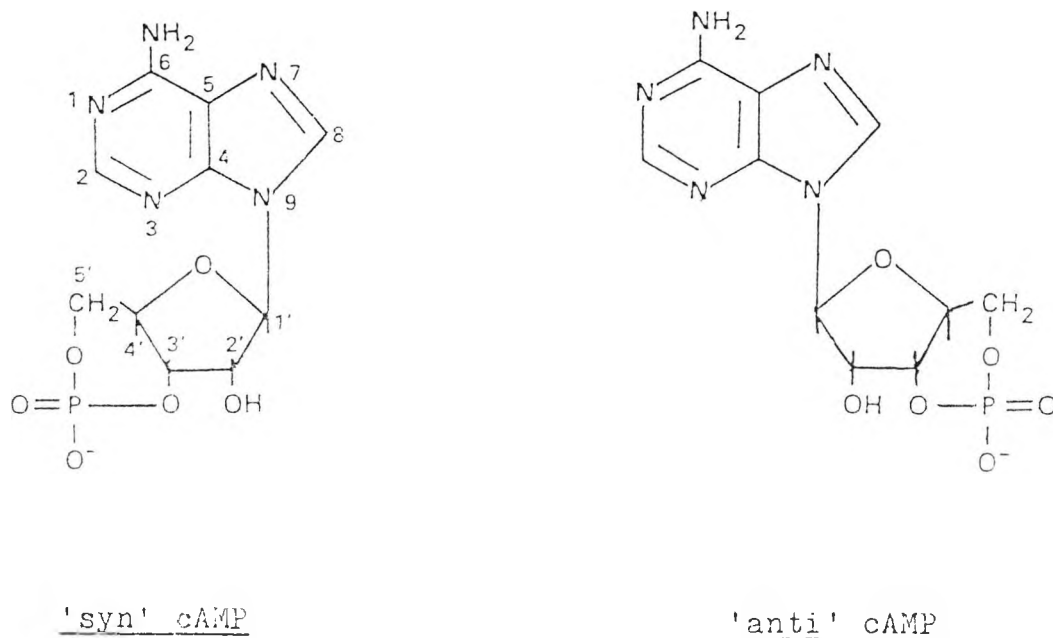


Fig. 3.6. Structures of 'syn' & 'anti' cAMP.

Despite early confusion concerning which conformational state of cAMP binds to CRP (21), it appears from crystallographic evidence (18), that cAMP in the 'anti' conformation binds to CRP.

Using the equilibrium dialysis technique to study the binding of cAMP to pure CRP, under various conditions of temperature, ionic strength (KCl) and pH, it has been categorically shown (17), that two binding sites for cAMP exist in dimeric CRP. At pH 8.0 and 20°C, using a concentration range of cAMP from  $2 \times 10^{-6}$  M to  $5 \times 10^{-4}$  M, two molecules of cAMP bind per CRP molecule. At low ionic strength, the co-operativity of cAMP binding is negative and becomes progressively positive as the ionic strength is increased. This negative co-operativity may be explained by the asymmetric dimer observed in the crystal structure.

The cAMP molecule is bound between the deep  $\beta$ -roll pocket and the C helix of the large domain in such a way, that it interacts with amino acid side-chains from both subunits of the dimer. The cAMP is bound with its phosphoribose moiety adjacent to strands 6 and 7 of the  $\beta$ -roll, and its adenine ring oriented toward the pair of C helices in the dimer interface.

Each part of the cAMP molecule is stabilised by hydrogen-bonding and non-polar contacts with the protein. Amino acid residues Ile-30, Val-49, Leu-61 to Leu-64 and Arg-82 to Val-86 from the  $\beta$ -strands, and residues Ile-70 to Leu-73 of the loop between strands  $\beta_6$  and  $\beta_7$  contribute to the cAMP-binding pocket.

Three of the eighteen nearest side chains are charged:

Glu-72, Arg-82 and Arg-123. The guanidinium group of Arg-123 is between the carboxyl groups of Asp-68 and Glu-72, and hence appears to form an interior salt bridge between the  $\beta$ -roll and the C helix. The phosphate group interacts with the guanidinium group of Arg-82, and the hydroxyl group of Ser-83 from strand 7 of the  $\beta$ -roll.

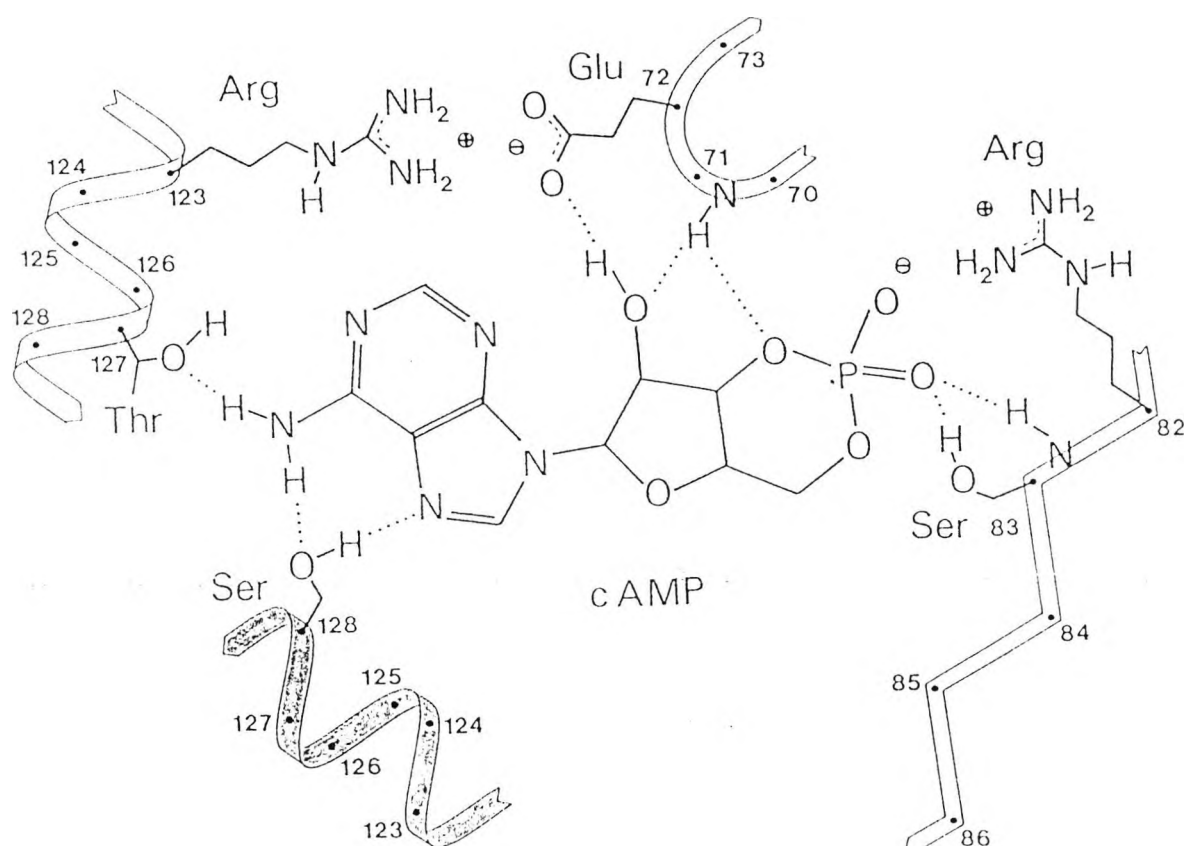


Fig. 3.7. A schematic representation of the cAMP binding sites in the CRP crystal structure. The hydrogen bonds are indicated as dotted lines, and charged groups that form ionic interactions are shown. The lower shaded  $\alpha$ -helix is from the adjacent subunit in the CRP dimer (18).

The 2'OH group of the ribose moiety is bound to the carboxyl side chain of Glu-72 and via the N-H group derived from the peptide bond between Ile-70 and Gly-71. The adenine ring interacts with residues from the two C helices; Thr-127

of the subunit in which the cAMP is bound, makes contact with the 6-amino group of the adenine ring; and Ser-128 from the opposite subunit interacts with the 6-amino group and 7-N atom of the adenine ring. Since opposite sides of the C helices face different subunits, side chains from each helix alternate between the two adenine rings from opposite subunits: Arg-123, Val-126 and Thr-127 are close to the cAMP molecule in one subunit, while Leu-124 and Ser-128 from the same helix interact with the cAMP molecule of the second subunit. The involvement of residues from both subunits in binding each cAMP molecule reinforces the theory of co-operative interactions (17).

The amino acid residues 71 to 73 form a bend into which the 2'OH group fits. The residues forming the cAMP binding pocket are stabilised by the hydroxyl group of Tyr-99, which forms hydrogen-bonds with the side-chain of Arg-82 and the carboxyl oxygen of Gly-71.

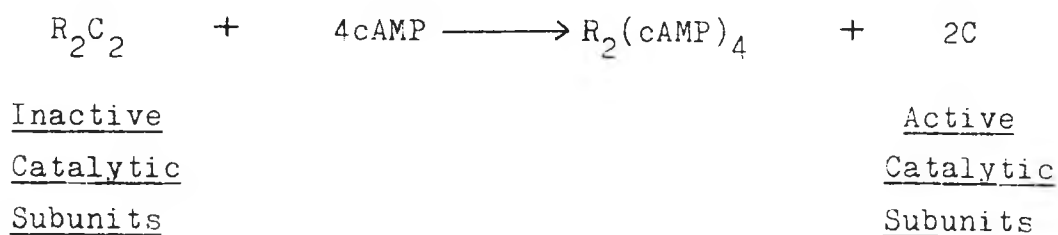
As intimated earlier, cAMP in the 'anti' conformation appears to bind to CRP. This contention is reinforced by visualising the interactions between 'syn' cAMP and the protein. If the adenine ring is rotated into the 'syn' conformation, there are bad contacts with Ser-128 within the 'open' subunit, and Ser-83 in the 'closed' subunit is too close. Thr-127 is too far from the N-6 atom of the adenine ring, to form a hydrogen-bond (18).

### 3.7.           HOMOLOGY BETWEEN CRP AND THE REGULATORY SUBUNIT                   OF cAMP-DEPENDENT PROTEIN KINASE.

It is clear that the action of cAMP is mediated by CRP

in prokaryotes. However, in eukaryotes, CRP is replaced by a protein kinase whose properties are mediated by cAMP.

cAMP-dependent protein kinase obtained from beef heart (isoenzyme II) has been isolated and characterised (22). The intact protein (holoenzyme) is inactive, consisting of two catalytic subunits and two regulatory subunits. In the presence of cAMP, the protein dissociates into two active catalytic subunits and a dimer of two regulatory subunits that are complexed with four cAMP molecules.



The active catalytic subunits may then perform their biological function of transferring phosphate from ATP to various protein substrates.

One regulatory unit from isoenzyme II ( $R_{II}$ ) is composed of 400 amino acids, and has a molecular weight of 56000 daltons. It appears to be composed of three domains: a small amino-terminal domain, a large carboxyl-terminal domain, and a region between these structures which probably interacts with the catalytic subunit within the holoenzyme. The carboxyl-terminal fragment, which appears to contain internal sequence homology between residues 135-256 and 257-400, may bind one cAMP molecule within each of these regions.

It has been shown (23) that there are homologous sequences between CRP and  $R_{II}$  which suggests that the cAMP-

binding domain is a conserved structure between the two cAMP-dependent proteins.

The best alignments of the two homologous domains of  $R_{II}$  ( $R_{II}A$  and  $R_{II}B$ ) with the CRP sequence, are as shown.

	$\alpha A$										$\beta 1$										$\beta 2$																																	
CRP	10	THR	LEU	GLU	TRP	PHE	LEU	SER	HIS	CYS	HIS	ILE	HIS	LYS	TYR	PRO	SER	LYS	SER	THR	LEU	ILE	HIS	GLN	GLY	GLU	20	ILE	HIS	LYS	TYR	PRO	SER	LYS	SER	THR	LEU	ILE	HIS	GLN	GLY	GLU	30	LEU	ILE	HIS	GLN	GLY	GLU					
R11A	143	GLN	LEU	SER	GLN	VAL	LEU	ASP	ALA	MET	PHE	GLU	ARG	THR	VAL	LYS	VAL	ASP	GLU	HIS	VAL	ILE	ASP	GLN	GLY	ASP	150	ALA	MET	PHE	GLU	ARG	THR	VAL	LYS	VAL	ASP	GLU	HIS	VAL	ILE	ASP	GLN	GLY	ASP	160	GLU	HIS	VAL	ILE	ASP	GLN	GLY	ASP
R11B	265	GLU	ARG	MET	LYS	ILE	VAL	ASP	ALA	ILE	GLY	GLU	LYS	VAL	TYR	LYS	ASP	GLY	GLU	ARG	ILE	ILE	THR	GLN	GLY	GLU	270	ALA	ILE	GLY	GLU	LYS	VAL	TYR	LYS	ASP	GLY	GLU	ARG	ILE	ILE	THR	GLN	GLY	GLU	280	GLU	ARG	ILE	ILE	THR	GLN	GLY	GLU

	$\beta 3$										$\beta 4$																																								
CRP	40	LYS	ALA	GLU	THR	LEU	TYR	TYR	ILE	VAL	LYS	GLY	SER	VAL	ALA	VAL	LEU	ILE	LYS	ASP	GLU	GLU	GLY	LYS	GLU	MET	50	VAL	ALA	VAL	LEU	ILE	LYS	ASP	GLU	GLU	GLY	LYS	GLU	MET											
R11A	170	ASP	GLY	ASP	ASN	PHE	TYR	VAL	ILE	GLU	ARG	GLY	THR	TYR	ASP	ILE	LEU	VAL	THR	LYS	ASP	ASN	GLN	THR	ARG	SER	180	VAL	ALA	VAL	LEU	ILE	LYS	ASP	GLU	GLU	GLY	LYS	GLU	MET											
R11B	290	LYS	ALA	ASP	SER	PHE	TYR	ILE	ILE	GLU	SER	GLY	GLU	VAL	SER	ILE	LEU	ILE	LYS	ASP	GLY	GLU	ASN	GLN	GLU	VAL	300	GLY	THR	TYR	ASP	ILE	LEU	VAL	THR	LYS	ASP	ASN	GLN	THR	ARG	SER	307	THR	LYS	ASP	ASN	GLN	THR	ARG	SER

	$\beta 5$										$\beta 6$										$\beta 7$																													
CRP	60	ILE	LEU	SER	TYR	LEU	ASN	GLN	GLY	ASP	PHE	ILE	GLY	GLU	LEU	GLY	LEU	PHE	GLU	GLU	GLY	GLN	GLU	ARG	SER	ALA	70	GLY	ASP	PHE	ILE	GLY	GLU	LEU	GLY	LEU	PHE	GLU	GLU	GLY	GLN	GLU	ARG	SER	ALA	80	GLU	ARG	SER	ALA
R11A	200	VAL	GLY	GLN	TYR	ASP	ASN	HIS	GLY	SER	PHE	GLY	GLU	LEU	ALA	LEU	MET	TYR	ASN	THR	PRO	ARG	ALA	ALA	210	GLY	ASP	PHE	ILE	GLY	GLU	LEU	GLY	LEU	PHE	GLU	GLU	GLY	GLN	GLU	ARG	SER	ALA	220	THR	PRO	ARG	ALA	ALA	
R11B	330	GLU	ILE	ALA	ARG	CYS	HIS	LYS	GLY	GLN	TYR	PHE	GLY	GLU	LEU	ALA	LEU	VAL	THR	ASN	LYS	PRO	ARG	ALA	ALA	340	GLY	SER	PHE	GLY	GLU	LEU	ALA	LEU	MET	TYR	ASN	THR	PRO	ARG	ALA	ALA	350	THR	PRO	ARG	ALA	ALA		

	$\beta 8$										$\alpha B$																																						
CRP	90	TRP	VAL	ARG	ALA	LYS	THR	ALA	CYS	GLU	VAL	ALA	GLU	ILE	SER	TYR	LYS	LYS	PHE	ARG	GLN	LEU	ILE	GLN	VAL	ASN	100	VAL	ALA	GLU	ILE	SER	TYR	LYS	LYS	PHE	ARG	GLN	LEU	ILE	GLN	VAL	ASN						
R11A	220	THR	ILE	VAL	ALA	THR	SER	GLU	GLY	SER	LEU	TRP	GLY	LEU	ASP	ARG	VAL	THR	PHE	ARG	ARG	ILE	ILE	VAL	LYS	ASN	230	VAL	ALA	GLU	ILE	SER	TYR	LYS	LYS	PHE	ARG	GLN	LEU	ILE	GLN	VAL	ASN	240	THR	PRO	ARG	ALA	ALA
R11B	350	SER	ALA	TYR	ALA	VAL	GLY	ASP	VAL	LYS	CYS	LEU	VAL	MET	ASP	VAL	GLN	ALA	PHE	GLU	ARG	LEU	LEU	GLY	PRO	CYS	360	VAL	ALA	GLU	ILE	SER	TYR	LYS	LYS	PHE	ARG	GLN	LEU	ILE	GLN	VAL	ASN	370	THR	PRO	ARG	ALA	ALA

	$\alpha C$																																																	
CRP	110	PRO	ASP	ILE	LEU	MET	ARG	LEU	SER	ALA	GLN	MET	ALA	ARG	ARG	LEU	GLN	VAL	THR	SER	GLU	LYS	VAL	GLY	ASN	LEU	120	GLN	MET	ALA	ARG	ARG	LEU	GLN	VAL	THR	SER	GLU	LYS	VAL	GLY	ASN	LEU	130	GLY	ASN	LEU			
R11A	250	ASN	ALA	LYS	LYS	ARG	LYS	MET	PHE	GLU	SER	PHE	ILE	GLU	SER	VAL	PRO	LEU	LEU	LYS	SER	LEU	GLU	VAL	SER	GLU	260	GLN	MET	ALA	ARG	ARG	LEU	GLN	VAL	THR	SER	GLU	LYS	VAL	GLY	ASN	LEU	265	GLY	ASN	LEU			
R11B	380	MET	ASP	ILE	MET	LYS	ARG	ASN	ILE	SER	HIS	TYR	GLU	GLU	GLN	LEU	VAL	LYS	MET	PHE	GLY	SER	SER	MET	ASP	LEU	390	GLN	MET	ALA	ARG	ARG	LEU	GLN	VAL	THR	SER	GLU	LYS	VAL	GLY	ASN	LEU	395	GLY	SER	SER	MET	ASP	LEU

Fig. 3.8. Alignment of two adjacent regions of the  $R_{II}$  sequence with the CRP sequence. Solid underlining indicates amino acids that are identical to one or more residues in the other sequences; dashed underlining indicates closely similar amino acids. Amino acids that are close to cAMP in CRP are indicated by an asterisk (23).

The homology is most apparent over a region of CRP residues 30-89, that includes  $\beta$ -strands 3-7, parts of  $\beta$ -strand 2, and  $\beta$ -strands 6 and 7. In the first homologous region, there are 18 identical and 9 homologous amino acids in this stretch of 60 residues, giving a total homology of 45%. In the second homologous region of R<sub>II</sub>, there are 23 identical and 5 homologous amino acids or 46.7% total homology. There is also extensive homology between R<sub>IIA</sub> and R<sub>IIB</sub>.

There is also some evidence of homology over a larger region from CRP  $\alpha$ -helix A through the eight  $\beta$ -strands to  $\alpha$ -helix B. The larger region; CRP residues 10-106 has 39.2% homology with residues 143-237 of R<sub>II</sub>, and 35.1% homology with the R<sub>II</sub> region comprising residues 265-367 in the carboxyl-terminal domain. It has been calculated that the statistical chance of homology over 60 residues is 14.2%, so these percentages of corresponding residues are very significant.

In view of the relationship between the two proteins, it appears that a common ancestral precursor protein capable of binding cAMP, has evolved into the appropriate receptor or transducer of cAMP levels in both bacteria and mammals. In prokaryotes, CRP interacts with DNA, while in mammals, cAMP-dependent protein kinase (when activated by cAMP) is involved in numerous intracellular processes, one of which is the participation in the first enzymatic reaction in a cascade which results in the breakdown of glycogen.

3.8. EVIDENCE FOR A CONFORMATIONAL CHANGE ELICITED  
IN CRP BY cAMP.

Since the cAMP molecule, on binding, makes numerous hydrogen-bonds as well as polar and non-polar interactions with the CRP, it may be deduced that the cAMP molecule elicits a conformational change in the protein.

In the absence of cAMP, CRP is resistant to attack by chymotrypsin and other proteases. Binding of cAMP alters the conformation of CRP, allowing for proteolytic attack on the carboxyl-proximal region. The resulting cores remain dimeric and bind cAMP, but no longer bind to DNA (10).

The stability of free CRP to chymotrypsin indicates that there is a stable interaction between regions of the amino-proximal and carboxyl-proximal polypeptides. When CRP is denatured by sodium dodecyl sulphate, one peptide bond (between Trp-85 and Val-86) inaccessible in free CRP, is hydrolysed by chymotrypsin resulting in the formation of the amino-proximal 9500 dalton fragment and the 13000 dalton carboxyl-proximal fragment (24).

CRP will only crystallise in the presence of cAMP (15), it follows, therefore, that free CRP and the CRP-cAMP complex must have different structures. As a result, the secondary structure of free CRP has not been fully determined.

However, the computer molecular model of free CRP, utilising the primary structure, has been deduced (25). It was found that only 23% homology was present in the amino-terminal domain between the free CRP and the CRP-cAMP complex. The computer programme used predicted an extremely long region comprising residues 68-108, with a strong propensity

to helix formation. Only a few terminal residues of this region have been observed to form helix in crystal; while in the rest of this region, the polypeptide chain folded into three consecutive sheets that are essential to create the pocket for cAMP binding. It was proposed that two different conformations of the same protein were being observed, and that cAMP binding elicits the change. This idea seemed likely, given that cAMP induces a conformational change in the protein on binding. Further support for this proposal, was gained from the fact that most contacts of cAMP with CRP fall in the 68-108 region.

Thus, free CRP seems to contain a long  $\alpha$ -helix comprising residues 68-108. Since helix 111-134 (part of  $\alpha$ -helix C), makes important contacts with the cAMP molecule, it is thought that cAMP first binds to it. This binding may destabilise helix 68-108 instead of which a  $\beta$ -roll is formed to create the hydrophobic pocket, into which the cAMP molecule fits.

Studies utilising mutant CRP molecules that have single amino acid alterations, have further elucidated the mechanism of CRP-cAMP interaction (26,27). These single mutations render the CRP molecule cAMP-independent, that is, cAMP is not necessary for the protein to bind to specific sites on DNA.

In the wild-type protein, glycine-141 in helix D of the carboxyl-terminal domain, is on the side that would be facing helix C of the amino-terminal domain, across the hinge. If this amino acid is replaced by a serine residue, an amino acid side chain would be present that is longer and more polar. This substitution, which renders the CRP molecule cAMP-

independent is thought, therefore, to alter either the distance or the orientation relationship between the two helices.

If, in this mutant, threonine-127 is replaced by an alanine residue, the cAMP-dependence of this mutant is partially restored. Since the hydroxyl group of threonine-127 in the wild-type molecule forms a hydrogen bond with the 6-amino group of cAMP; replacement by alanine would not allow this interaction to occur. Since the mutant can still be activated by cAMP, it is presumed that this interaction is not an essential part of the cAMP-induced conformational change, necessary for binding to DNA. This indicates that threonine-127 has a different role; because of the proximity of this amino acid to those of the other subunit (particularly serine-128), it is likely that threonine-127 is involved in subunit-subunit alignment. Substitution of alanine at position 127 prevents proper subunit-subunit alignment. cAMP can compensate for this by making additional amino acid contacts.

Alanine at position 144 in the wild-type CRP, is also present in helix D of the carboxyl-terminal domain; but faces away from helix C toward helix F of the carboxyl-terminal portion of the protein. Helix F is thought to interact with the DNA molecule. Substitution of this amino acid by a threonine residue, produces a modified protein which has a larger side group than does the wild-type. It is proposed that the larger side group of threonine in the mutant, pushes helix F away from the main body of the protein.

If, in this mutant, residues arginine-169 and glutamic acid-171 in helix E are replaced by other amino acids, the

cAMP-dependence is restored. It is thought that this loss of cAMP-independence is due to the amino- and carboxyl-terminal domains not aligning properly, with respect to each other. Since cAMP can restore the biological function of the mutant, it is thought that the cAMP molecule makes contact with amino acids in  $\beta$ -strands 2 and 7, which, as previously mentioned, are located in the amino-terminal domain but toward the carboxyl-terminal domain. It is proposed that such contacts help the  $\beta$ -sheets shift closer to the carboxyl-terminal domain, helping an interaction between the two domains.

In a particular mutant whereby threonine-127 is replaced by isoleucine, and glutamine-170 is replaced by lysine, these substitutions result in low cAMP-independent activity. If this mutant is subjected to a further amino acid substitution, where arginine-195 is replaced by leucine, the protein is endowed with high cAMP-independent activity. Since residue 195 is not present within the cAMP-binding site, this finding reinforces the proposal that cAMP plays a part in alignment of the two domains within each subunit.

Studies have been performed (28) using guanosine 3',5'-cyclic monophosphate (cGMP) and several other structural analogues of cAMP, to determine whether they elicit a similar response to cAMP with regard to CRP.

cGMP was found to bind to CRP with comparative affinity respective to cAMP, but failed to bring about a conformational change, and the CRP-cGMP complex produced would not bind specifically to DNA.

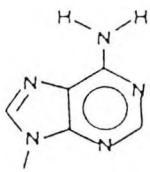
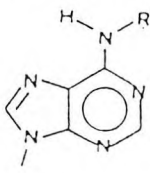
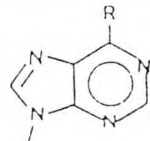
		Binding	Allostery	Activity
cAMP		+++	+++	+++
N-6-substituted	 R = -CH <sub>2</sub> CH <sub>3</sub> -CH <sub>2</sub> CH <sub>2</sub> CH <sub>2</sub> CH <sub>3</sub> -C <sub>6</sub> H <sub>5</sub> -CH <sub>2</sub> C <sub>6</sub> H <sub>5</sub> -CH(CH <sub>3</sub> )CH <sub>2</sub> C <sub>6</sub> H <sub>5</sub> -CH(CH <sub>3</sub> )CH <sub>2</sub> CH <sub>2</sub> C <sub>6</sub> H <sub>5</sub>	+++ +++ ++++ +++ ++++ ++++	++ +++ +++ ++ ++++ ++++	- - - - - -
C-6-substituted	 R = -H -CL -OCH <sub>3</sub> -N(CH <sub>3</sub> ) <sub>2</sub>	++ ++ ++ ++++	- - - -	- - - -

Fig. 3.9. Summary of the effects on CRP of ten cAMP analogues. Results of the assays of binding, conformational effects (allostery) and transcription (activity) are shown. + + + denotes an effect roughly equal to that of cAMP; + denotes a weak but definite effect; - denotes no effect (28).

Those cAMP analogues substituted at the N-6 position, bound to the CRP and produced a conformational change. However, the complex produced would not bind specifically to DNA. This indicates that the conformational change elicited by these analogues, does not parallel that observed with cAMP.

Those analogues substituted at the C-6 position also bound to the CRP but, in this case, failed to elicit a conformational change, and the complex produced would not

specifically interact with DNA. It was also found that 2'-deoxy-cAMP (that is, the 2'OH group is absent), failed to bind to CRP.

These findings indicate that the 6-amino group of the adenine ring must be present, in order to produce the conformational change within the protein, and subsequent binding of the complex to DNA. Further, it appears that the 2'OH group of the ribose moiety, must be present to allow binding to the protein.

Moreover, cAMP must induce CRP to assume more than one conformational state (29). Thus, CRP must exist in at least three conformational states, two of which are cAMP-dependent. At high cAMP concentrations, the CRP molecule has properties resembling the free protein. It has been found that binding of the first cAMP molecule, is approximately one to two orders of magnitude stronger than the second one. Thus, there is interaction between the sites and there is negative co-operativity in binding. Since there is interaction between the cAMP binding sites, the simplest model to fit these data, would be the existence of three ligation and three conformational states of the protein. In the simplest case, the single-ligated protein would assume an intermediate conformation, that is between that of the free and double-ligated protein. However, it has been demonstrated that the single-ligated state of CRP assumes a conformation, which is not merely an intermediate state. Therefore, the CRP system may be represented by a more general model, in which binding of cAMP to one subunit changes the conformation of this and

the neighbouring subunit. The fact that the two subunits of the CRP dimer are asymmetric (as discussed earlier), lends credence to this proposal.

3.9. BINDING OF THE CRP-cAMP COMPLEX TO DNA:  
MECHANISM OF ACTION.

In the absence of cAMP, CRP may bind non-specifically to DNA. The primary function of CRP, when complexed with cAMP, is to bind to specific DNA sites at or near promoters, where it either stimulates or inhibits the initiation of RNA synthesis (19).

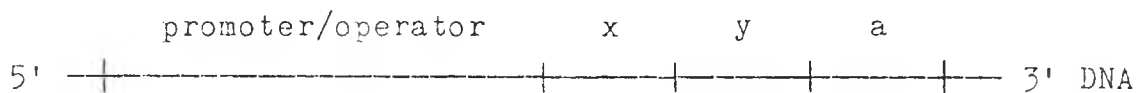


Fig. 3.10. The Lac Operon. CRP-cAMP complex binds near promoters, where it stimulates initiation of the transcription of structural genes x, y and a. x is the gene for  $\beta$ -galactosidase, y is the gene for  $\beta$ -galactoside permease and a is the gene for  $\beta$ -galactoside acetyltransferase.

The crystal structures of CRP and two other proteins also concerned with the regulation of transcription:  $\lambda$  phage cro protein (30) and a proteolytic fragment of  $\lambda$  cI repressor (31), have led to a number of general conclusions concerning the structural basis of DNA sequence recognition of proteins. The structures of CRP and the other proteins, contain an identical two  $\alpha$ -helix structure (32). Sequence homologies found between these proteins, suggest that this two-helix motif is directly involved in DNA sequence recognition.

The positive electrostatic charge density of the CRP dimer lies on the two carboxyl-terminal small domains, and extends along the outside of the two protruding  $F$   $\alpha$ -helices. The net negative electrostatic charge potential lies on the cAMP-binding amino-terminal domains (33). The location of positive electrostatic charge potential strongly suggests the orientation of B-DNA, bound to the small domains of CRP. If it is assumed that, in the CRP-DNA complex, the approximate two-fold axis of the CRP dimer is co-incident with the approximate two-fold axis of DNA; then there are only two parameters left to relate the DNA and the protein: their relative rotational orientation and the distance between them.

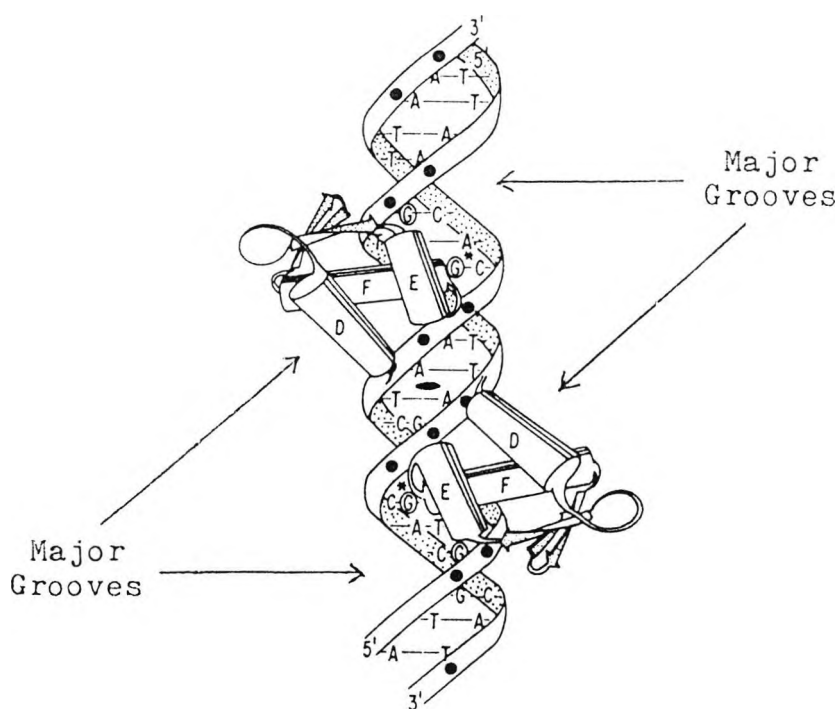


Fig. 3.11. A schematic diagram of the two DNA-binding domains of CRP, interacting with the CRP-binding site in the Lac Operon (34).

Only one relative orientation of DNA and protein strongly overlaps the negative electrostatic potential surfaces of the protein (33). This orientation also maximises the interactions between helices F and the major grooves of B-DNA.

On binding of the CRP-cAMP complex to the specific DNA sequence of the Lac Operon (that is, that stretch of bacterial DNA concerned with the production of the enzymes necessary for lactose degradation), hydrogen-bonds are formed between side-chains of the protein and the exposed edges of base-pairs in the major groove, and to the sugar-phosphate backbone.

Utilising chemical protection (35) and genetic (36) studies, it has been shown that the CRP-cAMP complex interacts with a portion of the DNA molecule showing the following sequence.

	5		10		15		20													
A	A	-	T	G	T	G	A	-	-	-	-	T	C	A	C	A	-	T	T	
T	T	-	A	C	A	C	T	-	-	-	-	-	A	G	T	G	T	-	A	A

Fig. 3.12. Base sequence of DNA recognised by the CRP-cAMP complex, which allows the latter to bind to specific sites on DNA. 'A' denotes adenine, 'G' denotes guanine, 'T' denotes thymine and 'C' denotes cytosine. Hyphens indicate the positions of any base.

The number of interactions between CRP and DNA can be increased by bending or kinking the DNA so that it contacts more of the protein surface, and is also closer to the positive electrostatic potential surface. Two arginine-180

side-chains, one from each F helix, now make hydrogen-bond interactions with two guanine bases instead of interacting mainly with the phosphate groups. Bending of the DNA, also allows additional interactions with the sugar-phosphate backbone, at the extreme ends of the site by lysine-201 and glutamine-170.

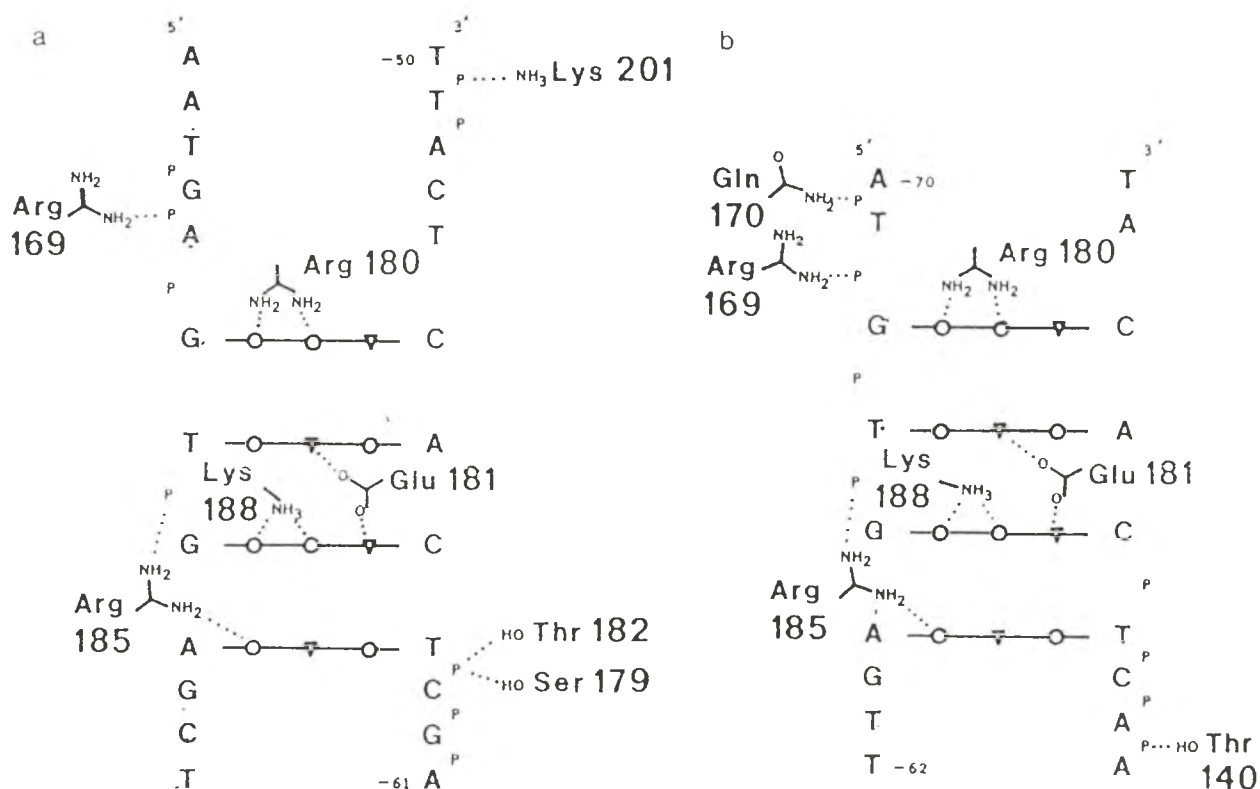


Fig. 3.13. A schematic diagram of some of the interactions proposed between the two small domains of the CRP dimer, and its DNA-binding site in the Lac Operon. Interactions made by each subunit with one-half of the DNA site, are shown separately in (a) and (b). Hydrogen-bond donors on the bases are indicated by '▽', and acceptors are shown by 'O'. Phosphate groups within 5 Å of protein atoms are indicated by 'P' (34).

The binding of the CRP-cAMP complex to DNA may produce

fourteen hydrogen-bonds, made between eight protein side-chains and the exposed edges of eight base-pairs in the major grooves. These are arginine-180, glutamate-181, arginine-185 and lysine-188 from helix F of each subunit. The position of glutamate-181, which makes hydrogen-bond interactions with two adjacent base-pairs, may be stabilised by salt bridges to arginine-180 or lysine-188. Moreover, nine hydrogen-bonds or salt links can be made to the phosphate groups of the DNA backbone.

The Glu-181 side chain carboxylate group of one subunit of the CRP dimer, is in hydrogen-bonded contact with the cytosine N-4 atom of the G-C base-pair at position 7 of the DNA site; and the Glu-181 side-chain carboxylate group of the opposite subunit of the CRP dimer, is in hydrogen-bonded contact with the cytosine N-4 atom of the C-G base-pair at position 16 of the DNA site. It has been shown that if Glu-181 is replaced by either valine or leucine, no functional contacts are made between residue-181 side-chain and positions 7 and 16 of the DNA site.

It is thought (37) that when CRP binds to DNA, supercoil formation occurs in the latter which serves to bring sequentially separated DNA regions into close physical proximity. The solenoidal coil formed on CRP association, constitutes a structurally unique site on the DNA, where it is partially unwound. This is an established factor in the potentiation of binding and transcription by RNA polymerase.

There is evidence (38) that the CRP-cAMP complex may also bind to RNA polymerase. Immunological studies (39) have shown that the CRP-cAMP complex binds to the  $\sigma$  (regulatory)

subunit of RNA polymerase. It has been observed that at low ionic concentrations (50 mM KCl), where RNA polymerase normally exists in the dimeric form, addition of an excess of CRP causes dissociation into monomers. This implies that CRP binds more tightly, perhaps exclusively, to the monomeric form. The simplest explanation of this observation is that CRP interacts with a region of RNA polymerase, that becomes shielded when monomers associate into dimers.

These findings provide strong corroborative evidence, that protein-protein contact is at least a component of the mechanism of gene activation by CRP.

It has been shown (29) that at cAMP concentrations at which the predominant species is the CRP-(cAMP)<sub>2</sub> complex, there is a significant decrease in the binding of CRP to a specific DNA site, as compared to the CRP-cAMP complex. Hence, it can be concluded that of the three species: free CRP, CRP-cAMP and CRP-(cAMP)<sub>2</sub>, only CRP-cAMP is active in binding to specific DNA sequences. In contrast, free CRP and CRP-(cAMP)<sub>2</sub> do not bind to a specific DNA sequence, or at least with significantly reduced affinity.

This finding may be rationalised as follows: as *E. coli* senses the presence of an alternative source of metabolites, for example, lactose, the cellular level of cAMP increases, resulting in an increased amount of CRP-cAMP complex which then binds to the Lac promoter, to activate the transcription of mRNA coding for the metabolic enzymes responsible for utilising the alternative energy source. Hence, it is acceptable to assume that both CRP-cAMP and CRP-(cAMP)<sub>2</sub> complexes can bind to the operon for metabolic enzymes.

However, CRP is an auto-regulator of the expression of its own gene (40). The CRP-cAMP complex serves to repress the expression of the CRP gene. It is logical that at higher concentrations of cAMP, the formation of CRP-(cAMP)<sub>2</sub> is favoured. This leads to dissociation of the CRP-cAMP complex for the CRP gene, resulting in an increase in the synthesis of more CRP to cope with the increased need of metabolic enzymes.

In addition to its own gene, CRP has been found to negatively regulate the synthesis of cAMP (41). The gene in *E. coli* responsible for the production of the enzyme (adenylate cyclase) necessary for the creation of cAMP, is called the cya gene. It has been found that the CRP specifically interacts with the unique CRP binding sequence, which overlaps with the RNA polymerase binding region or promoter. In addition, it has been shown that the RNA polymerase-promoter interaction is altered in the presence of CRP-cAMP.

The CRP-cAMP complex has also been shown to negatively regulate the production, in *E. coli*, of protein III: a major outer membrane protein (42) and also the enzymes concerned with glutamine metabolism (43). These effects are thought to be achieved by a mechanism analogous to that of the CRP and cya genes.

It has recently been found (44) that lateral wall synthesis in the *E. coli* cell cycle, is triggered by the CRP-cAMP complex. In this case, the CRP-cAMP complex is thought to control amino-sugar metabolism.

### 3.10. SUMMARY.

In summary, CRP from *E. coli*, is a dimeric protein of molecular weight 47238 daltons, with a pI value of 9.2. It has been purified to homogeneity, and its primary and secondary structures have been elucidated. Each monomer is composed of two domains: a large, amino-terminal domain concerned with the binding of one cAMP molecule, and a small, carboxyl-terminal domain, involved with DNA binding. Consequently, each CRP dimer binds two molecules of cAMP.

There is evidence that the protein undergoes a conformational change on binding cAMP. This conformational change permits the CRP-cAMP complex to bind to specific sites on the DNA helix, so that the former may carry out its function of regulating, either negatively or positively, the transcription of mRNA for enzyme synthetic control.

In view of the foregoing, CRP was considered an ideal candidate for further investigation.

3.11. REFERENCES.

1. Dienert, F.  
(1900) Ann. Inst. Pasteur, Paris 14 139
2. Makman, R.S. & Sutherland, E.W.  
(1965) J. Biol. Chem. 240 1309
3. Perlman, R.L. & Pastan, I.  
(1968) J. Biol. Chem. 243 5420
4. Ullmann, A. & Monod, J.  
(1968) FEBS Letters 2 57
5. Zubay, G., Schwartz, D. & Beckwith, J.  
(1970) Proc. Natl. Acad. Sci. USA 66 104
6. Emmer, M., de Crombrughe, B., Pastan, I. & Perlman, R.L.  
(1970) Proc. Natl. Acad. Sci. USA 66 480
7. Cook, D.I. & Revzin, A.  
(1980) J. Bacteriol. 141 1279
8. Riggs, A.D., Reiness, G. & Zubay, G.  
(1971) Proc. Natl. Acad. Sci. USA 68 1222
9. Pastan, I., Gallo, M. & Anderson, W.B.  
(1974) Meth. Enzymol. 38 367
10. Eilen, E., Pampero, C. & Krakow, J.S.  
(1978) Biochemistry 17 2469
11. Boone, T. & Wilcox, G.  
(1978) Biochim. Biophys. Acta 541 528
12. Zubay, G.  
(1980) Meth. Enzymol. 65 856
13. Aiba, H., Fujimoto, S. & Ozaki, N.  
(1982) Nucl. Acids Res. 10 1345
14. Cossart, P. & Gicquel-Sanzey, B.  
(1982) Nucl. Acids Res. 10 1363
15. McKay, D.B., Weber, I.T. & Steitz, T.A.  
(1982) J. Biol. Chem. 257 9518

16. McKay, D.B. & Steitz, T.A.  
(1981) Nature 290 744
17. Takahashi, M., Blazy, B. & Baudras, A.  
(1980) Biochemistry 19 5124
18. Weber, I.T. & Steitz, T.A.  
(1987) J. Mol. Biol. 198 311
19. de Crombrughe, B., Busby, S. & Buc, H.  
(1984) Science 224 831
20. Clore, G.M. & Gronenborn, A.M.  
(1982) FEBS Letters 145 197
21. Gronenborn, A.M., Clore, G.M., Blazy, B. & Baudras, A.  
(1981) FEBS Letters 136 160
22. Takio, K., Smith, S.B., Krebs, E.G., Walsh, K.A.  
& Titani, K.  
(1982) Proc. Natl. Acad. Sci. USA 79 2544
23. Weber, I.T., Takio, K., Titani, K. & Steitz, T.A.  
(1982) Proc. Natl. Acad. Sci. USA 79 7679
24. Aiba, H. & Krakow, J.S.  
(1981) Biochemistry 20 4774
25. Kypr, J. & Mrazek, J.  
(1985) Biochem. Biophys. Res. Commun. 131 780
26. Garges, S. & Adhya, S.  
(1988) J. Bacteriol. 170 1417
27. Harman, J.G., Peterkofsky, A. & McKenney, K.  
(1988) J. Biol. Chem. 263 8072
28. Ebright, R.H., LeGrice, S.F.J., Miller, J.P. & Krakow, J.S.  
(1985) J. Mol. Biol. 182 91
29. Heyduk, T. & Lee, J.C.  
(1989) Biochemistry 28 6914
30. Anderson, W.F., Ohlendorf, D.H., Takeda, Y. & Matthews, B.W.  
(1981) Nature 290 754
31. Pabo, C.O. & Lewis, M.  
(1982) Nature 298 443

32. Steitz, T.A., Ohlendorf, D.H., McKay, D.B., Anderson, W.F. & Matthews, B.W.  
(1982) Proc. Natl. Acad. Sci. USA 79 3097
33. Steitz, T.A., Weber, I.T. & Matthew, J.B.  
(1983) Cold Spring Harbour Symp. Quant. Biol. 47 419
34. Weber, I.T. & Steitz, T.A.  
(1984) Proc. Natl. Acad. Sci. USA 81 3973
35. Simpson, R.B.  
(1980) Nucl. Acids Res. 8 759
36. Kolb, A., Busby, S., Herbert, M., Kotlarz, D. & Buc, H.  
(1983) EMBO J. 2 217
37. Salemme, F.R.  
(1982) Proc. Natl. Acad. Sci. USA 79 5263
38. Pinkney, M. & Hoggett, J.G.  
(1988) Biochemical J. 250 897
39. Stender, W.  
(1980) Biochem. Biophys. Res. Commun. 96 320
40. Okamoto, K., Hara, S., Bhasin, R. & Freundlich, M.  
(1988) J. Bacteriol. 170 5076
41. Aiba, H.  
(1985) J. Biol. Chem. 260 3063
42. Mallick, U. & Herrlich, P.  
(1979) Proc. Natl. Acad. Sci. USA 76 5520
43. Prusiner, S., Miller, R.E. & Valentine, R.C.  
(1972) Proc. Natl. Acad. Sci. USA 69 2922
44. Utsumi, R., Noda, M., Kawamukai, M. & Komano, T.  
(1989) J. Bacteriol. 171 2909

CHAPTER 4.

EXPERIMENTAL PROCEDURES FOR THE SYNTHESIS  
OF FLUORESCENT PROBES.

4.1. SYNTHESIS OF BIS (1,10-PHENANTHROLINE)  
(BATHOPHENANTHROLINE DISULPHONYL CHLORIDE)  
RUTHENIUM (II) HEXAFLUOROPHOSPHATE  
DIHYDRATE.

4.1.1. Preparation of Bis (1,10-phenanthroline) dichloride,  
ruthenium (II) dihydrate. (C-1).

Ruthenium trichloride trihydrate (2.50 gm; 0.0096 mol), 1,10-phenanthroline (3.50 gm; 0.0194 mol) and lithium chloride (5.00 gm), were introduced into a 500 ml round-bottomed flask and heated together at reflux in dry dimethylformamide (50 ml), under nitrogen, for 7 hours with efficient stirring.

The purple-black solution was allowed to cool to room temperature. Acetone (250 ml) was added (stirring still maintained), and the flask was stoppered under nitrogen. This solution was left overnight at 0°C. A black, micro-crystalline solid was recovered by filtration, which was washed with water (6 x 50 ml) and diethyl ether (6 x 50 ml). The solid was then dried in vacuo at 40°C.

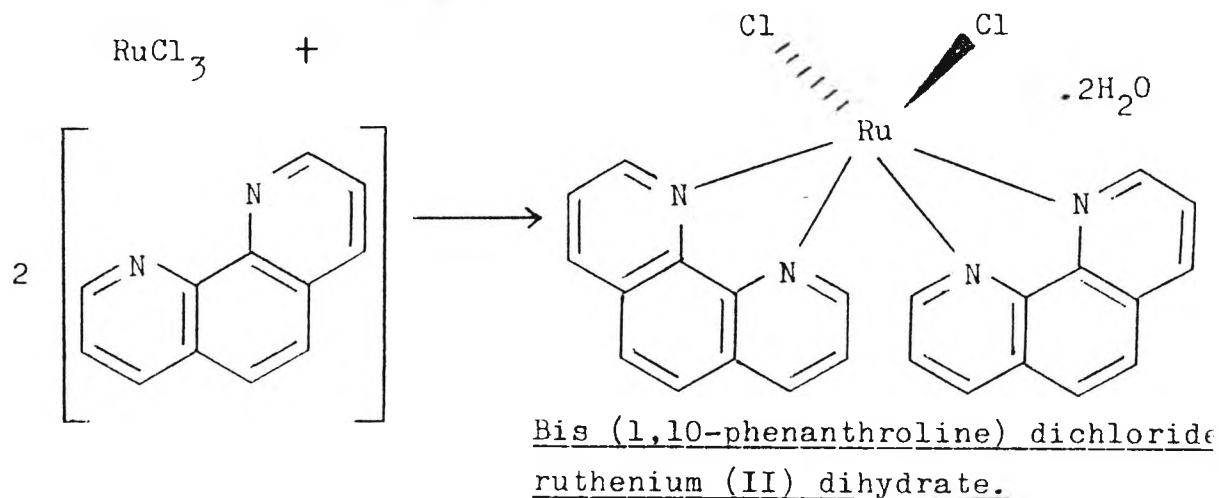


Fig. 4.1. The reaction for the preparation of  
Bis (1,10-phenanthroline) dichloride, ruthenium (II) dihydrate.

Weight of product obtained = 2.64 gm

Actual Yield = 39%

Bis (1,10-phenanthroline) dichloride, ruthenium (II) dihydrate was characterised from the following data:

Infra-red Spectrum Analysis (KBr disc)

cm<sup>-1</sup>

3438	O-H stretch (water of crystallisation)
3062	Aromatic C-H stretch
1626	Aryl-H vibration
1407	C-H deformation

C, H, N Microanalytical Data

C<sub>24</sub>H<sub>16</sub>N<sub>4</sub>RuCl<sub>2</sub>·2H<sub>2</sub>O

Calculated	(%)	C : 50.70	H : 3.52	N : 9.86
Found	(%)	C : 50.63	H : 3.50	N : 9.91

4.1.2. Preparation of Bis (1,10-phenanthroline) (Bathophenanthroline disulphonic acid, disodium salt) ruthenium (II) dihydrate. (C-2).

Bis (1,10-phenanthroline) dichloride, ruthenium (II) dihydrate, (C-1), (0.50 gm; 0.0008 mol) and bathophenanthroline disulphonic acid, disodium salt hydrate (0.50 gm; 0.0009 mol) were suspended in water (50 ml) in a 100 ml round-bottomed flask, and heated for 24 hours at reflux.

The solution was cooled, and the red-brown precipitate was collected and washed with distilled water (4 x 15 ml). The solid was then dried over sodium hydroxide pellets.

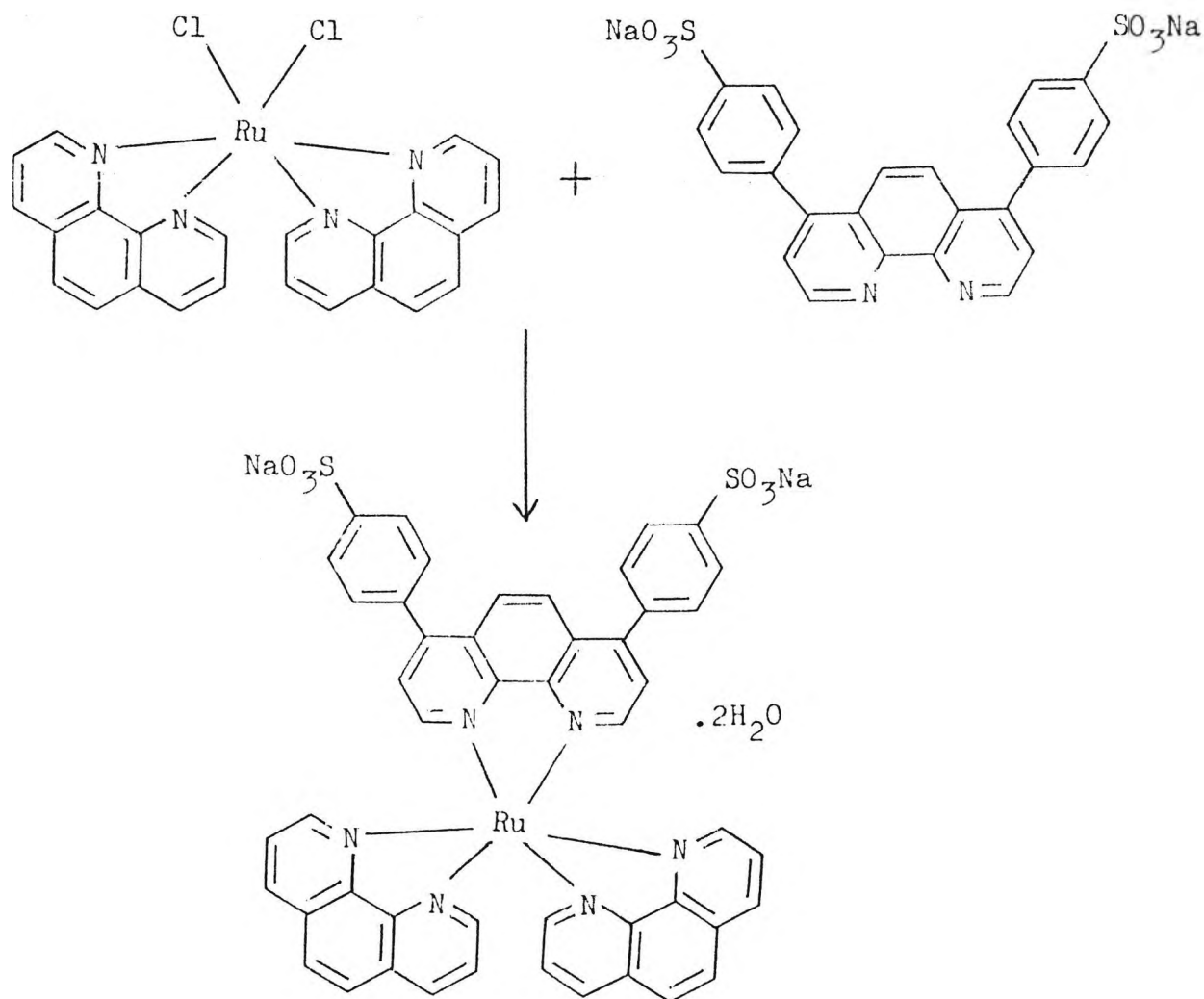


Fig. 4.2. The reaction for the preparation of Bis (1,10-phenanthroline) (bathophenanthroline disulphonic acid, disodium salt) ruthenium (II) dihydrate.

Weight of product obtained = 0.35 gm

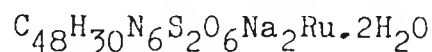
Actual Yield = 38%

Bis (1,10-phenanthroline) (Bathophenanthroline disulphonic acid, disodium salt) ruthenium (II) dihydrate was characterised from the following data:

Infra-red Spectrum Analysis (KBr disc)

cm <sup>-1</sup>	
3434	O-H stretch (water of crystallisation)
1411	C-H deformation
1195	O-H stretch of SO <sub>3</sub> H
1126	S=O symmetrical stretch
1034	C-S stretch
1010	O-H stretch of SO <sub>3</sub> H
620	O-H stretch of SO <sub>3</sub> H

C,H,N Microanalytical Data



Calculated (%)	C : 55.73	H : 3.29	N : 8.13
Found (%)	C : 55.62	H : 3.22	N : 8.20

4.1.3. Preparation of Bis (1,10-phenanthroline)  
(Bathophenanthroline disulphonyl chloride)  
ruthenium (II) hexafluorophosphate  
dihydrate. (C-3).

Bis (1,10-phenanthroline) (Bathophenanthroline disulphonic acid, disodium salt) ruthenium (II) dihydrate, (C-2), (0.10 gm; 0.0001 mol) was introduced into a boiling tube. Phosphorus oxytrichloride (2 ml), and an excess of phosphorus pentachloride were then added. The mixture was then heated at reflux, under nitrogen, with stirring for 17 hours. The resulting deep-red solution was then allowed to cool.

To water (50 ml) in a 250 ml beaker, was added hexafluorophosphoric acid (4 ml), ice was then added to a volume of 200 ml. The deep-red solution was slowly added to the ice-water mixture, with stirring. The reddish-brown precipitate was filtered on the frit, washed with water (3 x 10 ml) and dried in vacuo at 40°C.

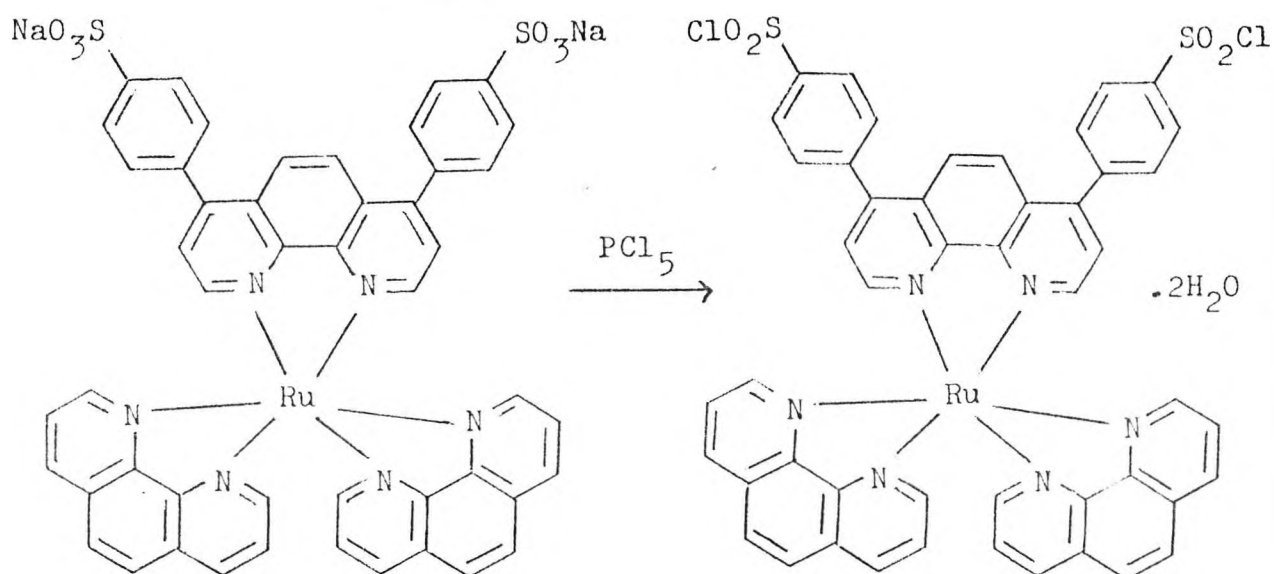


Fig. 4.3. The reaction for the preparation of the sulphonyl chloride derivative of Bis (1,10-phenanthroline) (Bathophenanthroline disulphonic acid, disodium salt) ruthenium (II) dihydrate.

Weight of product obtained = 0.0827 gm

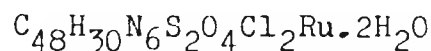
Actual Yield = 83%

The Sulphonyl Chloride derivative of Bis (1,10-phenanthroline)  
(Bathophenanthroline disulphonic acid, disodium salt)  
ruthenium (II) dihydrate was characterised from the following  
data:

Infra-red Spectrum Analysis (KBr disc)

$\text{cm}^{-1}$	
3418	O-H stretch (water of crystallisation)
3084	Aromatic C-H stretch
1412	C-H deformation
1373	S=O stretch of $\text{SO}_2\text{Cl}$
1225	S=O stretch
1173	S=O stretch
1126	S=O stretch of $\text{SO}_2\text{Cl}$

C,H,N Microanalytical Data



Calculated (%)	C : 56.14	H : 3.31	N : 8.18
Found (%)	C : 56.29	H : 3.17	N : 8.32

## 4.2. SYNTHESIS OF N-(1-PYRENE) MALEIMIDE (1).

### 4.2.1. Preparation of N-(1-Pyrene) Maleamic Acid. (C-4).

1-aminopyrene (0.90 gm; 4.2 mmol) was dissolved in ice-cold tetrahydrofuran (10.5 ml), and mixed with a solution of maleic anhydride (0.43 gm; 4.4 mmol) in ice-cold tetrahydrofuran (5.3 ml), in a 25 ml round-bottomed flask.

The mixture was allowed to react overnight with stirring at 4°C. A bright yellow precipitate resulted. The precipitate was collected via filtration at the pump, washed with ice-cold tetrahydrofuran (2 x 10 ml), and dried in vacuo at 40°C, to give N-(1-Pyrene) Maleamic Acid as a yellow, crystalline powder.

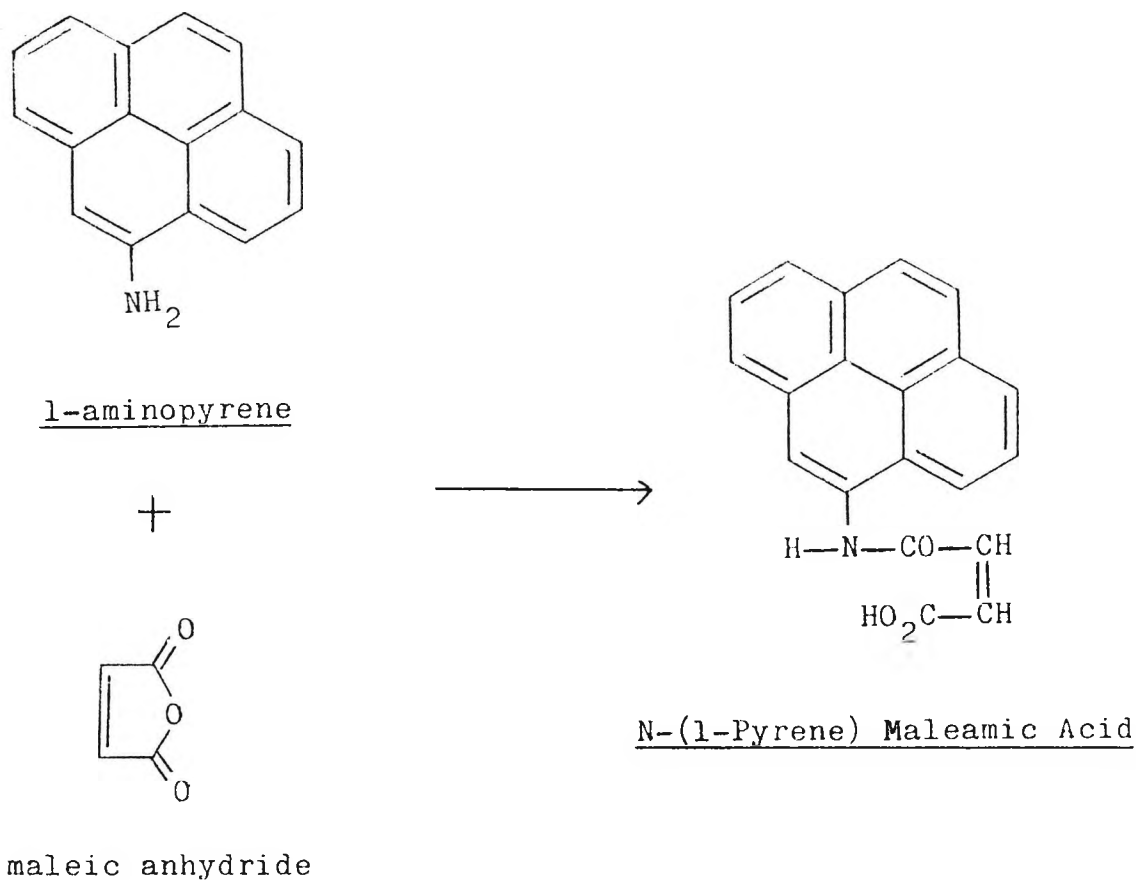


Fig. 4.4. The reaction for the preparation of N-(1-Pyrene) Maleamic Acid.

Weight of product obtained = 1.10 gm

Actual Yield = 84%

N-(1-Pyrene) Maleamic Acid was characterised by the following data:

Infra-red Spectrum Analysis (KBr disc)

cm<sup>-1</sup>

3224 } H-bonded O-H of  
3038 } carboxylic acid

1709 C=O stretch

1600 Aryl-H stretch

1579 Aryl-H stretch

C,H,N Microanalytical Data

C<sub>20</sub>H<sub>13</sub>NO<sub>3</sub>

Calculated (%) C : 76.19 H : 4.13 N : 4.44

Found (%) C : 76.27 H : 4.23 N : 4.60

Melting Point = 182-184°C

(literature value (1) = 183-185°C)

#### 4.2.2. Preparation of N-(1-Pyrene) Maleimide. (C-5).

N-(1-Pyrene) Maleamic Acid, (C-4), (0.22 gm; 0.70 mmol) was added to a solution of acetic anhydride (3.00 gm; 29.5 mmol) in a 10 ml round-bottomed flask containing sodium acetate (0.03 gm; 4.10 mmol). The resulting suspension was heated in an oil bath to 100°C, for 45 minutes with stirring. The reaction mixture was cooled to room temperature in a cold-water bath, and poured into ice-water (15 ml).

The precipitated product, N-(1-Pyrene) Maleimide, was removed by suction filtration, washed three times with ice-cold water (3 x 10 ml), and once with 'hexane' (b.p. 66-69°C) (10 ml), and dried in vacuo at 40°C.

N-(1-Pyrene) Maleimide was recrystallised by addition of water to its ethanolic solution, and finally from 100% ethanol, as gold needles.

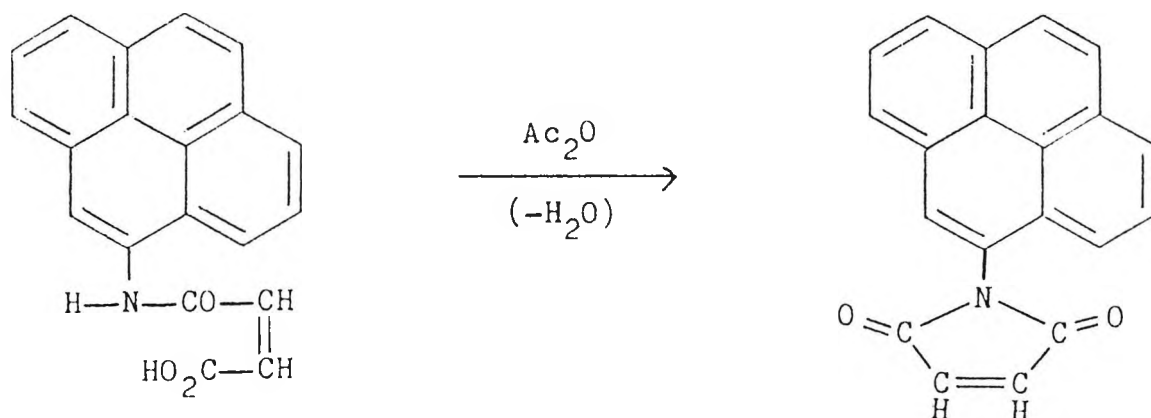


Fig. 4.5. The reaction for the preparation of N-(1-Pyrene) Maleimide.

Weight of product obtained = 0.10 gm

Actual Yield = 48%

N-(1-Pyrene) Maleimide was characterised by the following data:

Spectroscopic Analysis

Infra-red (KBr disc)

cm<sup>-1</sup>

1768 }  
1699 } C=O (maleimide)

<sup>1</sup>H Nuclear Magnetic Resonance (CDCl<sub>3</sub>/TMS)

δ 8.27 to 7.63 (multiplet, 9H, ArH)

δ 7.23 (singlet, 2H, vinyl)

C,H,N Microanalytical Data

C<sub>20</sub>H<sub>11</sub>NO<sub>2</sub>

Calculated (%) C : 80.79 H : 3.72 N : 4.71

Found (%) C : 80.10 H : 3.52 N : 4.45

Melting Point = 221-224°C

(literature value (1) = 223-225°C)

4.3. SYNTHESIS OF N-(IODOACETYLAMINOETHYL)-1-NAPHTHYLAMINE-8-SULPHONIC ACID. (1,8-IAEDANS).

4.3.1. Preparation of 1-Naphthol-8-Sulphonic Acid. (C-6). (2).

1-Naphthol-8-Sulphonic acid sultone (or Naphthosultone), (30 gm; 0.146 mol) was charged with distilled water (40 ml) in a 500 ml round-bottomed flask. The mixture was heated to 80°C, and aqueous sodium hydroxide solution (30% w/v, 24 ml) was added. The flask was then heated to 100°C and diluted with hot, distilled water (140 ml). Anhydrous sodium sulphite (0.4 gm; 0.003 mol) was added and the mixture was then acidified to pH 3 with concentrated hydrochloric acid.

Sodium chloride (20 gm; 0.342 mol) was added, and the mixture was then cooled. The precipitated product was filtered at the pump, washed with a small quantity of cold water and dried in vacuo at 40°C.

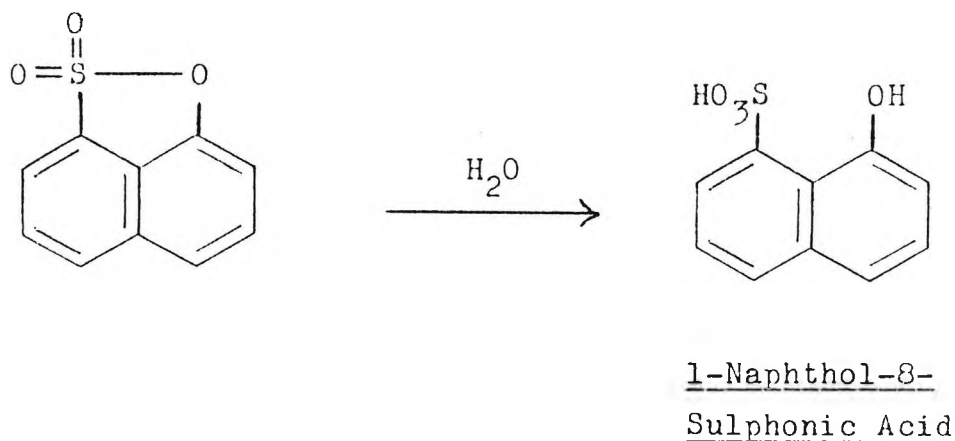


Fig. 4.6. The reaction for the preparation of 1-Naphthol-8-Sulphonic Acid

Weight of product obtained = 27.23 gm

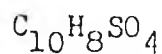
Actual Yield = 84%

1-Naphthol-8-Sulphonic Acid was characterised by the following data:

Infra-red Spectrum Analysis (KBr disc)

cm <sup>-1</sup>	
3052	-O-H (intermolecular hydrogen-bonded)
1601	Aryl-H vibration
1504	Aryl-H vibration
1403	-O-H bending
1053	S=O stretch

C,H,S Microanalytical Data



Calculated (%)	C : 53.57	H : 3.57	S : 14.29
Found (%)	C : 53.52	H : 3.48	S : 14.10

Melting Point = 105-107°C

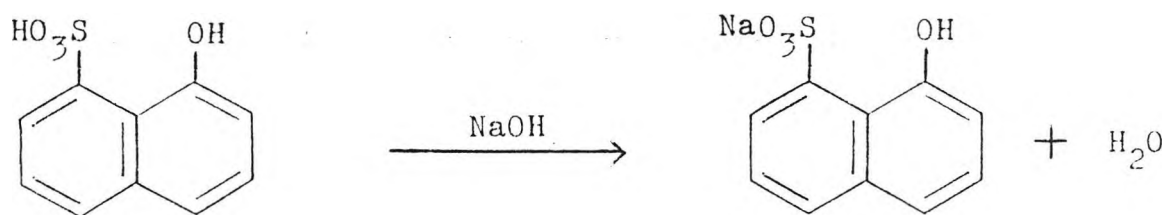
(literature value (3) = 106-107°C)

4.3.2. Preparation of 1-Naphthol-8-Sulphonic Acid, Sodium Salt. (C-7).

Sodium hydroxide (30 gm; 0.75 mol) was dissolved in distilled water (100 ml) in a 500 ml round-bottomed flask. Ethanol (200 ml) was then added and the mixture was heated to 70°C.

1-Naphthol-8-Sulphonic Acid, (C-6), (25 gm; 0.113 mol) was dissolved in aqueous ethanol (50% v/v, 200 ml) with heating to 70°C. The two solutions were then mixed.

The reaction mixture was cooled to room temperature, and finally in ice to complete precipitation of the sodium salt.



1-Naphthol-8-Sulphonic Acid, Sodium Salt.

Fig. 4.7. The reaction for the preparation of 1-Naphthol-8-Sulphonic Acid, Sodium Salt.

Weight of product obtained = 26.36 gm

Actual Yield = 96%

4.3.3. Preparation of p-Nitrophenyl Iodoacetate. (C-8). (4).

Iodoacetic acid (7.44 gm; 0.04 mol) and p-nitrophenol (6.68 gm; 0.048 mol) were dissolved in ethyl acetate (100 ml), in a 250 ml round-bottomed flask, at 5°C. To this solution was added, with stirring, 1,3-dicyclohexylcarbodiimide (8.24 gm; 0.04 mol). The by-product, 1,3-dicyclohexylurea started precipitating immediately. After complete dissolution of the dicyclohexylcarbodiimide, (approximately 2 hours), the temperature was held at 5°C for 30 minutes, with occasional stirring. The reaction mixture was allowed to attain room temperature and held there for one hour, after which time it was filtered. The precipitate was washed with ethyl acetate (150 ml), and the combined filtrate and washings were evaporated under reduced pressure, at room temperature, to dryness. The oily residue was recrystallised from ethanol, the final crystals being washed with cold ethanol (4 x 20 ml), to yield light yellow crystals. These crystals were air-dried, followed by drying in vacuo at 50°C.

Weight of product obtained = 6.19 gm

Actual Yield = 50%

The 1,3-dicyclohexylcarbodiimide acts as a dehydrating agent in the reaction, and the latter has been shown (5) to proceed via the following mechanism:

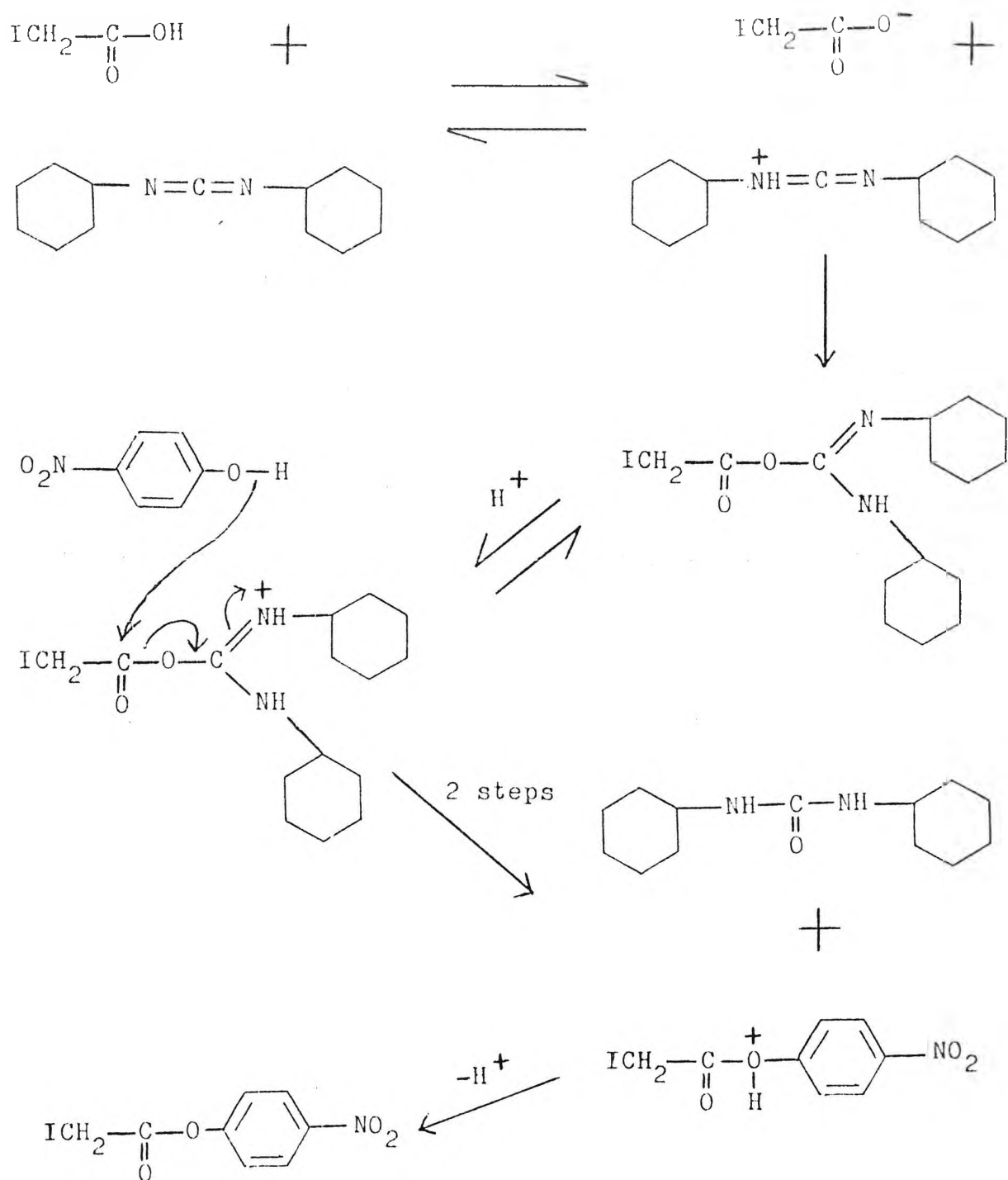


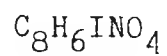
Fig. 4.8. The reaction mechanism for the preparation of p-nitrophenyl iodoacetate.

p-nitrophenyl iodoacetate was characterised by the following data:

Infra-red Spectrum Analysis (KBr disc)

cm <sup>-1</sup>	
3461	-O-H (intermolecular hydrogen-bonded)
3114	Aryl C-H stretch
3045	Aryl-H stretch
1590	C-N=O stretch
1533	C-NO <sub>2</sub> stretch
1348	C-N=O stretch
503	C-I stretch

C,H,N Microanalytical Data



Calculated (%)	C : 31.29	H : 1.96	N : 4.56
Found (%)	C : 31.28	H : 1.79	N : 4.43

Melting Point = 75-77°C

(literature value (6) = 76°C)

4.3.4. Preparation of N-(Aminoethyl)-1-Naphthylamine-8-Sulphonic Acid, (1,8-EDANS). (C-9) (4).

Sodium 1-naphthol-8-sulphonate, (C-7), (24 gm; 0.10 mol) was added to aqueous sodium bisulphite solution (25% w/v, 200 ml) in a 500 ml round-bottomed flask. Ethylenediamine (18 gm; (20 ml); 0.30 mol) was added, the pH adjusted to 8 with concentrated hydrochloric acid, and the mixture refluxed for 24 hours. A heavy precipitate slowly deposited. After cooling the reaction mixture to room temperature, the pH was adjusted to 7 with concentrated hydrochloric acid, cooled to 5°C for one hour, and filtered.

The clay-like residue was dissolved in water, by the addition of sufficient 10 M NaOH, and twice heated to boiling with activated charcoal, and filtered. The resulting solution was cooled to room temperature, adjusted to pH 7 with concentrated hydrochloric acid, and set at 5°C overnight.

After filtration at the pump, the precipitate was recrystallised twice from hot, distilled water, and dried in vacuo at 120°C for 24 hours.

Weight of product obtained = 11.21 gm

Actual Yield = 39%

This reaction is an example of the Bucherer reaction, and has been shown (7) to proceed as follows:

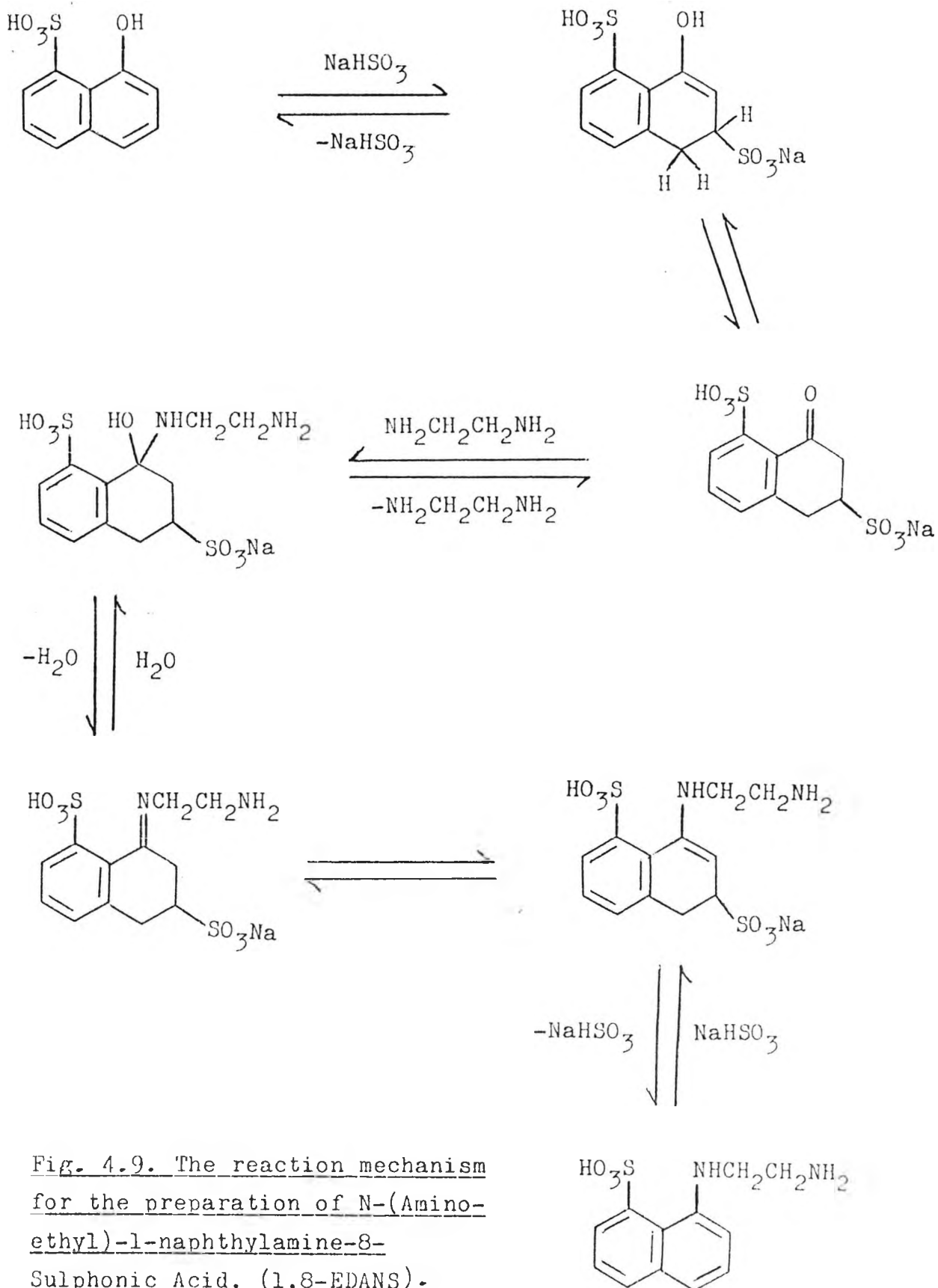


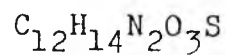
Fig. 4.9. The reaction mechanism for the preparation of N-(Aminoethyl)-1-naphthylamine-8-Sulphonic Acid, (1,8-EDANS).

N-(Aminoethyl)-1-naphthylamine-8-Sulphonic Acid, (1,8-EDANS)  
was characterised by the following data:

Infra-red Spectrum Analysis (KBr disc)

cm <sup>-1</sup>	
3443	-O-H (intermolecular hydrogen-bonded)
3305	N-H stretch
3167	Aryl C-H stretch
3045	Aryl C-H stretch
1572	-NH <sub>2</sub> (N-H bending)
1366	-SO <sub>2</sub> -O stretch
1191	-SO <sub>2</sub> -O stretch
1165	-SO <sub>2</sub> -O stretch
1046	S=O stretch

C,H,N Microanalytical Data



Calculated (%)	C : 54.12	H : 5.29	N : 10.51
Found (%)	C : 54.16	H : 5.31	N : 10.47

Thin-Layer Chromatography

Solvent: EtOH

Eluent: EtOH

R<sub>f</sub> 1,8-EDANS = 0.48 (literature value (4) = 0.48)

4.3.5. Preparation of N-(Iodoacetylaminoethyl)-1-Naphthylamine-8-Sulphonic Acid. (1,8-IAEDANS). (C-10). (4).

1,8-EDANS, (C-9), was initially converted to its sodium salt: 1,8-EDANS (5.00 gm; 0.019 mol) was dissolved in hot ethanol (200 ml), containing an excess of sodium hydroxide. Upon cooling, the salt (Na-EDANS) precipitated, and was filtered and dried in vacuo at 80°C. This material was utilised without further purification.

The remainder of the reaction steps were performed in the dark, due to the photosensitivity of the iodine-containing compound.

A mixture of Na-EDANS (1.44 gm; 0.005 mol) and dimethylformamide (12 ml) at 5°C, was stirred to maximum dissolution. A solution of p-nitrophenyl iodoacetate, (C-8), (2.30 gm; 0.0075 mol) in dimethylformamide (3 ml), cooled to 5°C, was rapidly added to the Na-EDANS solution, and allowed to react for 20 minutes. The mixture was then filtered rapidly at the pump. Concentrated hydriodic acid (2 ml; 0.011 mol) was added to the filtrate, followed by cold distilled water (60 ml) and cold acetone (20 ml). The filtrate was then stirred overnight, at 5°C. The solid formed was filtered at the pump, washed thoroughly with acetone (4 x 15 ml), and dried in vacuo at 80°C.

Weight of product obtained = 5.17 gm

Actual Yield = 70%

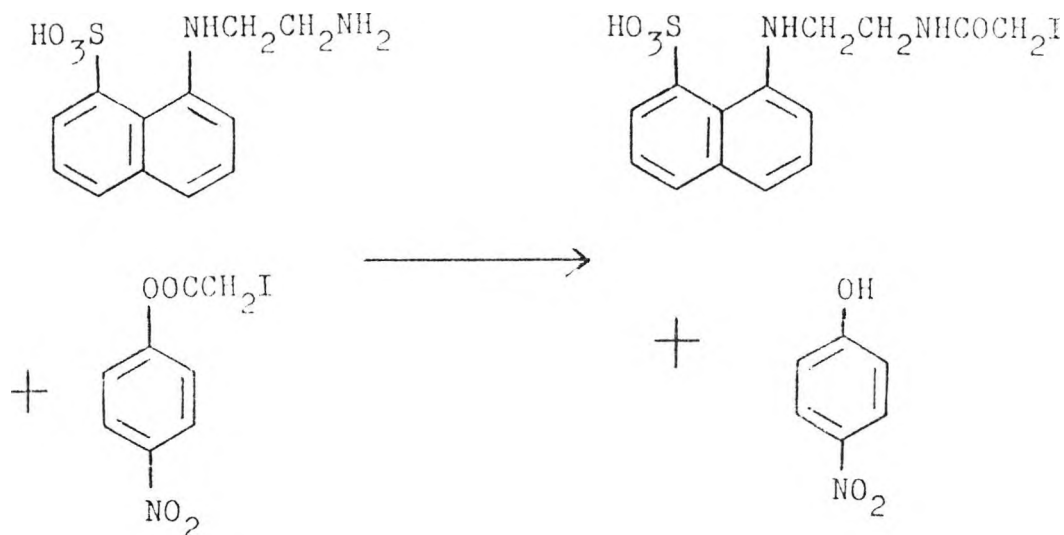


Fig. 4.10. The reaction for the preparation of N-(Iodoacetylaminoethyl)-1-naphthylamine-8-Sulphonic Acid.

N-(Iodoacetylaminoethyl)-1-naphthylamine-8-Sulphonic Acid, (1,8-IAEDANS), was characterised from the following data:

Spectroscopic Analysis

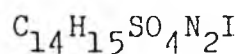
Infra-red (KBr disc)

cm <sup>-1</sup>	
3338	-O-H (intermolecular hydrogen-bonded)
3259	N-H stretch
1648	-C=O
525	C-I stretch

<sup>1</sup>H Nuclear Magnetic Resonance (DMSO-d<sub>6</sub>/TMS)

δ 7.50 to 8.50	(multiplet, 6H, ArH)
δ 2.50	(singlet, 1H, hydroxyl)

C,H,N Microanalytical Data



Calculated (%)	C : 38.72	H : 3.48	N : 6.45
Found (%)	C : 39.35	H : 3.44	N : 6.41

Thin-Layer Chromatography

Solvent: EtOH

Eluent: EtOH

R<sub>f</sub> 1,8-IAEDANS = 0.80 (literature value (4) = 0.82)

4.4. SYNTHESIS OF N-(1-ANILINONAPHTHYL-4) MALEIMIDE. (8).

4.4.1. Preparation of 4-p-sulphobenzeneazo-1-anilinonaphthalene. (C-11).

Sulphanilic acid (17.3 gm; 0.10 mol) was added to distilled water (100 ml) in a 250 ml round-bottomed flask. Anhydrous sodium carbonate (5.3 gm; 0.05 mol) was then added. After the effervescence had subsided and a clear solution was obtained, concentrated hydrochloric acid (25 ml) was added. The flask was then cooled to 5°C in ice.

Sodium nitrite (6.9 gm; 0.10 mol) was dissolved in distilled water (30 ml), and this solution was cooled to 5°C in ice. The sodium nitrite solution was then added dropwise to the cold acidified sulphanilic acid solution with stirring, and the temperature was not allowed to exceed 5°C. The sparingly soluble diazonium salt of sulphanilic acid, separated out as a white solid, and the addition was continued until an excess of nitrous acid was present; as detected by the immediate blue colouration, when tested with moist starch/potassium iodide paper.

N-phenyl-1-naphthylamine (21.9 gm; 0.10 mol) was dissolved in glacial acetic acid (90 ml), in a 250 ml conical flask, and distilled water (10 ml) was then added. The mixture was then cooled to 5°C in ice.

The suspension of the diazonium salt of sulphanilic acid was added dropwise to the cold N-phenyl-1-naphthylamine solution with stirring. Again, the temperature was not allowed to exceed 5°C. The azo-dye separated out as a purple solid and after the total addition of the diazonium salt, the

reaction mixture was allowed to stir for one hour.

The purple solid was then filtered off, washed with the minimum of cold water, and dried in vacuo at 80°C.

The reaction has been shown (9), to proceed as follows:

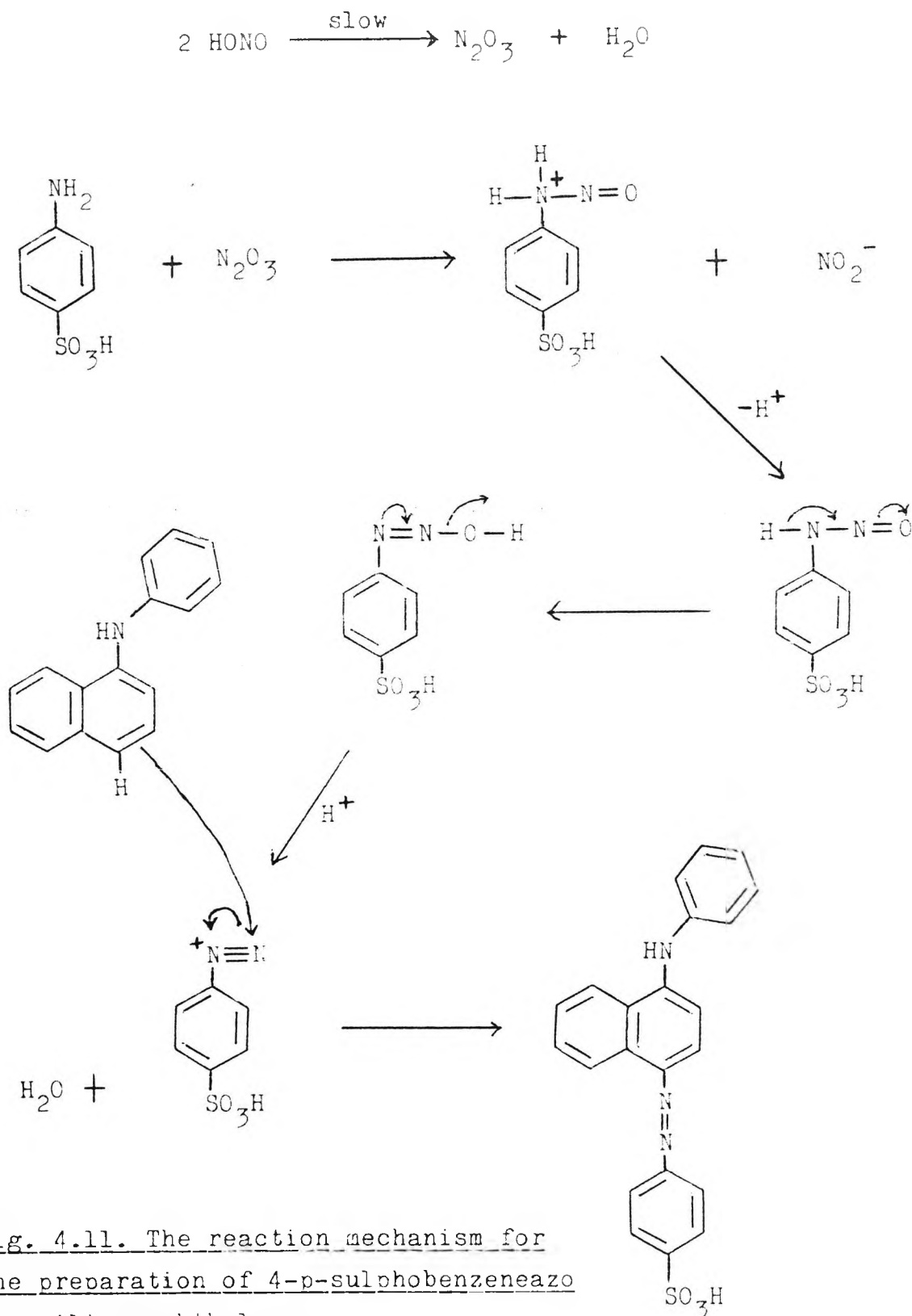


Fig. 4.11. The reaction mechanism for the preparation of 4-p-sulphobenzeneazo-1-anilinonaphthalene.

Weight of product obtained = 37.42 gm

Actual Yield = 93%

4-p-sulphobenzeneazo-1-anilinonaphthalene was characterised  
by the following data:

Infra-red Spectrum Analysis (KBr disc)

cm<sup>-1</sup>

3427	N-H stretch
1581	Aryl-H stretch
1491	Aryl-H stretch
1321	O-H bending
1060	S=O stretch

C,H,N Microanalytical Data

C<sub>22</sub>H<sub>17</sub>N<sub>3</sub>O<sub>3</sub>S

Calculated	(%)	C : 65.51	H : 4.22	N : 10.42
------------	-----	-----------	----------	-----------

Found	(%)	C : 65.37	H : 4.29	N : 10.56
-------	-----	-----------	----------	-----------

4.4.2. Preparation of 1-anilino-4-aminonaphthalene. (C-12).

4-p-sulphobenzeneazo-1-anilino-naphthalene, (C-11), (10.0 gm; 0.025 mol) was added to distilled water (100 ml) in a 250 ml conical flask. Aqueous sodium hydroxide (10% w/v) was added dropwise until neutralisation was complete. A blood-red solution was obtained. The solution was heated to 80°C on a hot plate, and sodium dithionite was added portionwise until decolourisation was complete.

The mixture was cooled to room temperature, and was extracted with portions of diethyl ether (4 x 25 ml), in a 100 ml round-bottomed flask. The ethereal solution of 1-anilino-4-aminonaphthalene was evaporated to dryness under reduced pressure. The purplish crystals obtained were recrystallised from ethanol.

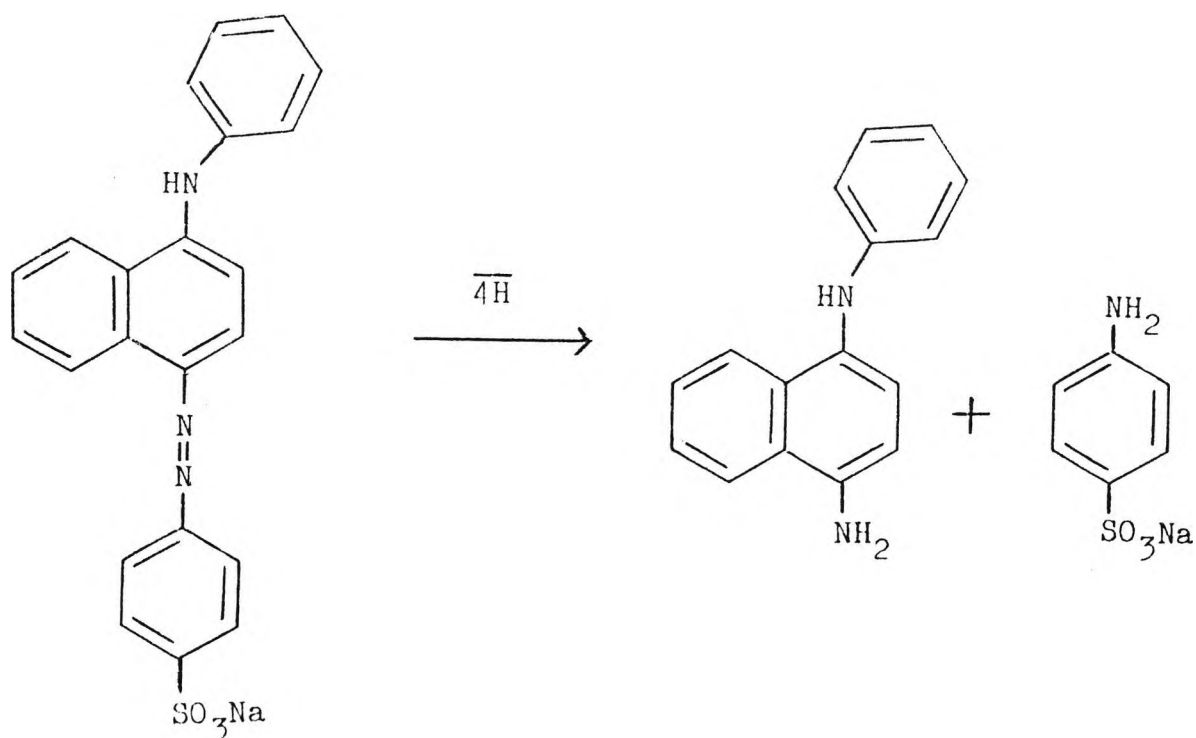


Fig. 4.12. The reaction for the preparation of 1-anilino-4-aminonaphthalene.

Weight of product obtained = 4.38 gm

Actual Yield = 80%

1-anilino-4-aminonaphthalene was characterised from the following data:

Spectroscopic Analysis

Infra-red (KBr disc)

cm<sup>-1</sup>

3414	N-H stretch
3387	-NH <sub>2</sub> stretch
3347	-NH <sub>2</sub> stretch
1591	Aryl-H stretch
1498	Aryl-H stretch

<sup>1</sup>H Nuclear Magnetic Resonance (CDCl<sub>3</sub>/TMS)

§ 5.5 (singlet, 2H, amine)

C,H,N Microanalytical Data

C<sub>16</sub>H<sub>14</sub>N<sub>2</sub>

Calculated (%)	C : 82.05	H : 5.98	N : 11.97
Found (%)	C : 82.17	H : 5.82	N : 11.90

Melting Point = 145-148°C

(literature value (8) = 147-149°C)

4.4.3. Preparation of N-(1-anilinonaphthyl-4) Maleamic Acid. (C-13).

1-anilino-4-aminonaphthalene, (C-12), (0.492 gm; 0.0021 mol) was dissolved in chloroform (15 ml) at 5°C, in a 25 ml round-bottomed flask, with stirring.

Maleic anhydride (0.30 gm; 0.003 mol) was dissolved in chloroform (5 ml) at 5°C, and was added to the amine solution.

The mixture was stirred overnight at 5°C, and the red precipitate formed was filtered at the pump, washed with cold chloroform (15 ml) and dried in vacuo at 80°C.

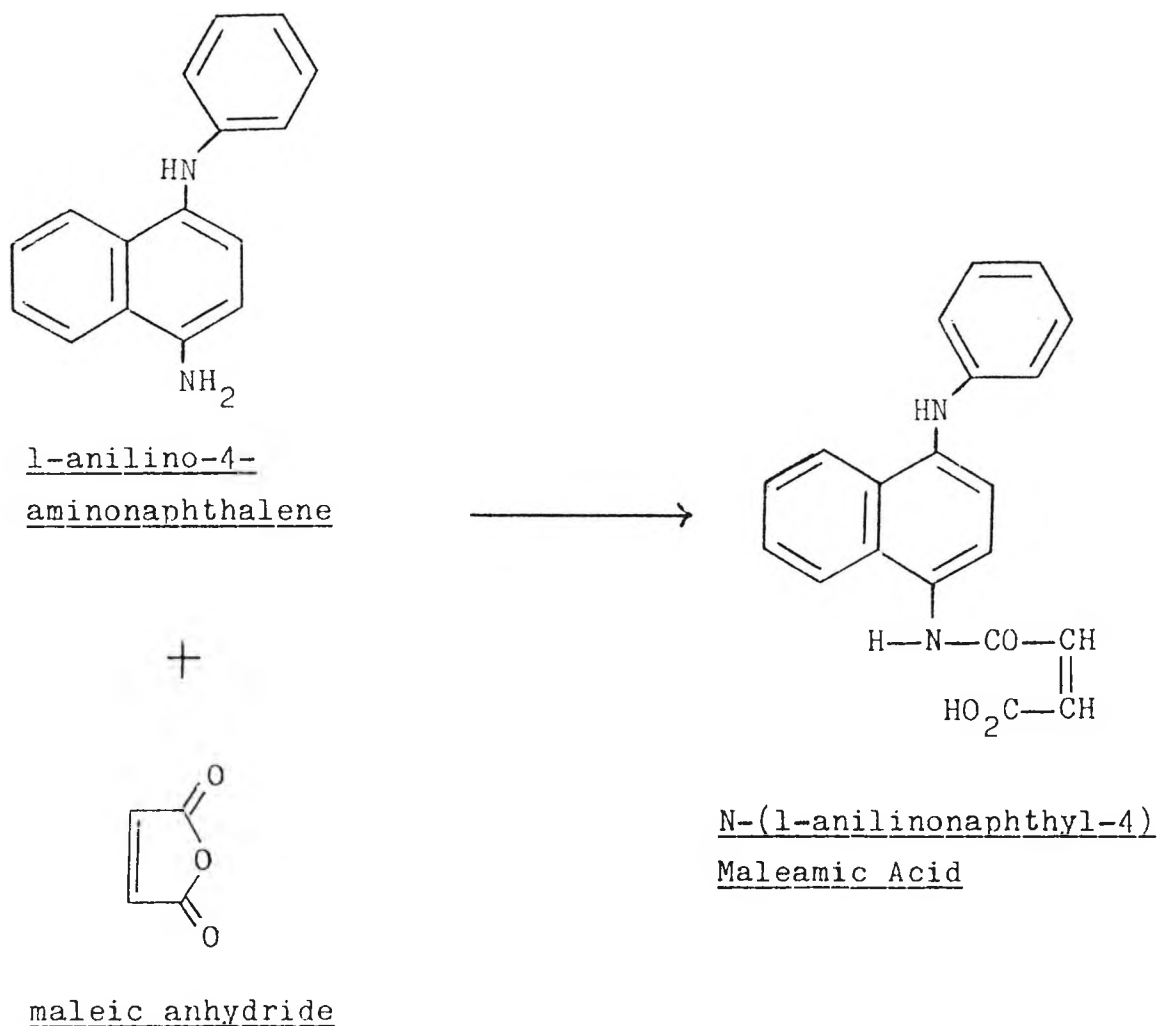


Fig. 4.13. The reaction for the preparation of N-(1-anilinonaphthyl-4) Maleamic Acid.

Weight of product obtained = 0.57 gm

Actual Yield = 81%

N-(1-anilinonaphthyl-4) Maleamic Acid was characterised from the following data:

Infra-red Spectrum Analysis (KBr disc)

cm<sup>-1</sup>

3426	N-H stretch
3224 ]	Hydrogen-bonded O-H bending of carboxylic acid
3049 ]	
1692	Conjugated CO <sub>2</sub> H
1582	Aryl-H stretch
1500	Aryl-H stretch

C, H, N Microanalytical Data

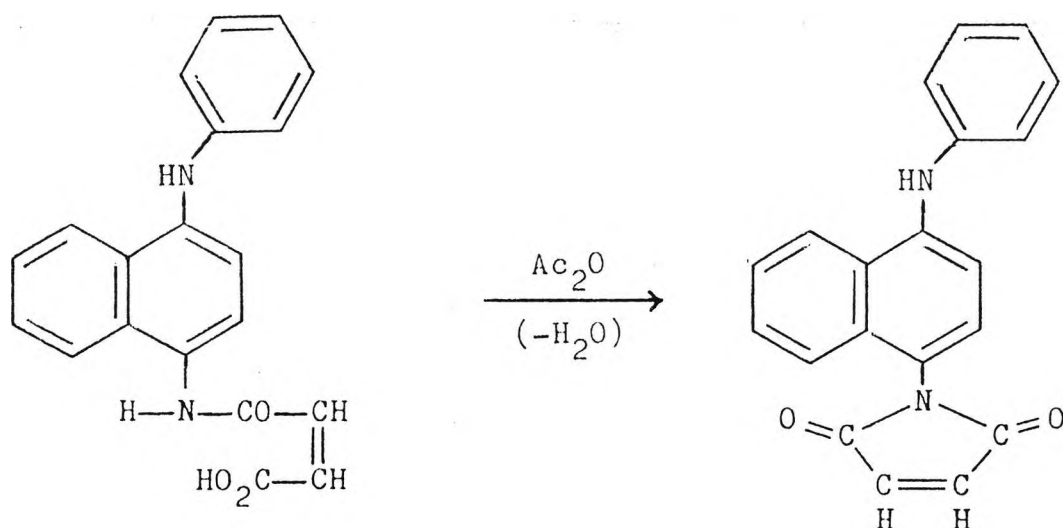
C<sub>20</sub>H<sub>16</sub>N<sub>2</sub>O<sub>3</sub>

Calculated	(%)	C : 72.29	H : 4.82	N : 8.43
Found	(%)	C : 72.38	H : 4.94	N : 8.56

4.4.4. Preparation of N-(1-anilinonaphthyl-4)  
Maleimide. (C-14).

N-(1-anilinonaphthyl-4) maleamic acid, (C-13), (0.33 gm; 0.001 mol) was added to a solution of acetic anhydride (6.0 gm (6 ml); 0.06 mol) containing sodium acetate (0.06 gm; 0.008 mol). The resulting suspension was heated to 100°C in an oil bath, with stirring, for two hours. The reaction mixture was cooled to room temperature in a cold water bath, poured into ice-water (30 ml) and vigorously stirred.

The red solid formed was collected at the pump, washed with distilled water (4 x 20 ml), and recrystallised from ethyl acetate to yield red prisms.



N-(1-anilinonaphthyl-4)  
Maleamic Acid

N-(1-anilinonaphthyl-4)  
Maleimide

Fig. 4.14. The reaction for the preparation  
of N-(1-anilinonaphthyl-4) Maleimide.

Weight of product obtained = 0.24 gm

Actual Yield = 77%

N-(1-anilinonaphthyl-4) Maleimide was characterised from the following data:

Spectroscopic Analysis

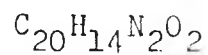
Infra-red (KBr disc)

cm <sup>-1</sup>	
3379	N-H stretch
1704	C=O stretch (maleimide)
1588	Aryl-H vibration
1528	N-H bending

<sup>1</sup>H Nuclear Magnetic Resonance (DMSO-d<sub>6</sub>/TMS)

§ 7.03 (singlet, 2H, vinyl)

C,H,N Microanalytical Data



Calculated (%)	C : 76.43	H : 4.46	N : 8.92
Found (%)	C : 76.52	H : 4.51	N : 8.87

Melting Point = 204-206°C

(literature value (8) = 207-208.5°C)

4.5. SYNTHESIS OF THE MALEIMIDYL BENZOATE ESTER  
OF BENZ(c,d)INDOL-2(1H)-ONE.

4.5.1. Preparation of Benz(c,d)indol-2(1H)-one.  
(Naphthostyryl). (C-15). (10,11).

Anhydrous aluminium chloride (14.63 gm; 0.11 mol) was added, with stirring, to anhydrous 1,2-dichlorobenzene (35 ml) in a 100 ml round-bottomed three-necked flask. The mixture was slowly heated to 160°C. It was then allowed to cool to 150°C, and a solution of 1-naphthyl isocyanate (8.5 ml; 0.05 mol) in anhydrous 1,2-dichlorobenzene (15 ml), was then slowly added over 30 minutes. The reaction mixture was then allowed to cool to 80°C, and hydrochloric acid (40 ml, 30% v/v) was cautiously added, together with anhydrous 1,2-dichlorobenzene (8 ml). The mixture was stirred at 95°C for 45 minutes, and was then allowed to cool to room temperature. The suspension was then centrifuged at 10000 g for 15 minutes, and the lower organic layer was isolated.

The organic layer was introduced into a 100 ml round-bottomed three-necked flask, and was mixed with sodium hydroxide solution (40 ml, 0.01 M) to pH 10, under nitrogen. Aqueous sodium hydroxide (8.4 ml, 2 M) was then added, the mixture was stirred at 95°C for one hour, and allowed to stand for a further hour at that temperature. The upper aqueous layer was isolated and was shaken with activated charcoal (0.5 gm). The mixture was filtered under a nitrogen atmosphere, and the residue was washed with distilled water (5 ml)

The filtrate was transferred to a 100 ml round-bottomed flask, and was heated with sodium dithionite (0.2 gm), to 95°C,

with stirring. Hydrochloric acid (30 ml, 18% v/v) at 90°C was added to the flask. The latter was maintained at 95°C for 30 minutes, and was then allowed to cool to 50°C. Yellow crystals deposited, and these were filtered at the pump, washed with distilled water (2 x 20 ml) and dried in vacuo at 80°C.

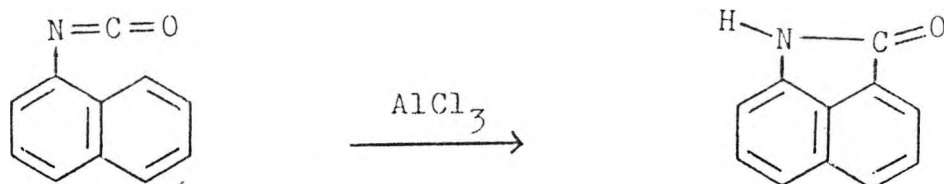


Fig. 4.15. The reaction for the preparation of Naphthostyryl.

Weight of product obtained = 5.38 gm

Actual Yield = 63%

Naphthostyryl was characterised by the following data:

Spectroscopic Analysis

Infra-red (KBr disc)

cm<sup>-1</sup>

3189 N-H stretch

1726 C=O stretch

<sup>1</sup>H Nuclear Magnetic Resonance (DMSO-d<sub>6</sub>/TMS)

δ 7.08 to 8.28 (multiplet, 6H, ArH)

C, H, N Microanalytical Data

C<sub>11</sub>H<sub>7</sub>NO

Calculated (%) C : 78.11 H : 4.14 N : 8.28

Found (%) C : 78.30 H : 4.28 N : 8.17

Melting Point = 179-180°C

(literature value (10,11) = 181°C)

4.5.2. Preparation of 1-hydroxy-methylbenz(c,d)indol-2  
(1H)-one. (Hydroxymethyl-naphthostyryl). (C-16). (12).

Naphthostyryl, (C-15), (4.0 gm; 0.023 mol) was dissolved, with stirring, in 1,4-dioxane (100 ml) at 60°C. To the clear solution obtained, was added aqueous formaldehyde (35% w/v, 5.1 gm (5.1 ml); 0.056 mol) and potassium carbonate (8.1 gm; 0.056 mol). The mixture was heated, and kept at 80°C, with stirring, for 30 minutes.

The mixture was filtered under suction, and the filtrate was evaporated to dryness under reduced pressure. The resulting residue was recrystallised from ethanol (25 ml), to yield yellow, hexagonal prisms.

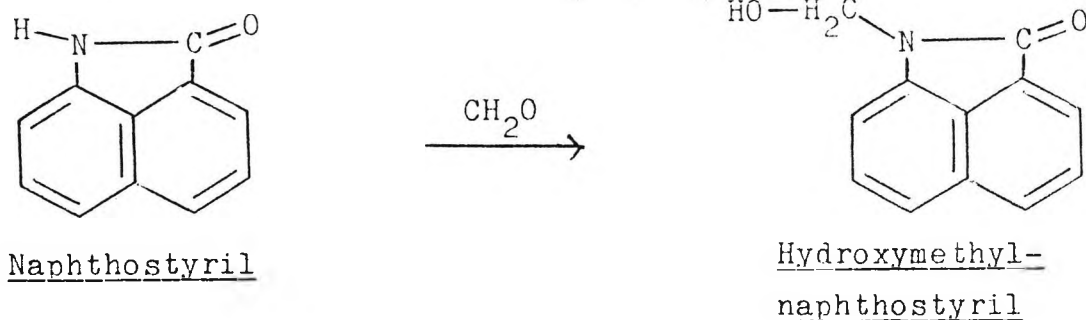


Fig. 4.16. The reaction for the preparation of Hydroxymethyl-naphthostyryl.

Weight of product obtained = 2.84 gm

Actual Yield = 60%

1-Hydroxymethyl-naphthostyryl was characterised from the following data:

Spectroscopic Analysis

Infra-red (KBr disc)

cm<sup>-1</sup>

3345 O-H stretch

1674 lactam ring

1630 C-O stretch

<sup>1</sup>H Nuclear Magnetic Resonance (DMSO-d<sub>6</sub>/TMS)

§ 7.33 to 8.21 (multiplet, 6H, ArH)

§ 5.35 (singlet, 2H, methylene)

§ 4.50 (singlet, 1H, hydroxyl)

C,H,N Microanalytical Data

C<sub>12</sub>H<sub>9</sub>NO<sub>2</sub>

Calculated (%) C : 72.36 H : 4.52 N : 7.04

Found (%) C : 72.51 H : 4.48 N : 7.11

Melting Point = 140-141°C

(literature value (12) = 141°C)

4.5.3. Preparation of 1-chloro-methylbenz(c,d)indol-2  
(1H)-one. (Chloromethyl-naphthostyryl). (C-17). (12).

Hydroxymethyl-naphthostyryl, (C-16), (0.24 gm; 0.12 mmol) was suspended in diethyl ether (2 ml), and cooled to 0°C.

Phosphorus pentachloride (0.25 gm; 1.2 mmol) was added, with stirring, and the resulting mixture was stirred at room temperature for two hours.

The suspension was then cooled to 0°C for one hour, and filtered at the pump. The greyish residue was recrystallised from cyclohexane, to yield a cream-coloured solid.

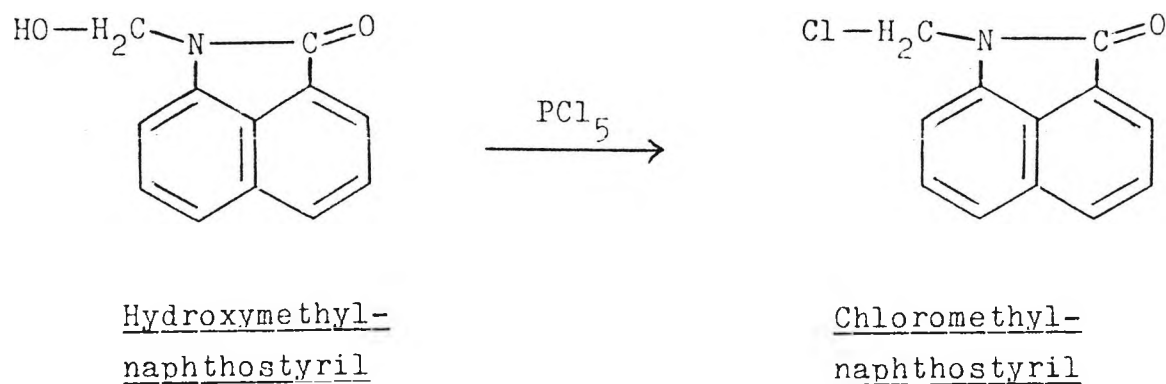


Fig. 4.17. The reaction for the preparation  
of Chloromethyl-naphthostyryl.

Weight of product obtained = 0.16 gm

Actual Yield = 63%

1-Chloromethyl-naphthostyryl was characterised from the following data:

Spectroscopic Analysis

Infra-red (KBr disc)

cm<sup>-1</sup>  
1721        lactam ring  
1633        C-O stretch  
777         C-Cl stretch

<sup>1</sup>H Nuclear Magnetic Resonance (DMSO-d<sub>6</sub>/TMS)

§ 7.07 to 8.00 (multiplet, 6H, ArH)

§ 5.87 (singlet, 2H, methylene)

C,H,N Microanalytical Data



Calculated (%)        C : 66.21        H : 3.68        N : 6.44

Found (%)        C : 66.33        H : 3.64        N : 6.41

Melting Point = 140-141°C

(literature value (12) = 141°C)

4.5.4. Preparation of N-(p-benzoic acid)

Maleamic Acid. (C-18).

p-aminobenzoic acid (1.15 gm; 8.4 mmol) was dissolved in ice-cold acetonitrile (22 ml), and mixed with a solution of maleic anhydride (0.86 gm; 8.8 mmol) in ice-cold acetonitrile (12 ml), in a 50 ml round-bottomed flask.

The mixture was allowed to react overnight, with stirring, at 4°C. A pale yellow precipitate resulted. The precipitate was collected via filtration at the pump, washed with ice-cold acetonitrile (3 x 10 ml), and dried in vacuo at 40°C; to give N-(p-benzoic acid) maleamic acid, as a yellow, crystalline solid.

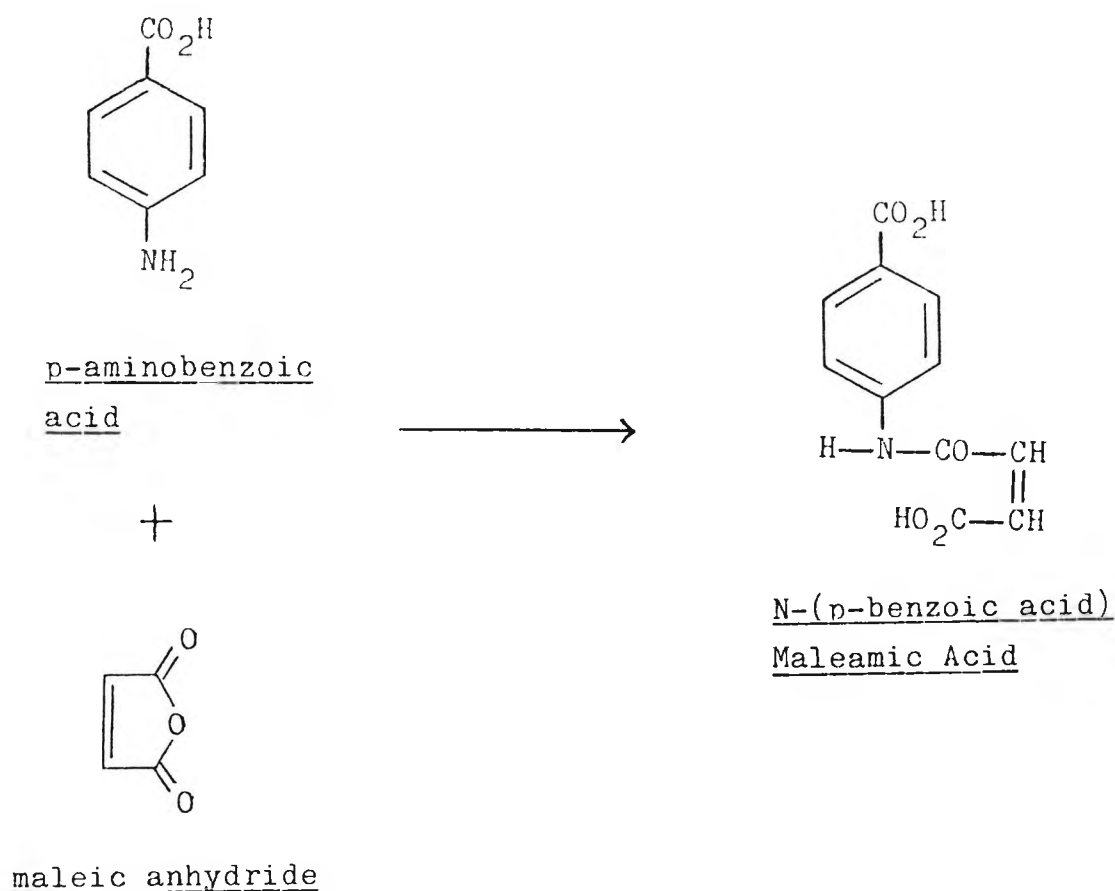


Fig. 4.18. The reaction for the preparation of N-(p-benzoic acid) Maleamic Acid.

Weight of product obtained = 1.49 gm

Actual Yield = 76%

N-(p-benzoic acid) Maleamic Acid was characterised from the following data:

Infra-red Spectrum Analysis (KBr disc)

cm<sup>-1</sup>

3315 } Hydrogen-bonded O-H bending  
3011 } of carboxylic acid

1693 C=O stretch

1626 >C=C< absorption

C,H,N Microanalytical Data

C<sub>11</sub>H<sub>9</sub>NO<sub>5</sub>

Calculated (%) C : 56.17 H : 3.83 N : 5.96

Found (%) C : 56.26 H : 3.82 N : 5.91

#### 4.5.5. Preparation of N-(p-benzoic acid) Maleimide. (C-19).

N-(p-benzoic acid) maleamic acid, (C-18), (0.33 gm; 1.40 mmol) was added to acetic anhydride (6.0 gm (6 ml); 0.06 mol) in a 10 ml round-bottomed flask, containing sodium acetate (0.06 gm; 8.2 mmol). The resulting suspension was heated in an oil bath to 100°C for 90 minutes, with stirring. The reaction mixture was cooled to room temperature in a cold water bath, and poured into ice-cold water (30 ml).

The precipitated product, N-(p-benzoic acid) maleimide was removed by suction filtration, washed with ice-cold water (3 x 15 ml) and hexane (66-69°C b.p., 1 x 10 ml), and was then dried in vacuo at 40°C.

N-(p-benzoic acid) maleimide was recrystallised by addition of water to its solution in acetonitrile, and finally from 100% acetonitrile, as pinkish crystals.

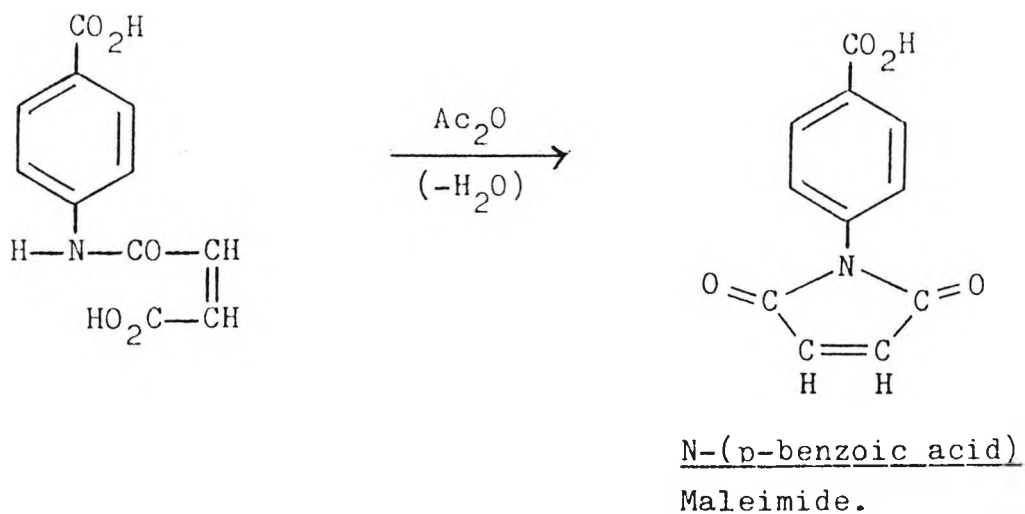


Fig. 4.19. The reaction for the preparation of N-(p-benzoic acid) maleimide.

Weight of product obtained = 0.16 gm

Actual Yield = 53%

N-(p-benzoic acid) Maleimide was characterised from the following data:

Spectroscopic Analysis

Infra-red (KBr disc)

cm<sup>-1</sup>

3087          O-H stretch of carboxylic acid

1798 }  
1716 }          C=O (maleimide)

<sup>1</sup>H Nuclear Magnetic Resonance (DMSO-d<sub>6</sub>/TMS)

δ 6.92 (singlet, 2H, vinyl)

C, H, N Microanalytical Data

C<sub>11</sub>H<sub>7</sub>NO<sub>4</sub>

Calculated (%)          C : 60.83          H : 3.23          N : 6.45

Found (%)          C : 60.89          H : 3.27          N : 6.38

4.5.6. Preparation of the Maleimidyl Benzoate Ester of Benz(c,d)indol-2(1H)-one. (C-20).

1-chloromethyl-naphthostyryl, (C-17), (0.05 gm; 0.23 mmol) and N-(p-benzoic acid) maleimide, (C-19), (0.05 gm; 0.23 mmol), were mixed, ground and placed together with dimethylformamide (1 ml), in a 5 ml round-bottomed flask fitted with a reflux condenser and calcium chloride tube. The mixture was heated, with stirring, to 100°C and maintained at this temperature for 20 minutes.

After cooling to 20°C, water (1 ml) was added drop-by-drop. The resulting precipitate was filtered, and crystallised from ethanol-water, to yield a beige, crystalline solid. The solid was finally dried in vacuo at 40°C

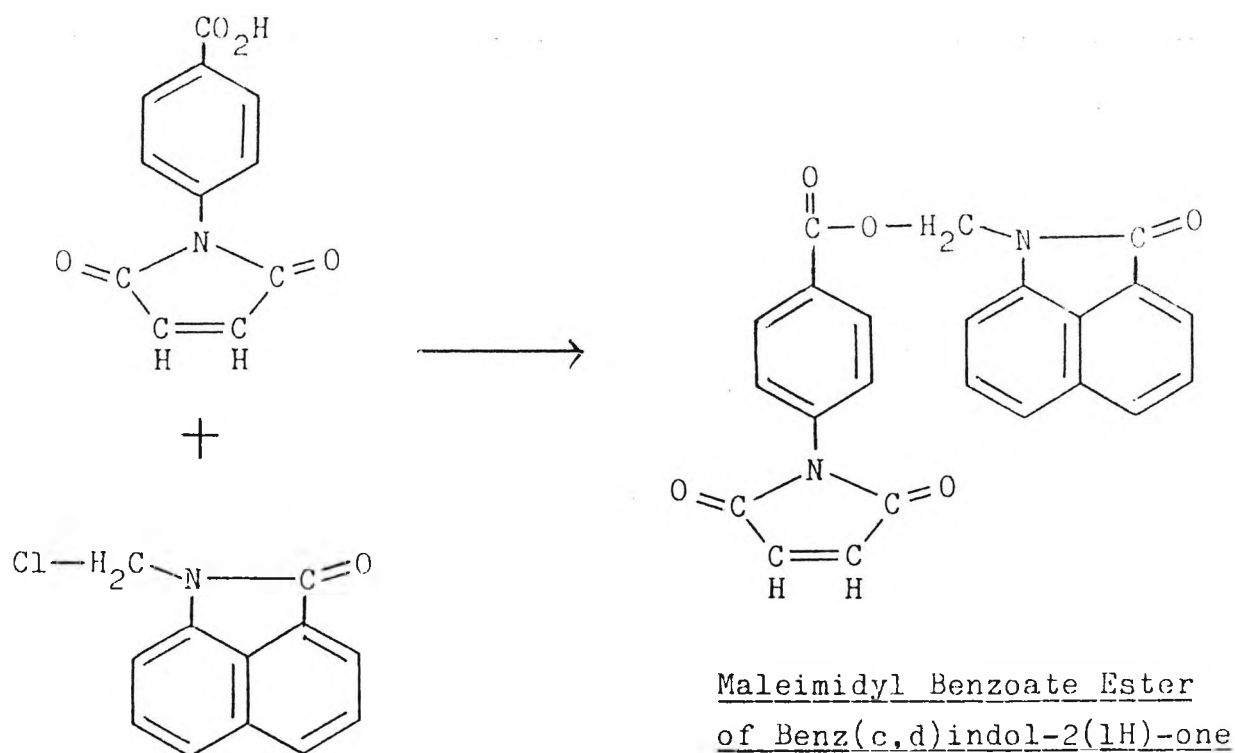


Fig. 4.20. The reaction for the preparation of the maleimidyl benzoate ester of Benz(c,d)indol-2(1H)-one.

Weight of product obtained = 0.43 gm

Actual Yield = 47%

The Maleimidyl Benzoate Ester of Benz(c,d)indol-2(1H)-one  
was characterised from the following data:

Infra-red Spectrum Analysis (KBr disc)

cm<sup>-1</sup>

1711 }  
1632 } C=O (maleimide)

701 >C=C< absorption

C,H,N Microanalytical Data

C<sub>23</sub>H<sub>14</sub>N<sub>2</sub>O<sub>5</sub>

Calculated (%) C : 69.35 H : 3.52 N : 7.04

Found (%) C : 69.28 H : 3.64 N : 7.09

4.6. SYNTHESIS OF SUCCINIMIDYL TRANS-PARINARATE. (C-21).

Trans-parinaric acid (0.055 gm; 0.2 mmol) and N-Hydroxysuccinimide (0.025 gm; 0.25 mmol) were dissolved in ethyl acetate (20 ml) in a 50 ml round-bottomed flask at 5°C. To this was added, with stirring, 1,3-dicyclohexylcarbodiimide (0.041 gm; 0.2 mmol). The by-product, 1,3-dicyclohexylurea, started precipitating immediately. After complete dissolution of the dicyclohexylcarbodiimide, (approximately 10 minutes), the temperature was held at 5°C for 10 minutes, with occasional stirring. The reaction mixture was allowed to attain room temperature, and held there for 30 minutes, after which time it was filtered.

The precipitate was washed with ethyl acetate (30 ml) and the combined filtrate and washings, were evaporated under reduced pressure, at room temperature, to dryness.

The solid was recrystallised from acetonitrile, to yield a cream-coloured powder.

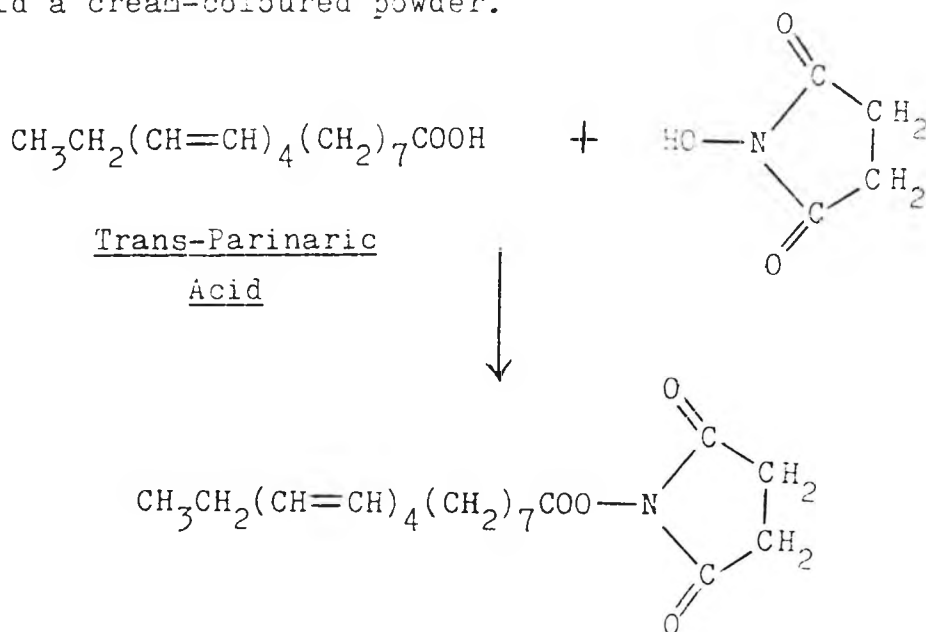


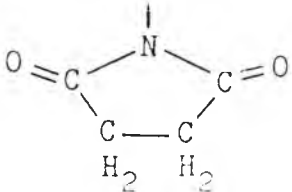
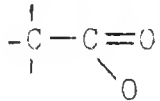
Fig. 4.21. The reaction for the preparation of Succinimidyl Trans-Parinarate.

Weight of product obtained = 0.065 gm

Actual Yield = 87%

Succinimidyl Trans-Parinarate was characterised from the following data:

Mass Spectrum Analysis

<u>Molecular Mass</u>	<u>% Abundance</u>	<u>Attributable Species</u>
98.0260	100.00	
56.0521	46.10	$-(CH_2)_4-$
56.0174	29.90	
55.0212	14.03	$-CH=CH-CH_2-CH_3$
98.1028	11.16	$-(CH_2)_7-$
99.0356	8.97	'Base Peak' + 1
70.0692	6.21	$-(CH_2)_5-$
100.0991	5.00	$-OOC-(CH_2)_4-$
142.1141	2.07	$-OOC-(CH_2)_7-$

C, H, N Microanalytical Data

C<sub>22</sub>H<sub>31</sub>NO<sub>4</sub>

Calculated (%)	C : 70.78	H : 8.31	N : 3.75
Found (%)	C : 70.82	H : 8.29	N : 3.79

#### 4.7. SYNTHESIS OF 9-BROMOMETHYLACRIDINE.

##### 4.7.1. Preparation of 9-Methylacridine. (C-22). (13).

A mixture of diphenylamine (5.0 gm; 0.03 mol) and glacial acetic acid (5.0 gm (5 ml); 0.08 mol) in the presence of anhydrous zinc chloride (20 gm), was heated, with stirring, to 220°C in a 50 ml round-bottomed flask. The excess acetic acid was thereby evaporated, and the mixture was then held at 225°C for six hours. The reaction mixture was then digested with hot, aqueous sulphuric acid (10% v/v), and then rendered strongly basic (approximately pH 10), with concentrated ammonia solution in order to dissolve the zinc chloride.

The insoluble residue was extracted with benzene (3 x 15 ml) and, after separation, the benzene layer was extracted again with aqueous sulphuric acid (10% v/v). The acidified extract was made basic by the addition of aqueous ammonia, upon which yellow crystals separated out.

Filtration yielded crude 9-methylacridine. A portion of the crude material (0.5 gm) was subjected to column chromatography utilising alumina, and was eluted with petroleum ether (60-80°C b.p.) and the collected fractions were pooled and evaporated to dryness under reduced pressure.

The pale yellow residue was recrystallised from the petroleum ether, to yield pale yellow crystals.

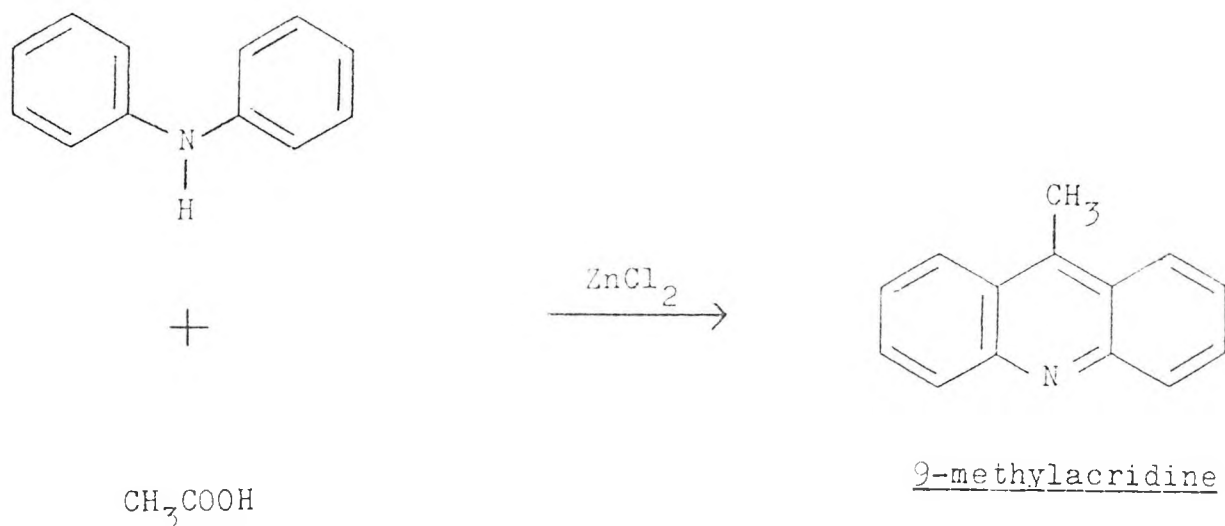


Fig. 4.22. The reaction for the preparation of 9-methylacridine.

9-methylacridine was characterised from the following data:

C,H,N Microanalytical Data

C<sub>14</sub>H<sub>11</sub>N

Calculated	(%)	C : 87.05	H : 5.70	N : 7.25
Found	(%)	C : 87.12	H : 5.78	N : 7.13

Melting Point = 115-117°C

(literature value (14) = 117-118°C)

4.7.2. Preparation of 9-Bromomethylacridine. (C-23). (15).

9-methylacridine, (C-22), (0.20 gm; 1.0 mmol) and N-Bromosuccinimide (0.20 gm; 1.12 mmol), were added to carbon tetrachloride (30 ml) containing benzoyl peroxide (0.003 gm), in a 50 ml round-bottomed flask. The mixture was refluxed for two hours during which time, succinimide, a white solid, was seen to rise to the surface.

The solution was evaporated under reduced pressure, and the residue was recrystallised from petroleum ether (60-80°C b.p.)

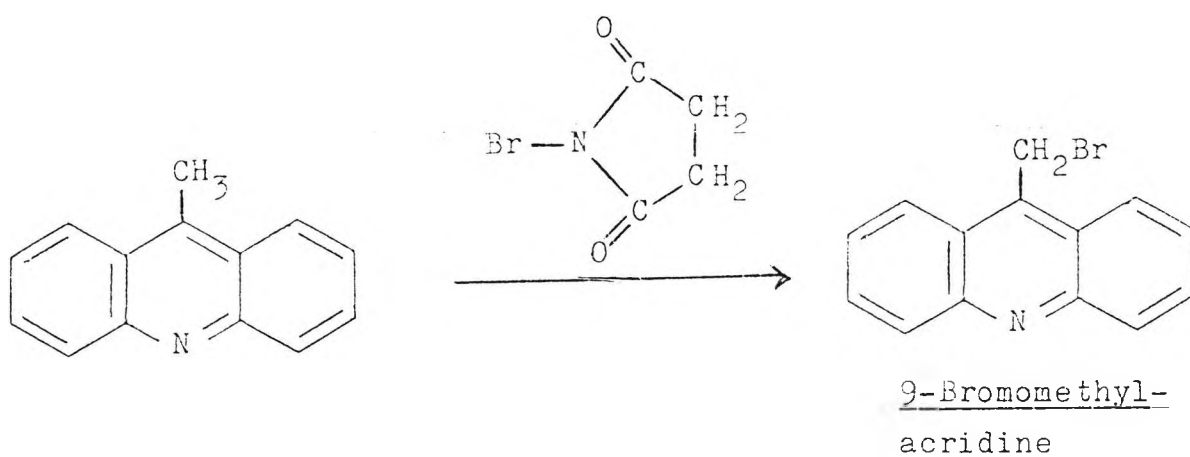


Fig. 4.23. The reaction for the preparation of 9-Bromomethylacridine.

Weight of product obtained = 0.23 gm

Actual Yield = 82%

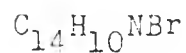
9-Bromomethylacridine was characterised from the following data:

<sup>1</sup>H Nuclear Magnetic Resonance Spectrum (CDCl<sub>3</sub>/TMS)

§ 7.80 to 8.80 (multiplet, 8H, ArH)

§ 6.1 (singlet, 2H, methylene)

C,H,N Microanalytical Data



Calculated (%)      C : 61.76      H : 3.68      N : 5.15

Found (%)      C : 61.82      H : 3.67      N : 5.12

Melting Point = 147-150°C

(literature value (15) = 147-151°C)

4.8. REFERENCES.

1. Weltman, J.K., Szaro, R.P., Frackelton, Jr., A.R., Dowben, R.M., Bunting, J.R. & Cathou, R.E.  
(1973) J. Biol. Chem. 248 3173
2. Donaldson, N.  
In The Chemistry & Technology of Naphthalene Compounds.  
(Publ: Edward Arnold) p 256
3. Handbook of Chemistry & Physics.  
(Ed: Robert C. Weast, CRC Press) 67th Edition (1988)
4. Hudson, E.N. & Weber, G.  
(1973) Biochemistry 12 4154
5. Smith, M., Moffatt, J.G. & Khorana, H.G.  
(1958) J. Amer. Chem. Soc. 80 6204
6. Lorand, L., Brennen, W.T. & Rule, N.G.  
(1962) Arch. Biochem. Biophys. 96 147
7. Drake, N.L.  
(1942) Org. Reactions 1 106
8. Kanaoka, Y., Machida, M., Machida, M. & Sekine, T.  
(1973) Biochim. Biophys. Acta 317 563
9. Ridd, J.H.  
(1961) Quart. Rev. Chem. Soc. 15 418
10. Harnisch, H.  
(1976) German Offen 2,635,693 (Bayer AG)
11. Harnisch, H.  
(1977) German Offen 2,700,649 (Bayer AG)
12. Wendelin, W., Gubitz, G. & Pracher, U.  
(1987) J. Heterocyclic Chem. 24 1381
13. Tsuge, O., Nishinohara, M. & Tashiro, M.  
(1963) Bull. Chem. Japan 36 1477
14. Jensen, H. & Rethwisch, F.  
(1928) J. Amer. Chem. Soc. 50 1144

15. Akasaka, K., Suzuki, T., Ohruai, H., Meguro, H.,  
Shindo, Y. & Takahashi, H.

(1987) Anal. Letters 20 1581

CHAPTER 5.

EXPERIMENTAL PROCEDURES FOR THE FLUORESCENT  
MODIFICATION OF cAMP RECEPTOR PROTEIN.

## 5.1. INTRODUCTION.

cAMP Receptor Protein (CRP) was provided by SmithKline Beecham Pharmaceuticals, as a buffered aqueous solution. In order to fluorescently modify the protein, it was necessary to determine the CRP concentration of the solution supplied. This was achieved by a standard protein assay procedure, and the result obtained dictated the amount of CRP solution utilised for each modification procedure.

The CRP was then labelled with a variety of amine reactive and sulphhydryl (thiol) reactive fluorescent probes, using adaptations of documented procedures.

## 5.2. CRP ASSAY.

### 5.2.1. Experimental Procedure. (1).

Bovine Serum Albumin (BSA, 100 mg) was dissolved in distilled water (1 ml).

Five tubes were set up, in duplicate, as follows:

Tubes 1 -	50.0 $\mu$ l BSA solution +	200.0 $\mu$ l water	(20 mg/ml)
Tubes 2 -	37.5 $\mu$ l BSA solution +	212.5 $\mu$ l water	(15 mg/ml)
Tubes 3 -	25.0 $\mu$ l BSA solution +	225.0 $\mu$ l water	(10 mg/ml)
Tubes 4 -	12.5 $\mu$ l BSA solution +	237.5 $\mu$ l water	( 5 mg/ml)
Tubes 5 -	250.0 $\mu$ l water		( 0 mg/ml)

Stock CRP solution was treated, in duplicate, as follows:

Tubes 6 -	250.0 $\mu$ l CRP solution	
Tubes 7 -	100.0 $\mu$ l CRP solution +	150.0 $\mu$ l water
Tubes 8 -	50.0 $\mu$ l CRP solution +	200.0 $\mu$ l water

Bradford Reagent (Coomassie Brilliant Blue G-250 (0.01% w/v), aqueous ethanol (4.70% v/v) and phosphoric acid solution (8.50% w/v), 1 ml) was added to each of the tubes, and the contents were thoroughly mixed. The tubes were allowed to stand for 10 minutes, and the absorbance of each of the tubes, at 595 nm, was then determined using the Beckman DU-50 Spectrophotometer.

A standard curve was plotted, and the CRP concentration, in mg/ml, was then determined.

### 5.2.2. Results.

#### BSA Solution.

<u>Tube Nos.</u>	<u>Absorbance at 595 nm</u>	<u>Concentration in mg/ml</u>
5	0.011	0.00
	0.014	0.00
4	0.207	5.00
	0.196	5.00
3	0.348	10.00
	0.332	10.00
2	0.461	15.00
	0.536	15.00
1	0.591	20.00
	0.622	20.00

Table 5.1. Absorbance readings, at 595 nm, for varying concentrations of BSA as detected by Bradford Reagent.

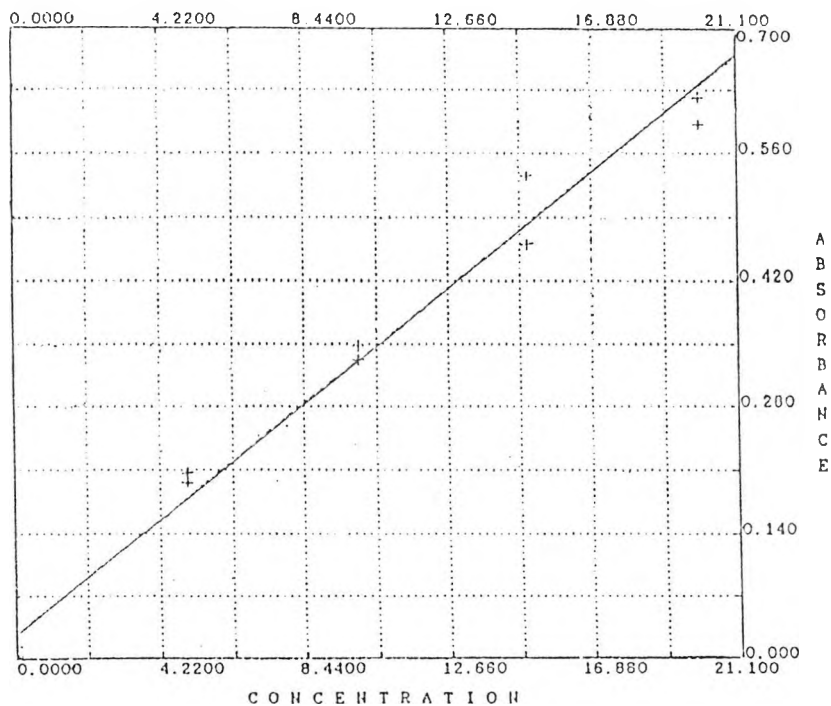


Fig. 5.1. Calibration Curve of Absorbance against Concentration (mg/ml), for the Assay of CRP Stock Solution.

CRP Solution.

<u>Tube Nos.</u>	<u>Absorbance at 595 nm</u>	<u>Conc.</u>	<u>Mean Conc.</u>	<u>Concentration in mg/ml</u>
8	0.119	3.016	2.801	2.80
	0.106	2.587		
7	0.289	8.616	7.447	(3.70)
	0.218	6.277		
6	0.416	12.80	13.02	2.60
	0.429	13.23		

Table 5.2. Absorbance readings, at 595 nm, for varying concentrations of CRP as detected by Bradford Reagent, for the deduction of the CRP concentration.

CRP concentration = 2.70 mg/ml at a dilution of 1:5.

Therefore, the stock CRP concentration = 13.50 mg/ml.

5.3. EXPERIMENTAL PROCEDURES FOR THE MODIFICATION OF THE  $\epsilon$ -AMINO GROUP OF LYSINE RESIDUES IN THE cAMP RECEPTOR PROTEIN (CRP).

5.3.1. Fluorescent Modification of CRP using Bis (1,10-phenanthroline) (Bathophenanthroline disulphonyl chloride) ruthenium (II) hexafluorophosphate dihydrate. (C-3, Ru Complex I).

The method utilised was that adapted from a documented procedure (2).

Ru Complex I (1.0 mg; 1.0  $\mu$ mol), as synthesised, was dissolved in carbonate buffer (0.05 M, 2.0 ml, pH 9.7) containing acetonitrile (1% v/v).

The above solution was divided into two equal portions. To one portion was added carbonate buffer (0.05 M, 1.0 ml, pH 9.7) containing n-butylamine (10% v/v).

Stock CRP solution (0.04 ml, 13.50 mg/ml) was dissolved in carbonate buffer (0.05 M, 0.96 ml), and this solution was added to the remaining portion.

The resulting solutions were allowed to stand overnight at 4°C. The protein-containing solution was then extensively dialysed (3 days), against phosphate buffered saline (0.10 M, 1000 ml, pH 7.4) using cellulose tubing which retains molecular weight species in excess of 12000 daltons.

The dialysand was then subjected to gel exclusion chromatography using Sephadex G-25 (20-80  $\mu$ m bead size, bed volume: approximately 10 ml), which had previously equilibrated with phosphate buffered saline (0.10 M, PBS) and was eluted with the PBS.

The collected fraction and the control sample were

diluted to 3 ml with PBS, and then subjected to U.V./visible and fluorescence spectral analysis.

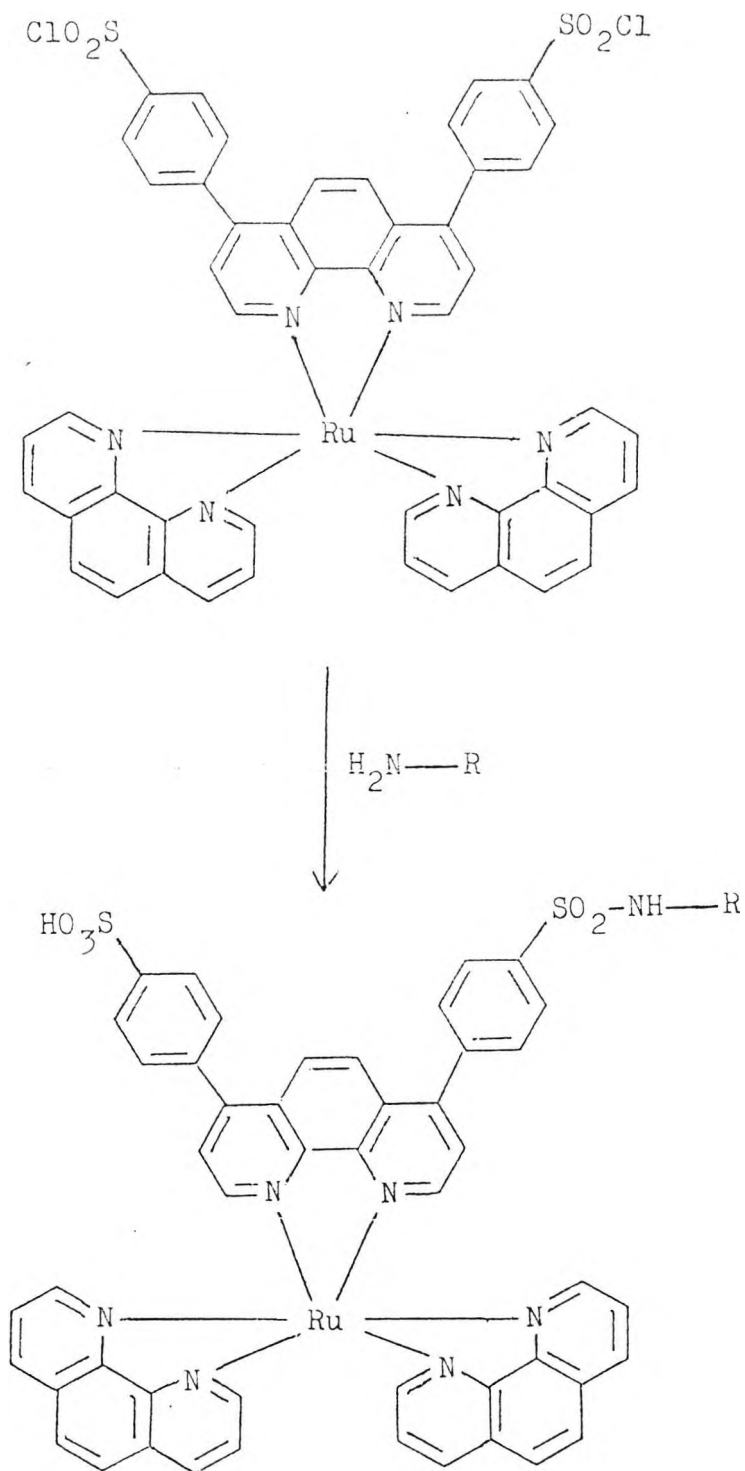


Fig. 5.2. The reaction for the preparation of a modified amine by the use of Ru Complex I.

### 5.3.2. Fluorescent Modification of CRP using Succinimidyl Trans-Parinarate. (C-21).

The method utilised was that adapted from a documented procedure (3).

Succinimidyl trans-parinarate (1.0 mg; 2.0  $\mu$ mol., as synthesised, was dissolved in carbonate buffer (0.05 M, 2.0 ml, pH 9.7) containing dimethyl sulphoxide (1% v/v).

The above solution was divided into two equal portions. To one portion was added carbonate buffer (0.05 M, 1.0 ml, pH 9.7) containing n-butylamine (10% v/v).

Stock CRP solution (0.04 ml, 13.50 mg/ml) was dissolved in carbonate buffer (0.05 M, 0.96 ml), and this solution was added to the remaining portion.

The resulting solutions were allowed to stand overnight at 4°C. The protein-containing solution was then extensively dialysed (3 days), against phosphate buffered saline (0.10 M, 1000 ml, pH 7.4) using cellulose tubing which retains molecular weight species in excess of 12000 daltons.

The dialysand was then subjected to gel exclusion chromatography using Sephadex G-25 (20-80  $\mu$ m bead size, bed volume: approximately 10 ml), which had previously equilibrated with phosphate buffered saline (0.10 M, PBS) and was eluted with the PBS.

The collected fraction and the control sample were diluted to 3 ml with PBS, and then subjected to U.V./visible and fluorescence spectral analysis.

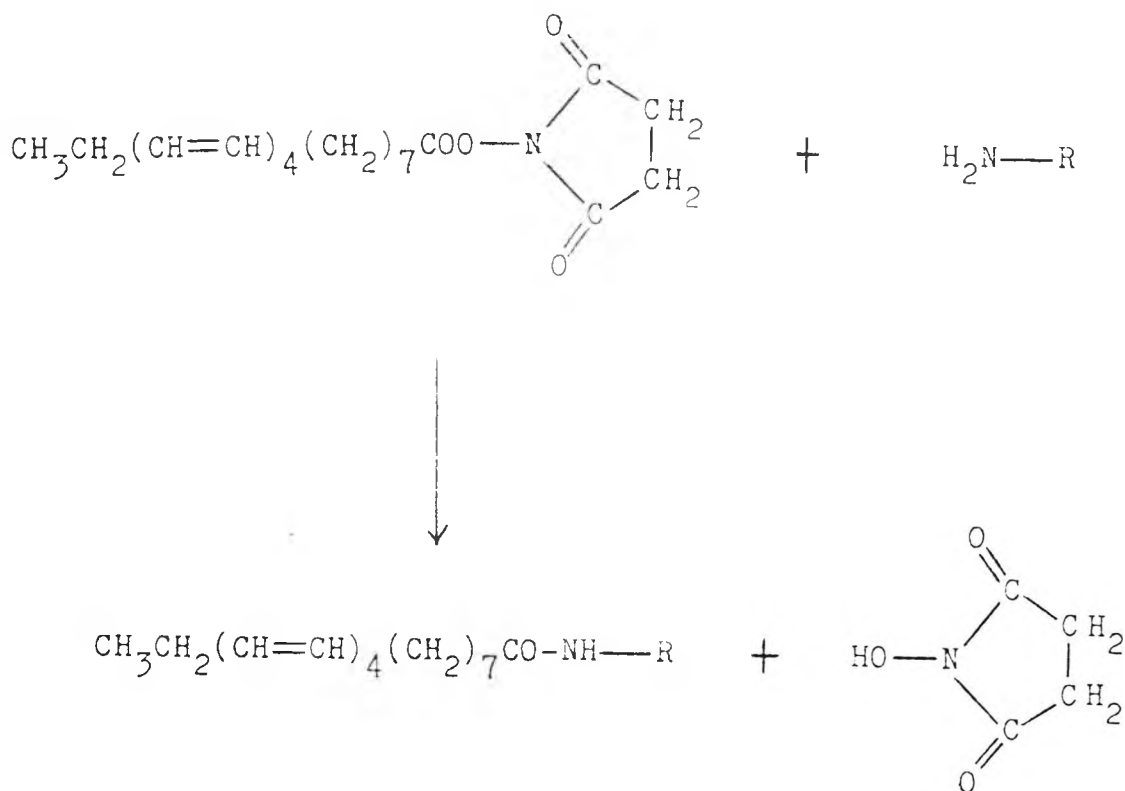


Fig. 5.3. The reaction for the preparation of a modified amine by the use of Succinimidyl Trans-Parinarate.

5.3.3. Fluorescent Modification of CRP using Sulphorhodamine Acid Chloride, (Texas Red).

The method utilised was that as outlined (2). Sulphorhodamine acid chloride (Texas Red) (1.0 mg; 1.6  $\mu\text{mol}$ ), was dissolved in carbonate buffer (0.05 M, 2.0 ml, pH 9.7) containing acetonitrile (1% v/v).

The above solution was divided into two equal portions. To one portion was added carbonate buffer (0.05 M, 1.0 ml, pH 9.7) containing n-butylamine (10% v/v).

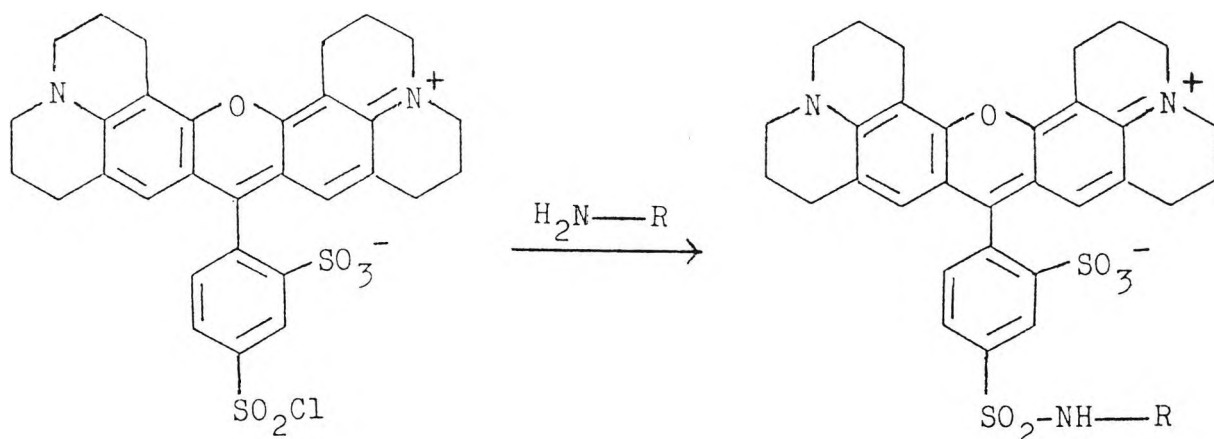
Stock CRP solution (0.04 ml, 13.50 mg/ml) was dissolved

in carbonate buffer (0.05 M, 0.96 ml), and this solution was added to the remaining portion.

The resulting solutions were allowed to stand overnight at 4°C. The protein-containing solution was then extensively dialysed (3 days), against phosphate buffered saline (0.10 M, 1000 ml, pH 7.4) using cellulose tubing which retains molecular weight species in excess of 12000 daltons.

The dialysand was then subjected to gel exclusion chromatography using Sephadex G-25 (20-80  $\mu\text{m}$  bead size, bed volume: approximately 10 ml), which had previously equilibrated with phosphate buffered saline (0.10 M, PBS) and was eluted with the PBS.

The collected fraction and the control sample were diluted to 3 ml with PBS, and then subjected to U.V./visible and fluorescence spectral analysis.



Sulphorhodamine Acid  
Chloride. (Texas Red).

Fig. 5.4. The reaction for the preparation  
of a modified amine by the use of  
Sulphorhodamine Acid Chloride, (Texas Red).

5.3.4. Fluorescent Modification of CRP using Succinimidyl 7-Amino-4-Methylcoumarin-3-Acetate.

The method utilised was that as outlined (3). Succinimidyl 7-amino-4-methylcoumarin-3-acetate (1.0 mg; 3.2  $\mu$ mol) was dissolved in carbonate buffer (0.05 M, 2.0 ml, pH 9.7), containing dimethyl sulphoxide (1% v/v).

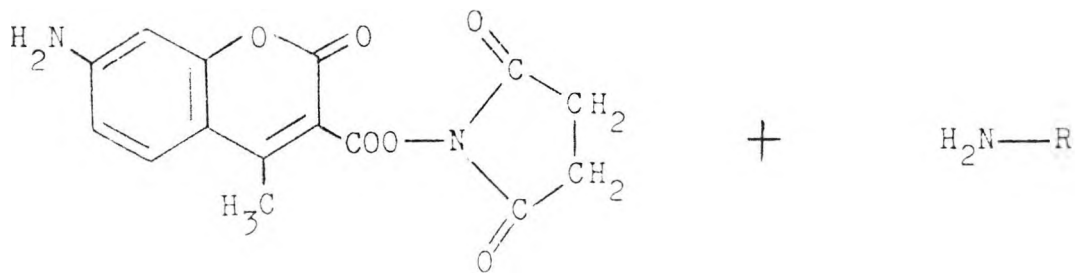
The above solution was divided into two equal portions. To one portion was added carbonate buffer (0.05 M, 1.0 ml, pH 9.7) containing n-butylamine (10% v/v).

Stock CRP solution (0.04 ml, 13.50 mg/ml) was dissolved in carbonate buffer (0.05 M, 0.96 ml), and this solution was added to the remaining portion.

The resulting solutions were allowed to stand overnight at 4°C. The protein-containing solution was then extensively dialysed (3 days), against phosphate buffered saline (0.01 M, 1000 ml, pH 7.4) using cellulose tubing which retains molecular weight species in excess of 12000 daltons.

The dialysand was then subjected to gel exclusion chromatography using Sephadex G-25 (20-80  $\mu$ m bead size, bed volume: approximately 10 ml), which had previously equilibrated with phosphate buffered saline (0.10 M, PBS) and was eluted with the PBS.

The collected fraction and the control sample were diluted to 3 ml with PBS, and then subjected to U.V./visible and fluorescence spectral analysis.



Succinimidyl 7-amino-4-  
methylcoumarin-3-acetate.

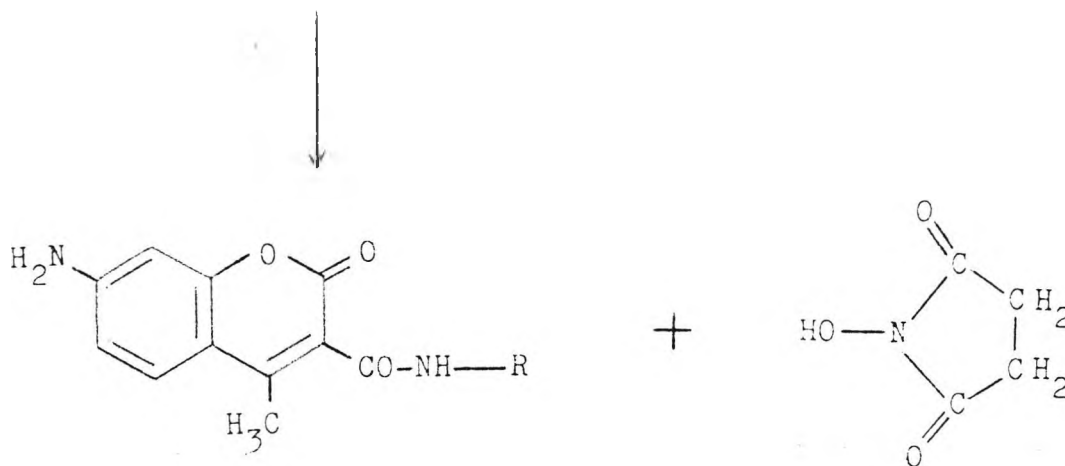


Fig. 5.5. The reaction for the preparation of a  
modified amine by the use of Succinimidyl 7-amino-  
4-methylcoumarin-3-acetate.

5.3.5. Fluorescent Modification of CRP using 5-Dimethyl-  
aminonaphthalene-1-Sulphonyl Chloride. ('Dansyl'  
Chloride).

The method utilised was that as outlined (4). 'Dansyl' Chloride (1.0 mg; 3.7  $\mu$ mol) was dissolved in carbonate buffer (0.05 M, 2.0 ml, pH 9.7), containing acetonitrile (1% v/v).

The above solution was divided into two equal portions. To one portion was added carbonate buffer (0.05 M, 1.0 ml,

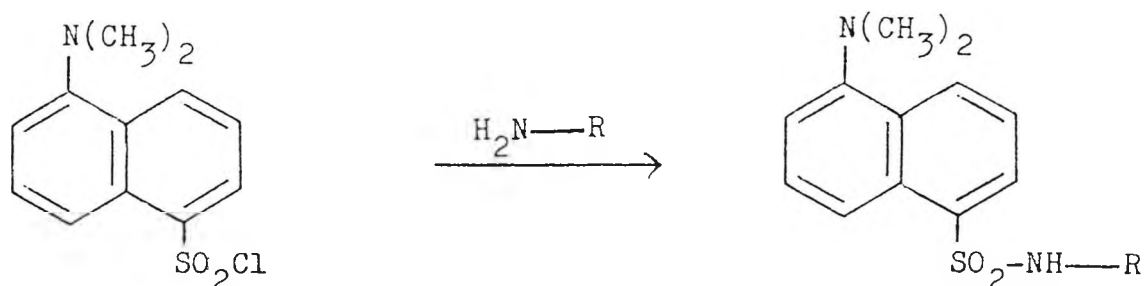
pH 9.7), containing n-butylamine (10% v/v).

Stock CRP solution (0.04 ml, 13.50 mg/ml) was dissolved in carbonate buffer (0.05 M, 0.96 ml), and this solution was added to the remaining portion.

The resulting solutions were allowed to stand overnight at 4°C. The protein-containing solution was then extensively dialysed (3 days), against phosphate buffered saline (0.10 M, 1000 ml, pH 7.4) using cellulose tubing which retains molecular weight species in excess of 12000 daltons.

The dialysand was then subjected to gel exclusion chromatography using Sephadex G-25 (20-80  $\mu$ m bead size, bed volume: approximately 10 ml), which had previously equilibrated with phosphate buffered saline (0.10 M, PBS) and was eluted with the PBS.

The collected fraction and the control sample were diluted to 3 ml with PBS, and then subjected to U.V./visible and fluorescence spectral analysis.



### 'Dansyl' Chloride

Fig. 5.6. The reaction for the preparation of a modified amine by the use of 'Dansyl' Chloride.

5.4. EXPERIMENTAL PROCEDURES FOR THE MODIFICATION OF THE THIOL GROUP OF CYSTEINE RESIDUES IN THE CAMP RECEPTOR PROTEIN (CRP).

5.4.1. Fluorescent Modification of CRP using Bis (2,2'-bipyridine) (4-Vinyl-4'-Methyl-2,2'-bipyridine) ruthenium (II) hexafluorophosphate. (Ru Complex II).

The method utilised was that adapted from a documented procedure (5).

Ru Complex II (1.0 mg; 1.64  $\mu\text{mol}$ ) was dissolved in phosphate buffered saline (0.10 M, 2.0 ml, pH 7.4, PBS) containing acetonitrile (1% v/v).

The above solution was divided into two equal portions. To one portion was added buffered (PBS) cysteine solution (1.0 ml, 1.0 mg/ml).

Stock CRP solution (0.04 ml, 13.50 mg/ml) was dissolved in PBS (0.10 M, 0.96 ml), and this solution was added to the remaining portion.

The resulting solutions were allowed to stand overnight at 4°C. The protein-containing solution was then extensively dialysed (3 days), against PBS (0.10 M, 1000 ml, pH 7.4) using cellulose tubing which retains molecular weight species in excess of 12000 daltons.

The dialysand was then subjected to gel exclusion chromatography using Sephadex G-25 (20-80  $\mu\text{m}$  bead size, bed volume: approximately 10 ml), which had previously equilibrated with PBS (0.10 M) and was eluted with the PBS.

The collected fraction and the control sample were diluted to 3 ml with PBS, and then subjected to U.V./visible and fluorescence spectral analysis.

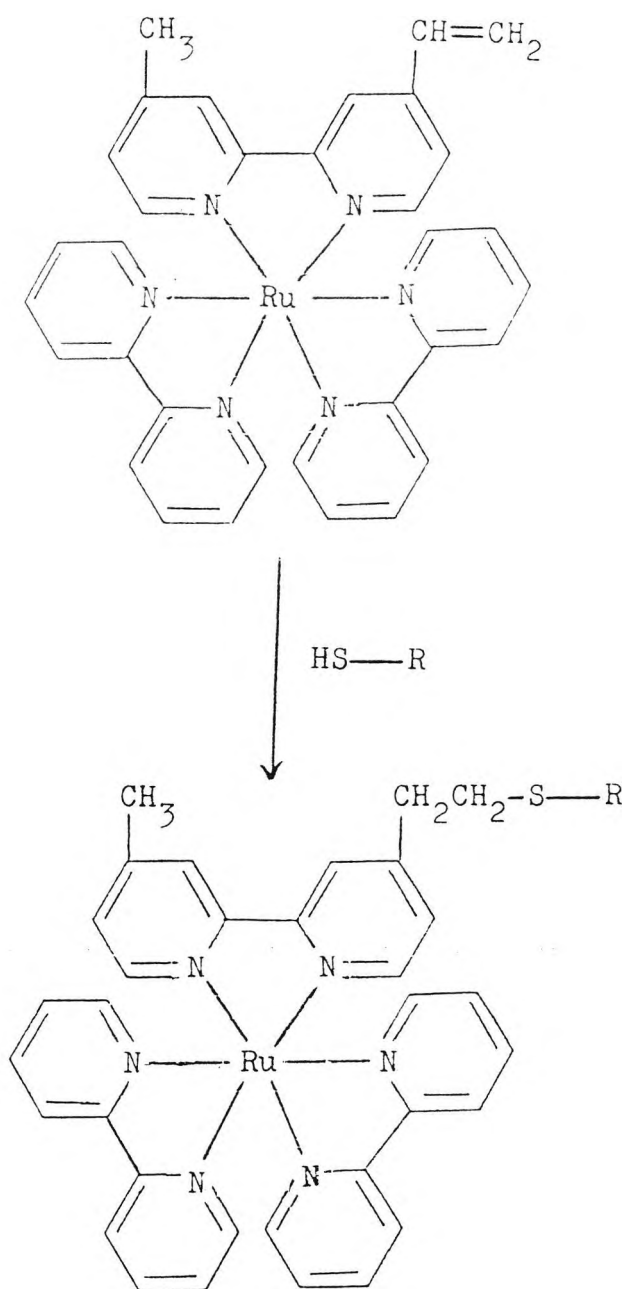


Fig. 5.7. The reaction for the preparation of a modified thiol by the use of Ru Complex II.

5.4.2. Fluorescent Modification of CRP using 9-Bromomethyl Acridine. (C-23).

The method utilised was that adapted from a documented procedure (6).

9-bromomethyl acridine (2.0 mg; 7.4  $\mu$ mol), as synthesised,

was dissolved in Tris-HCl/KCl/EDTA buffer (0.20 M, 3.0 ml, pH 8.0), containing 1,4-dioxane (1% v/v).

The above solution was divided into three equal portions. To one portion was added Tris-HCl/KCl/EDTA buffer (1.0 ml), and the resulting solution was immediately subjected to U.V./visible and fluorescence spectral analysis. To a second portion was added buffered (Tris-HCl/KCl/EDTA) cysteine solution (1.0 ml, 1.0 mg/ml).

Stock CRP solution (0.04 ml, 13.50 mg/ml) was dissolved in Tris-HCl/KCl/EDTA (0.20 M, 0.96 ml), and this solution was added to the remaining portion.

The two remaining solutions were allowed to stand overnight, protected from light, at 4°C. The protein-containing solution was then extensively dialysed (3 days), against Tris-HCl/KCl/MgCl<sub>2</sub>/dithiothreitol buffer (0.20 M, 1000 ml, pH 8.0) using cellulose tubing which retains molecular weight species in excess of 12000 daltons.

The dialysand was then subjected to gel exclusion chromatography using Sephadex G-25 (20-80 μm bead size, bed volume: approximately 10 ml), which had previously equilibrated with the Tris-HCl/KCl/EDTA buffer, and was eluted with this buffer.

The collected fraction and the cysteine-containing sample were diluted to 3 ml with the eluent buffer, and then subjected to U.V./visible and fluorescence spectral analysis.

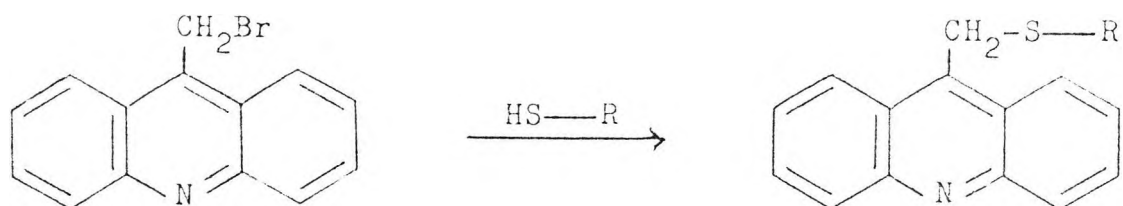


Fig. 5.8. The reaction for the preparation of a modified thiol by the use of 9-bromomethyl acridine.

5.4.3. Fluorescent Modification of CRP using N-(9-Acridinyl) Maleimide. (7).

The method utilised was that adapted from a documented procedure (8).

N-(9-acridinyl) maleimide (2.0 mg; 7.3  $\mu\text{mol}$ ) was dissolved in HEPES/KCl buffer (0.50 M, 3.0 ml, pH 7.4), containing 1,4-dioxane (1% v/v).

The above solution was divided into three equal portions. To one portion was added HEPES/KCl buffer (1.0 ml). To a second portion was added buffered (HEPES/KCl) cysteine solution (1.0 ml, 1.0 mg/ml).

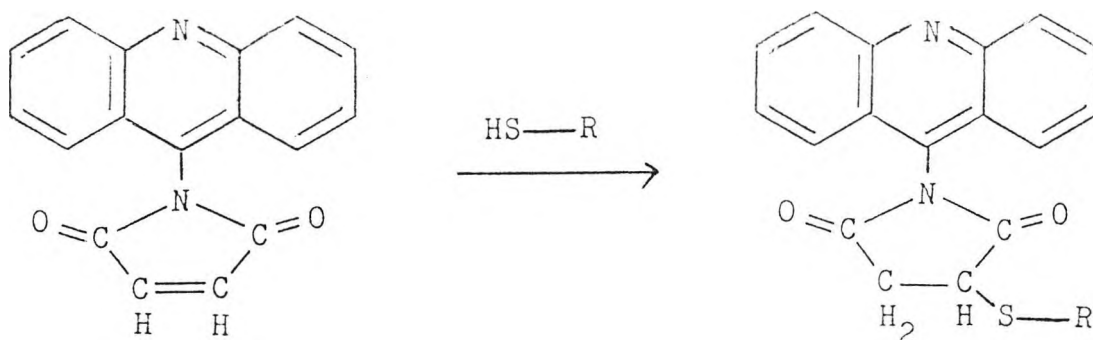
Stock CRP solution (0.04 ml, 13.50 mg/ml) was dissolved in HEPES/KCl (0.50 M, 0.96 ml), and this solution was added to the remaining portion.

The resulting solutions were allowed to stand overnight at 4°C. The protein-containing solution was then extensively dialysed (3 days), against the HEPES/KCl buffer (0.50 M, 1000 ml, pH 7.4) using cellulose tubing which retains molecular weight species in excess of 12000 daltons.

The dialysand was then subjected to gel exclusion

chromatography using Sephadex G-25 (20-80  $\mu$ m bead size, bed volume: approximately 10 ml), which had previously equilibrated with the HEPES/KCl buffer, and was eluted with this buffer.

The collected fraction and the control samples were diluted to 3 ml with HEPES/KCl, and then subjected to U.V./visible and fluorescence spectral analysis.



N-(9-acridinyl)  
Maleimide

Fig. 5.9. The reaction for the preparation of a modified thiol by the use of N-(9-acridinyl) maleimide.

#### 5.4.4. Fluorescent Modification of CRP using Tetramethylrhodamine-5 (and 6) Iodoacetamide. (5-IATR).

The method utilised was that adapted from a documented procedure (9).

5-IATR (2.0 mg; 3.5  $\mu$ mol) was dissolved in Tris-HCl/KCl/EDTA buffer (0.20 M, 3.0 ml, pH 8.0), containing acetonitrile (1% v/v).

The above solution was divided into three equal portions.

To one portion was added Tris-HCl/KCl/EDTA buffer (1.0 ml), and the resulting solution was immediately subjected to U.V./visible and fluorescence spectral analysis. To a second portion was added buffered (Tris-HCl/KCl/EDTA) cysteine solution (1.0 ml, 1.0 mg/ml).

Stock CRP solution (0.04 ml, 13.50 mg/ml) was dissolved in Tris-HCl/KCl/EDTA (0.20 M, 0.96 ml), and this solution was added to the remaining portion.

The two remaining solutions were allowed to stand overnight, protected from light, at 4°C. The protein-containing solution was then extensively dialysed (3 days), against Tris-HCl/KCl/MgCl<sub>2</sub>/dithiothreitol buffer (0.20 M, 1000 ml, pH 8.0) using cellulose tubing which retains molecular weight species in excess of 12000 daltons.

The dialysand was then subjected to gel exclusion chromatography using Sephadex G-25 (20-80 μm bead size, bed volume: approximately 10 ml), which had previously equilibrated with the Tris-HCl/KCl/EDTA buffer, and was eluted with this buffer.

The collected fraction and the cysteine-containing sample were diluted to 3 ml with the eluent buffer, and then subjected to U.V./visible and fluorescence spectral analysis.

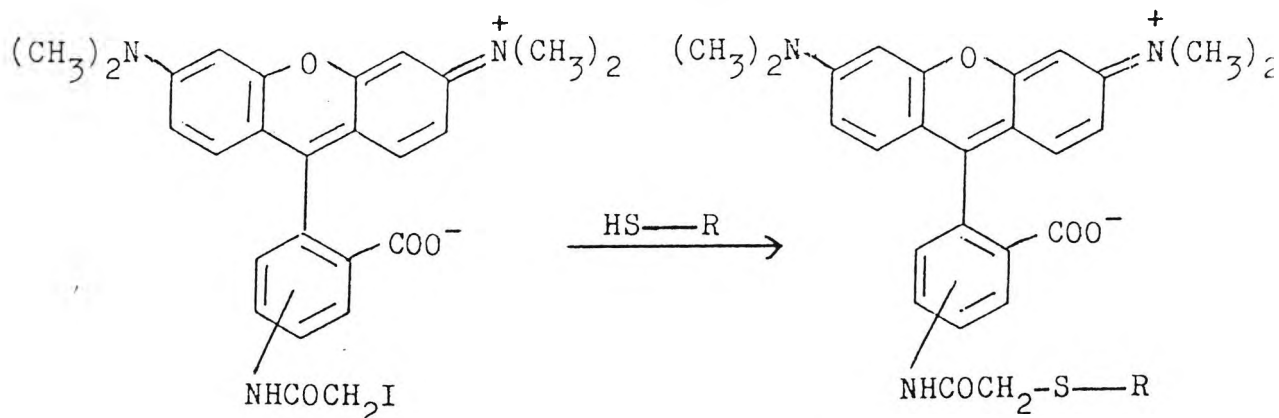


Fig. 5.10. The reaction for the preparation of a modified thiol by the use of 5-IATR.

5.4.5. Fluorescent Modification of CRP using  
5-Iodoacetamidofluorescein. (5-IAF).

The method utilised was that adapted from a documented procedure (10).

5-IAF (2.0 mg; 4.3  $\mu$ mol) was dissolved in Tris-HCl/KCl/EDTA buffer (0.20 M, 3.0 ml, pH 8.0), containing acetonitrile (1% v/v).

The above solution was divided into three equal portions. To one portion was added Tris-HCl/KCl/EDTA buffer (1.0 ml), and the resulting solution was immediately subjected to U.V./visible and fluorescence spectral analysis. To a second portion was added buffered (Tris-HCl/KCl/EDTA) cysteine solution (1.0 ml, 1.0 mg/ml).

Stock CRP solution (0.04 ml, 13.50 mg/ml) was dissolved in Tris-HCl/KCl/EDTA (0.20 M, 0.96 ml), and this solution was added to the remaining portion.

The two remaining solutions were allowed to stand overnight, protected from light, at 4°C. The protein-containing solution was then extensively dialysed (3 days), against Tris-HCl/KCl/MgCl<sub>2</sub>/dithiothreitol buffer (0.20 M, 1000 ml, pH 8.0) using cellulose tubing which retains molecular weight species in excess of 12000 daltons.

The dialysand was then subjected to gel exclusion chromatography using Sephadex G-25 (20-80  $\mu$ m bead size, bed volume: approximately 10 ml), which had previously equilibrated with the Tris-HCl/KCl/EDTA buffer, and was eluted with this buffer.

The collected fraction and the cysteine-containing

sample were diluted to 3 ml with the eluent buffer, and then subjected to U.V./visible and fluorescence spectral analysis.

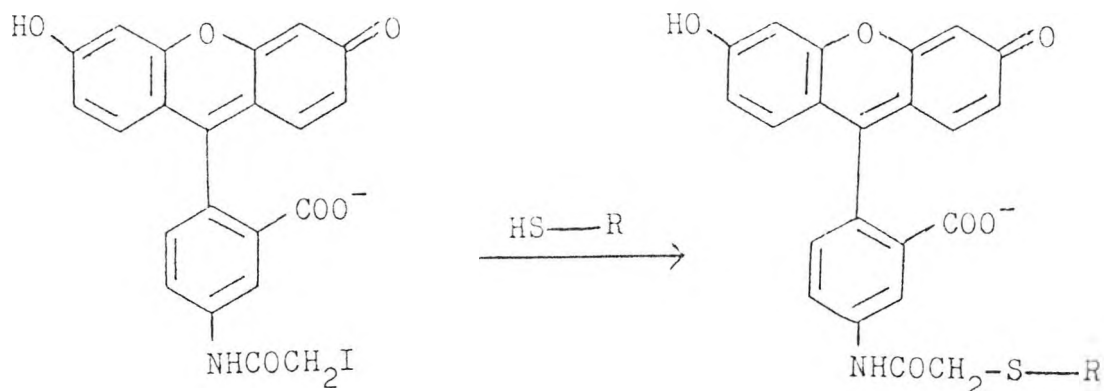


Fig. 5.11. The reaction for the preparation of a modified thiol by the use of 5-IAF.

#### 5.4.6. Fluorescent Modification of CRP using 4-Chloro-7-nitrobenz-2-oxa-1,3-diazole. (NBD-Chloride).

The method utilised was that adapted from a documented procedure (11).

NBD-Chloride (2.0 mg; 10  $\mu$ mol) was dissolved in Tris-HCl/KCl buffer (0.20 M, 3.0 ml, pH 7.4), containing ethanol (1% v/v).

The above solution was divided into three equal portions. To one portion was added Tris-HCl/KCl buffer (1.0 ml). To a second portion was added buffered (Tris-HCl/KCl) cysteine solution (1.0 ml, 1.0 mg/ml).

Stock CRP solution (0.04 ml, 13.50 mg/ml) was dissolved in Tris-HCl/KCl (0.20 M, 0.96 ml), and this solution was added to the remaining portion.

The resulting solutions were allowed to stand overnight at 4°C. The protein-containing solution was then extensively

dialysed (3 days), against Tris-HCl/KCl buffer (0.20 M, 1000 ml, pH 7.4) using cellulose tubing which retains molecular weight species in excess of 12000 daltons.

The dialysand was then subjected to gel exclusion chromatography using Sephadex G-25 (20-80  $\mu$ m bead size, bed volume: approximately 10 ml), which had previously equilibrated with the Tris-HCl/KCl buffer, and was eluted with this buffer.

The collected fraction and the control samples were diluted to 3 ml with the eluent buffer, and then subjected to U.V./visible and fluorescence spectral analysis.

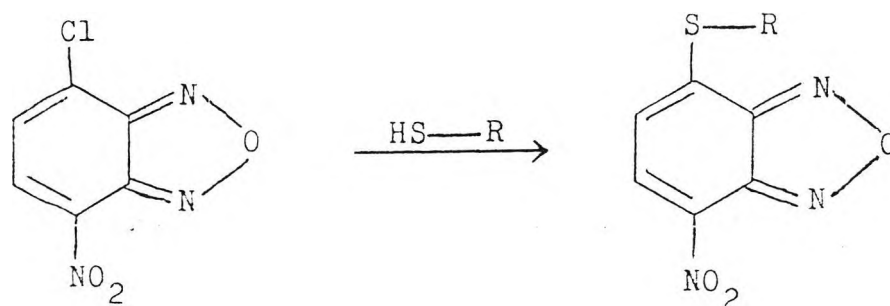


Fig. 5.12. The reaction for the preparation of a modified thiol by the use of NBD-Chloride.

#### 5.4.7. Fluorescent Modification of CRP using Protoporphyrin IX.

The method utilised was that adapted from a documented procedure (12).

Protoporphyrin IX (8,13-divinyl-3,7,12,17-tetramethyl-21H,23H-porphine-2,18-dipropionic acid, 1.0 mg; 1.78  $\mu$ mol) was dissolved in phosphate buffered saline (0.10 M, 2.0 ml, pH 7.4, PBS) containing 1,4-dioxane (5% v/v).

The above solution was divided into two equal portions.

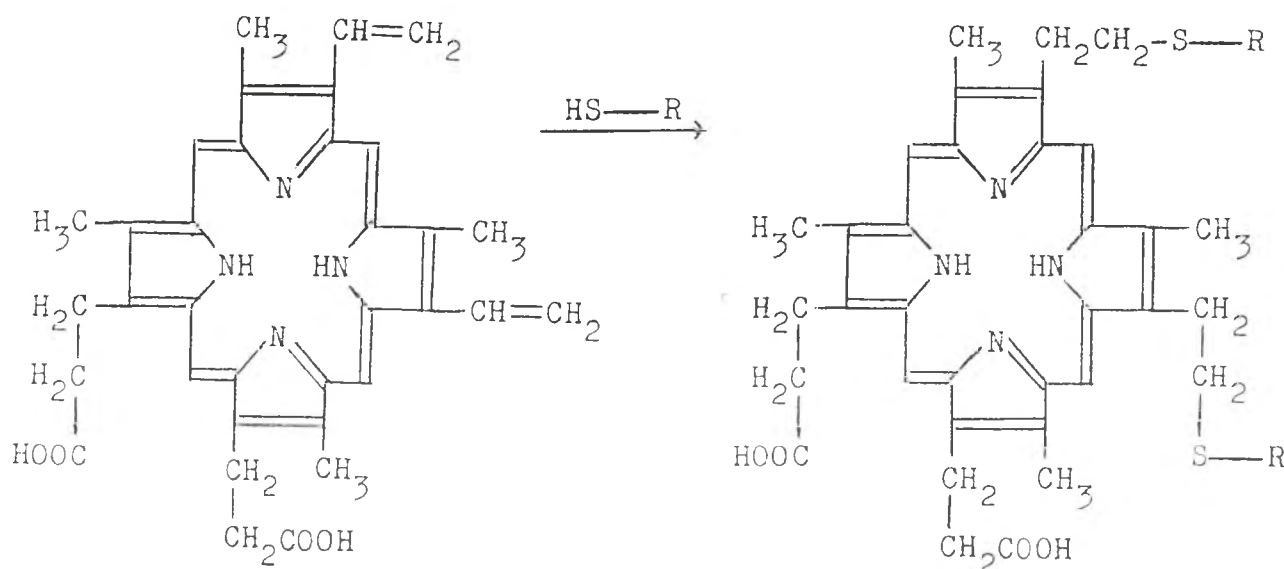
To one portion was added buffered (PBS) cysteine solution (1.0 ml, 1.0 mg/ml).

Stock CRP solution (0.04 ml, 13.50 mg/ml) was dissolved in PBS (0.10 M, 0.96 ml), and this solution was added to the remaining portion.

The resulting solutions were allowed to stand overnight at 4°C. The protein-containing solution was then extensively dialysed (3 days), against PBS (0.10 M, 1000 ml, pH 7.4) using cellulose tubing which retains molecular weight species in excess of 12000 daltons.

The dialysand was then subjected to gel exclusion chromatography using Sephadex G-25 (20-80 μm bead size, bed volume: approximately 10 ml), which had previously equilibrated with PBS (0.10 M) and was eluted with the PBS.

The collected fraction and the control sample were diluted to 3 ml with PBS, and then subjected to U.V./visible and fluorescence spectral analysis.



Protoporphyrin IX

Fig. 5.13. The reaction for the preparation of a modified thiol by the use of Protoporphyrin IX.

#### 5.4.8. Fluorescent Modification of CRP using Bilirubin.

The method utilised was that adapted from a documented procedure (12).

Bilirubin (1.0 mg; 1.70  $\mu\text{mol}$ ) was dissolved in phosphate buffered saline (0.10 M, 2.0 ml, pH 7.4, PBS), containing 1,4-dioxane (5% v/v).

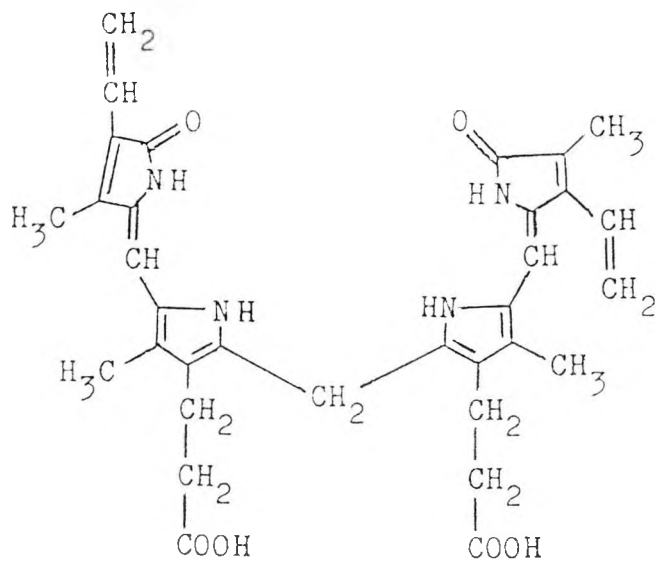
The above solution was divided into two equal portions. To one portion was added buffered (PBS) cysteine solution (1.0 ml, 1.0 mg/ml).

Stock CRP solution (0.04 ml, 13.50 mg/ml) was dissolved in PBS (0.10 M, 0.96 ml), and this solution was added to the remaining portion.

The resulting solutions were allowed to stand overnight at 4°C. The protein-containing solution was then extensively dialysed (3 days), against PBS (0.10 M, 1000 ml, pH 7.4) using cellulose tubing which retains molecular weight species in excess of 12000 daltons.

The dialysand was then subjected to gel exclusion chromatography using Sephadex G-25 (20-80  $\mu\text{m}$  bead size, bed volume: approximately 10 ml), which had previously equilibrated with PBS (0.10 M) and was eluted with the PBS.

The collected fraction and the control sample were diluted to 3 ml with PBS, and then subjected to U.V./visible and fluorescence spectral analysis.



Bilirubin

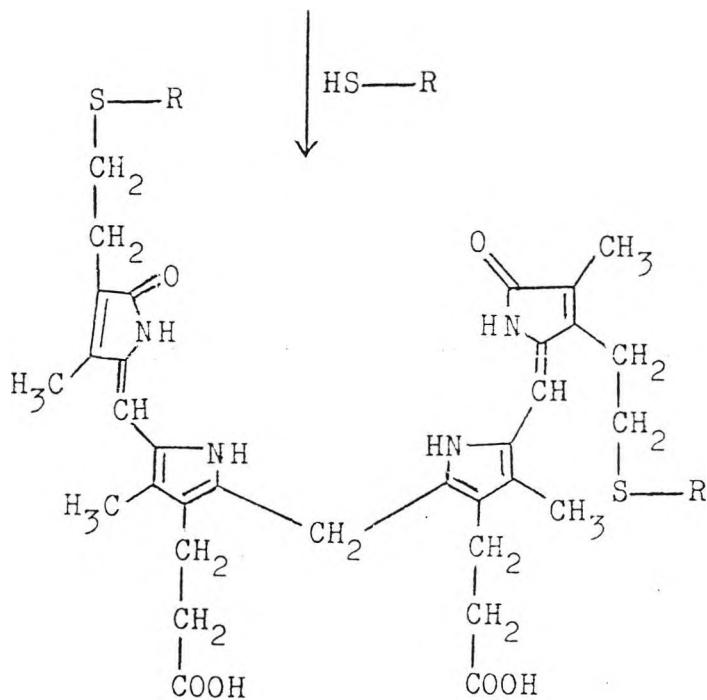


Fig. 5.14. The reaction for the preparation of a modified thiol by the use of Bilirubin.

5.4.9. Fluorescent Modification of CRP using N-(1-Pyrene) Maleimide. (C-5).

The method utilised was that as outlined (8). N-(1-Pyrene) maleimide (2.0 mg; 6.70  $\mu$ mol), as synthesised, was dissolved

in HEPES/KCl buffer (0.50 M, 3.0 ml, pH 7.4), containing 1,4-dioxane (1% v/v).

The above solution was divided into three equal portions. To one portion was added HEPES/KCl buffer (1.0 ml). To a second portion was added buffered (HEPES/KCl) cysteine solution (1.0 ml, 1.0 mg/ml).

Stock CRP solution (0.04 ml, 13.50 mg/ml) was dissolved in HEPES/KCl (0.50 M, 0.96 ml), and this solution was added to the remaining portion.

The resulting solutions were allowed to stand overnight at 4°C. The protein-containing solution was then extensively dialysed (3 days), against the HEPES/KCl buffer (0.50 M, 1000 ml, pH 7.4) using cellulose tubing which retains molecular weight species in excess of 12000 daltons.

The dialysand was then subjected to gel exclusion chromatography using Sephadex G-25 (20-80  $\mu$ m bead size, bed volume: approximately 10 ml), which had previously equilibrated with the HEPES/KCl buffer, and was eluted with this buffer.

The collected fraction and the control samples were diluted to 3 ml with HEPES/KCl, and then subjected to U.V./visible and fluorescence spectral analysis.

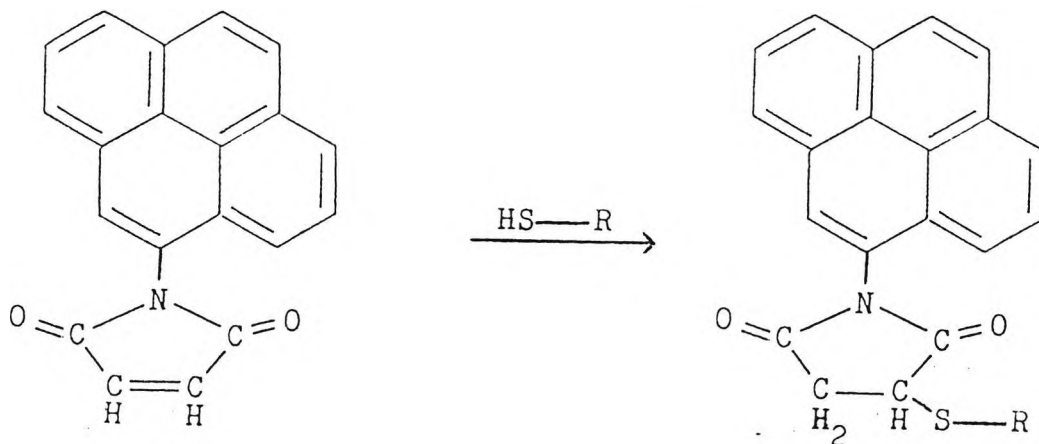


Fig. 5.15. The reaction for the preparation of a modified thiol by the use of N-(1-Pyrene) Maleimide.

5.4.10. Fluorescent Modification of CRP  
using Lucifer Yellow, VS.

The method utilised was that adapted from a documented procedure (5).

Lucifer Yellow, VS, (dilithium 4-amino-N-(3-(vinylsulphonyl)phenyl) naphthalimide-3,6-disulphonate, 1.0 mg; 1.80  $\mu$ mol) was dissolved in phosphate buffered saline (0.10 M, 2.0 ml, pH 7.4, PBS).

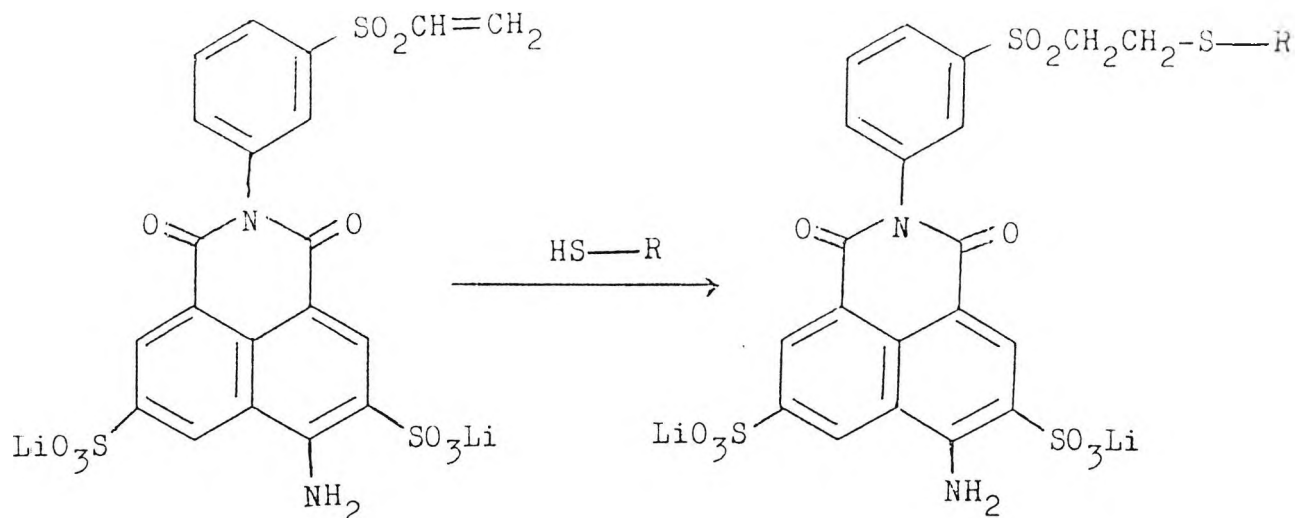
The above solution was divided into two equal portions. To one portion was added buffered (PBS) cysteine solution (1.0 ml, 1.0 mg/ml).

Stock CRP solution (0.04 ml, 13.50 mg/ml) was dissolved in PBS (0.10 M, 0.96 ml), and this solution was added to the remaining portion.

The resulting solutions were allowed to stand overnight at 4°C. The protein-containing solution was then extensively dialysed (3 days), against PBS (0.10 M, 1000 ml, pH 7.4) using cellulose tubing which retains molecular weight species in excess of 12000 daltons.

The dialysand was then subjected to gel exclusion chromatography using Sephadex G-25 (20-80  $\mu$ m bead size, bed volume: approximately 10 ml), which had previously equilibrated with PBS (0.10 M) and was eluted with the PBS.

The collected fraction and the control sample were diluted to 3 ml with PBS, and then subjected to U.V./visible and fluorescence spectral analysis.



Lucifer Yellow, VS

Fig. 5.16. The reaction for the preparation of a modified thiol by the use of Lucifer Yellow, VS.

5.4.11. Fluorescent Modification of CRP using N-(7-dimethylamino-4-methylcoumarinyl) Maleimide. (DACM).

The method utilised was that as outlined (13). DACM (2.0 mg; 6.71  $\mu\text{mol}$ ) was dissolved in Tris-HCl/KCl buffer (0.20 M, 3.0 ml, pH 7.4), containing dimethyl sulphoxide (1% v/v).

The above solution was divided into three equal portions. To one portion was added Tris-HCl/KCl buffer (1.0 ml). To a second portion was added buffered (Tris-HCl/KCl) cysteine solution (1.0 ml, 1.0 mg/ml).

Stock CRP solution (0.04 ml, 13.50 mg/ml) was dissolved in Tris-HCl/KCl (0.20 M, 0.96 ml), and this solution was added to the remaining portion.

The resulting solutions were allowed to stand overnight at 4°C. The protein-containing solution was then extensively

dialysed (3 days), against Tris-HCl/KCl buffer (0.20 M, 1000 ml, pH 7.4) using cellulose tubing which retains molecular weight species in excess of 12000 daltons.

The dialysand was then subjected to gel exclusion chromatography using Sephadex G-25 (20-80  $\mu$ m bead size, bed volume: approximately 10 ml), which had previously equilibrated with the Tris-HCl/KCl buffer, and was eluted with this buffer.

The collected fraction and the control samples were diluted to 3 ml with the eluent buffer, and then subjected to U.V./visible and fluorescence spectral analysis.

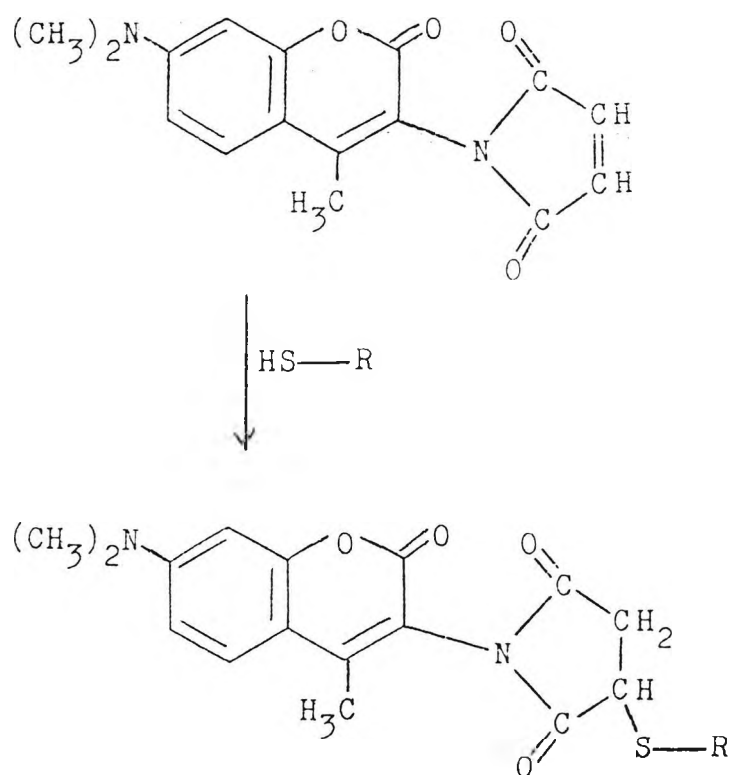


Fig. 5.17. The reaction for the preparation of a modified thiol by the use of DACM.

5.4.12. Fluorescent Modification of CRP using  
Maleimidyl Benzoate Ester of Benz(c,d)  
indol-2(1H)-one. (C-20).

The method utilised was that adapted from a documented procedure (14).

Maleimidyl benzoate ester of benz(c,d)indol-2(1H)-one (2.0 mg; 5.00  $\mu$ mol), as synthesised, was dissolved in Tris-HCl/KCl buffer (0.20 M, 3.0 ml, pH 7.4), containing ethanol (1% v/v).

The above solution was divided into three equal portions. To one portion was added Tris-HCl/KCl buffer (1.0 ml). To a second portion was added buffered (Tris-HCl/KCl) cysteine solution (1.0 ml, 1.0 mg/ml).

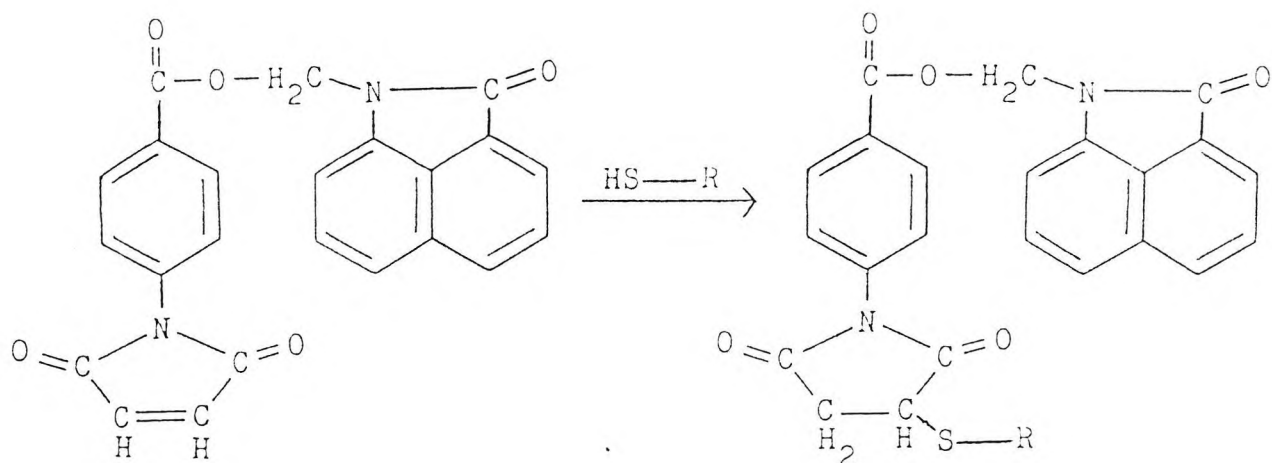
Stock CRP solution (0.04 ml, 13.50 mg/ml) was dissolved in Tris-HCl/KCl (0.20 M, 0.96 ml), and this solution was added to the remaining portion.

The resulting solutions were allowed to stand overnight at 4°C. The protein-containing solution was then extensively dialysed (3 days), against Tris-HCl/KCl buffer (0.20 M, 1000 ml, pH 7.4) using cellulose tubing which retains molecular weight species in excess of 12000 daltons.

The dialysand was then subjected to gel exclusion chromatography using Sephadex G-25 (20-80  $\mu$ m bead size, bed volume: approximately 10 ml), which had previously equilibrated with the Tris-HCl/KCl buffer, and was eluted with this buffer.

The collected fraction and the control samples were diluted to 3 ml with the eluent buffer, and then subjected

to U.V./visible and fluorescence spectral analysis.



Maleimidyl Benzoate Ester  
of Benz(c,d)indol-2(1H)-one

Fig. 5.18. The reaction for the preparation of a modified thiol by the use of maleimidyl benzoate ester of benz(c,d)indol-2(1H)-one.

5.4.13. Fluorescent Modification of CRP using  
N-(1-Anilino-naphthyl-4) Maleimide. (C-14).

The method utilised was that as outlined (15). N-(1-anilino-naphthyl-4) maleimide (2.0 mg; 6.37  $\mu$ mol, ANM), as synthesised, was dissolved in HEPES/KCl buffer (0.50 M, 3.0 ml, pH 7.4), containing 1,4-dioxane (1% v/v).

The above solution was divided into three equal portions. To one portion was added HEPES/KCl buffer (1.0 ml). To a second portion was added buffered (HEPES/KCl) cysteine solution (1.0 ml, 1.0 mg/ml).

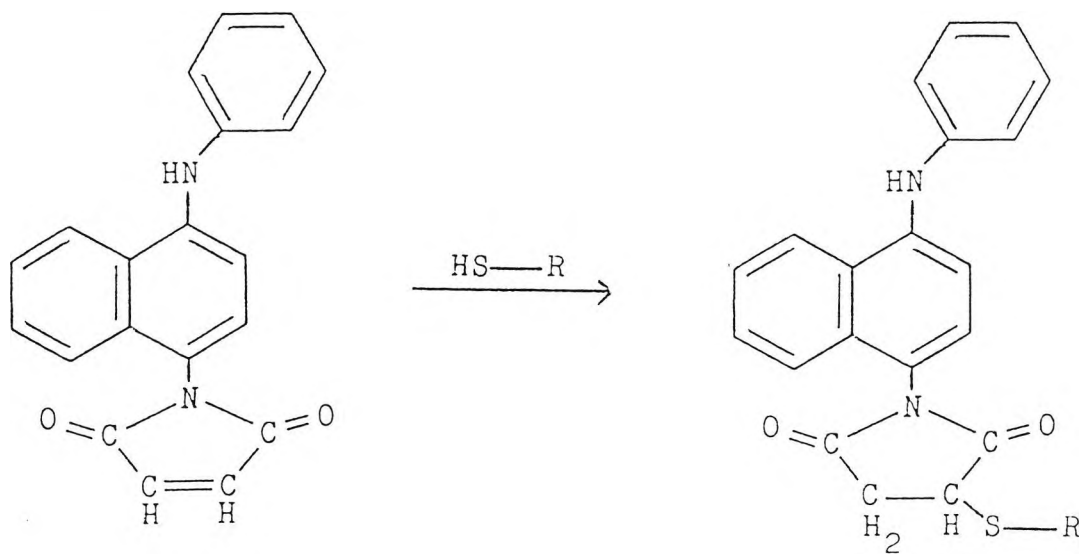
Stock CRP solution (0.04 ml, 13.50 mg/ml) was dissolved in HEPES/KCl (0.50 M, 0.96 ml), and this solution was

added to the remaining portion.

The resulting solutions were allowed to stand overnight at 4°C. The protein-containing solution was then extensively dialysed (3 days), against the HEPES/KCl buffer (0.50 M, 1000 ml, pH 7.4) using cellulose tubing which retains molecular weight species in excess of 12000 daltons.

The dialysand was then subjected to gel exclusion chromatography using Sephadex G-25 (20-80 μm bead size, bed volume: approximately 10 ml), which had previously equilibrated with the HEPES/KCl buffer, and was eluted with this buffer.

The collected fraction and the control samples were diluted to 3 ml with HEPES/KCl, and then subjected to U.V./visible and fluorescence spectral analysis.



N-(1-anilino-4-naphthyl)

Maleimide

Fig. 5.19. The reaction for the preparation of a modified thiol by the use of N-(1-anilino-4-naphthyl-4) maleimide.

5.4.14. Fluorescent Modification of CRP using 2-(4'-iodoacetamidoanilino)naphthalene-6-sulphonic acid, sodium salt. (IAANS).

The method utilised was that adapted from a documented procedure (16).

IAANS (2.0 mg; 4.15  $\mu$ mol) was dissolved in Tris-HCl/KCl/EDTA buffer (0.20 M, 3.0 ml, pH 8.0).

The above solution was divided into three equal portions. To one portion was added Tris-HCl/KCl/EDTA buffer (1.0 ml), and the resulting solution was immediately subjected to U.V./visible and fluorescence spectral analysis. To a second portion was added buffered (Tris-HCl/KCl/EDTA) cysteine solution (1.0 ml, 1.0 mg/ml).

Stock CRP solution (0.04 ml, 13.50 mg/ml) was dissolved in Tris-HCl/KCl/EDTA (0.20 M, 0.96 ml), and this solution was added to the remaining portion.

The two remaining solutions were allowed to stand overnight, protected from light, at 4<sup>o</sup>C. The protein-containing solution was then extensively dialysed (3 days), against Tris-HCl/KCl/MgCl<sub>2</sub>/dithiothreitol buffer (0.20 M, 1000 ml, pH 8.0) using cellulose tubing which retains molecular weight species in excess of 12000 daltons.

The dialysand was then subjected to gel exclusion chromatography using Sephadex G-25 (20-80  $\mu$ m bead size, bed volume: approximately 10 ml), which had previously equilibrated with the Tris-HCl/KCl/EDTA buffer, and was eluted with this buffer.

The collected fraction and the cysteine-containing sample were diluted to 3 ml with the eluent buffer, and then subjected to U.V./visible and fluorescence spectral analysis.

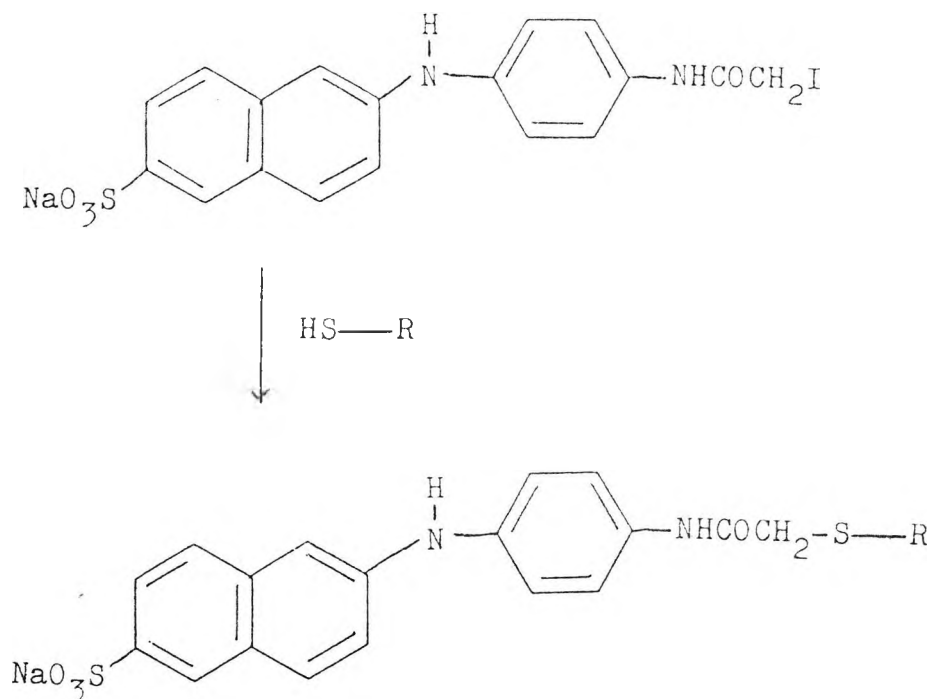


Fig. 5.20. The reaction for the preparation of a modified thiol by the use of 2-(4'-iodoacetamidoanilino)naphthalene-6-sulphonic acid, sodium salt. (IAANS).

5.4.15. Fluorescent Modification of CRP using N-(Iodoacetyl aminoethyl)-1-naphthylamine-8-sulphonic acid. (1,8-IAEDANS). (C-10) (17).

The method utilised was that as outlined (18).

1,8-IAEDANS (2.0 mg; 4.60  $\mu\text{mol}$ ), as synthesised, was dissolved in Tris-HCl/KCl/EDTA buffer (0.20 M, 3.0 ml, pH 8.0).

The above solution was divided into three equal portions. To one portion was added Tris-HCl/KCl/EDTA buffer (1.0 ml), and the resulting solution was immediately subjected to U.V./visible and fluorescence spectral analysis. To a second portion was added buffered (Tris-HCl/KCl/EDTA) cysteine solution (1.0 ml, 1.0 mg/ml).

Stock CRP solution (0.04 ml, 13.50 mg/ml) was dissolved

in Tris-HCl/KCl/EDTA (0.20 M, 0.96 ml), and this solution was added to the remaining portion.

The two remaining solutions were allowed to stand overnight, protected from light, at 4°C. The protein-containing solution was then extensively dialysed (3 days), against Tris-HCl/KCl/MgCl<sub>2</sub>/dithiothreitol buffer (0.20 M, 1000 ml, pH 8.0) using cellulose tubing which retains molecular weight species in excess of 12000 daltons.

The dialysand was then subjected to gel exclusion chromatography using Sephadex G-25 (20-80 μm bead size, bed volume: approximately 10 ml), which had previously equilibrated with the Tris-HCl/KCl/EDTA buffer, and was eluted with this buffer.

The collected fraction and the cysteine-containing sample were diluted to 3 ml with the eluent buffer, and then subjected to U.V./visible and fluorescence spectral analysis.

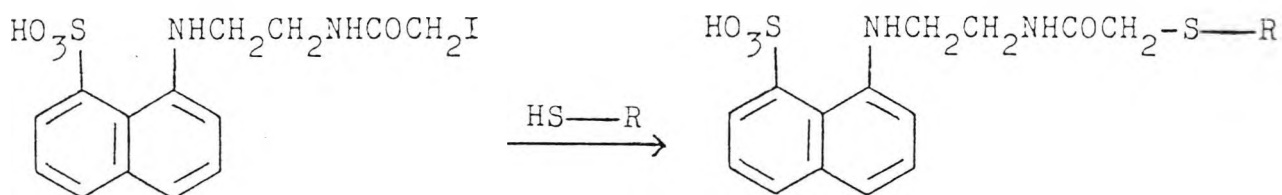


Fig. 5.21. The reaction for the preparation of a modified thiol by the use of 2-(4'-iodoacetamido-anilino)naphthalene-6-sulphonic acid. (1,8-IAEDANS).

5.4.16. Fluorescent Modification of CRP using 6-Acryloyl-2-Dimethylaminonaphthalene. (Acrylodan).

The method utilised was that adapted from a documented procedure (19).

Acrylodan (1.0 mg; 4.44  $\mu$ mol) was dissolved in HEPES/KCl buffer (0.50 M, 2.0 ml, pH 7.4), containing acetonitrile (1% v/v).

The above solution was divided into two equal portions. To one portion was added buffered (HEPES/KCl) cysteine solution (1.0 ml, 1.0 mg/ml).

Stock CRP solution (0.04 ml, 13.50 mg/ml) was dissolved in HEPES/KCl (0.50 M, 0.96 ml), and this solution was added to the remaining portion.

The resulting solutions were allowed to stand overnight at 4°C. The protein-containing solution was then extensively dialysed (3 days), against the HEPES/KCl buffer (0.50 M, 1000 ml, pH 7.4) using cellulose tubing which retains molecular weight species in excess of 12000 daltons.

The dialysand was then subjected to gel exclusion chromatography using Sephadex G-25 (20-80  $\mu$ m bead size, bed volume: approximately 10 ml), which had previously equilibrated with the HEPES/KCl buffer, and was eluted with this buffer.

The collected fraction and the control sample were diluted to 3 ml with HEPES/KCl, and then subjected to U.V./visible and fluorescence spectral analysis.

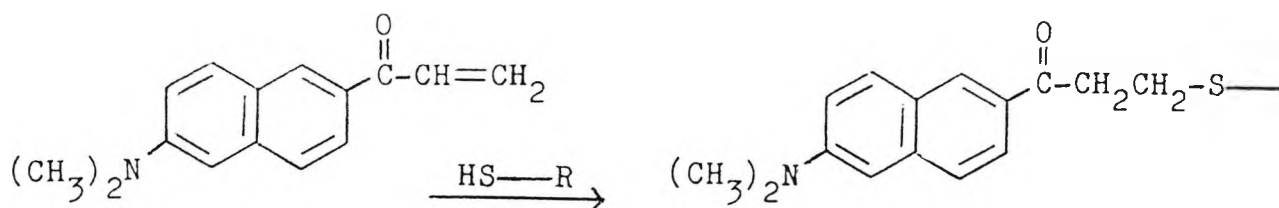


Fig. 5.22. The reaction for the preparation of a modified thiol by the use of 6-acryloyl-2-dimethylaminonaphthalene. (Acrylodan).

5.5. REFERENCES.

1. Bradford, M.M.  
(1976) Anal. Biochem. 72 248
2. Titus, J.A., Haugland, R.P., Sharrow, S.O. & Segal, D.M.  
(1982) J. Immunol. Methods 50 193
3. Khalfan, H., Abuknesha, R., Rand-Weaver, M., Price, R.G.  
& Robinson, D.  
(1986) Histochem. J. 18 497
4. Chen, R.F.  
(1969) Arch. Biochem. Biophys. 133 263
5. Stewart, W.W.  
(1981) Nature 292 17
6. Okamoto, M. & Morino, Y.  
(1972) Biochemistry 11 3188
7. Nara, Y. & Tuzimura, K.  
(1978) Agric. Biol. Chem. 42 793
8. Weltman, J.K., Szaro, R.P., Frackelton, Jr., A.R.,  
Dowben, R.M., Bunting, J.R. & Cathou, R.E.  
(1973) J. Biol. Chem. 248 3173
9. Tait, J.F. & Frieden, C.  
(1982) Arch. Biochem. Biophys. 216 133
10. Papakos, J.G. & Steinberg, M.  
(1982) Biochim. Biophys. Acta 693 493
11. Wong, P. & Harper, E.T.  
(1982) Biochim. Biophys. Acta 700 33
12. Holowka, D.A. & Hammes, G.G.  
(1978) Biochemistry 16 5538
13. Yamamoto, K., Takamitsu, S. & Kanaoka, Y.  
(1977) Anal. Biochem. 79 83
14. Gupte, S.S. & Lane, L.K.  
(1983) J. Biol. Chem. 258 5005
15. Kanaoka, Y., Machida, M., Machida, M. & Sekine, T.  
(1973) Biochim. Biophys. Acta 317 563

16. Price, N.C.  
(1979) Biochemical J. 177 603
17. Hudson, E.N. & Weber, G.  
(1973) Biochemistry 12 4154
18. Wu, F.Y.-H., Nath, K. & Wu, C.-W.  
(1974) Biochemistry 13 2567
19. Prendergast, F.G., Meyer, M., Carlson, G.L., Iida, S.  
& Potter, J.D.  
(1983) J. Biol. Chem. 258 7541

CHAPTER 6.

RESULTS AND DISCUSSION.

## 6.1. INVESTIGATION OF THE INTERACTION OF cAMP WITH THE UNLABELLED & LABELLED cAMP RECEPTOR PROTEIN. (CRP).

Since we are investigating the increase in fluorescence intensity and possible shifts in emission maxima, as reported by a fluorophore, in response to a conformational change induced in the protein by the binding of cAMP, it is imperative that the modification, caused by introducing a fluorescent probe, does not seriously impede cAMP binding to the protein.

### 6.1.1. CRP Assay.

#### 6.1.1.1. Experimental Procedure.

An aqueous buffered solution of CRP was supplied by SmithKline Beecham Pharmaceuticals. It was necessary to deduce the protein concentration of the solution provided, and this was achieved by the utilisation of a protein assay procedure derived from the Lowry method (1), and its improved modifications (2,3).

#### Preparation of Protein Standards.

Bovine Serum Albumin (BSA) standard solution (400  $\mu\text{g/ml}$ ) was prepared by adding distilled water (5 ml) to BSA (2 mg), in a glass vial. The contents were swirled gently, until complete dissolution occurred.

Five tubes were set up, in duplicate, as follows:

<u>Tube Nos.</u>	<u>Standard Protein Solution (ml)</u>	<u>Distilled Water (ml)</u>	<u>Final Protein Conc. (<math>\mu\text{g/ml}</math>)</u>
1	0.125	0.875	50
2	0.250	0.750	100
3	0.500	0.500	200
4	0.750	0.250	300
5	1.000	0.000	400

Table 6.1. The contents of each of the standard protein sample tubes.

A 'blank' tube was set up containing distilled water (1 ml).

CRP solution (10  $\mu\text{l}$ ) was introduced into each of two tubes, and these solutions were diluted to 1 ml with distilled water producing a final dilution of 1:100.

Lowry Reagent Solution (sodium carbonate (10% w/v), copper sulphate-tartrate (0.1% w/v  $\text{CuSO}_4$ ), potassium tartrate (0.2% w/v), 1 ml) was added to each tube, and the contents were thoroughly mixed.

All solutions were allowed to stand at room temperature for 20 minutes.

With rapid and immediate mixing, Folin & Ciocalteu's Phenol Reagent Working Solution (0.5 ml, 2 M) was added to each tube. Colour was allowed to develop for 30 minutes.

Solutions were transferred to cuvettes and the absorbance of the standards and samples, versus the blank, was determined at 595 nm. Readings were completed within 30 minutes.

6.1.1.2. Results.

<u>Tube Nos.</u>	<u>Protein conc.</u> <u>(<math>\mu\text{g/ml}</math>)</u>	<u>Absorbance .</u> <u>at 595 nm</u>	<u>Mean</u> <u>Absorbance</u>
Blank	0.00	0.050	0.050
1	50.00	0.296	0.300
	50.00	0.304	
2	100.00	0.558	0.550
	100.00	0.542	
3	200.00	0.970	0.976
	200.00	0.983	
4	300.00	1.346	1.340
	300.00	1.334	
5	400.00	1.783	1.785
	400.00	1.787	
CRP soln.		0.590	0.591
		0.592	

Table 6.2. Absorbance readings, at 595 nm, for varying concentrations of BSA and CRP as detected by Lowry Reagent.

Using the data obtained, a calibration curve was constructed.

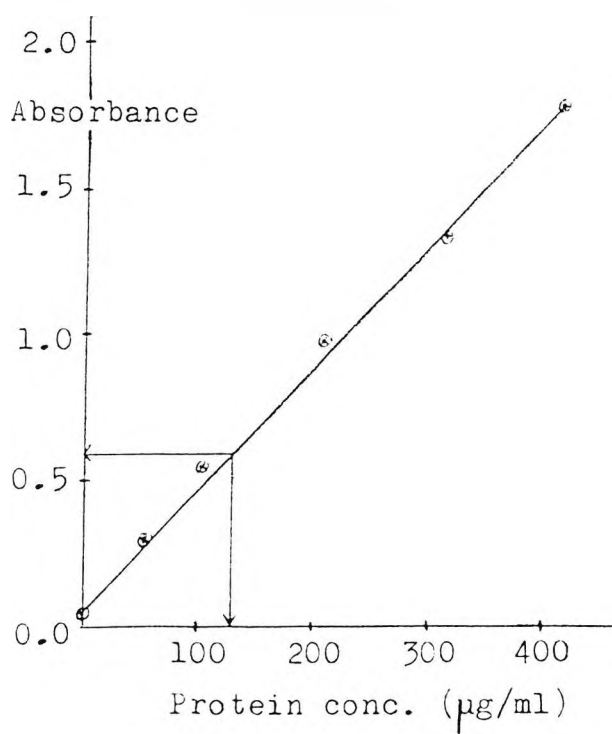


Fig. 6.1. Calibration Curve using standard protein solution for the assay of CRP.

From the calibration curve, it may be deduced that the concentration of the diluted CRP solution is 125  $\mu\text{g/ml}$  at a dilution of 1:100. Therefore, the stock CRP concentration is 12.50 mg/ml.

#### 6.1.2. cAMP Binding Assay of Unlabelled CRP.

It is fundamentally important for the protein to bind cAMP so that the former may report its conformational change, via changes in the fluorescence characteristics of the attendant fluorophore. Since organic solvents are usually necessary to effect dissolution of the fluorophores in the fluorescent modification process, it is important that the presence of organic solvent does not adversely affect the cAMP binding properties of the protein.

A cAMP binding assay of the unlabelled protein was followed, as derived from documented procedures (4,5), in order to investigate these effects.

##### 6.1.2.1. Experimental Procedure.

Five tubes were set up in duplicate. To each tube was added:

- i) 5'AMP solution (10  $\mu\text{l}$ , 20 mM),
- ii) 'Cold' + tritiated ( $^3\text{H}$ ) cAMP solution (10  $\mu\text{l}$ );  
produced by adding  $^3\text{H}$ -cAMP (5  $\mu\text{l}$ ) to 'cold' cAMP (220  $\mu\text{l}$ , 2  $\mu\text{M}$ ), producing a final  $^3\text{H}$ -cAMP concentration of 0.08  $\mu\text{M}$ .
- iii) Distilled water (20  $\mu\text{l}$ )

To one set of five tubes was added aqueous acetonitrile (5% v/v, 10  $\mu\text{l}$ ), and these were designated tubes 1A to 5A. To the other set of five tubes was added distilled water (10  $\mu\text{l}$ ),

and these were designated tubes 1B to 5B.

This experimental protocol was employed in order to ascertain the effect of organic solvent, on the ability of the protein to bind cAMP.

Each tube was then treated to varying concentrations of stock CRP solution (12.50 mg/ml) to a volume of 50  $\mu$ l.

Tube Nos.	1A/1B	2A/2B	3A/3B	4A/4B	5A/5B
CRP soln.	1:10	1:20	1:40	1:80	1:160

Table 6.3. The contents of each of the sample tubes with respect to CRP concentration.

A control tube was set up containing:

- i) 5'AMP solution (10  $\mu$ l, 20 mM)
- ii) 'Cold' + tritiated ( $^3\text{H}$ ) cAMP solution (10  $\mu$ l);  
produced by adding  $^3\text{H}$ -cAMP (5  $\mu$ l) to 'cold' cAMP (220  $\mu$ l 20 mM), producing a final  $^3\text{H}$ -cAMP concentration of 0.08  $\mu\text{M}$ .
- iii) Distilled water (30  $\mu$ l)
- iv) BSA solution (50  $\mu$ l, 1.25 mg/ml)

The tubes were then incubated on ice for 10 minutes. Saturated ammonium sulphate solution (1 ml) was added to each tube, and the latter were allowed to stand for a further 10 minutes.

The function of the control tube was to ascertain the radioactivity trapped non-specifically within the precipitated protein.

The contents of each tube was then subjected to millipore filtration (0.45  $\mu\text{m}$  pore size), and the residue on the filter paper was washed with saturated ammonium sulphate solution (2 x 3 ml). Each millipore filter paper was then introduced

into separate vials, Pico-Fluor Liquid Scintillation Fluid (10 ml) was added, and each vial was then subjected to radio-counting using a Liquid Scintillation Counter.

A total-count tube was set up by taking an aliquot (10  $\mu$ l) of a 'cold' + tritiated ( $^3\text{H}$ ) cAMP solution; produced by adding  $^3\text{H}$ -cAMP (5  $\mu$ l) to 'cold' cAMP solution (220  $\mu$ l, 20 mM), producing a final  $^3\text{H}$ -cAMP concentration of 0.08  $\mu$ M. This aliquot was then added to distilled water (90  $\mu$ l).

Pico-Fluor Liquid Scintillation Fluid (10 ml) was added to the final solution, and the vial was then directly subjected to radio-counting using a Liquid Scintillation Counter.

#### 6.1.2.2. Results.

Total Count = 134523 disintegrations per minute (d.p.m.)

Control Count = 4014 disintegrations per minute (d.p.m.)

#### cAMP Binding Assay of Acetonitrile Treated Unlabelled CRP.

<u>Tube No.</u>	<u>CRP Dilution</u>	<u>d.p.m.</u>	<u>Corrected d.p.m.</u>	<u>% Binding</u>
1A	1:10	93532	89518	67
2A	1:20	84728	80714	60
3A	1:40	66971	62957	47
4A	1:80	42918	38904	29
5A	1:160	12085	8071	6

Table 6.4. Results of the % binding of acetonitrile treated unlabelled CRP.

cAMP Binding Assay of Untreated, Unlabelled CRP.

<u>Tube No.</u>	<u>CRP Dilution</u>	<u>d.p.m.</u>	<u>Corrected d.p.m.</u>	<u>% Binding</u>
1B	1:10	92514	88500	66
2B	1:20	87418	83404	62
3B	1:40	66325	62311	46
4B	1:80	44183	40169	30
5B	1:160	10740	6726	5

Table 6.5. Results of the % binding of untreated, unlabelled CRP.

Thus, it may be seen that cAMP Receptor Protein efficiently binds cAMP, and that the presence of organic solvent (acetonitrile) has no effect on the capacity of the protein to bind cAMP.

6.1.3. cAMP Binding Assay of 6-Acryloyl-2-Dimethyl-aminonaphthalene (Acrylodan) Labelled CRP.

Since we are labelling CRP via cysteine residues, it is a requirement that fluorescent modification utilising thiol reagents, does not radically interfere with the binding of cAMP to the protein.

The modification procedure utilised was that adapted from a documented procedure (6), and the modified protein was subjected to the cAMP binding assay.

6.1.3.1. Experimental Procedure.

Acrylodan (1.0 mg; 4.44  $\mu$ mol) was dissolved in HEPES/KCl

buffer (0.50 M, 2.0 ml, pH 7.4), containing acetonitrile (1% v/v). Aliquots (30  $\mu$ l) of this solution were added to each of five tubes, in duplicate. Each tube contained varying concentrations of stock CRP solution (12.50 mg/ml), to a volume of 50  $\mu$ l.

Tube Nos.	1	2	3	4	5
CRP soln.	1:10	1:20	1:40	1:80	1:160

Table 6.6. The contents of each of the sample tubes with respect to CRP concentration.

The contents of each tube were thoroughly mixed, and the latter were allowed to stand overnight at 4°C. The following were then added to each tube:

- i) 5'AMP solution (10  $\mu$ l, 20 mM),
- ii) 'Cold' + tritiated ( $^3\text{H}$ ) cAMP solution (10  $\mu$ l);  
produced by adding  $^3\text{H}$ -cAMP (5  $\mu$ l) to 'cold' cAMP (220  $\mu$ l 20 mM), producing a final  $^3\text{H}$ -cAMP concentration of 0.08  $\mu\text{M}$ .

The tubes were then incubated in ice for 10 minutes. Saturated ammonium sulphate solution (1 ml) was added to each tube, and the the latter were allowed to stand at 0°C for a further 10 minutes.

The contents of each tube was then subjected to millipore filtration (0.45  $\mu\text{m}$  pore size), and the residue on the filter paper was washed with saturated ammonium sulphate solution (2 x 3 ml).

Each millipore filter paper was then introduced into a vial and Pico-Fluor Liquid Scintillation Fluid (10 ml) was added, and each vial was then subjected to radio-counting

using a Liquid Scintillation Counter.

6.1.3.2. Results.

Total Count = 134523 disintegrations per minute (d.p.m.)

Control Count = 4014 disintegrations per minute (d.p.m.)

cAMP Binding Assay of Acrylodan Labelled CRP.

<u>Tube Nos.</u>	<u>CRP Dilution</u>	<u>d.p.m.</u>	<u>Corrected d.p.m.</u>	<u>Mean d.p.m.</u>	<u>% cAMP Binding</u>
1	1:10	57823	53809	55154	41
	1:10	60513	56499		
2	1:20	51904	47890	46451	34
	1:20	49025	45011		
3	1:40	43080	39066	37946	28
	1:40	40839	36825		
4	1:80	29107	25093	24395	18
	1:80	27710	23696		
5	1:160	7771	3757	4111	3
	1:160	8479	4465		

Table 6.7. Results of the % cAMP binding of acrylodan labelled CRP.

6.1.4. cAMP Binding Assay of Bis (1,10-phenanthroline) (Bathophenanthroline disulphonyl chloride) ruthenium (II) hexafluorophosphate. (Ru Complex I).

Since we are also labelling CRP via lysine residues, it is necessary to ascertain whether fluorescent modification utilising amine reactive reagents, interferes with the binding of cAMP to the protein.

The modification procedure was that adapted from a

documented procedure (7), and the modified protein was subjected to the cAMP binding assay.

#### 6.1.4.1. Experimental Procedure.

Ru Complex I (1.0 mg; 1.0  $\mu\text{mol}$ ) was dissolved in carbonate buffer (0.05 M, 2.0 ml, pH 9.7), containing acetonitrile (1% v/v). Aliquots (30  $\mu\text{l}$ ) of this solution were added to each of five tubes, in duplicate. Each tube contained varying concentrations of stock CRP solution (12.50 mg/ml), to a volume of 50  $\mu\text{l}$ .

Tube Nos.	1	2	3	4	5
CRP soln.	1:10	1:20	1:40	1:80	1:160

Table 6.8. The contents of each of the sample tubes with respect to CRP concentration.

The contents of each tube were thoroughly mixed, and the latter were allowed to stand overnight at 4°C. The following were then added to each tube:

- i) 5'AMP solution (10  $\mu\text{l}$ , 20 mM)
- ii) 'Cold' + tritiated ( $^3\text{H}$ ) cAMP solution (10  $\mu\text{l}$ );  
produced by adding  $^3\text{H}$ -cAMP (5  $\mu\text{l}$ ) to 'cold' cAMP (220  $\mu\text{l}$  20 mM), producing a final  $^3\text{H}$ -cAMP concentration of 0.08  $\mu\text{M}$ .

The tubes were then incubated in ice for 10 minutes. Saturated ammonium sulphate solution (1 ml) was added to each tube, and the latter were allowed to stand at 0°C for a further 10 minutes.

The contents of each tube was then subjected to millipore filtration (0.45  $\mu\text{m}$  pore size), and the residue on

the filter paper was washed with saturated ammonium sulphate solution (2 x 3 ml).

Each millipore filter paper was then introduced into a vial and Pico-Fluor Liquid Scintillation Fluid (10 ml) was added, and each vial was then subjected to radio-counting using a Liquid Scintillation Counter.

#### 6.1.4.2. Results.

Total Count = 134523 disintegrations per minute (d.p.m.)

Control Count = 4014 disintegrations per minute (d.p.m.)

#### cAMP Binding Assay of Ru Complex I Labelled CRP.

<u>Tube Nos.</u>	<u>CRP Dilution</u>	<u>d.p.m.</u>	<u>Corrected d.p.m.</u>	<u>Mean d.p.m.</u>	<u>% cAMP Binding</u>
1	1:10	91608	87594	87040	65
	1:10	90500	86486		
2	1:20	83291	79277	79624	59
	1:20	83985	79971		
3	1:40	71267	67253	65466	49
	1:40	67693	63679		
4	1:80	48109	44095	41702	31
	1:80	43323	39309		
5	1:160	12323	8309	8300	6
	1:160	12304	8290		

Table 6.9. Results of the % cAMP binding of Ru Complex I labelled CRP.

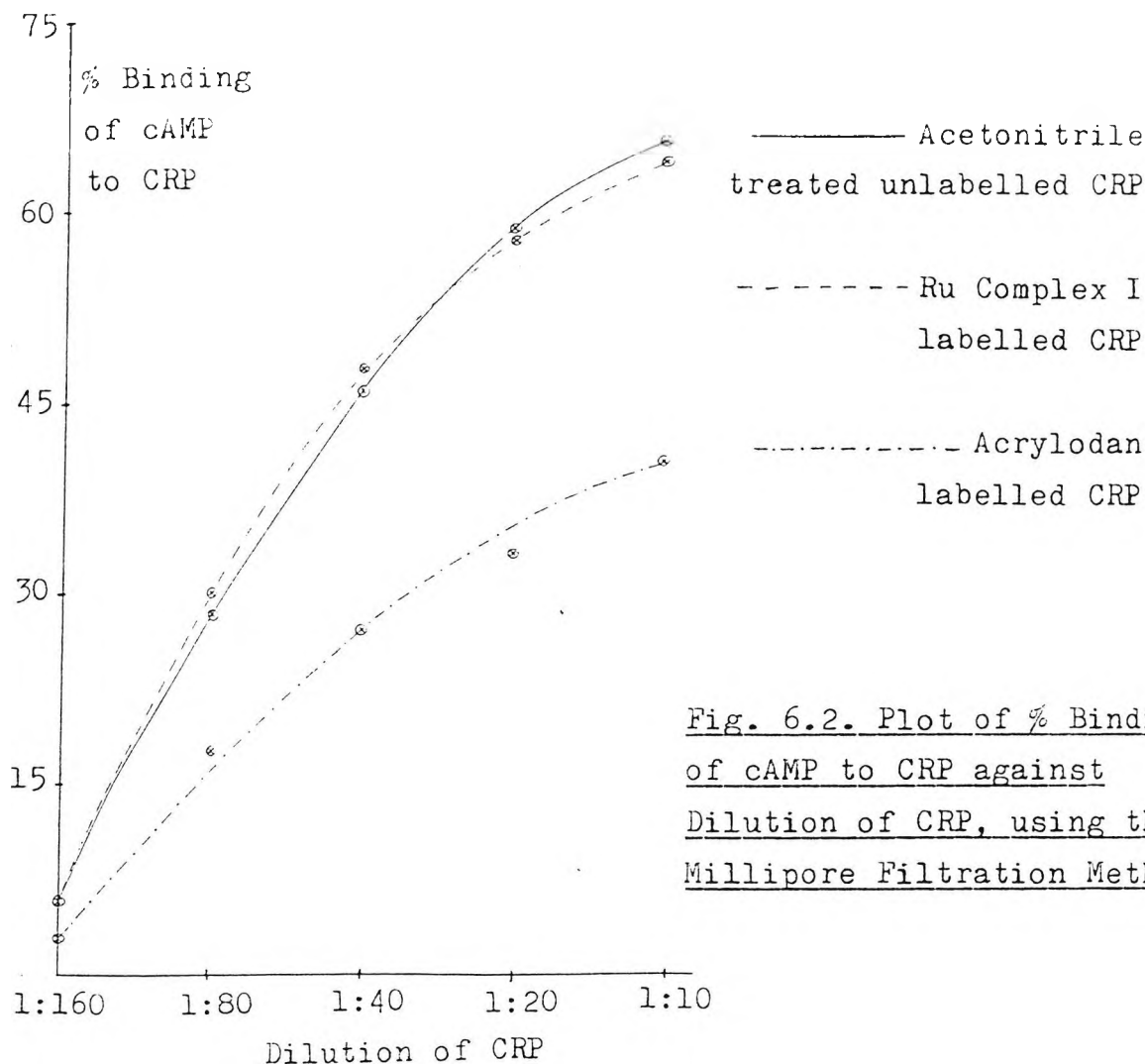


Fig. 6.2. Plot of % Binding of cAMP to CRP against Dilution of CRP, using the Millipore Filtration Method.

#### 6.1.4.3. Conclusion.

It may be seen from the graph that the ruthenium complex I labelled CRP, (that is, labelled via  $\epsilon$ -amino groups of lysine residues present in CRP) when present at a CRP concentration of 1:10, produces a minimal decrease (6%), in the efficacy of cAMP binding by the protein.

Acrylodan labelled CRP, (that is, labelled via thiol groups of cysteine residues present in CRP) produces a larger decrease (26%) in the efficiency of cAMP binding exhibited by CRP, when present at a concentration of 1:10.

Thus, fluorescent modification of CRP via both thiol and  $\epsilon$ -amino groups, does not seriously impede the capacity of cAMP to bind to the protein.

6.1.5. cAMP Binding Assay of Unlabelled CRP using the Aspirator Separation Method.

6.1.5.1. Experimental Procedure.

This method was used so as to validate the millipore filtration method.

Five tubes were set up in duplicate. To each tube was added:

- i) 5'AMP solution (10  $\mu$ l, 20 mM),
- ii) 'Cold' + tritiated ( $^3\text{H}$ ) cAMP solution (10  $\mu$ l);  
produced by adding  $^3\text{H}$ -cAMP (5  $\mu$ l) to 'cold' cAMP (220  $\mu$ l, 2  $\mu\text{M}$ ), producing a final  $^3\text{H}$ -cAMP concentration of 0.08  $\mu\text{M}$ ,
- iii) Distilled water (30  $\mu$ l).

Each tube was then treated to varying concentrations of stock CRP solution (12.50 mg/ml) to a volume of 50  $\mu$ l.

Tube Nos.	1	2	3	4	5
CRP soln.	1:10	1:20	1:40	1:80	1:160

Table 6.10. The contents of each of the sample tubes with respect to CRP concentration.

A control tube was set up containing:

- i) 5'AMP solution (10  $\mu$ l, 20 mM)
- ii) 'Cold' + tritiated ( $^3\text{H}$ ) cAMP solution (10  $\mu$ l);  
produced by adding  $^3\text{H}$ -cAMP (5  $\mu$ l) to 'cold' cAMP (220  $\mu$ l, 20 mM), producing a final  $^3\text{H}$ -cAMP concentration of 0.08  $\mu\text{M}$ .
- iii) Distilled water (30  $\mu$ l)
- iv) BSA solution (50  $\mu$ l, 1.25 mg/ml).

The tubes were then incubated on ice for 10 minutes. Saturated

ammonium sulphate solution (1 ml) was added to each tube, and the latter were allowed to stand for a further 10 minutes.

The function of the control tube was to ascertain the level of radioactivity trapped non-specifically within the pellet.

The tubes were then centrifuged at 10000 g for 10 minutes, and the supernatant was removed by aspiration. The pellets were each resuspended in water (0.2 ml), and the suspensions were introduced into separate vials. Pico-Fluor Liquid Scintillation Fluid (10 ml) was added to each vial, and the latter were then subjected to radio-counting using a Liquid Scintillation Counter.

A total-count tube was set up by taking an aliquot (10  $\mu$ l) of a 'cold' + tritiated ( $^3\text{H}$ ) cAMP solution; produced by adding  $^3\text{H}$ -cAMP (5  $\mu$ l) to 'cold' cAMP solution (220  $\mu$ l, 20 mM), producing a final  $^3\text{H}$ -cAMP concentration of 0.08  $\mu$ M. This aliquot was then added to distilled water (90  $\mu$ l).

Pico-Fluor Liquid Scintillation Fluid (10 ml) was added to the final solution, and the vial was then directly subjected to radio-counting using a Liquid Scintillation Counter.

#### 6.1.5.2. Results.

Total Count = 129872 disintegrations per minute (d.p.m.)

Control Count = 3878 disintegrations per minute (d.p.m.)

cAMP Binding Assay of Unlabelled CRP using the Aspirator Separation Method.

<u>Tube Nos.</u>	<u>CRP Dilution</u>	<u>d.p.m.</u>	<u>Corrected d.p.m.</u>	<u>Mean d.p.m.</u>	<u>% cAMP Binding</u>
1	1:10	93672	89794	90053	69
	1:10	94191	90313		
2	1:20	88970	85092	85936	66
	1:20	90659	86781		
3	1:40	81317	77439	77105	59
	1:40	80650	76772		
4	1:80	61178	57300	57689	44
	1:80	61957	58079		
5	1:160	30632	26754	27338	21
	1:160	31800	27922		

Table 6.11. Results of the % cAMP binding of unlabelled CRP as isolated via aspiration.

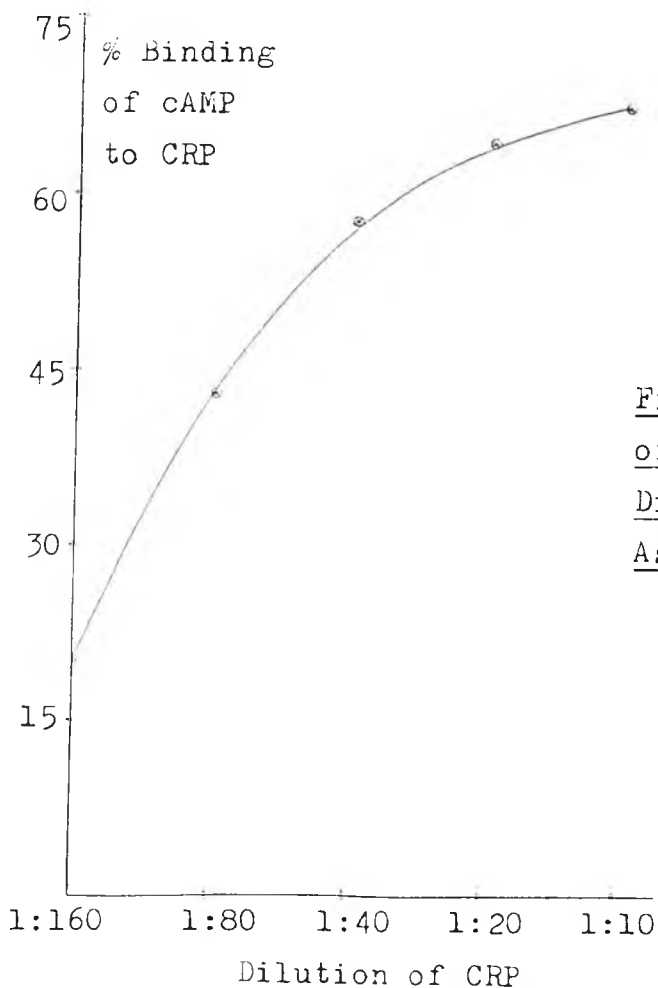


Fig. 6.3. Plot of % Binding of cAMP to CRP against Dilution of CRP, using the Aspirator Separation Method.

### 6.1.5.3. Conclusion.

It may be seen from the similarity of the shape of the two graphs, that the millipore filtration method is a valid means of isolating the cAMP-CRP complex, although the aspirator separation method is the more usual route taken.

## 6.2. INVESTIGATION OF THE CONFORMATIONAL CHANGE INDUCED IN CRP, BY cAMP BINDING, AS REPORTED BY A RANGE OF FLUOROPHORES.

Having established that neither the presence of organic solvent, nor the labelling of the CRP via thiol or  $\epsilon$ -amino groups, seriously impedes cAMP binding; we may examine the conformational change induced in CRP by the binding of cAMP, as reported by the fluorophore.

### 6.2.1. Fluorescence Data Derived from CRP Labelled via $\epsilon$ -amino Groups.

#### 6.2.1.1. Bis (1,10-phenanthroline) (Bathophenanthroline disulphonyl chloride) ruthenium (II) hexafluorophosphate, (Ru Complex I), Labelled CRP and Derivatised n-butylamine.

The U.V./visible spectrum exhibits a peak absorbance of both the protein-label conjugate, and the n-butylamine-modified label, at 433 nm. The concentration of the samples was adjusted to give a peak absorbance of 0.10, and were illuminated, at this wavelength.

The fluorescence spectrum of both samples shows a peak emission at 600 nm, thereby exhibiting a Stokes Shift of 167 nm and a relative fluorescence intensity of 220.

cAMP solution (sodium salt, 200  $\mu$ l, 1.5 mM) was added to both samples, producing a final cAMP concentration of approximately 100  $\mu$ M. The samples were allowed to incubate for 10 minutes, and both samples were then found to have a relative fluorescence intensity of 189, with no shift in the wavelength of peak emission.

The fluorescence spectrum was scanned utilising the following parameters:

Scan Range = 450-740 nm.  
Sample Sensitivity = 30  
Excitation  $\lambda$  = 433 nm.  
Peak Emission  $\lambda$  = 600 nm.  
Stokes Shift = 167 nm.

- (a) Relative Fluorescence Intensity  
of n-butylamine-bound probe = 220
- (b) Relative Fluorescence Intensity  
of (a) after cAMP addition = 189  
Fluorescence Change = -14%
- (c) Relative Fluorescence Intensity  
of protein-probe conjugate = 220
- (d) Relative Fluorescence Intensity  
of (c) after cAMP addition = 189  
Fluorescence Change = -14%

#### 6.2.1.2. Succinimidyl Trans-Parinarate (TPA) Labelled CRP and Derivatised n-butylamine.

The U.V./visible spectrum shows a peak absorbance of both the protein-label conjugate, and the n-butylamine-modified label, at 330 nm. The concentration of the samples was adjusted to give a peak absorbance of 0.10, and were

irradiated, at this wavelength.

The fluorescence spectrum of both samples exhibits three emission maxima at 360 nm, 400 nm and 460 nm, giving Stokes Shifts of 30 nm, 70 nm and 130 nm respectively, with a relative fluorescence intensity of 715.

cAMP solution (sodium salt, 200  $\mu$ l, 1.5 mM) was added to both samples, producing a final cAMP concentration of approximately 100  $\mu$ M. The samples were allowed to incubate for 10 minutes, and both samples were then found to have a relative fluorescence intensity of 624, with no shift in emission maxima.

The fluorescence spectrum was scanned utilising the following parameters:

Scan Range = 340-540 nm.  
Sample Sensitivity = 10  
Excitation  $\lambda$  = 330 nm.  
Peak Emission  $\lambda$  = 360 nm, 400 nm, 460 nm.  
Stokes Shift = 30 nm, 70 nm, 130 nm.

- (a) Relative Fluorescence Intensity  
of n-butylamine-bound probe = 715
- (b) Relative Fluorescence Intensity  
of (a) after cAMP addition = 624  
Fluorescence Change = -13%
- (c) Relative Fluorescence Intensity  
of protein-label conjugate = 715
- (d) Relative Fluorescence Intensity  
of (c) after cAMP addition = 624  
Fluorescence Change = -13%

6.2.1.3. Sulphorhodamine Acid Chloride (Texas Red)  
Labelled CRP and Derivatised n-butylamine.

The U.V./visible spectrum exhibits a peak absorbance of both the protein-label conjugate, and the n-butylamine-modified label at 587 nm. The concentration of the samples was adjusted to give a peak absorbance of 0.10, and were illuminated, at this wavelength.

The fluorescence spectrum of both samples shows a peak emission at 605 nm, thereby exhibiting a Stokes Shift of 18 nm and a relative fluorescence intensity of 121.

cAMP solution (sodium salt, 200  $\mu$ l, 1.5 mM) was added to both samples, producing a final cAMP concentration of approximately 100  $\mu$ M. The samples were allowed to incubate for 10 minutes, and both samples were then found to have a relative fluorescence intensity of 104, with no shift in peak emission.

The fluorescence spectrum was scanned utilising the following parameters:

Scan Range = 590-650 nm.  
Sample Sensitivity = 0.3  
Excitation  $\lambda$  = 587 nm.  
Peak Emission  $\lambda$  = 605 nm  
Stokes Shift = 18 nm.

- (a) Relative Fluorescence Intensity  
of n-butylamine-bound probe = 121
- (b) Relative Fluorescence Intensity  
of (a) after cAMP addition = 104
- Fluorescence Change = -14%

- (c) Relative Fluorescence Intensity  
of protein-label conjugate = 121
- (d) Relative Fluorescence Intensity  
of (c) after cAMP addition = 104
- Fluorescence Change = -14%

6.2.1.4. Succinimidyl 7-amino-4-methylcoumarin-3-Acetate  
(AMCA) Labelled CRP and Derivatised n-butylamine.

The U.V./visible spectrum shows a peak absorbance of both the protein-label conjugate, and the n-butylamine-modified probe, at 335 nm. The concentration of the samples was adjusted to give a peak absorbance of 0.10, and were irradiated, at this wavelength.

The fluorescence spectrum of both samples exhibits a peak emission at 452 nm, thereby exhibiting a Stokes Shift of 117 nm, and a relative fluorescence intensity of 490.

cAMP solution (sodium salt, 200  $\mu$ l, 1.5 mM) was added to both samples, producing a final cAMP concentration of approximately 100  $\mu$ M. The samples were allowed to incubate for 10 minutes, and both samples were then found to have a relative fluorescence intensity of 432, with no shift in peak emission.

The fluorescence spectrum was scanned utilising the following parameters:

Scan Range = 340-580 nm.  
Sample Sensitivity = 1  
Excitation  $\lambda$  = 335 nm.  
Peak Emission  $\lambda$  = 452 nm.  
Stokes Shift = 117 nm.

- (a) Relative Fluorescence Intensity  
of n-butylamine-bound probe = 490
- (b) Relative Fluorescence Intensity  
of (a) after cAMP addition = 432  
Fluorescence Change = -12%
- (c) Relative Fluorescence Intensity  
of protein-label conjugate = 490
- (d) Relative Fluorescence Intensity  
of (c) after cAMP addition = 432  
Fluorescence Change = -12%

6.2.1.5. 5-dimethylaminonaphthalene-1-sulphonyl chloride  
('Dansyl' Chloride) Labelled CRP and Derivatised  
n-butylamine.

The U.V./visible spectrum exhibits a maximal absorbance of both the protein-label conjugate, and the n-butylamine-modified label, at 340 nm. The concentration of the samples was adjusted to give a peak absorbance of 0.10, and were irradiated, at this wavelength.

The fluorescence spectrum of both samples exhibits a maximal emission at 530 nm, thereby giving a Stokes Shift of 190 nm and a relative fluorescence intensity of 248.

cAMP solution (sodium salt, 200  $\mu$ l, 1.5 mM) was added to both samples, producing a final cAMP concentration of approximately 100  $\mu$ M. The samples were allowed to incubate for 10 minutes, and both samples were then found to have a relative fluorescence intensity of 222, with no shift in peak emission.

The fluorescence spectrum was scanned utilising the following parameters:

Scan Range = 400-600 nm.  
Sample Sensitivity = 30  
Excitation  $\lambda$  = 340 nm.  
Peak Emission  $\lambda$  = 530 nm.  
Stokes Shift = 190 nm.

(a) Relative Fluorescence Intensity  
of n-butylamine-bound probe = 248

(b) Relative Fluorescence Intensity  
of (a) after cAMP addition = 222  
Fluorescence Change = -11%

(c) Relative Fluorescence Intensity  
of protein-label conjugate = 248

(d) Relative Fluorescence Intensity  
of (c) after cAMP addition = 222  
Fluorescence Change = -11%

### 6.2.2. Fluorescence Data Derived from CRP Labelled via Thiol Groups.

#### 6.2.2.1. Bis (2,2'-bipyridine) (4-vinyl-4'-methyl-2,2'-bipyridine) ruthenium (II) hexafluorophosphate. (Ru Complex II), Labelled CRP and Derivatised Cysteine.

The U.V./visible spectrum shows a maximal absorbance of the cysteine-modified label at 455 nm, whilst that of the protein-label conjugate occurs at 450 nm. The concentration of the samples was adjusted to give a peak absorbance of 0.10, and were illuminated, at their respective peak absorbances.

The fluorescence spectrum of the cysteine-modified label

exhibits a maximal emission at 620 nm, thereby giving a Stokes Shift of 165 nm and with a relative fluorescence intensity of 210. The fluorescence spectrum of the protein-label conjugate shows a peak emission at 605 nm, thereby exhibiting a Stokes Shift of 150 nm and a relative fluorescence intensity of 267.

cAMP solution (sodium salt, 200  $\mu$ l, 1.5 mM) was added to both samples, producing a final cAMP concentration of approximately 100  $\mu$ M. The samples were allowed to incubate for 10 minutes, and the cysteine-modified probe was found to have a relative fluorescence intensity of 192, whilst that of the protein-probe conjugate was shown to be 336, with no further shift in peak emission.

The fluorescence spectrum was scanned utilising the following parameters:

Scan Range = 465-650 nm.

Sample Sensitivity = 30

For cysteine-modified probe:

Excitation  $\lambda$  = 455 nm.

Peak Emission  $\lambda$  = 620 nm.

Stokes Shift = 165 nm.

For protein-probe conjugate:

Excitation  $\lambda$  = 450 nm.

Peak Emission  $\lambda$  = 605 nm.

Stokes Shift = 155 nm.

(a) Relative Fluorescence Intensity

of cysteine-modified probe = 210

(b) Relative Fluorescence Intensity

of protein-probe conjugate = 267

Fluorescence Change = +27%

and a hypsochromic (blue) shift of = 15 nm.

(c) Relative Fluorescence Intensity

of (a) after cAMP addition = 192

Fluorescence Change = -8%

and no further shift

(d) Relative Fluorescence Intensity  
of (b) after cAMP addition = 336

Fluorescence Change = +26%  
and no further shift

6.2.2.2. 9-bromomethylacridine (9-BrMeAc) Labelled CRP,  
Derivatised Cysteine and the Free Probe.

The U.V./visible spectrum exhibits a peak absorbance of the free probe, as well as the cysteine-modified probe and the protein-probe conjugate, at 380 nm. The concentration of the samples was adjusted to give a peak absorbance of 0.10, and were irradiated, at this wavelength.

The fluorescence spectrum of the free-probe shows no emission, whilst that of the remaining samples exhibits a peak emission at 475 nm, thereby showing a Stokes Shift of 95 nm. The cysteine-modified probe shows a relative fluorescence intensity of 666, whilst that of the protein-probe conjugate is 672.

cAMP solution (sodium salt, 200  $\mu$ l, 1.5 mM) was added to the modified samples, producing a final cAMP concentration of approximately 100  $\mu$ M. The samples were allowed to incubate for 10 minutes, and the cysteine-modified sample was found to have a relative fluorescence intensity of 604, whilst that of the protein-probe conjugate was shown to be 610, with no shift in peak emission.

The fluorescence spectrum was scanned utilising the following parameters:

Scan Range = 400-600 nm.  
Sample Sensitivity = 3  
Excitation  $\lambda$  = 380 nm.  
Peak Emission  $\lambda$  = 475 nm.

Stokes Shift = 95 nm.

- (a) Relative Fluorescence Intensity  
of free probe = NIL
- (b) Relative Fluorescence Intensity  
of cysteine-modified probe = 666
- (c) Relative Fluorescence Intensity  
of (b) after cAMP addition = 604  
Fluorescence Change = -9%
- (d) Relative Fluorescence Intensity  
of protein-probe conjugate = 672
- (e) Relative Fluorescence Intensity  
of (d) after cAMP addition = 610  
Fluorescence Change = -9%

6.2.2.3. N-(9-acridinyl) Maleimide (N9AM) Labelled CRP,  
Derivatised Cysteine and the Free Probe.

The U.V./visible spectrum shows a maximal absorbance of the free probe, as well as the cysteine-modified label and the protein-probe conjugate, at 360 nm. The concentration of the samples was adjusted to give a peak absorbance of 0.10, and were irradiated, at this wavelength.

The fluorescence spectrum of the free probe shows no emission, whilst that of the remaining samples exhibits a peak emission at 400 nm, thereby showing a Stokes Shift of 40 nm, and with a relative fluorescence intensity of 580.

cAMP solution (sodium salt, 200  $\mu$ l, 1.5 mM) was added to the modified samples, producing a final cAMP concentration of approximately 100  $\mu$ M. The samples were allowed to incubate for 10 minutes, and both samples were found to have a

relative fluorescence intensity of 510, with no shift in peak emission.

The fluorescence spectrum was scanned utilising the following parameters:

Scan Range = 360-580 nm.  
Sample Sensitivity = 30  
Excitation  $\lambda$  = 360 nm.  
Peak Emission  $\lambda$  = 400 nm.  
Stokes Shift = 40 nm.

(a) Relative Fluorescence Intensity  
of free probe = NIL

(b) Relative Fluorescence Intensity  
of cysteine-modified probe = 580

(c) Relative Fluorescence Intensity  
of (b) after cAMP addition = 510

Fluorescence Change = -12%

(d) Relative Fluorescence Intensity  
of protein-probe conjugate = 580

(e) Relative Fluorescence Intensity  
of (d) after cAMP addition = 510

Fluorescence Change = -12%

#### 6.2.2.4. Tetramethylrhodamine-5 (and 6) Iodoacetamide (5-IATR) Labelled CRP, Derivatised Cysteine and the Free Probe.

The U.V./visible spectrum exhibits a maximal absorbance of the free probe, as well as the cysteine-modified label and the protein-probe conjugate, at 550 nm. The concentration of the samples was adjusted to give a peak absorbance of 0.10, and were irradiated, at this wavelength.

The fluorescence spectrum of the free probe, the cysteine-

modified label and the protein-probe conjugate, all exhibit a peak emission at 585 nm, thereby showing a Stokes Shift of 35 nm, and with relative fluorescence intensities of 130, 150 and 150 respectively.

cAMP solution (sodium salt, 200  $\mu$ l, 1.5 mM) was added to the modified samples, producing a final cAMP concentration of approximately 100  $\mu$ M. The samples were allowed to incubate for 10 minutes, and both samples were found to have a relative fluorescence intensity of 135, with no shift in peak emission.

The fluorescence spectrum was scanned utilising the following parameters:

Scan Range = 560-630 nm.  
Sample Sensitivity = 0.1  
Excitation  $\lambda$  = 550 nm.  
Peak Emission  $\lambda$  = 585 nm.  
Stokes Shift = 35 nm.

- (a) Relative Fluorescence Intensity  
of free probe = 130
- (b) Relative Fluorescence Intensity  
of cysteine-modified probe = 150  
Fluorescence Change = +15%
- (c) Relative Fluorescence Intensity  
of (b) after cAMP addition = 135  
Fluorescence Change = -11%
- (d) Relative Fluorescence Intensity  
of protein-probe conjugate = 150
- (e) Relative Fluorescence Intensity  
of (d) after cAMP addition = 135  
Fluorescence Change = -11%

6.2.2.5. 5-iodoacetamidofluorescein (5-IAF) Labelled CRP,  
Derivatised Cysteine and the Free Probe.

The U.V./visible spectrum shows maximal absorbance of the free probe, as well as the cysteine-modified label and the protein-probe conjugate, at 480 nm. The concentration of the samples was adjusted to give maximal absorbance of 0.10, and were excited, at this wavelength.

The fluorescence spectrum of the free probe, the cysteine-modified label and the protein-probe conjugate, all exhibit a peak emission at 515 nm, thereby showing a Stokes Shift of 35 nm, and with relative fluorescence intensities of 265, 300 and 300 respectively.

cAMP solution (sodium salt, 200  $\mu$ l, 1.5 mM) was added to the modified samples, producing a final cAMP concentration of approximately 100  $\mu$ M. The samples were allowed to incubate for 10 minutes, and both samples were found to have a relative fluorescence intensity of 270, with no shift in peak emission.

The fluorescence spectrum was scanned utilising the following parameters:

Scan Range = 480-600 nm.  
Sample Sensitivity = 0.1  
Excitation  $\lambda$  = 480 nm.  
Peak Emission  $\lambda$  = 515 nm.  
Stokes Shift = 35 nm.

(a) Relative Fluorescence Intensity  
of free probe = 265

(b) Relative Fluorescence Intensity  
of cysteine-modified probe = 300

Fluorescence Change = +13%

(c) Relative Fluorescence Intensity  
of (b) after cAMP addition = 270  
Fluorescence Change = -10%

(d) Relative Fluorescence Intensity  
of protein-probe conjugate = 300

(e) Relative Fluorescence Intensity  
of (d) after cAMP addition = 270  
Fluorescence Change = -10%

6.2.2.6. 4-chloro-7-nitrobenz-2-oxa-1,3-diazole (NBD-Cl)  
Labelled CRP, Derivatised Cysteine and the Free Probe.

The U.V./visible spectrum exhibits a peak absorbance of the free probe, as well as the cysteine-modified label and the protein-probe conjugate, at 430 nm. The concentration of the samples was adjusted to give a maximal absorbance of 0.10, and were illuminated, at this wavelength.

The fluorescence spectrum of the free probe shows no emission, whilst that of the remaining samples exhibits a peak emission at 475 nm, thereby showing a Stokes Shift of 45 nm, and with a relative fluorescence intensity of 242.

cAMP solution (sodium salt, 200  $\mu$ l, 1.5 mM) was added to the modified samples, producing a final cAMP concentration of approximately 100  $\mu$ M. The samples were allowed to incubate for 10 minutes, and both samples were found to have a relative fluorescence intensity of 210, with no shift in peak emission.

The fluorescence spectrum was scanned utilising the following parameters:

Scan Range = 400-600 nm.  
Sample Sensitivity = 10

Excitation  $\lambda$  = 430 nm.  
Peak Emission  $\lambda$  = 475 nm.  
Stokes Shift = 45 nm.

- (a) Relative Fluorescence Intensity  
of free probe = NIL
- (b) Relative Fluorescence Intensity  
of cysteine-modified probe = 242
- (c) Relative Fluorescence Intensity  
of (b) after cAMP addition = 210  
Fluorescence Change = -13%
- (d) Relative Fluorescence Intensity  
of protein-probe conjugate = 242
- (e) Relative Fluorescence Intensity  
of (d) after cAMP addition = 210  
Fluorescence Change = -13%

6.2.2.7. Protoporphyrin IX Labelled CRP and Derivatized Cysteine.

The U.V./visible spectrum shows a peak absorbance of both the protein-label conjugate, and the cysteine-modified probe, at 400 nm, with minor peaks at 500, 535, 569, 624 and 663 nm. The concentration of the samples was adjusted to give a peak absorbance of 0.10, and were irradiated, at this wavelength.

The fluorescence spectrum of both samples, exhibits three emission maxima at 625 nm, 663 nm and 690 nm, giving Stokes Shifts of 225 nm, 263 nm and 290 nm, respectively. The cysteine-modified probe exhibited a relative fluorescence intensity of 120, whilst that of the probe-protein conjugate was found to be 175.

cAMP solution (sodium salt, 200  $\mu$ l, 1.5 mM) was added to both samples, producing a final cAMP concentration of approximately 100  $\mu$ M. The samples were allowed to incubate for 10 minutes, and the cysteine-modified probe was found to have a relative fluorescence intensity of 109, whilst that of the protein-probe conjugate was found to be 158, with no shift in peak emission.

The fluorescence spectrum was scanned utilising the following parameters:

Scan Range = 410-760 nm.  
Sample Sensitivity = 10  
Excitation  $\lambda$  = 400 nm.  
Peak Emission  $\lambda$  = 625 nm, 663 nm, 690 nm.  
Stokes Shift = 225 nm, 263 nm, 290 nm.

- (a) Relative Fluorescence Intensity  
of cysteine-modified probe = 120
- (b) Relative Fluorescence Intensity  
of protein-probe conjugate = 175  
Fluorescence Change = +46%
- (c) Relative Fluorescence Intensity  
of (a) after cAMP addition = 109  
Fluorescence Change = -9%
- (d) Relative Fluorescence Intensity  
of (b) after cAMP addition = 158  
Fluorescence Change = -10%

#### 6.2.2.8. Bilirubin Labelled CRP and Derivatized Cysteine.

The U.V./visible spectrum exhibits a maximal absorbance of the cysteine-modified probe, as well as the protein-probe

conjugate, at 400 nm. The concentration of the samples was adjusted to give maximal absorbance of 0.10, and were excited, at this wavelength.

The fluorescence spectrum of the cysteine-modified probe shows no emission, whilst that of the protein-probe conjugate exhibits a peak emission at 452 nm, thereby showing a Stokes Shift of 52 nm and with a relative fluorescence intensity of 785.

cAMP solution (sodium salt, 200  $\mu$ l, 1.5 mM) was added to the protein-probe sample, producing a final cAMP concentration of approximately 100  $\mu$ M. The sample was allowed to incubate for 10 minutes, and the sample was found to have a relative fluorescence intensity of 695, with no shift in peak emission.

The fluorescence spectrum was scanned utilising the following parameters:

Scan Range = 390-700 nm.  
Sample Sensitivity = 3  
Excitation  $\lambda$  = 400 nm.  
Peak Emission  $\lambda$  = 452 nm.  
Stokes Shift = 52 nm.

- (a) Relative Fluorescence Intensity  
of cysteine-modified probe = NIL
- (b) Relative Fluorescence Intensity  
of protein-probe conjugate = 785
- (c) Relative Fluorescence Intensity  
of (b) after cAMP addition = 695
- Fluorescence Change = -11%

6.2.2.9. N-(1-Pyrene) Maleimide (N1PM) Labelled CRP,  
Derivatised Cysteine and the Free Probe.

The U.V./visible spectrum shows a peak absorbance of the free probe, as well as the cysteine-modified label and the protein-probe conjugate, at 345 nm. The concentration of the samples was adjusted to give a maximal absorbance of 0.10, and were irradiated, at this wavelength.

The fluorescence spectrum of the free probe shows no emission, whilst that of the remaining samples exhibits absorbance maxima at 368 nm, 386 nm and 409 nm, thereby showing Stokes Shifts of 23 nm, 41 nm and 64 nm respectively, and with a relative fluorescence intensity of 165.

cAMP solution (sodium salt, 200  $\mu$ l, 1.5 mM) was added to the modified samples, producing a final cAMP concentration of 100  $\mu$ M. The samples were allowed to incubate for 10 minutes, and the cysteine-modified label was found to have a relative fluorescence intensity of 151. The protein-probe sample was shown to exhibit a further peak in emission at 465 nm, producing a relative fluorescence intensity of 177.

The fluorescence spectrum was scanned utilising the following parameters:

Scan Range = 350-500 nm.  
Sample Sensitivity = 10  
Excitation = 345 nm.  
Peak Emission = 368 nm, 386 nm, 409 nm.  
(and for the protein-probe conjugate, 465 nm.)  
Stokes Shift = 23 nm, 41 nm, 64 nm.  
(and for the protein-probe conjugate, 120 nm.)

(a) Relative Fluorescence Intensity  
of free probe = NIL

- (b) Relative Fluorescence Intensity  
of cysteine-modified probe = 165
- (c) Relative Fluorescence Intensity  
of (b) after cAMP addition = 151  
Fluorescence Change = -8%
- (d) Relative Fluorescence Intensity  
of protein-probe conjugate = 165
- (e) Relative Fluorescence Intensity  
of (d) after cAMP addition = 177  
Fluorescence Change = +7%  
and an extra peak in emission at 465 nm.

6.2.2.10. Dilithium-4-amino-N-(3-(vinylsulphonyl)phenyl)  
naphthalimide-3,6-disulphonate, (Lucifer Yellow),  
Labelled CRP and Derivatised Cysteine.

The U.V./visible spectrum exhibits a maximal absorbance of both the cysteine-modified probe and the protein-probe conjugate, at 425 nm. The concentration of the samples was adjusted to give a peak absorbance of 0.10, and were illuminated, at this wavelength.

The fluorescence spectrum of both samples shows a peak emission at 530 nm, thereby exhibiting a Stokes Shift of 105 nm, and with a relative fluorescence intensity of 540.

cAMP solution (sodium salt, 200  $\mu$ l, 1.5 mM) was added to both samples, producing a final cAMP concentration of approximately 100  $\mu$ M. The samples were allowed to incubate for 10 minutes, and both samples were then found to have a relative fluorescence intensity of 485, with no shift in the wavelength of peak emission.

The fluorescence spectrum was scanned utilising the

following parameters:

Scan Range = 520-720 nm.  
Sample Sensitivity = 30  
Excitation  $\lambda$  = 425 nm.  
Peak Emission  $\lambda$  = 530 nm.  
Stokes Shift = 105 nm.

- (a) Relative Fluorescence Intensity  
of cysteine-modified probe = 540
- (b) Relative Fluorescence Intensity  
of (a) after cAMP addition = 485  
Fluorescence Change = -10%
- (c) Relative Fluorescence Intensity  
of protein-probe conjugate = 540
- (d) Relative Fluorescence Intensity  
of (b) after cAMP addition = 485  
Fluorescence Change = -10%

6.2.2.11. N-(7-dimethylamino-4-methylcoumarinyl) Maleimide,  
(DACM), Labelled CRP, Derivatised Cysteine and  
the Free Probe.

The U.V./visible spectrum shows a maximal absorbance of the free probe, as well as the cysteine-modified label, at 400 nm, whilst that of the protein-probe conjugate occurs at 385 nm. The concentration of the samples was adjusted to give a maximal absorbance of 0.10, and were irradiated, at their respective peak absorbances.

The fluorescence spectrum of the free-probe shows no emission, whilst that of the remaining samples exhibits a peak emission at 475 nm, thereby showing a Stokes Shift of 75 nm, and with a relative fluorescence intensity of 220.

cAMP solution (sodium salt, 200  $\mu$ l, 1.5 mM) was added to the modified samples, producing a final cAMP concentration of approximately 100  $\mu$ M. The samples were allowed to incubate for 10 minutes, and the cysteine-modified sample was found to have a relative fluorescence intensity of 197, whilst that of the protein-probe conjugate was shown to be 245, with no shift in peak emission.

The fluorescence spectrum was scanned utilising the following parameters:

Scan Range = 420-550 nm.  
Sample Sensitivity = 0.3  
Excitation  $\lambda$  = 400 nm.  
Peak Emission  $\lambda$  = 475 nm.  
Stokes Shift = 75 nm.

- (a) Relative Fluorescence Intensity  
of free probe = NIL
- (b) Relative Fluorescence Intensity  
of cysteine-modified probe = 220
- (c) Relative Fluorescence Intensity  
of (b) after cAMP addition = 197  
Fluorescence Change = -10%
- (d) Relative Fluorescence Intensity  
of protein-probe conjugate = 220
- (e) Relative Fluorescence Intensity  
of (d) after cAMP addition = 245  
Fluorescence Change = +11%

6.2.2.12. Maleimidyl Benzoate Ester of Benz(c,d)indol-2(1H)-one  
Labelled CRP, Derivatised Cysteine and the Free Probe.

The U.V./visible spectrum exhibits a maximal absorbance

of the free probe, as well as the cysteine-modified label at 370 nm, whilst that of the protein-probe conjugate occurs at 362 nm. The concentration of the samples was adjusted to give a maximal absorbance of 0.10, and were irradiated, at their respective peak absorbances.

The fluorescence spectrum of the free probe and the cysteine-modified probe, both show emission maxima at 520 nm, thereby exhibiting a Stokes Shift of 150 nm, with relative fluorescence intensities of 216 and 220 respectively. The fluorescence spectrum of the protein-probe conjugate shows a peak emission of 510 nm, thereby exhibiting a Stokes Shift of 148 nm, with a relative fluorescence intensity of 313.

cAMP solution (sodium salt, 200  $\mu$ l, 1.5 mM) was added to the modified samples, producing a final cAMP concentration of approximately 100  $\mu$ M. The samples were allowed to incubate for 10 minutes, and the cysteine-modified sample was found to have a relative fluorescence intensity of 197, whilst that of the protein-probe conjugate was shown to be 215, with no shift in peak emission.

The fluorescence spectrum was scanned utilising the following parameters:

Scan Range = 400-720 nm.

Sample Sensitivity = 3

For cysteine-modified probe:

Excitation  $\lambda$  = 370 nm.

Peak Emission  $\lambda$  = 520 nm.

Stokes Shift = 150 nm.

For protein-probe conjugate:

Excitation  $\lambda$  = 362 nm.

Peak Emission  $\lambda$  = 510 nm.

Stokes Shift = 148 nm.

(a) Relative Fluorescence Intensity

of free probe = 216

- (b) Relative Fluorescence Intensity  
of cysteine-modified probe = 220  
Fluorescence Change = +2%
- (c) Relative Fluorescence Intensity  
of free probe = 216
- (d) Relative Fluorescence Intensity  
of protein-probe conjugate = 313  
Fluorescence Change = +45%
- (e) Relative Fluorescence Intensity  
of (b) after cAMP addition = 197  
Fluorescence Change = -9%
- (f) Relative Fluorescence Intensity  
of (d) after cAMP addition = 215  
Fluorescence Change = -2%

6.2.2.13. N-(1-Anilino-naphthyl-4) Maleimide (ANM) Labelled  
CRP, Derivatised Cysteine and the Free Probe.

The U.V./visible spectrum shows a maximal absorbance of the free probe, as well as the cysteine-modified label and the protein-probe conjugate, at 351 nm. The concentration of the samples was adjusted to give a maximal absorbance of 0.10, and were irradiated, at this wavelength.

The fluorescence spectrum of the free probe shows no emission, whilst that of the cysteine-modified sample exhibits a peak emission at 430 nm, thereby showing a Stokes Shift of 79 nm, with a relative fluorescence intensity of 390. The Peak emission of the protein-probe conjugate occurs at 405 nm, thereby exhibiting a Stokes Shift of 64 nm, with a relative fluorescence intensity of 487.

cAMP solution (sodium salt, 200  $\mu$ l, 1.5 mM) was added to the modified samples, producing a final cAMP concentration of approximately 100  $\mu$ M. The samples were allowed to incubate for 10 minutes, and the cysteine-modified sample was found to have a relative fluorescence intensity of 355, whilst that of the protein-probe conjugate fell to 458, with no further shift in peak emission.

The fluorescence spectrum was scanned utilising the following parameters:

Scan Range = 380-550 nm.

Sample Sensitivity = 3

Excitation  $\lambda$  = 351 nm.

For cysteine-modified probe:

Peak Emission  $\lambda$  = 430 nm.

Stokes Shift = 79 nm.

For protein-probe conjugate:

Peak Emission  $\lambda$  = 405 nm.

Stokes Shift = 64 nm.

(a) Relative Fluorescence Intensity  
of free probe = NIL

(b) Relative Fluorescence Intensity  
of cysteine-modified probe = 390

(c) Relative Fluorescence Intensity  
of protein-probe conjugate = 487

Fluorescence Change = +23%

and a hypsochromic (blue) shift of = 15 nm.

(d) Relative Fluorescence Intensity  
of (b) after cAMP addition = 355

Fluorescence Change = -9%

(e) Relative Fluorescence Intensity  
of (c) after cAMP addition = 458

Fluorescence Change = -6%  
and no further shift

6.2.2.14. 2-(4'-iodoacetamidoanilino)naphthalene-6-sulphonic acid, sodium salt, (IAANS), Labelled CRP, Derivatised Cysteine and the Free Probe.

The U.V./visible spectrum exhibits a maximal absorbance of the free probe, as well as the cysteine-modified label, at 340 nm, whilst that of the protein-probe conjugate occurs at 334 nm. The concentration of the samples was adjusted to give a maximal absorbance of 0.10, and were irradiated, at their respective peak absorbances.

The fluorescence spectrum of the free probe and the cysteine-modified probe, both show emission maxima of 455 nm, thereby exhibiting a Stokes Shift of 115 nm, with relative fluorescence intensities of 102 and 125 respectively.

The fluorescence spectrum of the protein-probe conjugate, exhibits a peak emission at 400 nm, thereby showing a Stokes Shift of 66 nm, with a relative fluorescence intensity of 315.

cAMP solution (sodium salt, 200  $\mu$ l, 1.5 mM) was added to the modified samples, producing a final cAMP concentration of approximately 100  $\mu$ M. The samples were allowed to incubate for 10 minutes, and the cysteine-modified sample was found to have a relative fluorescence intensity of 111, whilst that of the protein-probe conjugate was shown to be 327, with no further shift in peak emission.

The fluorescence spectrum was scanned utilising the following parameters:

Scan Range = 380-550 nm.

Sample Sensitivity = 0.3

For free probe and cysteine-  
modified probe:

Excitation  $\lambda$  = 340 nm.  
Peak Emission  $\lambda$  = 455 nm.  
Stokes Shift = 115 nm.

For protein-probe conjugate:

Excitation  $\lambda$  = 334 nm.  
Peak Emission  $\lambda$  = 400 nm.  
Stokes Shift = 66 nm.

(a) Relative Fluorescence Intensity  
of free probe = 102

(b) Relative Fluorescence Intensity  
of cysteine-modified probe = 125  
Fluorescence Change = +22%

(c) Relative Fluorescence Intensity  
of free probe = 102

(d) Relative Fluorescence Intensity  
of protein-probe conjugate = 315  
Fluorescence Change = +208%  
and a hypsochromic (blue) shift of = 55 nm.

(e) Relative Fluorescence Intensity  
of (b) after cAMP addition = 111  
Fluorescence Change = -11%

(f) Relative Fluorescence Intensity  
of (d) after cAMP addition = 327  
Further Fluorescence Change = +4%  
and no further shift

6.2.2.15. N-(Iodoacetylaminoethyl)-1-naphthylamine-8-  
Sulphonic Acid, (1,8-IAEDANS). Labelled CRP.  
Derivatised Cysteine and the Free Probe.

The U.V./visible spectrum shows a maximal absorbance of the free probe, as well as the cysteine-modified label, at 340 nm, whilst that of the protein-probe conjugate occurs at 330 nm. The concentration of the samples was adjusted

to give a maximal absorbance of 0.10, and were irradiated, at their respective peak absorbances.

The fluorescence spectrum of the free probe and the cysteine-modified probe, both show emission maxima at 515 nm, thereby exhibiting a Stokes Shift of 175 nm, with relative fluorescence intensities of 103 and 118, respectively. The fluorescence spectrum of the protein-probe conjugate exhibits a peak emission at 470 nm, thereby showing a Stokes Shift of 140 nm, with a relative fluorescence intensity of 470.

cAMP solution (sodium salt, 200  $\mu$ l, 1.5 mM) was added to the modified samples, producing a final cAMP concentration of approximately 100  $\mu$ M. The samples were allowed to incubate for 10 minutes, and the cysteine-modified sample was found to have a relative fluorescence intensity of 109, whilst the protein-probe conjugate exhibits a peak emission at 460 nm, with a relative fluorescence intensity of 490.

The fluorescence spectrum was scanned utilising the following parameters:

Scan Range = 400-650 nm.

Sample Sensitivity = 3

For free probe and cysteine-modified probe:

Excitation  $\lambda$  = 340 nm.  
Peak Emission  $\lambda$  = 515 nm.  
Stokes Shift = 175 nm.

For protein-probe conjugate:

Excitation  $\lambda$  = 330 nm.  
Peak Emission  $\lambda$  = 470 nm.  
Stokes Shift = 140 nm.

(a) Relative Fluorescence Intensity  
of free probe = 103

(b) Relative Fluorescence Intensity  
of cysteine-modified probe = 118

Fluorescence Change = +15%

- (c) Relative Fluorescence Intensity  
of free probe = 103
- (d) Relative Fluorescence Intensity  
of protein-probe conjugate = 470  
Fluorescence Change = +356%  
and a hypsochromic (blue) shift of = 45 nm.
- (e) Relative Fluorescence Intensity  
of (b) after cAMP addition = 109  
Fluorescence Change = -8%
- (f) Relative Fluorescence Intensity  
of (d) after cAMP addition = 490  
Further Fluorescence Change = +4%  
and a further hypsochromic (blue)  
shift of = 10 nm.

6.2.2.16. 6-Acryloyl-2-dimethylaminonaphthalene (Acrylodan),  
Labelled CRP and Derivatized Cysteine.

The U.V./visible spectrum exhibits a maximal absorbance of the cysteine-modified probe at 385 nm, whilst that of the protein-probe conjugate occurs at 374 nm. The concentration of the samples was adjusted to give a maximal absorbance of 0.10, and were irradiated, at their respective peak absorbances.

The fluorescence spectrum of the cysteine-modified probe shows an emission maximum at 530 nm, thereby exhibiting a Stokes Shift of 145 nm, with a relative fluorescence intensity of 140. The fluorescence spectrum of the protein-probe conjugate exhibits a peak emission at 485 nm, thereby showing a Stokes Shift of 111 nm, with a relative fluorescence intensity of 580.

cAMP solution (sodium salt, 200  $\mu$ l, 1.5 mM) was added to

the modified samples, producing a final cAMP concentration of approximately 100  $\mu\text{M}$ . The samples were allowed to incubate for 10 minutes, and the cysteine-modified sample was found to have a relative fluorescence intensity of 128, whilst that of the protein-probe conjugate was found to be 612, with a further hypsochromic (blue) shift of 10 nm.

The fluorescence spectrum was scanned utilising the following parameters:

Scan Range = 400-650 nm.

Sample Sensitivity = 3

For cysteine-modified probe:

Excitation  $\lambda$  = 385 nm.

Peak Emission  $\lambda$  = 530 nm.

Stokes Shift = 145 nm.

For protein-probe conjugate:

Excitation  $\lambda$  = 374 nm.

Peak Emission  $\lambda$  = 485 nm.

Stokes Shift = 111 nm.

(a) Relative Fluorescence Intensity

of cysteine-modified probe = 140

(b) Relative Fluorescence Intensity

of protein-probe conjugate = 580

Fluorescence Change = +314%

and a hypsochromic (blue) shift of = 45 nm.

(c) Relative Fluorescence Intensity

of (a) after cAMP addition = 128

Fluorescence Change = -9%

(d) Relative Fluorescence Intensity

of (b) after cAMP addition = 612

Further Fluorescence Change = +6%

and a further hypsochromic (blue)

shift of = 10 nm.

### 6.2.3. Discussion of the Performance of the Various Fluorophores Utilised.

All fluorescent probes were modified by either n-butylamine or cysteine, for comparison between the fluorescence of the probe and that of the protein-probe conjugate. This was done in order to nullify any effects of the reactive moiety, on the fluorescence of the probe.

The absorbance and fluorescence characteristics of both n-butylamine and cysteine, were investigated to discount any interfering emission from either of these. Cysteine was found to absorb maximally at 204 nm, and showed no fluorescence emission. N-butylamine was found to absorb maximally at 210 nm, and also showed no fluorescence emission.

All of the U.V./visible spectra were baselined against the appropriate buffer used. A final cAMP concentration of 100  $\mu\text{M}$  was chosen, since this concentration was found to produce a conformational change within the CRP (8,9). The sodium salt of cAMP was used in the titration procedures, so as to obviate any effects on fluorescence intensity from pH changes on cAMP addition.

Usually, the excited state of fluorescent organic molecules, has a much higher dipole moment than the ground state. As a consequence, energy is lost by dipole-dipole interaction with the solvent molecules during the lifetime of the excited state, and, as the amount of interaction increases, the emission moves further toward the red portion of the visible spectrum. Generally, emission occurs at longer wavelengths in highly polar environments and, conversely,

emission occurs at shorter wavelengths in highly non-polar environments (10).

It may be seen from the results obtained from the fluorescent modification of CRP via the  $\epsilon$ -amino group of lysine residues, that neither a shift of peak emission, nor fluorescence enhancement is evident, even though the fluorescence characteristics of 'dansyl' chloride are known to be sensitive to changes in the hydrophobicity of its environment (11). This suggests that labelling via  $\epsilon$ -amino groups places the fluorophore in a position (possibly on the surface of the protein), whereby possible increases in hydrophobicity induced in the protein by the binding of cAMP, will not be reported by the fluorophore.

Bis (2,2'-bipyridine)(4-vinyl-4'-methyl-2,2'-bipyridine) ruthenium (II) hexafluorophosphate, (Ru Complex II), possesses the vinyl group and will label CRP via the thiol group of susceptible cysteine residues, at the pH employed. Since a fluorescence enhancement of 27% was reported by the probe when CRP-bound, concomitant with a hypsochromic shift of 15 nm, as compared to the cysteine-modified probe, it is evident that the position of the probe is in a more hydrophobic environment when labelled via thiol groups. Addition of cAMP solution to the cysteine-modified probe, reduced fluorescence intensity by 8%, and this may be ascribed to a dilution effect. When cAMP binds to the protein, a further fluorescence enhancement of 26% was observed. This indicates that cAMP binding induces a conformational change within the protein, which places the probe in an even greater hydrophobic environment.

Free 9-bromomethylacridine (9-BrMeAc) was found to be non-fluorescent. This is a consequence of the interaction between the bromine atom and the excited singlet state of the fluorophore, which renders the acridine nucleus non-fluorescent. Removal of the bromine by derivatisation of cysteine, restored the fluorescence characteristics of the acridine chromophore. The protein-label conjugate exhibited a slight increase in fluorescence as compared to the cysteine-modified probe, but both species lose approximately 9% of their total emission on the addition of cAMP solution, and is attributable to the effect of dilution.

Free N-(9-acridinyl) maleimide (N9AM) was found to be non-fluorescent. This effect is due to the presence of the maleimide moiety, which involves the olefinic endo double bond, and this is responsible for the observed quenching of fluorescence emission (12). It is known (13), that maleimide derivatives generally react rapidly and specifically with thiol groups in proteins (at neutral pH), by an electrophilic addition mechanism to give an addition product. Again, the fluorescence intensity of both the protein-probe conjugate and the cysteine-modified probe were reduced (by approximately 12%), on addition of cAMP solution. The dilution of the samples is the cause of the decrease. It would appear therefore, that the acridine chromophore is, in this case, not a good candidate for reporting changes in the polarity of its environment.

Both tetramethylrhodamine-5 (and 6) iodoacetamide (5-IATR) and 5-iodoacetamidofluorescein (5-IAF) suffer from the

disadvantage of small Stokes Shifts (35 nm). This renders the task of the separation of the incident and emitted radiation quite difficult, since filters with very sharp cut-off points will need to be used. Both compounds possess the iodoacetamide group, which serves as the reactive moiety for the modification procedure. Although the iodoacetamide group may react with both thiols and amines, the pH of the conjugation reaction ensures exclusive reaction with the thiol group. It is evident that both free probes are quite strongly fluorescent. This is due to the position of the iodine atom which, unlike the bromine atom of 9-bromomethylacridine, is not directly attached to the chromophore, and may therefore not exert its effect quite so strongly. However, it is seen that removal of the iodine atom by the modification reaction, increases the fluorescence intensity of the rhodamine and fluorescein chromophores by 15% and 13% respectively. Addition of cAMP solution to the modified samples, reduces fluorescence intensity by 11% and 10% respectively. This reduction is ascribed to the effect of dilution, and consequently both the rhodamine and fluorescein chromophores, are not sufficiently sensitive to the polarity of their environment for our purposes.

Free 4-chloro-7-nitrobenz-2-oxa-1,3-diazole (NBD-Cl) (14), was found to be non-fluorescent. This is a consequence of the electron-withdrawing effect of the chlorine atom, which is directly attached to the chromophore. Removal of the chlorine atom by the modification reaction (15), provides a mildly fluorescent species. Addition of cAMP solution reduced the relative fluorescence intensity by approximately 13%, and may be attributed to an effect of dilution. Thus, NBD-Cl is

not sufficiently sensitive to the polarity of its surroundings, it also suffers the disadvantage of a small Stokes Shift (45 nm).

Protoporphyrin IX possesses two vinyl groups, and may therefore (at neutral pH), selectively modify thiol groups. The protein-probe conjugate exhibits an increase in fluorescence intensity of 46%, as compared to the cysteine-modified probe. It would appear therefore, that the porphyrin chromophore is quite sensitive to the polarity of its microenvironment. However, addition of cAMP solution did not enhance the relative fluorescence intensity, but decreases the latter by approximately 10%. This may be ascribed to a dilution effect.

Like protoporphyrin IX, bilirubin also possesses two vinyl groups, and may therefore selectively modify thiol groups at neutral pH. However, unlike cysteine-modified protoporphyrin IX, the modified bilirubin molecule exhibited no fluorescence emission. This may be attributable to the conformers of bilirubin which are in dynamic equilibrium. As a consequence, bilirubin may lose its excited state energy via non-radiative pathways, (for example, thermally). Protoporphyrin IX on the other hand has a more rigid structure, and is more likely to lose its excited state energy via emissive pathways. The bilirubin probe-protein conjugate is strongly fluorescent, and it is possible that the protein constrains the bilirubin molecule into a particular conformation, thereby allowing the chromophore to lose its excited state energy via fluorescence emission. The addition of cAMP solution reduces relative fluorescence intensity by approximately 11%, and this may be ascribed to the effect of dilution.

An experimental procedure was followed in order to encapsulate bilirubin within the water-soluble clathrate, cyclohepta-amylose, or  $\beta$ -cyclodextrin (16).

Bilirubin (0.05 gm) was dissolved in chloroform (10 ml). A concentrated aqueous solution (2% w/v, 10 ml) of  $\beta$ -cyclodextrin, was shaken with the bilirubin solution. An orange precipitate was found to be deposited. This was removed by filtration, and washed with chloroform (2 x 2 ml). The orange solid was dried in air. The U.V./visible spectrum of the aqueous, encapsulated bilirubin exhibited peak absorbance at 400 nm. The concentration of the sample was adjusted to give a maximal absorbance of 0.10, and was excited, at this wavelength.

The fluorescence spectrum of the encapsulated chromophore, showed a peak emission at 505 nm, with a relative fluorescence intensity of 510. This compares to the peak emission at 452 nm of the protein-probe conjugate, with a relative fluorescence intensity of 785.

The fluorescence spectrum was scanned utilising the following parameters:

Scan Range = 415-645 nm.  
Sample Sensitivity = 3  
Excitation  $\lambda$  = 400 nm.  
Peak Emission  $\lambda$  = 505 nm.  
Stokes Shift = 105 nm.

It would appear that the  $\beta$ -cyclodextrin also constrains the bilirubin molecule in a particular conformation, so as to ensure loss of excited state energy via emissive pathways. The bilirubin when present as a protein-probe conjugate must

be within a more hydrophobic environment, than when encapsulated within  $\beta$ -cyclodextrin, as evidenced by the increased fluorescence intensity (+35%), and by the hypsochromic shift of 53 nm.

It is known (17), that  $\beta$ -cyclodextrin preferentially complexes with the left-handed (or negative) chiral enantiomer of bilirubin.

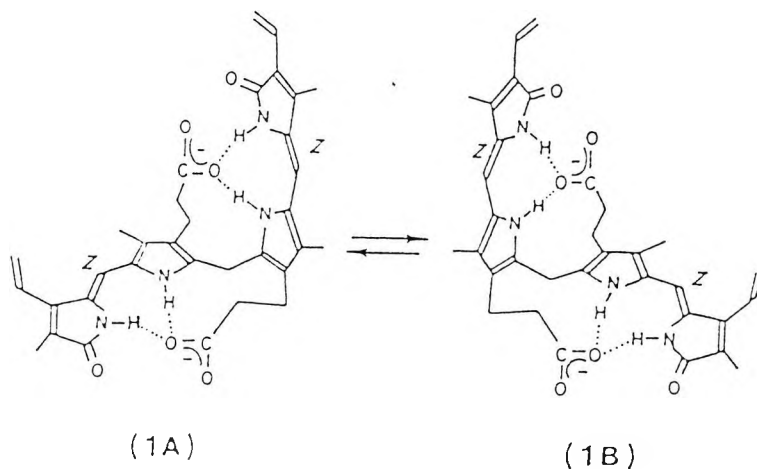


Fig. 6.4. Interconverting enantiomeric, intramolecularly hydrogen-bonded conformers of bichromophoric (4Z,15Z)-bilirubin IX bispropionate anion. Conformer 1A exhibits a left-handed or negative chirality; Conformer 1B exhibits a right-handed or positive chirality (17).

Free N-(1-Pyrene) maleimide (N1PM) (18), was found to be non-fluorescent. On reaction with cysteine, the resulting adduct was found to be fairly fluorescent; (relative fluorescence intensity = 165) and its fluorescence spectrum describes three peaks of emission. On addition of cAMP solution, the relative fluorescence intensity was seen to decrease by approximately 8%, and may be attributed to the effect of dilution.

The protein-probe conjugate exhibited the same degree of

fluorescence intensity, as did the cysteine adduct. However, on addition of cAMP solution, the fluorescence spectrum exhibited four peaks; the extra peak of emission occurring at 465 nm, producing an increased (+7%) relative fluorescence intensity. The extra peak may be attributed to fluorescence emitted from an excited dimer (excimer), of pyrene molecules. This indicates that two cysteine residues are labelled, and they are in close proximity to each other. This phenomenon has also been observed when  $\text{Ca}^{2+}$  binds to pyrene-labelled Troponin I (19).

Dilithium 4-amino-N-(3-(vinylsulphonyl)phenyl) naphthalimide-3,6-disulphonate, (Lucifer Yellow, VS) (20), possesses the vinyl-sulphone group and will act as a thiol-reactive agent at neutral pH. Cysteine-modified lucifer yellow is strongly fluorescent and addition of cAMP solution, reduces the relative fluorescence intensity by approximately 10%. Likewise, the protein-probe conjugate exhibits a similar fluorescence intensity to the cysteine-modified probe, and again, addition of cAMP solution reduces the relative fluorescence intensity by approximately 10%. The reductions in the relative fluorescence intensity may be ascribed to a dilution effect, and as a consequence, lucifer yellow is not sufficiently sensitive to the changes in the polarity of its environment.

N-(7-dimethylamino-4-methylcoumarinyl) maleimide (DACM) (21), possesses the maleimide moiety and consequently, will modify thiol groups at neutral pH. The free probe is non-fluorescent and the cysteine-modified probe, exhibited very strong fluor-

escence intensity. Upon addition of cAMP solution, the relative fluorescence intensity was reduced by approximately 10%, and this may be ascribed to the effect of dilution.

The protein-label conjugate exhibits a relative fluorescence intensity similar to that of the cysteine-transformed probe. However, on addition of cAMP solution, the relative fluorescence intensity was seen to increase by approximately 11%. No shift in peak emission was in evidence.

It is clear that DACM is responding to the increase in the hydrophobicity of its environment, by an increase in the relative fluorescence intensity. During the modification procedure, the probe undergoes a series of structural changes; from a close-type adduct to an open-type adduct. The higher the pH, the greater the rate of ring opening. All probe molecules were in the open-type form within 24 hours at pH 7.2.

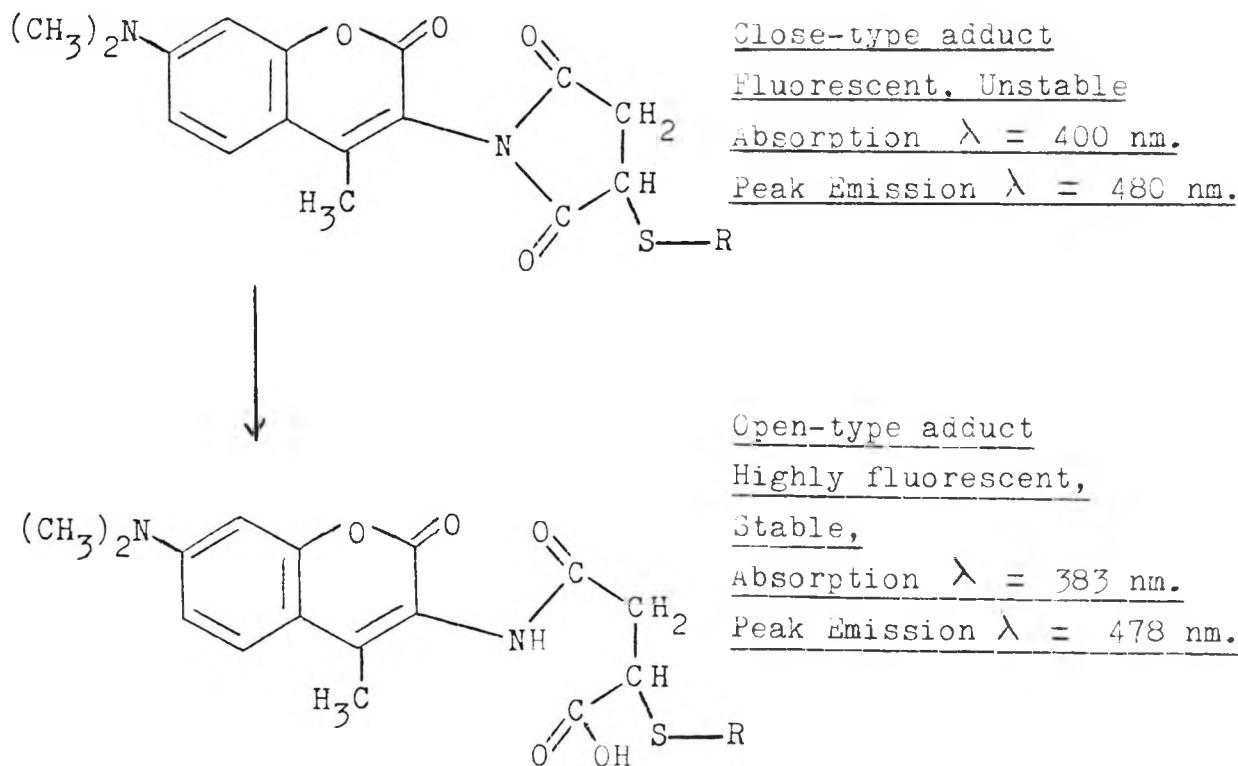


Fig. 6.5. The reaction for the ring-opening of the thiol adduct of DACM.

Clearly, the structure investigated, is the open-type adduct, as evidenced by the wavelengths of absorption and emission.

Although the maleimidyl benzoate ester of benz(c,d) indol-2(1H)-one (Naph-Mal) (22), possesses the maleimide moiety, and will consequently modify thiol groups at neutral pH, and the former is not directly attached to the naphthalene nucleus (chromophore). As a result, the free probe exhibited fairly strong fluorescence emission. A slight increase in the relative fluorescence intensity was seen to decrease by approximately 3%. This may be attributed to the effect of dilution. A much larger increase in the relative fluorescence intensity was exhibited in the protein-probe conjugate (+45%), when compared to the free probe. On cAMP addition, the relative fluorescence intensity was shown to decrease, but to a much lesser extent (-2%). This may indicate, that the loss of relative fluorescence intensity by the effect of dilution, was offset by the increase in the relative fluorescence intensity of the probe in response to the increase in the hydrophobicity of its environment, when the protein bound to cAMP. No shifts in peak emission were evident. The probe also exhibited a large Stokes Shift of 150 nm.

Free N-(1-anilinonaphthyl-4) maleimide (ANM) (23), is non-fluorescent. Since it possesses the maleimide moiety, at neutral pH, it may act as a thiol modifying agent. The cysteine-modified probe exhibits strong fluorescence emission and the relative fluorescence intensity of the protein-probe conjugate, was seen to increase by approximately 23%; concomitant with a hypsochromic shift of 15 nm, as compared to the cysteine-modified probe. This showed that the ANM is

sensitive to the polarity of its microenvironment. Upon addition of cAMP solution, to the cysteine-modified probe, the relative fluorescence intensity of the latter, was seen to diminish by approximately 9%. Addition of cAMP solution to the protein-probe conjugate yielded a decrease of 6% in the relative fluorescence intensity of the latter, with no further shift in peak emission.

2-(4'-iodoacetamidoanilino) naphthalene-6-sulphonic acid, sodium salt (IAANS), possesses the iodoacetamide group, and as a consequence, it may react with thiol groups at neutral pH. The free probe is strongly fluorescent; the fluorescence quenching effect of the iodine atom is minimised, due to its position away from the naphthalene chromophore. The cysteine-modified probe exhibited an increase in the relative fluorescence intensity of 22%, when compared to the free probe. This increase is a consequence of the loss of the iodine atom. Upon addition of cAMP solution, the relative fluorescence intensity of the cysteine-modified probe was seen to decrease by approximately 11%, and may be ascribed to the effect of dilution.

The protein-probe conjugate exhibited an increase in the relative fluorescence intensity of approximately 208%, as compared to the free probe, concomitant with a hypsochromic shift of 55 nm. The probe is therefore extremely sensitive to the polarity of its environment. Addition of cAMP solution further increased the relative fluorescence intensity of the protein-probe conjugate by approximately 4%, although no further shift in peak emission was evident. IAANS has been used to great effect on the investigation of the interaction

of  $\text{Ca}^{2+}$  with cardiac troponin and Troponin C (24).

N-(Iodoacetyl aminoethyl)-1-naphthylamine-8-Sulphonic acid (1,8-IAEDANS) (25), possesses the iodoacetamide moiety and will therefore react with thiol groups at neutral pH. The free probe is quite fluorescent, and the relative fluorescence intensity of the cysteine-modified probe demonstrated a 15% increase, compared with that of the free probe. This increase was due to the loss of the iodine atom. Addition of cAMP solution to this preparation gave a relative fluorescence intensity decrease of approximately 8%, which may be ascribed to a dilution effect.

The protein-probe conjugate exhibited a relative fluorescence intensity increase of 356%, concomitant with a hypsochromic shift of 45 nm, when compared to the free probe. Addition of cAMP solution to this species, yielded a further relative fluorescence intensity increase of approximately 4% with a further hypsochromic shift of 10 nm. Therefore, this probe is extremely sensitive to the polarity of its environment. The Stokes Shift for the protein-probe conjugate was 140 nm.

6-acryloyl-2-dimethylaminonaphthalene (Acrylodan) (6), possesses an acryloyl group and will therefore react with thiol groups at neutral pH. The cysteine-modified probe is strongly fluorescent and the relative fluorescence intensity of this adduct, is reduced by 9% on addition of cAMP solution. This is attributed to the effect of dilution.

The protein-probe conjugate exhibited a relative fluorescence intensity increase of 314%, when compared to the cysteine-modified adduct together with a hypsochromic shift of 45 nm. Addition of cAMP solution further enhanced the

relative fluorescence intensity of the protein-probe conjugate by approximately 6%, concomitant with a further hypsochromic shift of 10 nm. The probe is therefore exquisitely sensitive to the polarity of its environment.

Compounds possessing the 6-acyl-2-dimethylamino-naphthalene moiety, are known to be extremely sensitive to the polarity of their environment (26). The environment sensitivity of this moiety is derived from the large dipole moment developed in the excited state, as a consequence of facile charge delocalisation between the 2-dimethylamino moiety and the carbonyl group in the 6-position of the naphthalene chromophore.

Thus, it is clear that thiol modification of cysteine residues within the protein, has been much more successful than has production of the protein-probe conjugate by labelling of the  $\epsilon$ -amino group of lysine. When introduced onto the protein via thiol groups, the ruthenium complex (Ru Complex II), coumarin (DACM) and naphthalene (1,8-IAEDANS, Acrylodan) chromophore, exhibited shifts in peak emission and increases in the relative fluorescence intensity of the probe. When these chromophores, ruthenium complex (Ru Complex I), coumarin (AMCA) and naphthalene ('dansyl' chloride), are introduced onto the protein via  $\epsilon$ -amino groups, no positive results are detected.

It was therefore decided at an early stage, that modification of the protein via thiol transformation, would be the more profitable avenue to explore. This explains the preponderance of the use of thiol reactive probes as compared to  $\epsilon$ -amino modifying probes.

It is evident from the foregoing, that fluorophores possessing the naphthalene chromophore were the most successful of the probes investigated. However, larger chromophores such as ruthenium complex II and protoporphyrin IX, exhibited less dramatic increases in the relative fluorescence intensity of the protein-probe conjugate.

### 6.3. CORRELATION OF THE POLARITY OF THE HYDROPHOBIC POCKET OF CRP, WITH A RANGE OF ORGANIC SOLVENTS POSSESSING DIFFERENT POLARITIES.

It is possible to ascertain the extent of the hydrophobicity of the pocket present in CRP, by correlating the fluorescence characteristics of environmentally sensitive fluorophores with respect to polarity, when protein-bound and when dissolved in a range of organic solvents possessing different polarities. A quantitative relationship has been derived (27), between the position of the peak absorbance and emission, by taking into consideration the dielectric constant and the dipole moments of the solvent and the solute.

#### 6.3.1. Experimental Procedure.

1,8-IAEDANS and Acrylodan were selected for this investigation. Solutions of Acrylodan and 1,8-IAEDANS were individually prepared (0.10 mg per 3 ml), in a range of organic solvents with differing polarities.

The U.V./visible spectrum of each solution was scanned, and the concentration of each sample was diluted to achieve a peak absorbance of 0.10. The fluorescence spectrum was then scanned when excited at the wavelength of peak absorbance.

### 6.3.2. Results.

<u>SOLVENT</u>	<u>ACRYLODAN</u>		<u>1,8-IAEDANS</u>	
	<u>Absorbance</u> <u><math>\lambda</math> (nm)</u>	<u>Emission</u> <u><math>\lambda</math> (nm)</u>	<u>Absorbance</u> <u><math>\lambda</math> (nm)</u>	<u>Emission</u> <u><math>\lambda</math> (nm)</u>
Methanol	385	495	335	468
Ethanol	382	479	333	455
Acetonitrile	378	455	329	435
1,4-Dioxane	375	435	327	428

Table 6.12. Results for the effect of a range of solvents on the wavelengths of absorbance and emission of two fluorophores.

These results were compared with those obtained for the protein-probe conjugate, both before and after cAMP addition.

	<u>ACRYLODAN</u>		<u>1,8-IAEDANS</u>	
	<u>Absorbance</u> <u><math>\lambda</math> (nm)</u>	<u>Emission</u> <u><math>\lambda</math> (nm)</u>	<u>Absorbance</u> <u><math>\lambda</math> (nm)</u>	<u>Emission</u> <u><math>\lambda</math> (nm)</u>
Protein-probe conjugate	374	485	330	470
+ cAMP	374	475	330	460

Table 6.13. Tabulated results for the wavelengths of the absorbance and emission of two CRP-bound fluorophores, in the presence and absence of cAMP.

### 6.3.3. Conclusion.

The results obtained indicate that the hydrophobic pocket of CRP in the absence of cAMP, most closely resembles the polarity of methanol (which has a dielectric constant of

approximately 31 debyes). Upon cAMP addition, the polarity of the microenvironment surrounding the probe, acquires a polarity which equates most closely to ethanol (which has a dielectric constant of approximately 26 debyes).

A definitive system has been developed (28), whereby solvents may be categorised with respect to their polarity, by the designation of a Z-value. The Z-values for water, methanol, ethanol, acetonitrile and aqueous 1,4-dioxane (90% v/v) are 94.6, 83.6, 79.6, 71.3 and 76.7 respectively.

Bovine Serum Albumin (BSA) has a large, hydrophobic pocket and when labelled via  $\epsilon$ -amino groups by 'dansyl' chloride (10), the emission maximum of the probe occurs at 500 nm. This corresponds to a comparative hydrophobicity of 1,4-dioxane, (which has a dielectric constant of 3 debyes). Clearly, BSA possesses a non-polar pocket which is much more hydrophobic than that of CRP.

#### 6.4. DETERMINATION OF THE EFFECT OF cAMP ON THE ABILITY OF CRP TO UNDERGO THIOL MODIFICATION.

It is advantageous to know whether the CRP-cAMP complex will undergo thiol modification, since this would provide information regarding the interaction of the modification site and the amino acids comprising the cAMP binding site. As a consequence, experimental procedures were followed in order to ascertain whether fluorescent modification via thiol groups, could be achieved in the presence of cAMP.

##### 6.4.1. Experimental Procedure (8).

1,8-IAEDANS (1.0 mg) was dissolved in Tris-HCl/KCl/EDTA

buffer (0.20 M, 2.0 ml, pH 8.0).

The above solution was divided into two equal portions. Stock CRP solution (0.04 ml, 12.50 mg/ml) was dissolved in Tris-HCl/KCl/EDTA (0.20 M, 0.96 ml), and this solution was added to one portion.

To stock CRP solution (0.04 ml) was added cAMP solution (sodium salt, 0.20 ml, 1.5 mM), and the mixture was allowed to incubate for 10 minutes. Tris-HCl/KCl/EDTA buffer (0.20 M, 0.76 ml) was added to the CRP-cAMP complex solution, and the resulting solution was added to the remaining portion of the probe solution. The final cAMP concentration was in excess of 100  $\mu$ M.

The solutions were allowed to stand overnight, protected from light, at 4°C. Both solutions were then extensively dialysed (3 days), against Tris-HCl/KCl/MgCl<sub>2</sub>/dithiothreitol buffer (0.20 M, 1000 ml, pH 8.0) using cellulose tubing which retains molecular weight species in excess of 12000 daltons.

The dialysands were then subjected separately to gel exclusion chromatography using Sephadex G-25 (20-80  $\mu$ m bead size, bed volume: approximately 10 ml), which had previously equilibrated with the Tris-HCl/KCl/EDTA buffer, and the columns were eluted with this buffer.

The collected fractions were diluted to 3 ml with the eluent buffer, and then subjected to U.V./visible and fluorescence spectral analysis.

The labelling procedure was repeated using Acrylodan with the utilisation of HEPES/KCl buffer (0.50 M, pH 7.4) instead of the Tris-HCl buffers.

#### 6.4.2. Results.

The U.V./visible spectrum of the 1,8-IAEDANS labelled sample in the absence of cAMP, exhibited a peak absorbance at 330 nm. The fluorescence spectrum of this sample was found to show peak emission at 470 nm.

The U.V./visible spectrum of the purified conjugation medium on prior incubation with cAMP, exhibited no such peak. No fluorescence emission was detected in this sample.

The U.V./visible spectrum of the Acrylodan labelled sample in the absence of cAMP, exhibited a peak absorbance at 375 nm. The fluorescence spectrum of this sample was found to show peak emission at 485 nm.

The U.V./visible spectrum of the purified conjugation medium on prior incubation with cAMP, exhibited no such peak. No fluorescence emission was detected in this sample.

#### 6.4.3. Conclusion.

These results indicate that CRP may not be fluorescently modified via thiol groups, when the protein had been previously incubated with cAMP. It would appear, therefore, that thiol modification of CRP is communicated to the cAMP binding site, and that consequently there is interaction between the portions of the CRP molecule involved.

#### 6.5. INVESTIGATION OF THE NATURE OF THE CRP-PROBE CONJUGATE.

It is advantageous to deduce the dye : protein ratio of the fluorescently modified protein, so as to determine the number of accessible sites for modification. This

knowledge may provide an insight into the conformation of the protein.

As a result, procedures were followed in order to determine the stoichiometry of labelling of CRP via thiol modification.

### 6.5.1. Determination of the Stoichiometry of the Labelling of CRP via Thiol Modification.

#### 6.5.1.1. Experimental Procedure.

The protein-1,8-IAEDANS conjugate sample as previously prepared, in the absence of cAMP, was diluted by a factor of two with buffer, and the U.V./visible spectrum was utilised, in order to calculate the dye : protein ratio.

#### 6.5.1.2. Results.

From the Beer-Lambert law,  $D = \epsilon \cdot c \cdot l$

For a pathlength of 1 cm,  $D = \epsilon \cdot c$

$$c = \frac{D}{\epsilon}$$

For the probe,  $c = \frac{0.053}{\text{at } 340 \text{ nm}}$   $\epsilon$  at 340 nm = 6300  
(Ref. 25)

$$c = \frac{0.053}{6300} = \underline{8.4 \times 10^{-6} \text{ M.}}$$

For the protein,  $c = \frac{0.162}{\text{at } 278 \text{ nm}}$   $\epsilon$  at 278 nm = 20000  
(Ref. 29)

$$c = \frac{0.162}{20000} = \underline{8.1 \times 10^{-6} \text{ M.}}$$

Thus, the dye : protein ratio is 1 : 1.

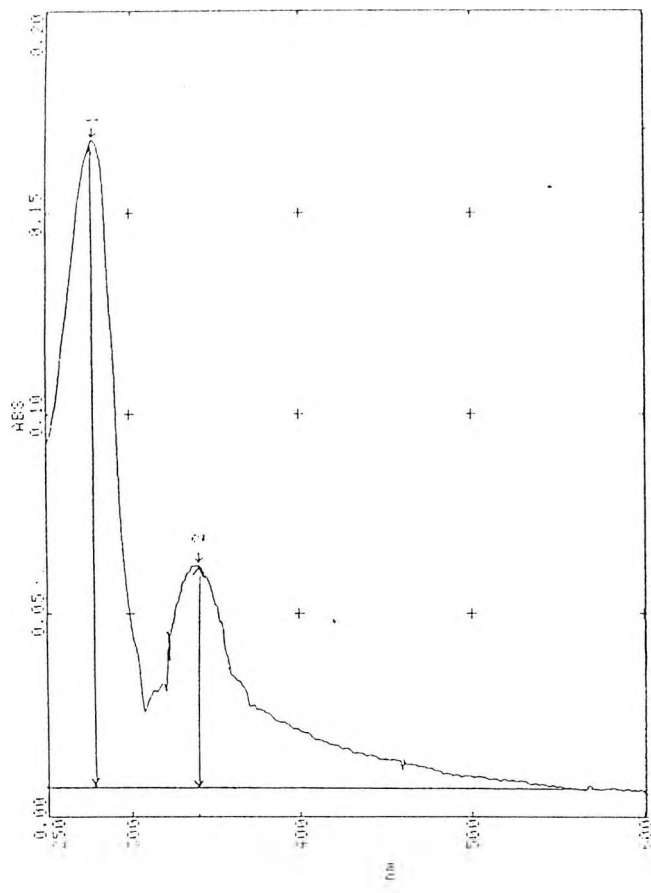


Fig. 6.6. The U.V./visible spectrum of CRP-1,8-IAEDANS conjugate, baselined against Tris-HCl buffer.

This procedure was repeated using DACM, in order to preclude possible binding of other susceptible amino acid residues, for example, histidine. Similarly, the dye : protein ratio was found to be 1 : 1.

6.5.2. Determination of the Specificity of the Labelling of CRP via Thiol Groups.

Having established that the dye : protein ratio of labelling is 1 : 1, it is necessary to investigate the nature of the protein-probe conjugate, with respect to covalent labelling of the protein. This may be achieved by the use of Sodium Dodecyl Sulphate-Polyacrylamide Gel Electrophoresis, (SDS-PAGE).

#### 6.5.2.1. Experimental Procedure.

The technique employed was that as outlined (30). The resolving gel (10%), was prepared from stock acrylamide solution (30% w/v) and N,N'-bis-methylene acrylamide solution (0.8% w/v), in Tris-HCl buffer (0.375 M, pH 8.8), containing SDS (0.1% w/v).

The stacking gel (3%), was prepared from stock acrylamide solution (30% w/v) and N,N'-bis-methylene acrylamide solution (0.8% w/v), in Tris-HCl buffer (0.125 M, pH 6.8), containing SDS (0.1% w/v).

Both gels were polymerised by the addition of tetra-methylethylenediamine (TEMED, 0.025% w/v), and ammonium persulphate.

The resolving gel occupied 100 mm of two 150 mm glass tubes, of internal diameter 6 mm. The stacking gel occupied 10 mm of these tubes.

The electrophoretic separation was performed in electrode buffer (pH 8.3), containing Tris-HCl (0.025 M) and glycine (0.192 M), plus SDS (0.1% w/v).

CRP was labelled with 1,8-IAEDANS as previously described, and two aliquots (2 x 200  $\mu$ l) were taken from the conjugation medium. One drop of bromophenol blue solution in Tris-HCl, pH 8.0, (0.001% w/v), was added to each aliquot. Each aliquot was then directly applied to one of the stacking gels.

The current was set at 3 mA per gel, and the current was applied for 90 minutes. The gels were removed from the tubes, and viewed under U.V. radiation at 375 nm.

### 6.5.2.2. Results.

A fluorescent band was observed approximately 40 mm from the bromophenol blue marker in both gels. No other fluorescent band was observed.

The gels were then fixed in trichloroacetic acid (10% v/v) overnight, and were stained by placing the gels in Coomassie Brilliant Blue (0.1% w/v) in trichloroacetic acid (10% v/v) for one hour at 37°C. The gels were then washed in aqueous acetic acid (7% v/v).

The gels were viewed in daylight and a blue band was observed approximately 40 mm from the bromophenol blue marker in both gels. No other protein band was observed.

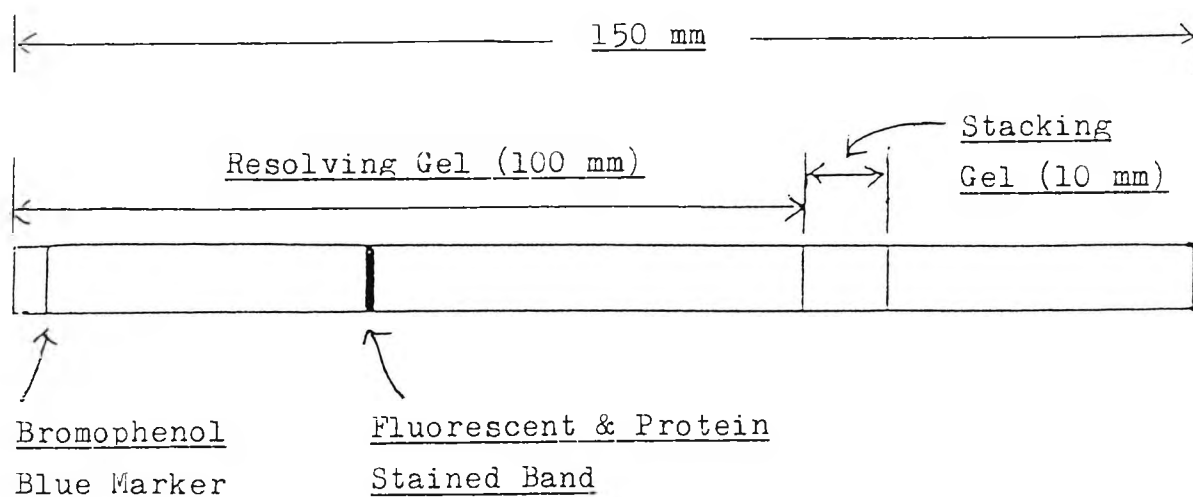


Fig. 6.7. Scale drawing of the electrophoretic gel of the CRP-1,8-IAEDANS conjugate.

### 6.5.3. Conclusion.

Thus, the label and the protein migrate as a single band, and this indicates that the probe is covalently bound to the protein. This is an important deduction, since introduction of the protein-probe conjugate into the cell when the probe is interacting non-specifically with the protein,

may result in loss of the probe when the protein interacts with cellular components.

#### 6.5.4. Discussion.

It is known (31) that hydrophobic probes will interact non-specifically with CRP. 8-anilino-1-naphthalene sulphonic acid (ANS) is such a probe, and its interaction with CRP produces a dramatic increase in fluorescence intensity, with a concomitant shift in peak emission from 530 nm to 480 nm. It was found that there are two ANS binding sites per CRP dimer.

When the ANS-CRP complex was titrated with cAMP, a quenching of the fluorescence signal was observed. The pattern of quenching was apparently biphasic. The first phase occurred in the cAMP concentration range of 0 to 200  $\mu\text{M}$ , whereas the second phase occurred at millimolar concentrations of cAMP.

Binding of ANS to CRP in the presence of 200  $\mu\text{M}$  cAMP, showed that the number of ANS binding sites per dimer was reduced to 1.2. This suggested that the first phase of fluorescence quenching of ANS-CRP in the presence of cAMP, corresponds to the dissociation of one ANS molecule from the ANS-CRP complex. It is possible that the second phase of quenching is due to the dissociation of the second ANS molecule from the CRP dimer. These observations indicate that the ANS is binding to the protein, in the vicinity of the cAMP binding site.

The CRP molecule possesses three cysteine residues at positions 18, 92 and 178 (32,33), of which only cysteine-178 is available for modification in the native protein, while

cysteine residues 18 and 92 are inaccessible (34). Cysteine-178 is present on a stretch of polypeptide connecting helices E and F, which form part of the DNA-binding site of the protein (35).

It is known (29) that in the absence of cAMP, the CRP exists in a monomeric state. cAMP binding promotes the formation of cysteine-178/cysteine-178 disulphide linkages (36), thereby producing CRP dimers. The distance between the thiol groups of these cysteine residues, was seen to decrease by at least 3 <sup>0</sup> A. This finding would explain the extra peak in the emission spectrum of N-(1-Pyrene) maleimide-bound CRP, observed on the addition of cAMP. In the absence of cAMP, the probe labels the monomeric protein via thiol groups present on cysteine residues at position 178. On cAMP binding, protein dimers are formed and the probe molecules are closer together, giving rise to the excited dimer (excimer) peak of fluorescence at 465 nm. Also, the observation that CRP may not be labelled via thiol modification of cysteine, on prior incubation with cAMP, may be rationalised, since cysteine-178/cysteine-178 disulphide linkages are formed in the presence of cAMP. As a result, no thiol groups are available for labelling.

Glutamate-181, which is in very close proximity to cysteine-178, has been found to be intimately involved in the mechanism of DNA binding by the protein (37). It has been postulated (31), that the binding of cAMP to one subunit changes the conformation of this and its neighbouring subunit. Thus, there is interaction between the sites, and there is

negative co-operativity in binding.

It is clear, therefore, that the binding of cAMP to the amino-terminal portion of the protein, induces a profound conformational change in the carboxyl-terminal part of the protein.

Conversely, we may contend that events occurring at the carboxyl-terminal portion of the protein, serves to increase the affinity of the protein for cAMP. Thus, when the thiol group of cysteine-178 is modified, it is unavailable for cysteine-178/cysteine-178 intersubunit disulphide linkage formation. This may disallow a preferred conformational change in the protein, and may render the latter with a reduced affinity for the cAMP molecule. This contention may provide an explanation for the finding that thiol modified CRP appears to possess a reduced affinity for cAMP, as compared to  $\epsilon$ -amino modified CRP.

The results obtained indicate that the following processes occur, and these may be represented schematically.

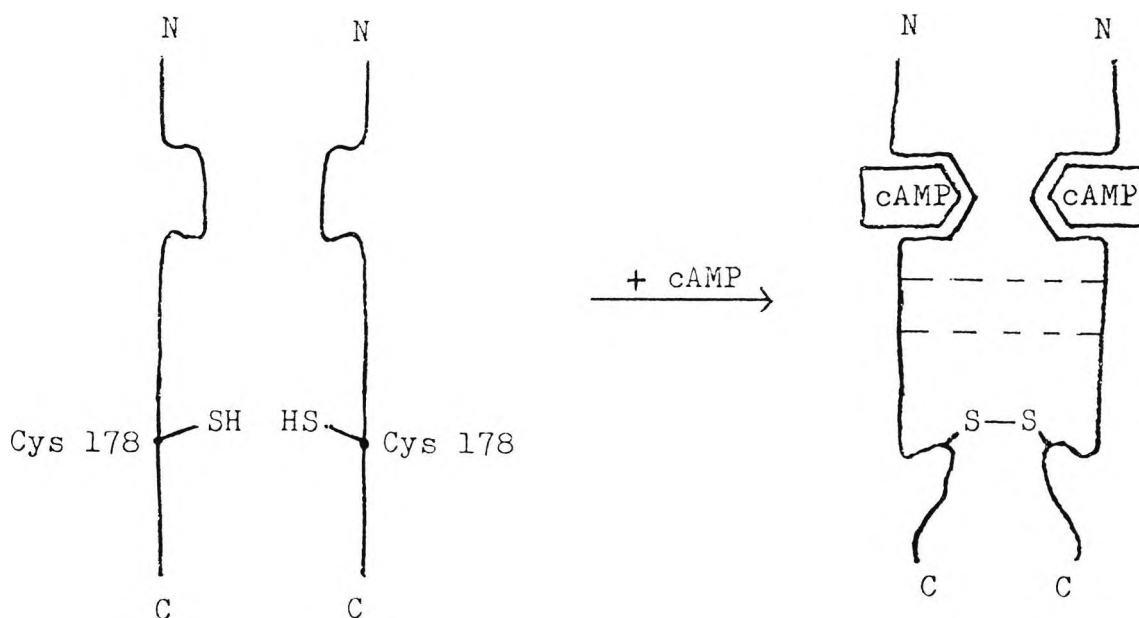


Fig. 6.8. Formation of the CRP dimer by the binding of cAMP.

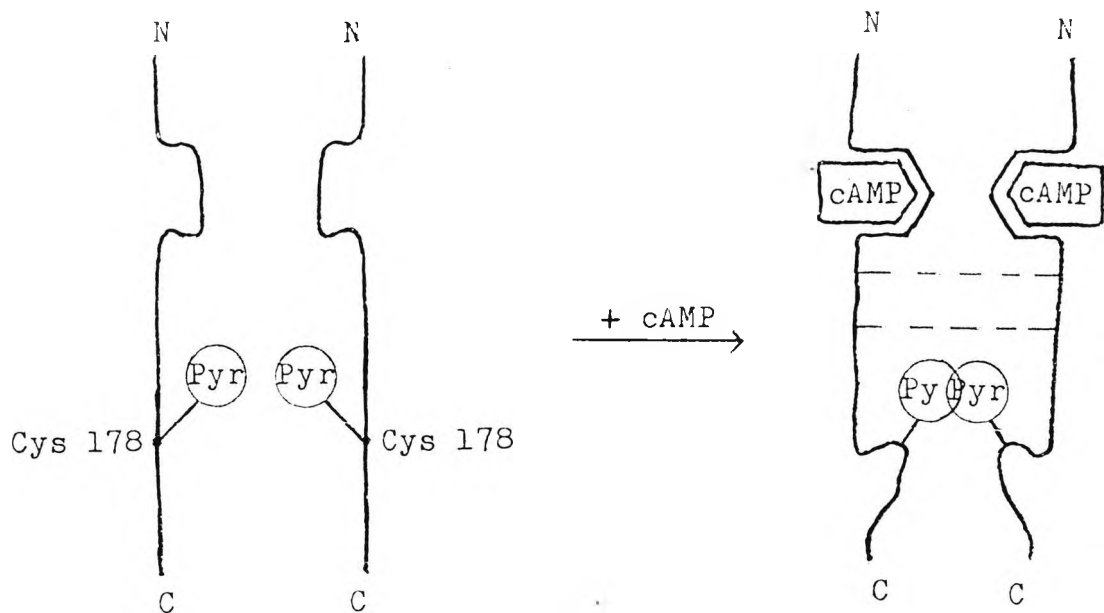


Fig. 6.9. Pyrene labelled CRP producing excimer emission via formation of the CRP dimer.

6.6. INVESTIGATION OF THE INTERACTION OF cAMP WITH THE cAMP BINDING SITE OF CRP AND R<sub>II</sub>.

The cAMP binding site of CRP (cABS) was supplied by SmithKline Beecham Pharmaceuticals, as a buffered aqueous solution, and it was considered that this protein may give a more profound conformational change on cAMP binding.

The protein possesses the same primary structure as the amino-terminal section of CRP, and the carboxyl-terminal amino acid is glutamate-125, which is present in helix C.

The regulatory subunit from cAMP-dependent protein kinase, obtained from bovine heart (R<sub>II</sub>) (38,39), was also supplied by SmithKline Beecham Pharmaceuticals as a buffered aqueous solution, to provide a comparison for cABS.

6.6.1. cABS and R<sub>II</sub> Assay.

6.6.1.1. Experimental Procedure.

The cABS and R<sub>II</sub> proteins were assayed utilising the procedure as previously described (1,2,3), in Section 6.1.1.1.

6.6.1.2. Results.

<u>Tube Nos.</u>	<u>Protein conc.</u> <u>(ug/ml)</u>	<u>Absorbance</u> <u>at 595 nm</u>	<u>Mean</u> <u>Absorbance</u>
Blank	0.00	0.150	0.150
1	50.00	0.394	0.390
	50.00	0.385	
2	100.00	0.496	0.501
	100.00	0.506	
3	200.00	0.980	0.982
	200.00	0.983	
4	300.00	1.368	1.373
	300.00	1.378	
5	400.00	1.796	1.800
	400.00	1.805	
cABS soln.		0.930 0.956	0.943
R <sub>II</sub>		0.168	0.172
		0.176	

Table 6.14. Absorbance readings, at 595 nm, for varying concentrations of BSA, cABS and R<sub>II</sub> as detected by Lowry Reagent.

Using the data obtained, a calibration curve was constructed. The concentration of the CRP solution was determined from the calibration curve.

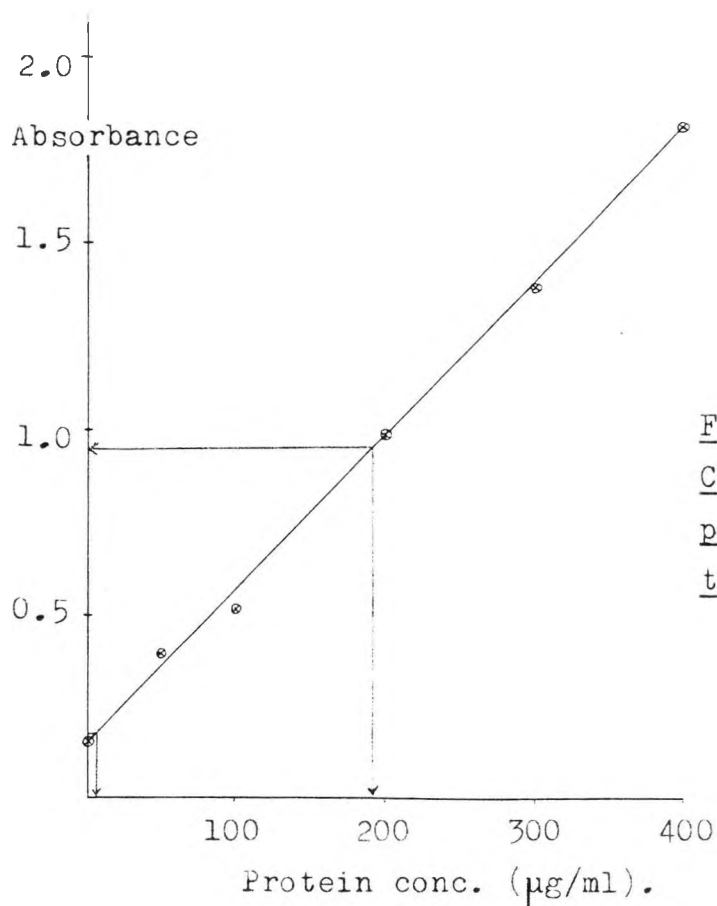


Fig. 6.10. Calibration Curve using standard protein solution for the assay of cABS and R<sub>II</sub>.

From the calibration curve, it may be deduced that the concentration of the diluted cABS solution is 192.5 µg/ml, at a dilution of 1:100. Therefore, the stock cABS concentration is 19.25 mg/ml.

From the calibration curve, it may be deduced that the concentration of the diluted R<sub>II</sub> solution is 6.20 µg/ml, at a dilution of 1:100. Therefore, the stock R<sub>II</sub> concentration is 0.62 mg/ml.

The cABS solution was diluted to a final concentration of 12.50 mg/ml, in order to facilitate direct comparison with CRP.

### 6.6.2. cAMP Binding Assay of Unlabelled cABS and R<sub>II</sub>.

#### 6.6.2.1. Experimental Procedure.

The cAMP binding assay of both cABS and R<sub>II</sub> (unlabelled),

was then performed utilising the procedure as previously described (4,5), in Section 6.1.2.1., in the presence of acetonitrile. The cABS was used at dilutions of 1:10, 1:20, 1:40, 1:80 and 1:160.  $R_{II}$  was utilised at dilutions of 1:2, 1:4 and 1:8.

#### 6.6.2.2. Results.

Total Count = 199326 disintegrations per minute (d.p.m.)

Control Count = 4276 disintegrations per minute (d.p.m.)

#### cAMP Binding Assay of Acetonitrile Treated Unlabelled cABS.

<u>Tube Nos.</u>	<u>CRP Dilution</u>	<u>Concentration</u>	<u>d.p.m.</u>	<u>Corrected d.p.m.</u>	<u>% Binding</u>
1A	1:10	1.250 mg/ml	50024	45748	23
2A	1:20	0.625 mg/ml	43589	39313	20
3A	1:40	0.310 mg/ml	32716	28440	14
4A	1:80	0.156 mg/ml	27990	23714	12
5A	1:160	0.078 mg/ml	13147	8871	4

Table 6.15. Results of the % binding of acetonitrile treated unlabelled cABS.

#### cAMP Binding Assay of Acetonitrile Treated Unlabelled $R_{II}$ .

<u>Tube Nos.</u>	<u>CRP Dilution</u>	<u>Concentration</u>	<u>d.p.m.</u>	<u>Corrected d.p.m.</u>	<u>% Binding</u>
1B	1:2	0.310 mg/ml	156466	152190	76
2B	1:4	0.155 mg/ml	117595	113319	57
3B	1:8	0.078 mg/ml	79445	75169	38

Table 6.16. Results of the % binding of acetonitrile treated unlabelled  $R_{II}$ .

A graph of % cAMP binding against protein concentration was then plotted.

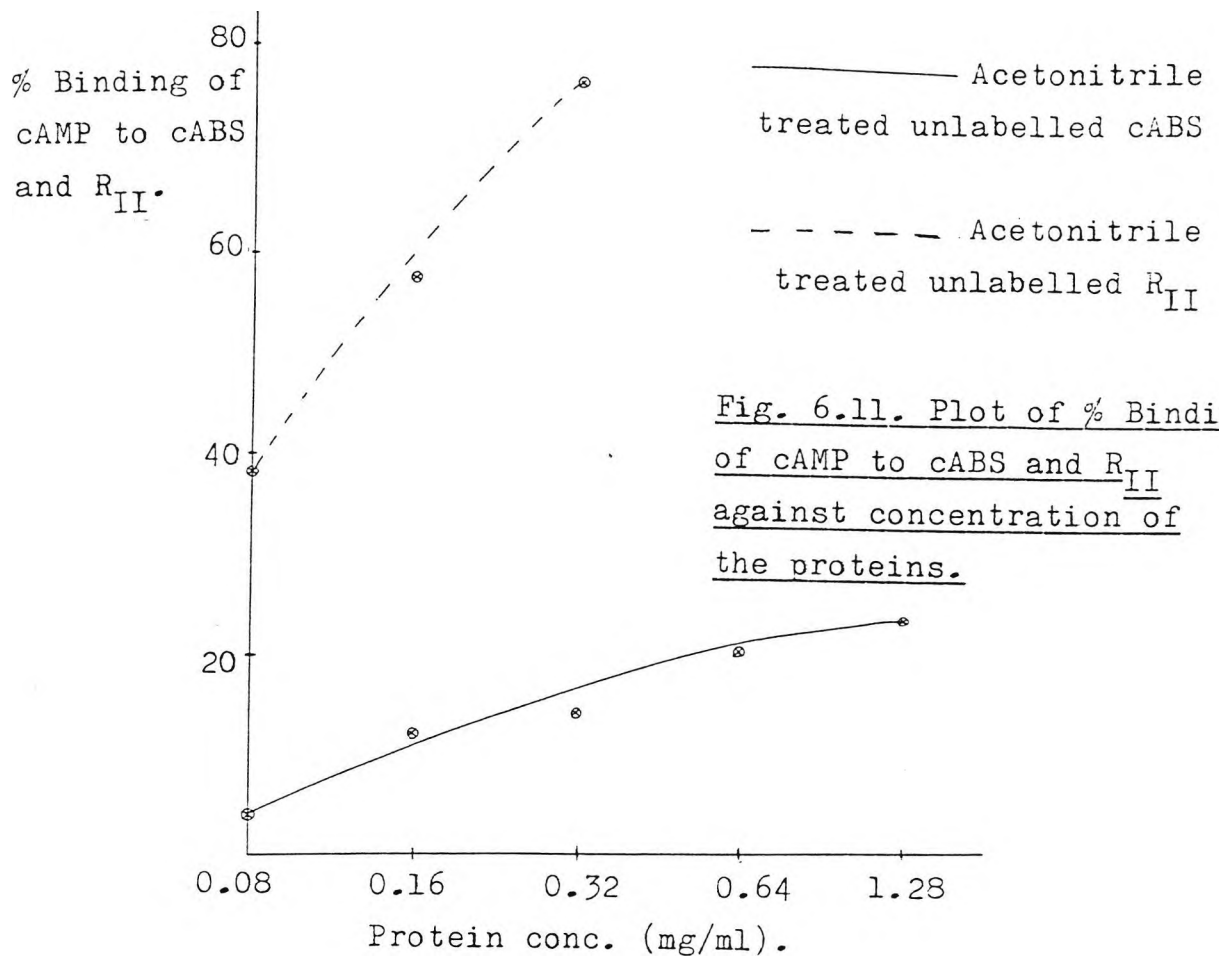


Fig. 6.11. Plot of % Binding of cAMP to cABS and R<sub>II</sub> against concentration of the proteins.

### 6.6.3. Conclusion.

It may be seen from the graph that cABS and R<sub>II</sub>, both present at a concentration of approximately 0.156 mg/ml, possess a cAMP binding capacity of 12% and 57% respectively. The capacity of CRP for cAMP at the same protein concentration, (1:80 dilution), is 29%. This finding reflects the observation that R<sub>II</sub> will bind two molecules of cAMP (40).

Also, it is clear that CRP possesses a much greater affinity for cAMP, than does cABS. Since the cABS is devoid of a DNA binding site, this finding gives credence to the contention, that the carboxyl-terminal segment of the protein is of profound importance for the binding of cAMP. The cysteine-178/cysteine-178 disulphide linkage which stabilises

cAMP binding in CRP, may not occur in cABS. As a consequence, cABS would be expected to have a reduced affinity for cAMP as compared to CRP.

#### 6.7. INVESTIGATION OF THE NATURE OF THE PROTEIN- PROBE CONJUGATES.

Since the cABS is devoid of cysteine-178, it is not expected to undergo fluorescent modification via thiol groups of cysteine residues. This assumption was investigated by the reaction of cABS with 1,8-IAEDANS as previously described (8), in Section 6.4.1. R<sub>II</sub> was labelled likewise.

The U.V./visible spectrum of the purified protein-probe conjugate showed that the protein did, in fact, undergo modification. The U.V./visible spectrum of the R<sub>II</sub> conjugate, exhibited similar peaks.

##### 6.7.1. Determination of the Stoichiometry of Labelling.

In order to deduce the stoichiometry of labelling of cABS via thiol modification, it is necessary to determine the molar extinction coefficient of cABS.

##### 6.7.1.1. Calculation of the Molar Extinction Coefficient of cABS.

Diluted stock cABS solution (20  $\mu$ l), at a final concentration of 10 mg/ml, was added to Tris-HCl (2.98 ml, pH 8.0) in a cuvette. The absorbance, at 278 nm, of this solution was found to be 0.076, when baselined against this buffer.

Calculation of cABS solution: 20  $\mu$ l per 3 ml = 6.66  $\mu$ l/ml.

6.66  $\mu$ l of 10 mg/ml solution = 0.067 mg/ml.

Molecular Weight of Protein = 14387

$$\text{Thus, molarity of protein} = \frac{0.067}{14387} = \underline{4.6 \times 10^{-6} \text{ M.}}$$

From the Beer-Lambert law,  $D = \epsilon \cdot c \cdot l$

For pathlength of 1 cm,  $D = \epsilon \cdot c$

$$\epsilon = \frac{D}{c} = \frac{0.076}{4.6 \times 10^{-6}} = 16521$$

$\epsilon$ , at 278 nm, of cABS = 16521 litre mol<sup>-1</sup> cm<sup>-1</sup>.

#### 6.7.1.2. Calculation of the Stoichiometry of the Labelling of cABS via Thiol Modification.

From the U.V./visible spectrum of the protein-probe conjugate, the probe was found to have an absorbance, at 340 nm, of 0.046, when baselined against the buffer used (tris-HCl).

$$\begin{aligned} \text{For the probe, } c &= \frac{D}{\epsilon} \\ c &= \frac{0.046}{6300} = \underline{7.3 \times 10^{-6} \text{ M.}} \\ & \text{(Ref. 25)} \end{aligned}$$

For the protein, absorbance at 278 nm, was found to be 0.112.

$$\begin{aligned} \text{For the protein, } c &= \frac{D}{\epsilon} \\ c &= \frac{0.112}{16500} = \underline{6.8 \times 10^{-6} \text{ M.}} \end{aligned}$$

Therefore, the dye : protein ratio is 1 : 1.

This procedure was repeated using DACM, in order to preclude possible binding of other susceptible amino acid residues, for example, histidine. The dye : protein ratio was also found to be 1 : 1.

### 6.7.2. Determination of the Specificity of Labelling.

#### 6.7.2.1. Experimental Procedure.

For the establishment of covalent modification of the cABS by the thiol probe, 1,8-IAEDANS, SDS-PAGE was performed as previously described (30), in Section 6.5.2.1. The procedure was performed in duplicate.

#### 6.7.2.2. Results.

After removal of the gels from the tubes, the former were viewed under U.V. radiation at 375 nm. A fluorescent band was observed approximately 25 mm from the bromophenol blue marker in both gels. No other fluorescent band was observed.

After fixing and staining, the gels were viewed in daylight, and a blue band was observed approximately 25 mm from the bromophenol blue marker in both gels. No other protein band was observed.

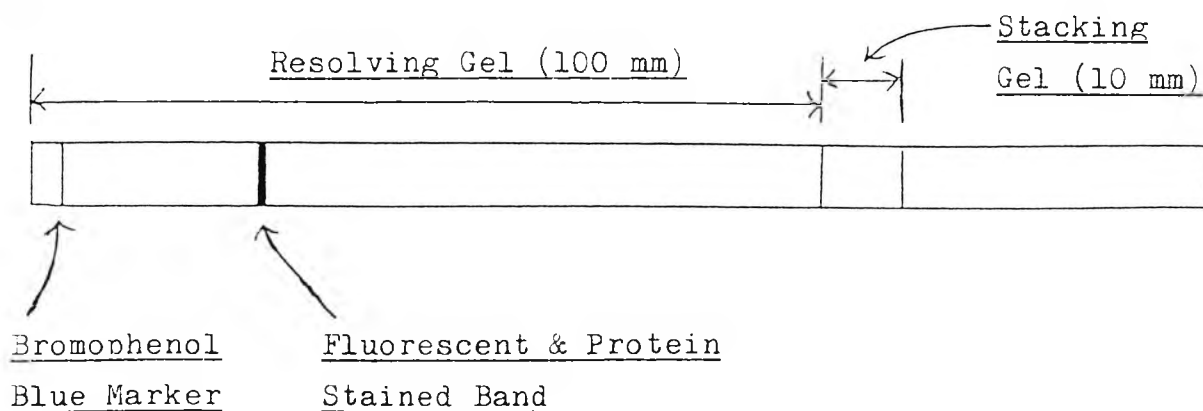


Fig. 6.12. Scale drawing of the electrophoretic gel of the cABS-1,8-IAEDANS conjugate.

### 6.7.3. Conclusion.

Thus, the label and the protein migrate as a single band, and this indicates that the probe is covalently bound to the protein.

### 6.8. DETERMINATION OF THE EFFECT OF THIOL MODIFICATION OF cABS AND R<sub>II</sub> ON THE CAPACITY FOR cAMP BINDING.

In order to elicit shifts in peak emission together with fluorescence enhancement, on the binding of cAMP, it is necessary for fluorescently labelled cABS to be capable of binding cAMP. R<sub>II</sub> was similarly investigated.

#### 6.8.1. Experimental Procedure.

The reactions were performed using Acrylodan as previously described in Section 6.1.3.1., utilising cABS at dilutions of 1:40, 1:80 and 1:160. R<sub>II</sub> was utilised at dilutions of 1:2, 1:4 and 1:8.

#### 6.8.2. Results.

##### cAMP Binding Assay of Thiol Modified cABS.

Tube Nos.	CRP Dilution	Conc. (mg/ml)	d.p.m.	Mean d.p.m.	Corrected d.p.m.	% Binding
1A	1:40	0.310	5042 4972	5007	731	0.37
2A	1:80	0.155	4685 4827	4756	480	0.24
3A	1:160	0.078	4623 4487	4555	279	0.14

Table 6.17. Results of the % cAMP binding of acrylodan labelled cABS.

Total Count = 199326 disintegrations per minute (d.p.m.)

Control Count = 4276 disintegrations per minute (d.p.m.)

cAMP Binding Assay of Thiol Modified R<sub>II</sub>.

<u>Tube</u> <u>Nos.</u>	<u>CRP</u> <u>Dilution</u>	<u>Conc.</u> <u>(mg/ml)</u>	<u>d.p.m.</u>	<u>Mean</u> <u>d.p.m.</u>	<u>Corrected</u> <u>d.p.m.</u>	<u>%</u> <u>Binding</u>
1B	1:2	0.310	139268 139230	139249	134973	68
2B	1:4	0.155	96552 96508	96530	92254	46
3B	1:8	0.078	54514 54466	54490	50214	25

Table 6.18. Results of the % cAMP  
binding of acrylodan labelled R<sub>II</sub>.

6.8.3. Conclusion.

These results show that thiol modification of cABS prevents the binding of cAMP. In contrast, thiol modified R<sub>II</sub> will bind cAMP.

6.9. DETERMINATION OF THE ABILITY OF cAMP BOUND cABS  
AND R<sub>II</sub> TO UNDERGO THIOL MODIFICATION.

6.9.1. Experimental Procedure.

Procedures were followed in order to ascertain whether fluorescent modification of cABS and R<sub>II</sub>, may be achieved in the presence of cAMP. cABS was utilised at dilutions of 1:40 and 1:80; R<sub>II</sub> was employed at dilutions of 1:2 and 1:4. The reaction was performed using Acrylodan as previously described, in Section 6.4.1.

### 6.9.2. Results.

The U.V./visible spectrum of the  $R_{II}$  samples on prior incubation with cAMP, exhibited a peak absorption at 372 nm. The fluorescence spectrum of these samples was found to show peak emission at 462 nm.

The U.V./visible spectrum of the cABS samples on prior incubation with cAMP, exhibited no such peak. No fluorescence emission was detected in these samples.

### 6.9.3. Discussion.

These results show that  $R_{II}$  may be fluorescently modified via thiol groups, in the presence of cAMP. However, cABS may not be fluorescently labelled via thiol groups when the protein had been previously incubated with cAMP.

cABS possesses two cysteine residues, at positions 18 and 92. Only one cysteine residue is modified during the derivatisation reaction, and this process prevents cAMP binding. Also, the finding that cAMP binding prevents fluorescent modification, indicates that the residue in question must be in the vicinity of the cAMP binding pocket. Since cysteine-92 is known to be located in this area (35,41), it is postulated that this amino acid is the site of fluorescent modification.

Since cysteine-92 in CRP is inaccessible to thiol reactive probes, it follows that CRP and cABS must possess different tertiary structures. Also, since cysteine-178/cysteine-178 disulphide linkage may not occur in cABS, it follows that the latter must exist solely in the monomeric form.

The results obtained indicate that the following processes occur, and these may be represented schematically.

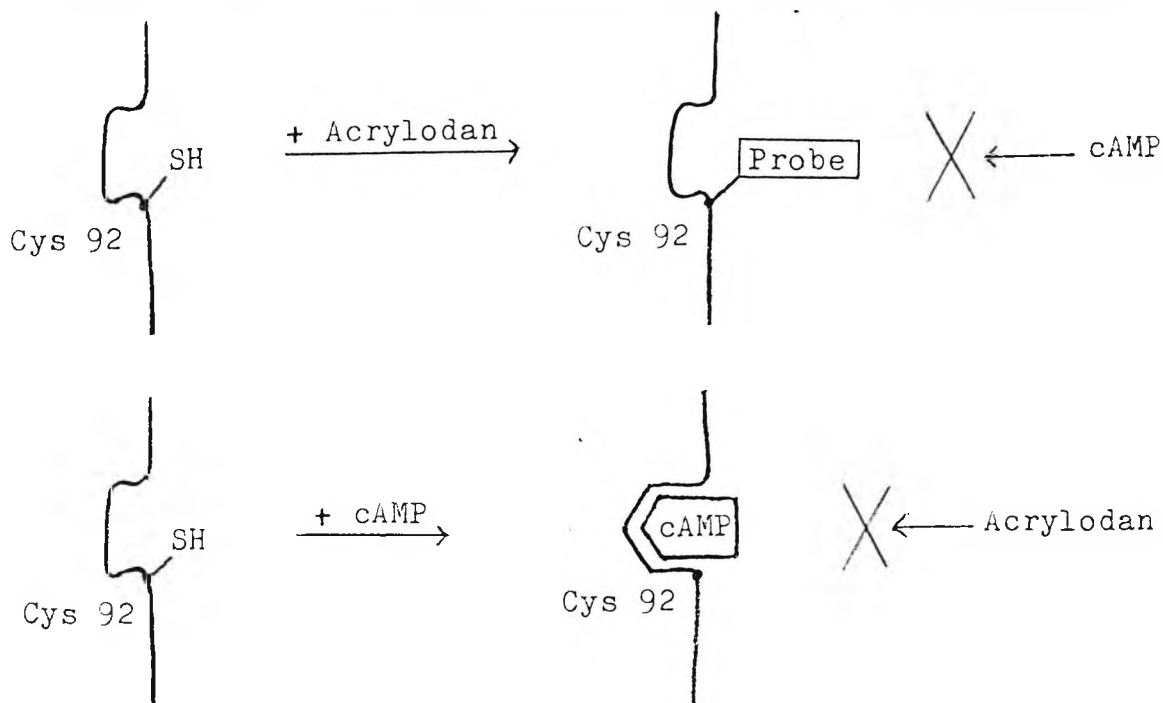


Fig. 6.13. Schematic Summary of the results obtained.

#### 6.10. IDEAS FOR FURTHER WORK.

Use of a fluorophore to label CRP, which may produce excited dimer (excimer) emission, at a longer wavelength than that produced by N-(1-Pyrene) maleimide. This could possibly be achieved by increasing the conjugation of the pyrene nucleus. The excimer emission of the probe is 465 nm, which shows blue fluorescence. Blue emission is not readily detectable by the naked eye; green/yellow fluorescence ( $\lambda =$  approximately 550 nm) is ideal for visualisation. The monitoring of excimer emission, is a good qualitative indicator of cAMP binding, since this emission only occurs on cAMP binding to the CRP.

Mutant CRP molecules have been produced (42,43,44,45),

which interact with cGMP to produce a conformational change in the protein. Use of the more suitable probes (for example, naphthalenes and possibly the pyrene) on this protein, may yield positive results.

It may be postulated that the use of a larger protein than CRP, for fluorescent modification may elicit a greater conformational change on cAMP binding, and thereby exhibit a greater hypsochromic shift in the emission spectrum together with a greater fluorescence enhancement. This is indicated by the greater hypsochromic shift (13 nm) as exhibited by the labelling of R<sub>II</sub> with Acrylodan, compared to CRP. However, it is expected that a larger protein will comprise more than one available cysteine residue, for fluorescence labelling. If, as in CRP, disulphide linkages are formed on cAMP binding, it may be possible to incubate the protein with cAMP allowing formation of the disulphide linkages. These cysteine residues are now not available for modification. Reaction of the protein with iodoacetamide (46,47), in order to block the thiol groups of less critical cysteine residues, may be performed. Removal of cAMP by dialysis will restore the thiol groups, and these may then be labelled by a suitable fluorescent, thiol-reactive agent. Subsequent rebinding of cAMP to the modified protein, will result in shifts in the emission spectrum, concomitant with enhancement of fluorescence.

In order for this strategy to be effective, the cAMP must be removed from the protein by dialysis.

This has been investigated as follows:

Two tubes were set up in duplicate. To each tube was added:

- i) 5'AMP solution (10  $\mu$ l, 20 mM),
- ii) 'Cold' + tritiated ( $^3\text{H}$ ) cAMP solution (10  $\mu$ l);  
produced by adding  $^3\text{H}$ -cAMP (5  $\mu$ l) to 'cold' cAMP (220  $\mu$ l, 2  $\mu$ M), producing a final  $^3\text{H}$ -cAMP concentration of 0.08  $\mu$ M.
- iii) Distilled water (230  $\mu$ l).

To one set of two tubes was added 1:40 (0.310 mg/ml) cABS solution (50  $\mu$ l).

To the other set of two tubes was added 1:2 (0.310 mg/ml)  $R_{II}$  solution (50  $\mu$ l).

One control tube was set up containing:

- i) 5'AMP solution (10  $\mu$ l, 20 mM),
- ii) Distilled water (240  $\mu$ l),
- iii) 1:40 cABS (50  $\mu$ l, 0.310 mg/ml).

A second control tube was set up containing i) and ii) plus 1:2  $R_{II}$  (50  $\mu$ l, 0.310 mg/ml).

Aliquots (100  $\mu$ l) were taken from each tube, and were introduced into separate vials. Pico-Fluor Liquid Scintillation Fluid (10 ml) was added, and each vial was then subjected to radio-counting using a Liquid Scintillation Counter.

A total count tube was set up by taking an aliquot (30  $\mu$ l) of a 'cold' + tritiated ( $^3\text{H}$ ) cAMP solution; produced by adding  $^3\text{H}$ -cAMP (5  $\mu$ l) to 'cold' cAMP solution (220  $\mu$ l, 20 mM), producing a final  $^3\text{H}$ -cAMP concentration of 0.08  $\mu$ M. This aliquot was then added to distilled water (270  $\mu$ l).

Aliquots (100  $\mu$ l) were taken from this, and the four sample tubes, and each aliquot was placed in separate vials.

Pico-Fluor Liquid Scintillation Fluid (10 ml) was added to each vial, and the latter were then directly subjected to radio-counting using a Liquid Scintillation Counter.

The remainder of each sample was extensively dialysed (3 days), against Tris-HCl/KCl/MgCl<sub>2</sub> (0.20 M, 1000 ml, pH 8.0) containing activated charcoal (2 gm) with stirring, using cellulose tubing which retains molecular weight species in excess of 8000 daltons.

After dialysis, aliquots (100 µl) were taken from each dialysand. These were radio-counted as above. The dialysis of R<sub>II</sub> was allowed to proceed for a further 24 hours, and the dialysands were again radio-counted.

### Results.

Total Count = 205192 d.p.m.

Control Count for cABS = 63 d.p.m.

Control Count for R<sub>II</sub> = 83 d.p.m.

### For cABS.

<u>Status</u>	<u>Protein Dilution</u>	<u>d.p.m.</u>	<u>Mean d.p.m.</u>	<u>Corrected d.p.m.</u>	<u>% Binding</u>
After Dialy-sis	1:40	860 912	886	823	0.40

Table 6.19. Results of the % cAMP binding to cABS after extensive dialysis.

For R<sub>II</sub>-

<u>Status</u>	<u>Protein Dilution</u>	<u>d.p.m.</u>	<u>Mean d.p.m.</u>	<u>Corrected d.p.m.</u>	<u>% Binding</u>
After Dialysis	1:2	98992 108080	103536	103453	50
After Further Dialysis	1:2	52864 60020	56442	56359	27

Table 6.20. Results of the % cAMP binding to R<sub>II</sub> after extensive dialysis.

The results show that cAMP may be readily removed from cABS by dialysis. Virtually all radioactivity was removed from the dialysis sack, after 72 hours dialysis.

R<sub>II</sub>, possessing a much greater affinity for cAMP, retains up to 30% of the radiolabelled cAMP after 96 hours dialysis. It has been suggested (40), that it is more likely for cAMP to dissociate from R<sub>II</sub> and then rebind, before the cAMP can exit from the dialysis sack.

Clearly, R<sub>II</sub> is not a good candidate for the strategy previously outlined.

#### 6.11. SUMMARY.

It was shown that cAMP Receptor Protein (CRP) was capable of binding cAMP when unlabelled, and when fluorescently labelled via  $\epsilon$ -amino groups and thiol groups.

The interaction between cAMP and thiol-labelled CRP

was found to yield the best results, especially when the latter was modified using a probe containing the naphthalene chromophore.

It was found that the hydrophobic pocket, present within the CRP, was much less lipophilic than that present within Bovine Serum Albumin (BSA), and it was also evident that CRP could not be fluorescently labelled when present as the CRP-cAMP complex. This was due to the formation of a cysteine-178/cysteine-178 disulphide bridge, between the two protein monomers, on cAMP binding. Since this amino acid residue undergoes modification on reaction with a thiol-reactive fluorophore, its thiol group was not available for modification in the presence of cAMP.

The dye : protein ratio was found to be 1 : 1 for thiol modification, and the labelling process was found to be covalent in nature, by the migration of a single band on SDS-PAGE.

The cAMP binding site of CRP (cABS), possessing residues 1 to 125 inclusive of those of CRP, supplied by SmithKline Beecham Pharmaceuticals, was found to bind cAMP although to a lesser extent than CRP. Although cysteine-178 is absent in cABS, it was still able to undergo fluorescent modification, and the dye : protein ratio was found to be 1 : 1. The amino acid residue concerned was shown to be cysteine-92. Thus, cABS possesses a different tertiary structure to CRP.

As with CRP, cABS would not undergo fluorescent modification in the presence of cAMP. Also, unlike CRP, the modified protein would not bind cAMP. This indicated that cysteine-92 must be

near the cAMP binding site of CRP.

The regulatory subunit of cAMP-dependent protein kinase ( $R_{II}$ ), was found to bind cAMP to a much greater extent than CRP. Fluorescent modification of the protein did not interfere with cAMP binding.

6.12.      REFERENCES.

1. Lowry, O.H., Rosebrough, N.J., Farr, A.L. & Randall, R.J.  
(1951) J. Biol. Chem. 193 265
2. Peterson, G.L.  
(1977) Anal. Biochem. 83 346
3. Bensadoun, A. & Weinstein, D.  
(1976) Anal. Biochem. 70 241
4. Anderson, W.B., Schneider, A.B., Emmer, M.,  
Perlman, R.L. & Pastan, I.  
(1971) J. Biol. Chem. 246 5929
5. Donoso-Pardo, J.L., Turner, P.C. & King, R.W.  
(1987) Eur. J. Biochem. 168 687
6. Prendergast, F.G., Meyer, M., Carlson, G.L., Iida, S.  
& Potter, J.D.  
(1983) J. Biol. Chem. 258 7541
7. Titus, J.A., Haugland, R.P., Sharrow, S.O. & Segal, D.M.  
(1982) J. Immunol. Methods 50 193
8. Wu, F.Y.-H., Nath, K. & Wu, C.-W.  
(1974) Biochemistry 13 2567
9. Kumar, S.A., Murthy, N.S. & Krakow, J.S.  
(1980) FEBS Letters 109 121
10. Chen, R.F.  
(1967) Arch. Biochem. Biophys. 120 609
11. Chen, R.F.  
(1969) Arch. Biochem. Biophys. 133 263
12. Kanaoka, Y., Machida, M., Kokubun, H. & Sekine, T.  
(1968) Chem. Pharm. Bull. 16 1747
13. Cecil, R.  
In The Proteins Vol. 1.  
(Ed: H. Neurath, Academic Press, New York) p 402 (1963)
14. Ghosh, P.B. & Whitehouse, M.W.  
(1968) Biochemical J. 108 155
15. Birkett, D.J., Price, N.C., Radda, G.K. & Salmon, A.G.  
(1970) FEBS Letters 6 346

16. Saenger, W.  
(1980) *Angew. Chem. Int. Ed. Engl.* 19 344
17. Lightner, D.A., Gawronski, J.K. & Gawronska, K.  
(1985) *J. Amer. Chem. Soc.* 107 2456
18. Weltman, J.K., Szaro, R.P., Frackelton, Jr., A.R.,  
Dowben, R.M., Bunting, J.R. & Cathou, R.E.  
(1973) *J. Biol. Chem.* 248 3173
19. Strasburg, G.M., Leavis, P.C. & Gergely, J.  
(1985) *J. Biol. Chem.* 260 366
20. Stewart, W.W.  
(1981) *Nature* 292 17
21. Yamamoto, K., Sekine, T. & Kanaoka, Y.  
(1977) *Anal. Biochem.* 79 83
22. Wendelin, W., Gubitz, G. & Pracher, U.  
(1987) *J. Heterocyclic Chem.* 24 1381
23. Kanaoka, Y., Machida, M., Machida, M. & Sekine, T.  
(1973) *Biochim. Biophys. Acta* 317 563
24. Johnson, J.D., Collins, J.H., Robertson, S.P. & Potter, J.D.  
(1980) *J. Biol. Chem.* 255 9635
25. Hudson, E.N. & Weber, G.  
(1973) *Biochemistry* 12 4154
26. Weber, G. & Farris, F.J.  
(1979) *Biochemistry* 18 3075
27. Lippert, E.  
(1957) *Hoppe Seylers Zeitschrift für Electrochemie* 61 962
28. Kosower, E.M.  
(1958) *J. Amer. Chem. Soc.* 80 3253
29. Saxe, S.A. & Revzin, A.  
(1979) *Biochemistry* 18 255
30. Laemmlli, U.K.  
(1970) *Nature* 227 680
31. Heyduk, T. & Lee, J.C.  
(1989) *Biochemistry* 28 6914

32. Aiba, H., Fujimoto, S. & Ozaki, N.  
(1982) Nucl. Acids Res. 10 1345
33. Cossart, P. & Gicquel-Sanzey, B.  
(1982) Nucl. Acids Res. 10 1363
34. Ebright, R.H., LeGrice, S.F.J., Miller, J.P. & Krakow, J.S.  
(1985) J. Mol. Biol. 182 91
35. Weber, I.T. & Steitz, T.A.  
(1987) J. Mol. Biol. 198 311
36. Eilen, E. & Krakow, J.S.  
(1977) J. Mol. Biol. 114 47
37. Ebright, R.H., Kolb, A., Buc, H., Kunkel, T.A.,  
Krakow, J.S. & Beckwith, J.  
(1987) Proc. Natl. Acad. Sci. USA 84 6083
38. Takio, K., Smith, S.B., Krebs, E.G., Walsh, K.A.  
& Titani, K.  
(1982) Proc. Natl. Acad. Sci. USA 79 2544
39. Weber, I.T., Takio, K., Titani, K. & Steitz, T.A.  
(1982) Proc. Natl. Acad. Sci. USA 79 7679
40. Corbin, J.D., Sugden, P.H., West, L., Flockhart, D.A.,  
Lincoln, T.M. & McCarthy, D.  
(1978) J. Biol. Chem. 253 3997
41. Kypr, J. & Mrazek, J.  
(1985) Biochem. Biophys. Res. Commun. 131 780
42. Garges, S. & Adhya, S.  
(1985) Cell 41 745
43. Aiba, H., Nakamura, T., Mitani, H. & Mori, H.  
(1985) EMBO J. 4 3329
44. Harman, J.G., McKenney, K. & Peterkofsky, A.  
(1986) J. Biol. Chem. 261 16332
45. Harman, J.G., Peterkofsky, A. & McKenney, K.  
(1988) J. Biol. Chem. 263 8072
46. Foster, M. & Harrison, J.H.  
(1973) J. Biochem. (Tokyo) 73 705
47. Harada, M. & Irie, M.  
(1974) Biochim. Biophys. Acta 351 295